



TECHNISCHE
UNIVERSITÄT
WIEN

Master Thesis

NON-NATURAL SUGAR ALCOHOLS AS POTENTIAL PHASE CHANGE MATERIALS

carried out for the purpose of obtaining the degree of Master of Science (MSc),

by

Nina Biedermann, BSc

Johann-Haberl-Straße 22
3830 Waidhofen an der Thaya

under the supervision of

Dipl.-Ing. Dr.techn. Christian Stanetty
Associate Prof. Dipl.-Ing. Dr.techn. Michael Schnürch

Institute of Applied Synthetic Chemistry, E163

submitted at the Technische Universität Wien,
Faculty of Technical Chemistry



Die approbierte gedruckte Originalversion dieser Diplomarbeit ist an der TU Wien Bibliothek verfügbar
The approved original version of this thesis is available in print at TU Wien Bibliothek.

*Everything is
theoretically impossible,
until it is done.*

Robert A. Heinlein



Die approbierte gedruckte Originalversion dieser Diplomarbeit ist an der TU Wien Bibliothek verfügbar
The approved original version of this thesis is available in print at TU Wien Bibliothek.

Acknowledgements

The last year has been the most challenging time of my life so far. However, it was an exciting time in which I was accompanied and supported by many people. Therefore, I would like to take the opportunity to express my deepest gratitude.

First of all, I would like to thank Associate Prof. Dr.techn. Michael Schnürch for the supervision of my master thesis, the opportunity to work on this interesting project, and his expert input during the practical work and writing process of my thesis.

Special thanks go to my second supervisor, Senior Scientist Dr.techn. Christian Stanetty, who introduced me to the quite challenging world of sugar chemistry. I am very grateful that he gave me the great opportunity to be a part of his "sugar team", and shared his knowledge with me that goes beyond chemistry. He was the person that I have learned the most from in the last year. At last, I want to thank him for his input and corrections during the writing process of my thesis.

I also want to thank Associate Prof. Dr.techn. Florian Rudroff and Univ.Prof. Dr.techn. Marko Mihovilovic for their qualified input during our seminars and the opportunity to conduct my master thesis in the BSC research group.

Furthermore, a big thank you goes to Dr.techn. Markus Draskovits for always having a helping hand in the lab and answering multiple questions, even though he often had to stand my whining at first.

Many thanks go to the HPLC-MS and NMR operators, especially Markus, Johanna, Clemens, and David, for countless measurements and their help whenever questions came up.

What I really appreciated in the last year was the great working environment in the research group. Therefore, I would like to thank all my colleagues Astrid, Blanca, Christoph, Clemens, Dominik, Eleni, Freddy, Hubert, Jakob, Johanna, Julia, Kathi, Kathi, Lydia, Markus, Raheleh, Richard, Sebastian, Stefan, Tobi, Tom and Viktor for their support and making the time in- and outside of the lab enjoyable.

Liebe Johanna, in dir habe ich nicht nur eine wundervolle Kollegin, sondern auch eine beste Freundin gefunden. Du hast mich in der Zeit meiner Masterarbeit unterstützt, wo du nur konntest, und deine Tür war immer für mich offen. Obwohl deine Ohren in Momenten der Verzweiflung einiges ertragen mussten, hast du immer die passenden Worte gefunden, um mir wieder ein Lächeln ins Gesicht zu zaubern und mich zu stärken. Das letzte Jahr ohne dich – für mich einfach unvorstellbar. Danke für alles!

Zuallerletzt möchte ich meiner Familie sowie meinen langjährigen Freunden aus der Schulzeit von Herzen danken, insbesondere meinen Eltern Melitta und Fritz und meiner Schwester Lydia. Ohne Eure zahlreichen motivierenden und stärkenden Worte wäre ich in meinem Leben nicht da, wo ich jetzt bin. Danke, dass ihr immer an mich glaubt, hinter mir steht und mich auf all meinen Wegen bestmöglich unterstützt!

Die approbierte gedruckte Originalversion dieser Diplomarbeit ist an der TU Wien Bibliothek verfügbar
The approved original version of this thesis is available in print at TU Wien Bibliothek.

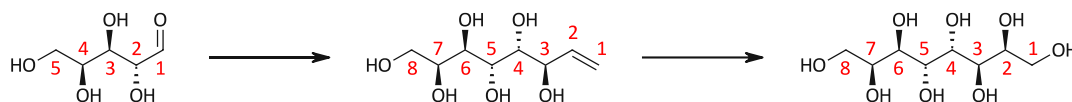


General remarks

All compounds prepared or used as starting materials in this thesis are numbered in bold Arabic numerals in order of their appearance. Compounds that are unknown to literature are additionally underlined.

Literature references are stated with superscript Arabic numerals in order of their appearance.

In all sugar species, numbering of the carbon atoms is started from the (former) reducing end of the sugar, even though this does not match with the IUPAC rules in some cases. This way the nomenclature utilizing stereochemical descriptors like *manno* or *galacto* can be used throughout the thesis.



Measurements of the open-chain contents were conducted by Dipl.Ing. Hubert Kalas.

Die approbierte gedruckte Originalversion dieser Diplomarbeit ist an der TU Wien Bibliothek verfügbar
The approved original version of this thesis is available in print at TU Wien Bibliothek.



Abbreviations

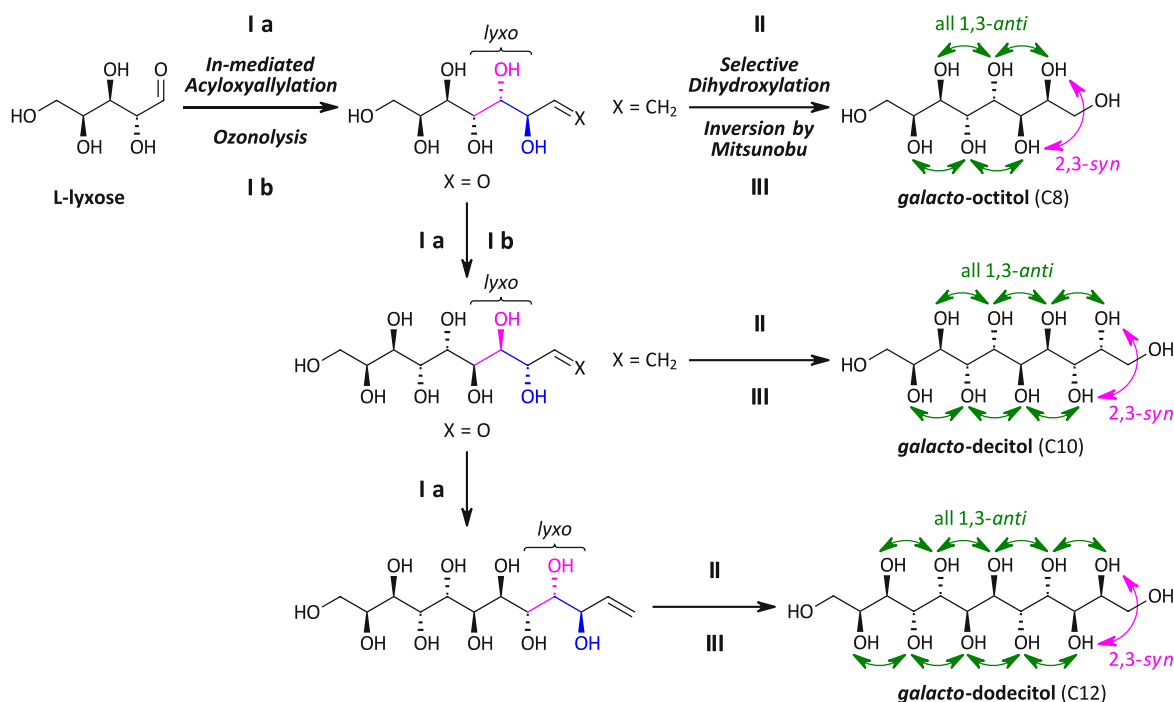
Ac	acetyl
AD	asymmetric dihydroxylation
aq.	aqueous
Bn	benzyl
Bz	benzoyl
conc.	concentrated
COSY	correlated spectroscopy (2D-NMR)
d	doublet (NMR)
DABCO	1,4-diazabicyclo[2.2.2]octane
DCM	dichloromethane
ddd	doublet of doublets of doublets (NMR)
ddt	doublet of doublets of triplets (NMR)
DEAD	diethyl azodicarboxylate
DH	dihydroxylation
DIAD	diisopropyl azodicarboxylate
DMF	<i>N,N</i> -dimethylformamide
DMAP	dimethylaminopyridine
DMSO	dimethyl sulfoxide
DSC	differential scanning calorimetry
dt	doublet of triplets (NMR)
equiv.	molar equivalents
EtOAc	ethyl acetate
EWG	electron withdrawing group
HMBC	heteronuclear multiple bond correlation (2D-NMR)
HPLC	high performance liquid chromatography
HPLC-MS	high performance liquid chromatography – mass spectroscopy
HPTLC	high performance thin layer chromatography
HR-MS	high resolution – mass spectrometry
HSQC	heteronuclear single quantum coherence (2D-NMR)
IMA	indium-mediated acyloxyallylation
<i>J</i>	coupling constant
LHS	latent heat storage
LP	light petroleum
m	multiplet (NMR)
MeOH	methanol
MW	molecular weight
NMM	<i>N</i> -methylmorpholine
NMO	<i>N</i> -methylmorpholine <i>N</i> -oxide
NMR	nuclear magnetic resonance spectroscopy

Nuc	nucleophile
OCC	open-chain content
PCM	phase change material
PEG	poly(ethylene glycol)
Piv	pivaloyl
PNB	4-nitrobenzoyl
ppm	parts per million
prep.	preparative
<i>p</i>-TSA	<i>para</i> -toluenesulfonic acid
q	quartet (NMR)
quant.	quantitative
R_f	retention factor
rt	room temperature
s	singlet (NMR)
SA	sugar alcohol
sat.	saturated
SC	stereocentre
SHS	sensible heat storage
SM	starting material
t	triplet (NMR)
TBS	<i>tert</i> -butyldimethylsilyl
TCS	thermochemical heat storage
td	triplet of doublets (NMR)
TG	thermogravimetric analysis
TEA	triethylamine
THF	tetrahydrofuran

Abstract

In the last years, sugar alcohols aroused great interest within the class of organic phase change materials (PCMs), as they possess high thermal storage densities. In a recent computational study, outstandingly large thermal storage densities for organic PCMs of up to 450–500 kJ/kg have been predicted for non-natural sugar alcohols that fulfill three structural criteria: a linear carbon backbone a stereochemical configuration with all hydroxy groups in 1,3-*anti*-relationship, and an even number of carbon atoms. The predicted values for the "*manno*-series" were already partly confirmed by us experimentally and based upon this, we designed a new series of stereochemically defined sugar alcohols in cooperation with Ishida and Inagaki, the authors of this study. The new "*galacto*-series" was derived from the naturally occurring galactitol, and non-natural sugar alcohols with 8, 10, and 12 carbon atoms in the backbone which also fulfil the stated rules.

In general, higher sugar species are accessible *via* indium-mediated acyloxyallylation (IMA), which is a useful tool for the elongation of aldoses by three carbon atoms. This transformation shows high diastereoselectivity and has deeply been investigated in our group. Including this reaction, we aimed to develop an efficient strategy for the synthesis of higher sugar alcohols with a *syn*-relationship between the two hydroxy groups at the terminal stereocentres and a 1,3-*anti*-relationship of all hydroxy groups ("*galacto*-series"). This protocol should allow the synthesis of the presented *galacto*-sugar alcohols in order to determine their physical properties and estimate their potential as PCMs to confirm and refine the model of the Ishida and Inagaki group.



The development of this general sequence was elaborated with the synthesis of the *L-threo-D-galacto*-octitol, the C8-sugar alcohol of the "*galacto*-series". The synthetic path towards this compound was thoroughly investigated and the targeted substance was obtained from the *L*-lyxose *via* IMA **I a** and subsequent transformation of the sugar-enitol species into the corresponding sugar alcohol. This was achieved by stereoselective dihydroxylation **II**, which included the formation of a new, third stereocentre, though with the wrong stereochemistry, but with high selectivity. However, the desired polyalcohol with all hydroxy groups in a 1,3-*anti*-relationship was accessible *via* subsequent Mitsunobu reaction **III** that lead to the inversion of the newly formed stereocentre and upon deprotection the desired *galacto*-octitol sugar alcohol.

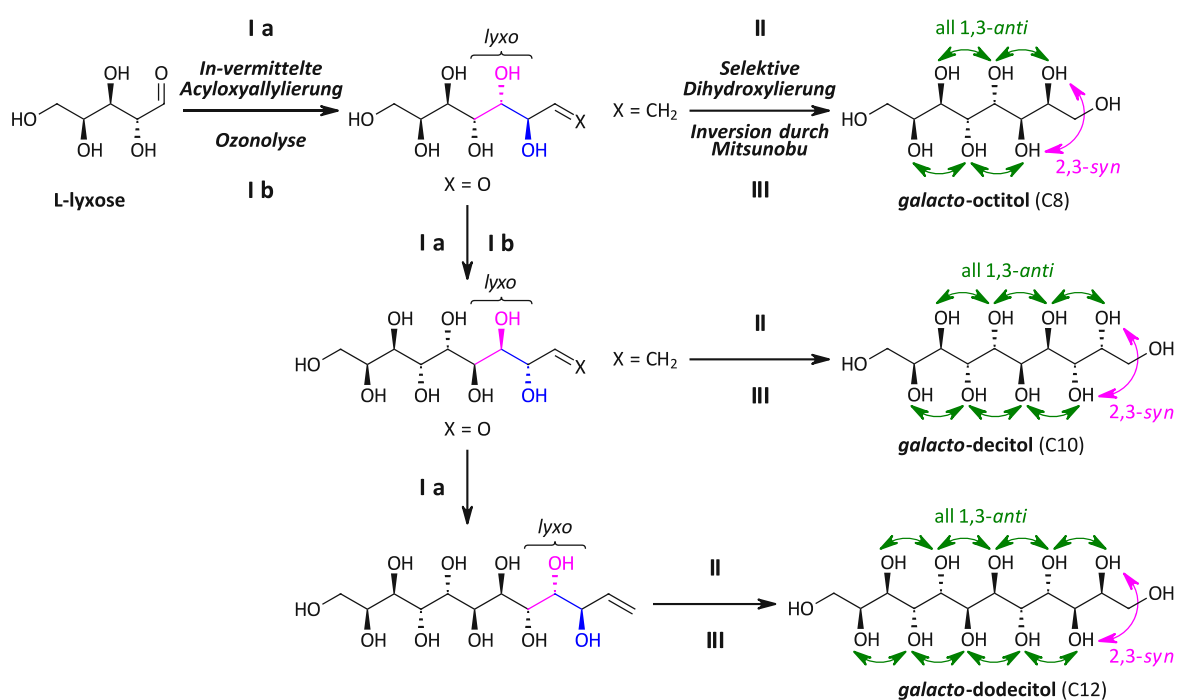
The developed sequence then served as blueprint to synthesis the two carbon longer *L-galacto-L-galacto*-decitol (C10). The required heptose as a starting material was obtained *via* IMA **1 a** of the *L*-lyxose and subsequent ozonolysis **1 b**, which is an established sequence for the elongation of aldoses by two carbon atoms. However, for the following IMA towards the enitol, an improved protocol was necessary, that allows the effective transformation of unreactive aldoses like the heptose. This was successfully achieved by developing a two-step Grignard protocol, using a different solvent, as well as reagent, eventually allowing the synthesis of the C10-enitol species and consequently *galacto*-decitol. The work towards the corresponding dodecitol is currently ongoing, first additional challenges arising from the growing polyhydroxylated chain are already discussed within this thesis.

In order to evaluate the potential as PCMs of this substance class, simultaneous thermal analysis (STA), a method that combines thermogravimetry and differential scanning calorimetry, of the synthesised *galacto*-octitol was performed. The melting point was found to be ~240 °C and a thermal storage density of 368 kJ/kg was measured. These values are quite promising considering the potential of this substance as a PCM and fuel our interest in these sugar species further.

Kurzfassung

In den letzten Jahren haben Zuckeralkohole innerhalb der Klasse der organischen Phasen-Wechsel-Materialien (PCMs) großes Interesse geweckt, da sie hohe thermische Speicherdichten besitzen. In einer kürzlich durchgeführten theoretischen Studie wurden für synthetische Zuckeralkohole außerordentlich große Speicherdichten für organische PCMs von bis zu 450–500 kJ/kg vorhergesagt, wenn diese die folgenden drei Voraussetzungen erfüllen: ein lineares Kohlenstoffrückgrat, eine stereochemische Konfiguration mit allen Hydroxygruppen in 1,3-*anti*-Beziehung, sowie eine gerade Anzahl an Kohlenstoffatomen. Die vorausgesagten Werte für die "*manno*-Serie" wurden bereits teilweise von uns experimentell bewiesen und basierend darauf eine neue Serie von stereochemisch definierten Zuckeralkoholen in Zusammenarbeit mit den Autoren dieser Studie entworfen. Die neue "*galacto*-Serie" wurde vom natürlich vorkommenden Galactitol abgeleitet, und synthetische Zuckeralkohole mit 8, 10 und 12 Kohlenstoffatomen im Rückgrat nach den genannten Regeln postuliert.

Generell sind höhere Zuckerspezies durch die Iridium-vermittelte Acyloxyallylierung (IMA) zugänglich, die ein nützliches Werkzeug für die Verlängerung von Aldosen um drei Kohlenstoffatome ist. Diese Transformation zeigt hohe Diastereoselektivität und wurde in unserer Gruppe eingehend untersucht. Mit Hilfe dieser Reaktion wollten wir folglich eine effiziente Strategie für die Synthese höherer Zuckeralkohole mit einer *syn*-Beziehung zwischen den beiden Hydroxygruppen an den terminalen Stereozentren und 1,3-*anti*-Beziehung aller Hydroxygruppen ("*galacto*-Serie") entwickeln. Dieses Protokoll soll die Synthese der dargestellten *galacto*-Zuckeralkohole ermöglichen, um ihre physikalischen Eigenschaften bestimmen und ihr Potential als PCMs abschätzen zu können, um das Modell der Ishida und Inagaki Gruppe zu bestätigen und weiter zu entwickeln.



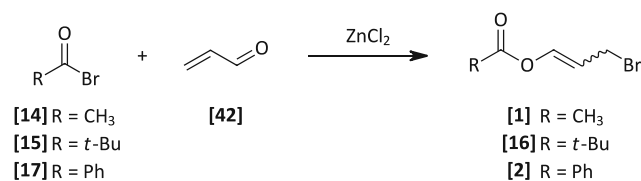
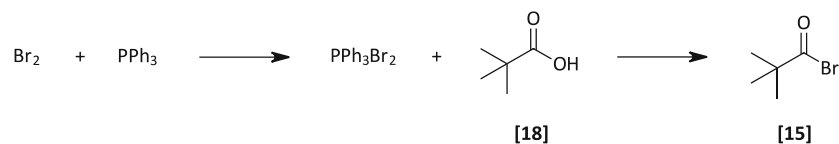
Die Entwicklung dieser allgemeinen Sequenz wurde mit der Synthese des *L-threo-D-galacto*-octitols, dem C8-Zuckeralkohol der "*galacto*-Serie", begonnen. Der Syntheseweg für diese Verbindung wurde umfassend untersucht und die Zielsubstanz ausgehend von *L*-Lyxose durch IMA **I a** und anschließende Umsetzung der Zuckerenitol-Spezies zum entsprechenden Zuckeralkohol erhalten. Dies wurde durch stereoselektive Dihydroxylierung **II** erreicht, wodurch ein neues, drittes Stereozentrum eingeführt wurde, jedoch mit der unerwünschten Stereochemie, aber mit hoher Selektivität. Dennoch war der Polyalkohol mit allen Hydroxygruppen in einer 1,3-*anti*-Beziehung über anschließende Mitsunobu Reaktion **III**, die zur Inversion des neu gebildeten Stereozentrums führte, zugänglich, und der gewünschte *galacto*-Octitol Zuckeralkohol wurde durch anschließende Entschützung erhalten.

Die entwickelte Sequenz diente dann als Vorlage für die Synthese des zwei Kohlenstoffatome längeren *L-galacto-L-galacto*-Decitols (C10). Die als Ausgangsmaterial benötigte Heptose wurde über IMA **I a** der *L*-Lyxose und anschließende Ozonolyse **I b** erhalten, was eine bewährte Sequenz für die Verlängerung von Aldosen um zwei Kohlenstoffatome darstellt. Für die anschließende IMA zum Enitol war jedoch ein verbessertes Protokoll notwendig, das die effektive Umsetzung von unreaktiven Aldosen wie der Heptose erlaubt. Dies gelang durch die Entwicklung eines zweistufigen Grignard-Protokolls, die Verwendung eines anderen Lösungsmittels, sowie Reagenzes, was möglicherweise die Synthese der C10-Enitolspezies und folglich des *galacto*-Decitols erlaubt. Die Arbeiten zum entsprechenden Dodecitol sind derzeit im Gange, erste zusätzliche Herausforderungen, die sich aus der wachsenden polyhydroxylierten Kette ergeben, werden bereits in dieser Arbeit diskutiert.

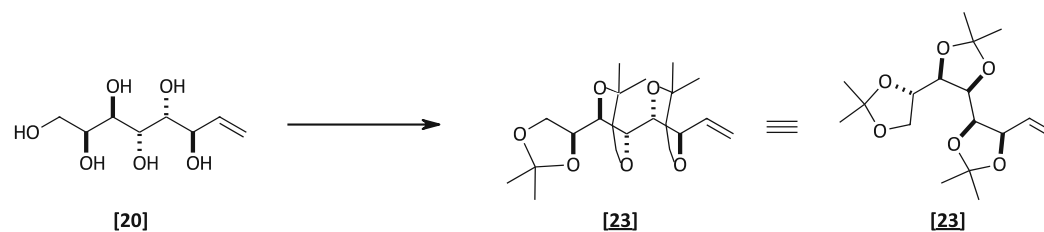
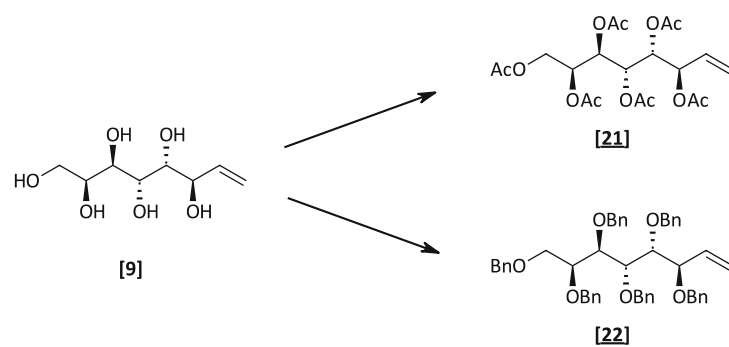
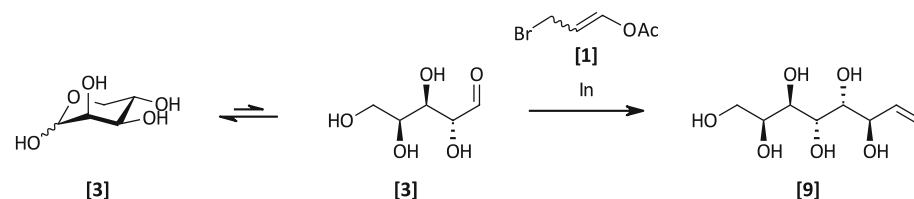
Um das Potential dieser Substanzklasse als PCMs zu bewerten, wurde simultane Thermoanalyse (STA), eine Methode, die Thermogravimetrie und Differential-Scanning-Kalorimetrie vereint, des synthetisierten *galacto*-Octitols durchgeführt. Es wurde ein Schmelzpunkt von ~240 °C gemessen, sowie eine thermische Energiespeicherdichte von 368 kJ/kg. Diese Werte sind recht vielversprechend, wenn man diese Substanzklasse bezüglich ihres Potentials als PCMs betrachtet, und wecken unsere Interesse an diesen Zuckerspezies weiter.

General schemes

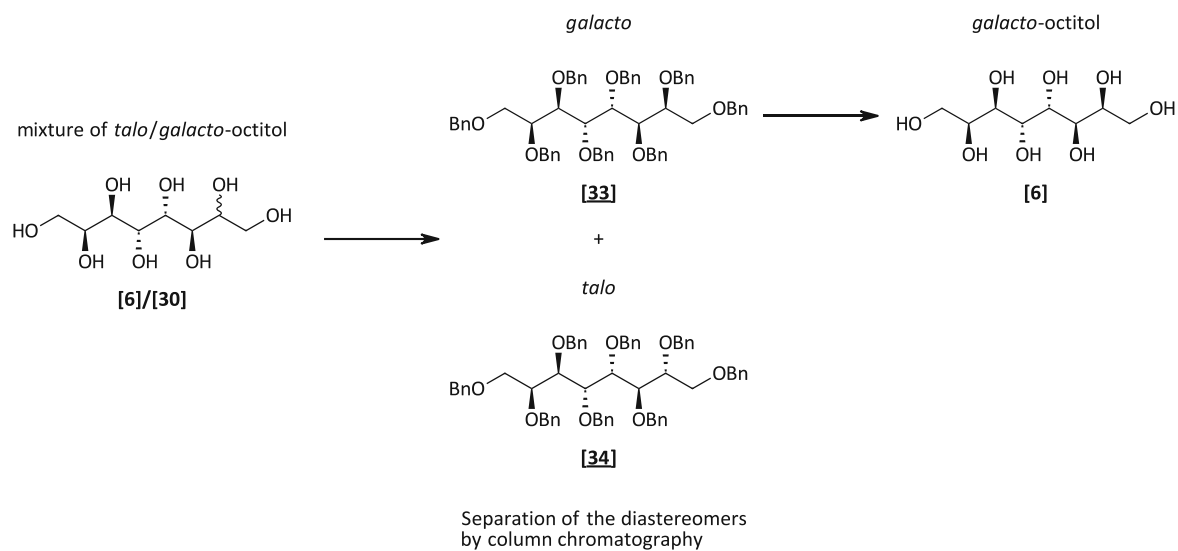
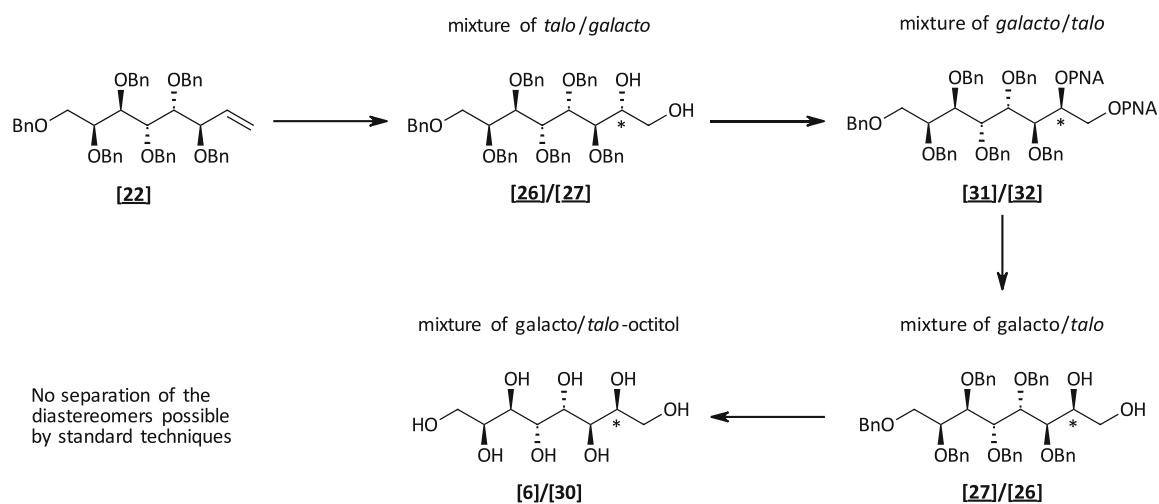
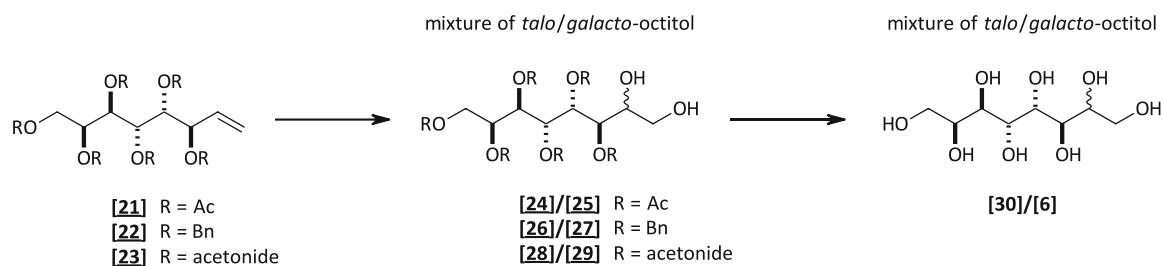
Synthesis of 3-bromopropenyl esters for the indium mediated acyloxyallylation



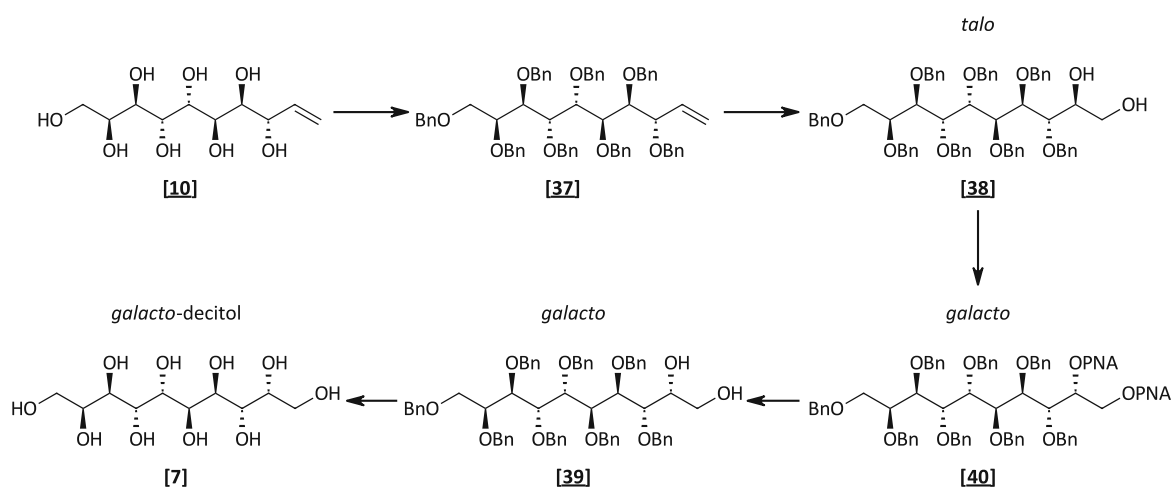
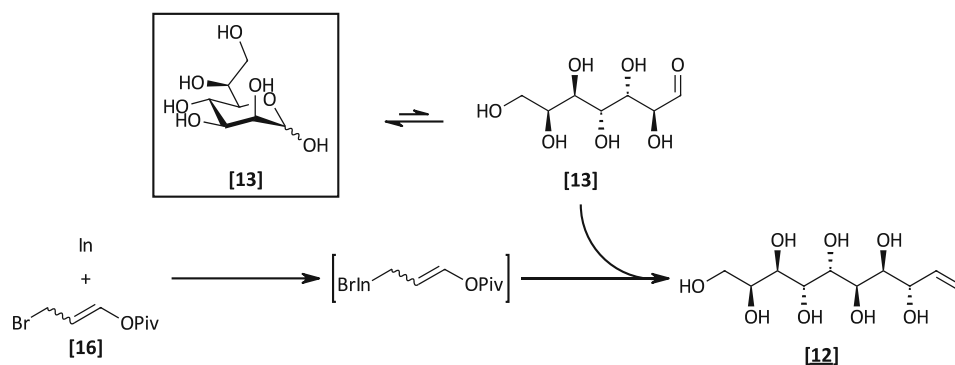
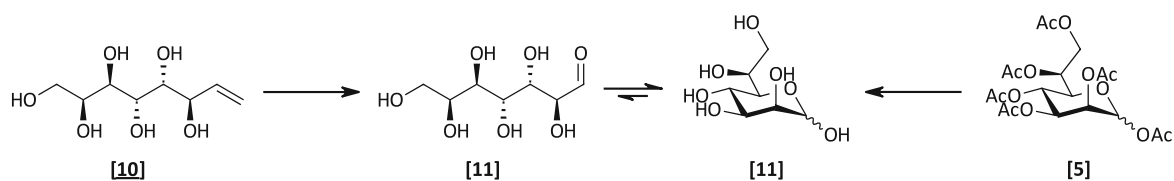
Synthesis of *L*-threo-*D*-galacto-octitolⁱ



ⁱ For clarity, the transformation is depicted with *L*-lyxose [3], although it was undertaken with the cheaper *D*-enantiomer [19], and [9] already available in the laboratory was used for the next steps.



Synthesis of L-galacto-L-galacto-decitol



Towards L-threo-D-galacto-D-galacto-dodecitol

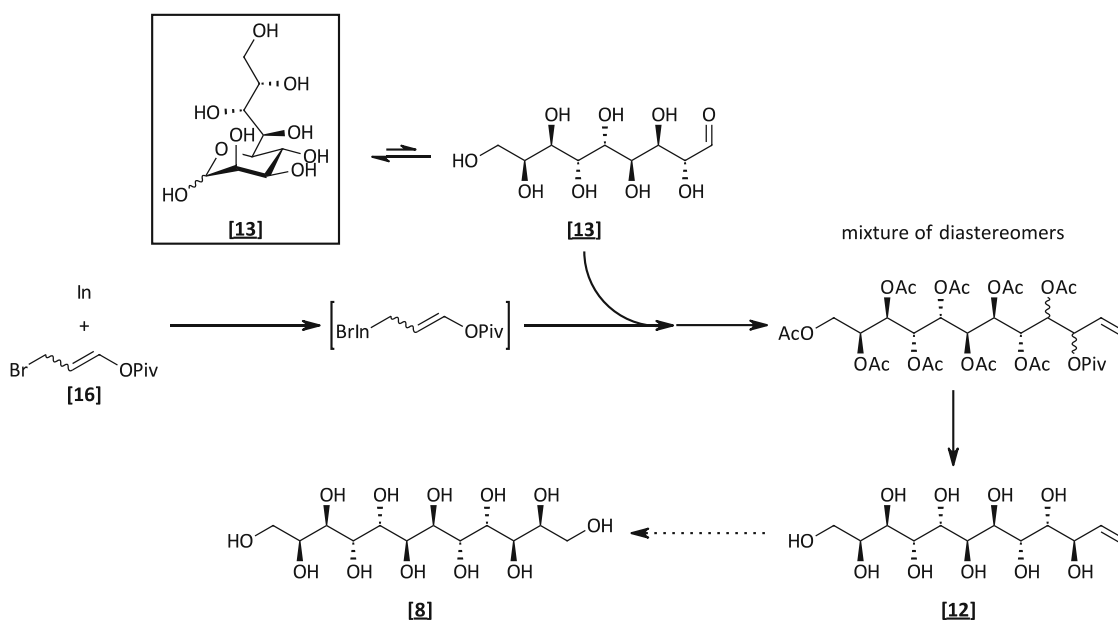
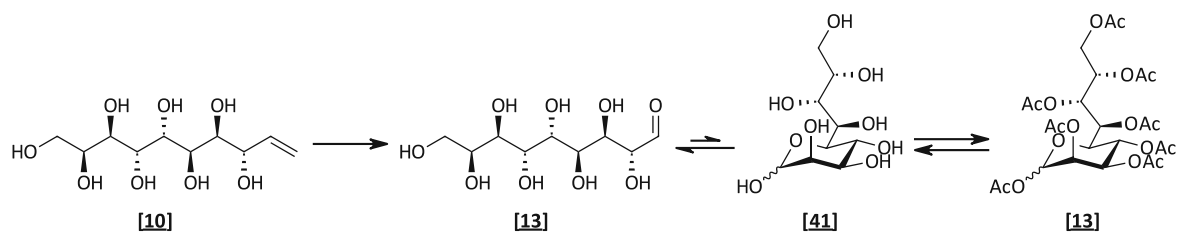


Table of content

ACKNOWLEDGEMENTS	I
GENERAL REMARKS	III
ABBREVIATIONS	V
ABSTRACT	VII
KURZFASSUNG	IX
GENERAL SCHEMES	XI
SYNTHESIS OF 3-BROMOPROPENYL ESTERS FOR THE INDIUM MEDIATED ACYLOXYALLYLATION.....	XI
SYNTHESIS OF L-THREO-D-GALACTO-OCTITOL.....	XI
SYNTHESIS OF L-GALACTO-L-GALACTO-DECTITOL.....	XIII
TOWARDS L-THREO-D-GALACTO-D-GALACTO-DODECITOL.....	XIV
TABLE OF CONTENT	XV
A INTRODUCTION	1
A 1 CARBOHYDRATES.....	1
A 1.1 Carbohydrates in general.....	1
A 1.2 Structure and classification of carbohydrates.....	1
A 1.2.1 Configurational isomers of monosaccharides.....	2
A 1.3 Nomenclature of higher aldoses.....	3
A 1.4 Ring-chain tautomerism of monosaccharides.....	3
A 1.4.1 Hemiacetal formation.....	3
A 1.4.2 Open-chain content of aldoses (OCC).....	4
A 1.5 Sugar alcohols and their applications.....	5
A 2 THE ELONGATION OF CARBOHYDRATES BY ADDITION TO THE ANOMERIC CENTRE.....	7
A 2.1 Addition of carbanions.....	7
A 2.1.1 The Kiliani ascension.....	7
A 2.1.2 The Baylis-Hillman reaction.....	8
A 2.2 Organometallic addition reactions.....	10
A 2.2.1 Elongation with organomagnesium and -lithium reagents.....	10
A 2.2.2 Tin- and indium-mediated allylation.....	11
A 2.2.3 Indium-mediated acyloxyallylation.....	12
A 3 THERMAL ENERGY STORAGE.....	17
A 3.1 Types of thermal energy storage systems.....	18
A 3.1.1 Sensible heat storage systems.....	19
A 3.1.2 Latent heat storage systems.....	19
A 3.1.3 Thermochemical heat storage systems.....	20

A 3.2	Comparison of SHS, LHS and TCS	20
A 4	PHASE CHANGE MATERIALS	21
A 4.1	Classification of PCMs	22
A 4.2	Inorganic phase change materials	23
A 4.2.1	Salts and salt hydrates.....	23
A 4.2.2	Metals and metal alloys	24
A 4.3	Organic phase change materials	25
A 4.3.1	Paraffin waxes	25
A 4.3.2	Nonparaffin organic PCMs.....	25
A 4.4	Non-natural sugar alcohols as potential PCMs.....	28
A 5	AIM OF THE THESIS.....	32
B	RESULTS AND DISCUSSION	35
B 1	RETROSYNTHETIC ANALYSIS	35
B 2	SYNTHESIS OF THE 3-BROMOPROPENYL ESTERS USED FOR IMA.....	37
B 3	THE SYNTHETIC ROUTE TOWARDS THE GALACTO-OCTITOL.....	38
B 3.1	Indium-mediated acyloxyallylation of lyxose towards the <i>glycero-manno</i> -octenitol	38
B 3.2	Introduction of protecting groups to the octenitol	39
B 3.2.1	Introduction of acetate groups to the octenitol.....	40
B 3.2.2	Introduction of benzyl groups to the octenitol	40
B 3.2.3	Synthesis of the 3,4:5,6:7,8- <i>O</i> -triisopropylidene-octenitol	41
B 3.3	Dihydroxylation of the protected octenitol	42
B 3.3.1	Evaluation and investigation of different dihydroxylation conditions	42
B 3.3.2	Results for the screening of substrates and reaction conditions	47
B 3.3.3	Dihydroxylation of the Bn-protected octenitol with high selectivity for the 2,3- <i>anti</i> -product	51
B 3.4	Inverting the stereochemistry <i>via</i> a Mitsunobu protocol.....	51
B 3.5	Deprotection towards the octitol	53
B 3.6	Purification of the enantiomeric mixture	54
B 3.7	Summary of the synthesis route towards the <i>L-threo-D-galacto</i> -octitol	55
B 4	SYNTHESIS OF GALACTO-DECITOL – APPLICATION OF THE DEVELOPED SYNTHETIC ROUTE.....	58
B 4.1	Preparation of <i>L-glycero-D-manno</i> -heptose <i>via</i> ozonolysis	58
B 4.2	Indium-mediated acyloxyallylation of <i>L-glycero-D-manno</i> -heptose towards the <i>manno</i> -decenitol	59
B 4.2.1	Performing the IMA using the Barbier-type protocol	60
B 4.2.2	A two-step Grignard protocol for the IMA	61
B 4.2.3	Synthesis of the <i>L-lyxo-L-manno</i> -decenitol	63
B 4.3	Protection and dihydroxylation of the <i>manno</i> -decenitol	64
B 4.4	Mitsunobu reaction and ester cleavage towards the octabenzyl- <i>galacto</i> - decitol	66

B 4.5	Deprotection towards the L- <i>galacto</i> -L- <i>galacto</i> -decitol.....	67
B 4.6	Summary of the synthesis route towards the L- <i>galacto</i> -L- <i>galacto</i> -decitol.....	69
B 5	FIRST STEPS TOWARDS THE GALACTO-DODECITOL	71
B 5.1	Preparation of L- <i>lyxo</i> -L- <i>manno</i> -nonose <i>via</i> ozonolysis	71
B 5.2	Indium-mediated acyloxyallylation of L- <i>lyxo</i> -L- <i>manno</i> -nonose towards the <i>manno</i> -dodecenitol	72
B 5.2.1	The open-chain contents of L- <i>glycero</i> -D- <i>manno</i> -heptose and L- <i>lyxo</i> -L- <i>manno</i> -nonose.....	74
B 5.2.2	Considerations on the low reactivity of the L- <i>lyxo</i> -L- <i>manno</i> -nonose in the performed IMA	75
B 6	PHYSICAL PROPERTIES OF MANNITOL, GALACTITOL AND GALACTO-OCTITOL	76
C	CONCLUSION AND OUTLOOK.....	81
D	EXPERIMENTAL PART.....	85
D 1	MATERIALS AND METHODS	85
D 2	SYNTHETIC PROCEDURES AND ANALYTICAL DATA.....	87
D 2.1	3-Bromoprop-1-en-1-yl acetate [1]	87
D 2.2	1,2-Dideoxy-D- <i>glycero</i> -L- <i>manno</i> -oct-1-enitol [20] – method A	89
D 2.3	1,2-Dideoxy-D- <i>glycero</i> -L- <i>manno</i> -dec-1-enitol [20] – method B.....	91
D 2.4	3,4,5,6,7,8-Hexa- <i>O</i> -acetyl-1,2-dideoxy-L- <i>glycero</i> -D- <i>manno</i> -oct-1- enitol [21].....	93
D 2.5	3,4,5,6,7,8-Hexa- <i>O</i> -benzyl-1,2-dideoxy-L- <i>glycero</i> -D- <i>manno</i> -oct-1- enitol [22].....	94
D 2.6	1,2-Dideoxy-3,4:5,6:7,8-tri- <i>O</i> -isopropylidene-D- <i>glycero</i> -L- <i>manno</i> -oct-1- enitol [23].....	96
D 2.7	Screening of octenitol substrates and dihydroxylation conditions, followed by deprotection to determine the ratio of the octitol isomers (¹³ C-NMR).....	97
D 2.7.1	Dihydroxylation of the protected octenitols [21], [22] and [23] on analytical scale.....	97
D 2.7.2	Deprotection of the semi-protected octitol mixtures [24]/[25], [26]/[27] and [28]/[29].....	98
D 2.7.3	Results of the substrate and method screening, including obtained yields and product ratios [6]/[30]	99
D 2.8	3,4,5,6,7,8-Hexa- <i>O</i> -benzyl-L- <i>threo</i> -D- <i>talo</i> octitol [26] – method A.....	100
D 2.9	3,4,5,6,7,8-Hexa- <i>O</i> -benzyl-L- <i>threo</i> -D- <i>talo</i> -octitol [26] – method B	101
D 2.10	3,4,5,6,7,8-Hexa- <i>O</i> -benzyl-1,2-di- <i>O</i> -(<i>p</i> -nitrobenzoyl)-L- <i>threo</i> -D- <i>galacto</i> - octitol [31].....	102
D 2.11	3,4,5,6,7,8-Hexa- <i>O</i> -benzyl-L- <i>threo</i> -D- <i>galacto</i> -octitol [27]	104
D 2.12	L- <i>Threo</i> -D- <i>galacto</i> -octitol [6] – method A	105
D 2.13	L- <i>Threo</i> -D- <i>galacto</i> -octitol [6] – method B	106

D 2.14	1,2,3,4,5,6,7,8-Octa- <i>O</i> -benzyl- <i>L</i> -threo- <i>D</i> -galacto-octitol [33] & 1,2,3,4,5,6,7,8-octa- <i>O</i> -benzyl- <i>L</i> -threo- <i>D</i> -talo-octitol [34]	107
D 2.15	3-Bromoprop-1-en-1-yl benzoate [2].....	109
D 2.16	3-Bromoprop-1-en-1-yl pivalate [16].....	111
D 2.17	<i>L</i> -Glycero- <i>D</i> -manno-heptose [11] – method A	113
D 2.18	<i>L</i> -Glycero- <i>D</i> -manno-heptose [11] – method B	114
D 2.19	1,2-Dideoxy- <i>L</i> -lyxo- <i>L</i> -manno-dec-1-enitol [10]	115
D 2.20	3,4,5,6,7,8,9,10-Octa- <i>O</i> -benzyl-1,2-dideoxy- <i>L</i> -lyxo- <i>L</i> -manno-dec-1- enitol [37].....	117
D 2.21	3,4,5,6,7,8,9,10-Octa- <i>O</i> -benzyl- <i>L</i> -galacto- <i>L</i> -talo-decitol [38]	119
D 2.22	3,4,5,6,7,8,9,10-Octa- <i>O</i> -benzyl-1,2-di- <i>O</i> -(<i>p</i> -nitrobenzoyl)- <i>L</i> -galacto- <i>L</i> - galacto-decitol [40].....	121
D 2.23	3,4,5,6,7,8,9,10-Octa- <i>O</i> -benzyl- <i>L</i> -galacto- <i>L</i> -galacto-decitol [39]	123
D 2.24	<i>L</i> -Galacto- <i>L</i> -galacto-decitol [7]	125
D 2.25	<i>L</i> -Lyxo- <i>L</i> -manno-nonose [13] – method A	126
D 2.26	<i>L</i> -Lyxo- <i>L</i> -manno-nonose [13] – method B	128
D 2.27	<i>L</i> -Lyxo- <i>L</i> -manno-nonose octaacetate [41]	129
D 2.28	1,2-Dideoxy- <i>L</i> -glycero- <i>D</i> -manno- <i>D</i> -manno-dodecenitol [12]	131
D 2.29	General procedure for the ABAO assay used for the determination of the OCC of <i>L</i> -glycero- <i>D</i> -manno-heptose [11] and <i>L</i> -lyxo- <i>L</i> -manno-nonose [13]..	133
E	APPENDIX	135
E 1	CURRICULUM VITAE.....	135
E 2	REFERENCES	137

A Introduction

A 1 Carbohydrates

A 1.1 Carbohydrates in general

Polyhydroxy alcohols with a straight chain of carbon atoms, a carbonyl functionality, and at least three carbon atoms are known as monosaccharides and are the building blocks of all carbohydrates.¹ The name "carbohydrates" originates from earlier times when chemists assumed that carbohydrates are hydrates of the element carbon due to their general molecular formula $C_n(H_2O)_n$. Later research on their structure showed that this is not correct, but the term remained unchanged.² Besides polyhydroxy aldehydes and ketones with the formula $C_n(H_2O)_n$, also closely related molecules and oligomers or polymers of these structures are indicated as carbohydrates.³

A 1.2 Structure and classification of carbohydrates

Monosaccharides are classified according to their number of carbon atoms and whether their carbonyl functionality is an aldehyde or keto group. Aldoses is the term for monosaccharides with an aldehyde function, ketoses for those with a keto function. The classification by their number of carbon atoms is the following: trioses (3), tetroses (4), pentoses (5), hexoses (6), heptoses (7), etc. (Figure 1).¹

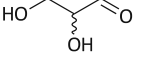
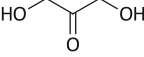
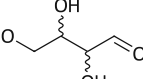
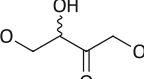
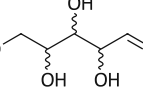
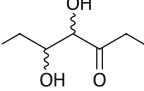
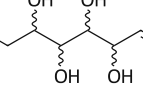
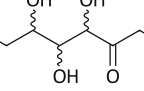
	Aldoses	Ketoses
Trioses		
Tetroses		
Pentoses		
Hexoses		

Figure 1. Classification of monosaccharides

The carbon atoms along the chain are all chiral, except the terminal ones and those that carry the carbonyl group. In the Fischer projection, the configuration of monosaccharides can be easily determined. If the hydroxy group at the chiral centre that is furthest away from the carbonyl functionality points to the right, the sugar is in the D-configuration. If it is to the left, the sugar is in the L-form (Figure 2).¹

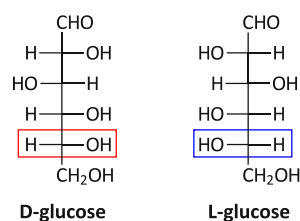


Figure 2. D- and L-form of the monosaccharide glucose, a pair of enantiomers (Fischer projection)

A 1.2.1 Configurational isomers of monosaccharides

Next to the already mentioned enantiomers, further configurational isomers of monosaccharides include diastereomers, epimers, and anomers.

- **Enantiomers** are stereoisomers that are mirror images, like the D- and L-form when it comes to sugars. An enantiomeric pair shows the same physical properties except for the rotation direction of plane-polarised light.
- **Diastereomers** are stereoisomers that are not mirror images. For sugars, the two hexoses D-glucose and D-altrose are diastereomers, for example. Diastereomers possess different physical properties (e.g. boiling point, refractive index, etc.).
- **Epimers** are a special form of diastereomeric sugars that differ in only one chiral centre, e.g. D-glucose and D-galactose.
- **Anomers** are a special form of diastereomers when it comes to sugars in the hemiacetal/-ketal form (see Chapter A 1.4.1). Two anomeric sugars only differ in the configuration around the anomeric carbon atom, meaning that α -D-glucopyranose and β -D-glucopyranose are called anomers.²

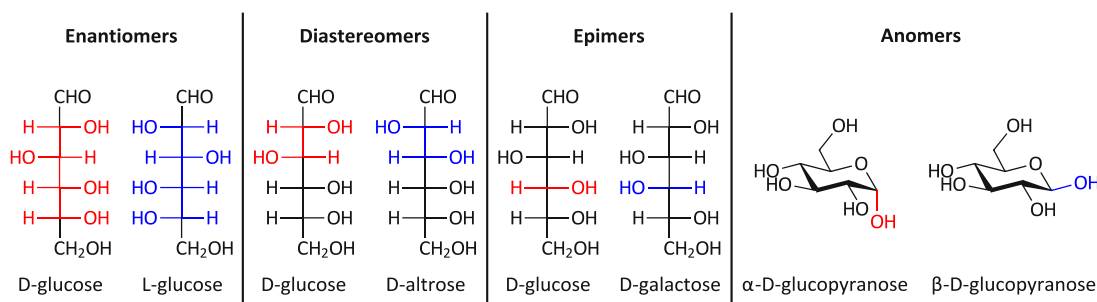


Figure 3. Configurational isomers of monosaccharides

A 1.3 Nomenclature of higher aldoses

Up to six carbon atoms, monosaccharides have trivial names (e.g. D-glucose) that are preferred over systematic names (*D-manno*-hexose). When it comes to aldoses that contain more than four chiral centres (heptoses, octoses, etc.), their names are generated by adding two or more configurational prefixes to the stem name. The carbon sugar is divided into groups of up to four chiral centres starting from the chiral centre proximal to C-1. Then the prefixes for the groups are assigned, and the name is built by putting the prefix of the group that is farthest from C-1 first. This group may contain less than four carbon atoms.⁴ Two examples for the nomenclature of higher aldoses are shown in Figure 4.

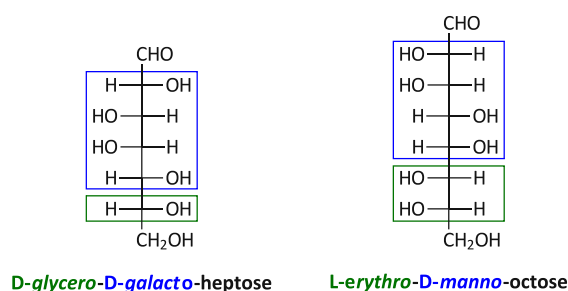


Figure 4. Nomenclature of higher aldoses that are shown in the Fischer projection

A 1.4 Ring-chain tautomerism of monosaccharides

A 1.4.1 Hemiacetal formation

The hydroxy groups of monosaccharides can react intramolecularly with the aldehyde or keto group to form cyclic hemiacetals or hemiketals. A six-membered ring (pyranose) or a five-membered ring (furanose) is formed, whereby pyranoses are thermodynamically more stable. With this cyclisation, a new chiral centre is formed at the so-called anomeric carbon atom. The two different diastereomers are called the α - or β -anomer (Figure 5).⁴ These anomeric prefixes, α and β , refer to the relative configuration at the anomeric centre to the asymmetric carbon atom of the compound. In the Fischer projection, if the anomeric and the reference carbon atom have the same configuration, the anomer is designated α .⁵

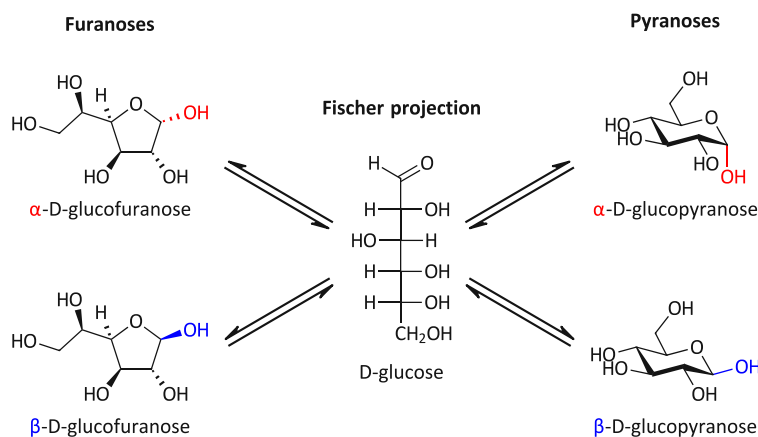


Figure 5. Cyclic forms of D-glucose

In solution, the open-chain and cyclic structures are in chemical equilibrium. When α -D-glucose, for example, is dissolved in water, it is mainly present in the cyclic pyranose form, and the concentration of the acyclic form is relatively low. However, as the hemiacetal formation is reversible, the cyclic form can react back to the open-chain form, and the anomeric β -D-glucopyranose can be formed. This back-and-forth reaction can lead to a substance-specific equilibrium, and the reaction that leads to this equilibrium is called mutarotation.³

A 1.4.2 Open-chain content of aldoses (OCC)

As already mentioned, aldoses are predominantly present in the cyclic hemiacetal form, but this cyclic form is in equilibrium with the open-chain aldehyde. The percentage of the acyclic form present in an aqueous solution of a sugar is known as the open-chain content (OCC).⁶⁻⁷ This value plays a significant role in understanding the differing reactivities of aldoses as aldehydes and their stability.⁸ If the availability of the open-chain form with the aldehyde functionality is low, reactions that occur at the aldehyde moiety of the sugar will be slower. In order to this, by considering the OCC, the different reactivity of various aldoses in some reactions can be partially explained.

The following Table 1 shows the OCCs of selected treoses, pentoses and hexoses determined by ^{13}C -NMR spectroscopy where the C-1 of the aldose was selectively ^{13}C -labelled^{6,9-10} (left column) and by a kinetic photometric assay⁷ (right column). The latter one is a fast, new method for open-chain aldose quantification that has been developed in our group, in which the adduct formation of the aldose with 2-amniobenzamidoxime (ABAO) is followed *via* photometric measurements due to the UV-absorption of the formed adducts.⁷

Table 1. OCC values of selected aldoses determined by ^{13}C -NMR spectroscopy and a kinetic photometric assay (ABAO assay)⁷

Entry	Name	OCC (%) ^{6,9-10} (^{13}C -NMR)	OCC (%) ⁷ (ABAO assay)
1	L-erythrose	12.0-12.5	12.5
2	D-threose	10.6-12.0	11.7
3	D-lyxose	0.097	0.11
4	D-xylose	0.071	0.072
5	D-galactose	0.052	0.054
6	D-glucose	0.099	0.010
7	D-mannose	0.026	0.032

A 1.5 Sugar alcohols and their applications

The products from the reduction of reducing sugars are polyols that contain a straight carbon chain where each carbon atom has a hydroxy group as a substituent. Generally, the classification of sugar alcohols is done according to the number of hydroxy groups as tetritols, pentitols, hexitols, heptitols, etc. Alditol is a term that is used for polyols that are obtained from aldoses. Due to the reduction, the two ends of the carbon chain of some aldoses are made identical, and the resulting sugar alcohols only exist in one form (no D- and L-form anymore), the mesoform, as they possess an internal symmetry plane.³ Meso compounds are achiral molecules even though they contain asymmetric carbon atoms because the molecule as a whole is symmetrical.¹¹ In the history of monosaccharides, sugar alcohols played an essential role in the determination of the configuration of sugars that was achieved by Emil Fischer and co-workers in the late 19th century.¹²⁻¹³ The two pentitols xylitol and L-arabitol could be distinguished due to their optical rotation, as xylitol did not show rotation and a small negative rotation was observed for arabinitol after the addition of borax. The same observations were made for the corresponding trihydroxyglutaric acids that show higher values compared to sugar alcohols, in general. From this, Fischer concluded that xylitol is a molecule that possesses a symmetry plane (meso compound) which was a further proof on his way to the determination of configurational relationships in monosaccharides.¹²

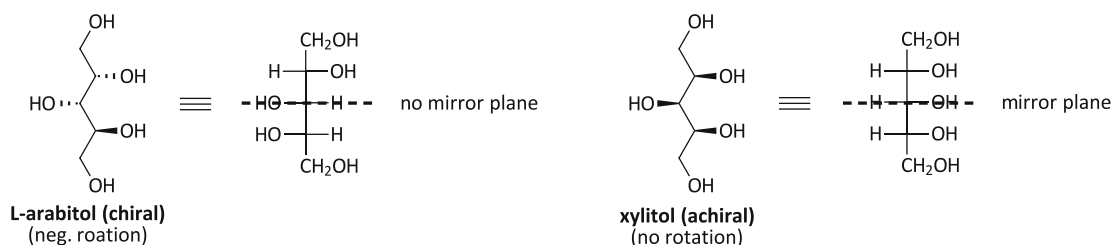
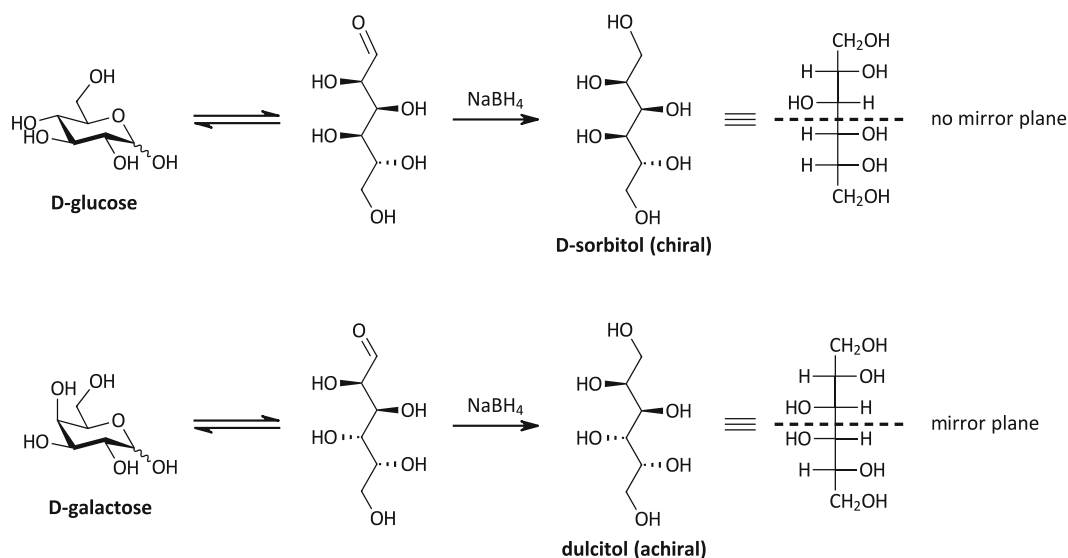


Figure 6. The pentitols L-arabitol and xylitol – a proof for the correlation between configuration and optical activity

Nowadays, sugar alcohols, especially hexitols and their derivatives, are of high interest for different fields like the food industry, pharmaceuticals, cosmetic, etc. In foods, sugar alcohols can be used to replace sugar as they are sweet too but less harmful to the human body due to properties like insulin-independent metabolism, no contribution to the development of dental caries, and lower caloric values. For pharmaceuticals, they play an essential role as bases for tablets as they provide a sweet taste, can easily be dissolved, and further mask the unpleasant taste of some drugs.¹⁴

In the last couple of years, sugar alcohols got more attraction in the field of phase change materials (PCMs) for thermal energy storage applications. This interest arises from their physical properties as high latent heat of fusion compared to other known organic phase change materials and melting points in a region that is suitable for their application in thermal energy storage of waste heat or solar energy.¹⁵ Among sugar alcohols, erythritol¹⁶⁻¹⁸, D-mannitol^{15-17,19-20}, and *myo*-inositol^{15,20} (cyclic sugar alcohol) received the most attention and were studied intensively. The application and potential of sugar alcohols as PCMs will be discussed later on in Chapter A 4.3.2.4 and A 4.4.

On industrial scale, commercial sugar alcohols like sorbitol, mannitol, and xylitol are manufactured by catalytic hydrogenation of the corresponding reducing sugar using a Raney nickel catalyst. In general, the reduction of the carbonyl group of aldoses can also be performed with reducing agents like NaBH₄ (lab scale) (Scheme 1).¹⁴



Scheme 1. Reduction of D-glucose and D-galactose to the corresponding sugar alcohols with NaBH₄

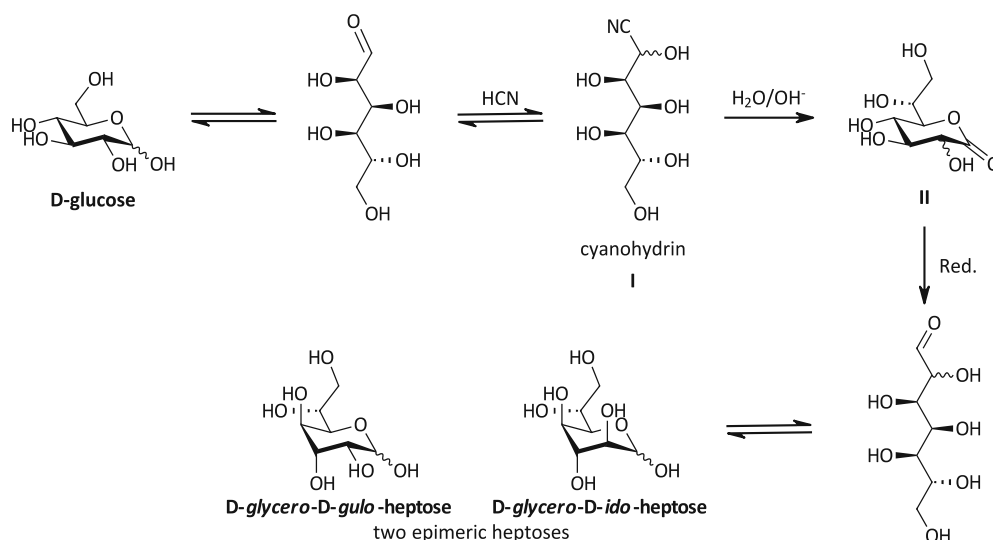
A 2 The elongation of carbohydrates by addition to the anomeric centre

Within this chapter, different methods for the elongation of carbohydrates, more precisely reducing monosaccharides, by addition to the carbonyl moiety are presented, broadening the synthetic scope of carbohydrates. The biggest challenge in the formation of new C–C bonds at the anomeric centre is the control of diastereoselectivity, as it depends on the nature of the aldehyde and used nucleophile. Further, most of the transformations require protection of the sugar, making the synthesis of higher sugar species more complex and elaborate.²¹ With the use of organoindium species as elongation reagents, that have been intensely investigated for reducing sugars in the last couple of years²²⁻²⁴, a method was developed allowing the use of completely unprotected carbohydrates as substrates. One of those methods is the indium-mediated acyloxyallylation, short IMA, which is a useful tool for the synthesis of higher, non-natural sugar species, as it allows the direct elongation of aldoses by three carbon atoms with control of the diastereoselectivity. As this thesis deals with the synthesis of non-natural sugar alcohols, a more in-depth look is taken into the strength of these methods but also its limitation and challenges.

A 2.1 Addition of carbanions

A 2.1.1 The Kiliani ascension

The elongation of the carbon chain in carbohydrates by the addition of hydrogen cyanide is known as the Kiliani ascension.²⁵ This elongation reaction is one of the longest-known reactions in carbohydrate chemistry.²¹ In Scheme 2, the Kiliani ascension of the aldose D-glucose is shown. In the first step, the cyanide performs a nucleophilic attack at the carbonyl carbon, giving a cyanohydrin **I** as the intermediate that is elongated by one carbon atom compared to the starting material. Upon hydrolysis, the corresponding aldonic acid is formed that immediately cyclises to form the lactone **II**. Final reduction leads to two epimeric heptoses. So, the product of the Kiliani ascension is an aldose that was extended by one carbon atom.²⁶

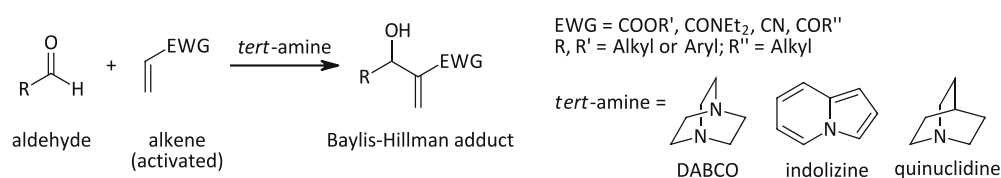


Scheme 2. Kiliani ascension of D-glucose, a reducing sugar, to achieve elongation by one carbon towards two epimeric heptoses

As already mentioned, the reaction gives two epimeric heptoses due to the nucleophilic attack of the cyanide at the aldehyde function that can occur from two sides. The nature of the cyanide cannot be adapted. Therefore, the selectivity relies on the substrate but also the experimental conditions giving rise to the *2,3-threo*- and *2,3-erythro*-configured sugars in ratios varying from 70:30 to 28:72 (*threo/erythro*). The separation of the two epimers can be achieved by fractional crystallisation of derivatives, such as alkaloid salts or phenylhydrazones, in the lactone form. Nevertheless, the Kiliani ascension is a quite useful reaction to elongate a reducing sugar by one carbon that can easily be performed, as no protection of the carbohydrate species is necessary. Further, this method is an easy tool when it comes to ^{13}C - and ^{14}C -labelled derivatives, as the prices of the used reagents are reasonable and make it affordable.²⁶

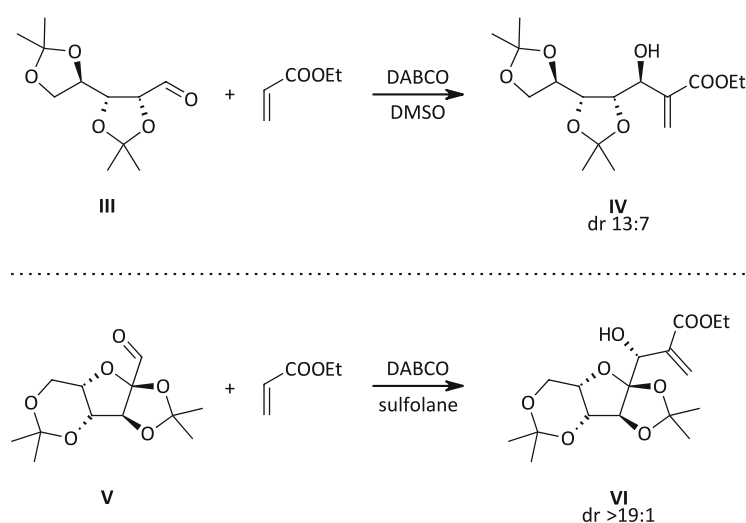
A 2.1.2 The Baylis-Hillman reaction

The Baylis-Hillman reaction was first published by Baylis and Hillman in 1972 in a German patent.²⁷ They described a reaction of activated alkenes (α,β -unsaturated esters, amides, nitriles, and ketones) with aldehydes, catalysed by tertiary bicyclic amines (DABCO, indolizine, or quinuclidine), as it is shown in Scheme 3.²⁸



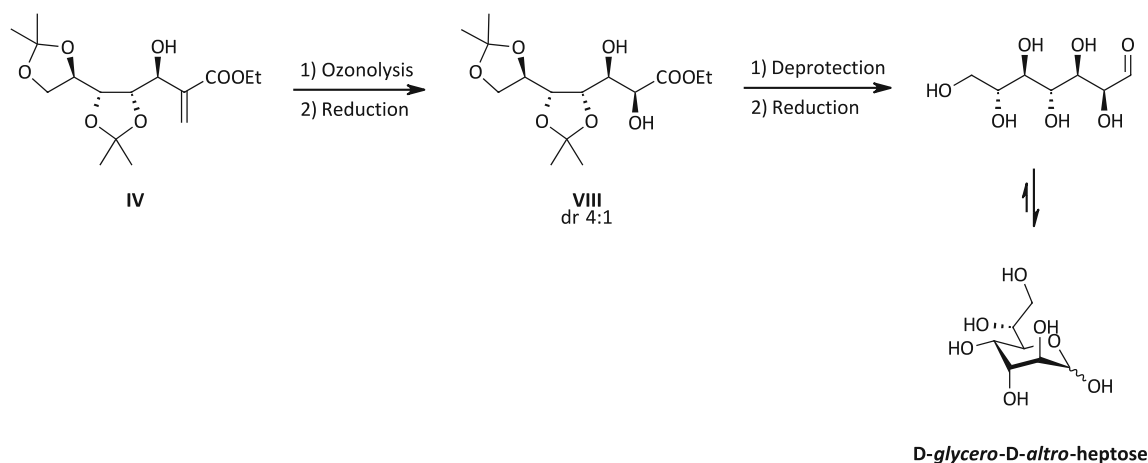
Scheme 3. Original patent information of the Baylis-Hillman reaction

For aldoses, this reaction can be used to elongate the carbon chain by two carbon atoms in a synthesis sequence with only a few steps. Typically, the reaction is performed with DABCO as a catalyst in either DMSO or a dioxane/water mixture. As the aldehyde derives from an aldose that is a chiral molecule, substance controlled stereoselectivity is observed in the addition of the olefin.²¹ The aldehyde **III** shown in Scheme 4a, that can be obtained in three steps from 2,3-*O*-isopropylidene-*D*-ribose, was treated with ethyl acrylate under standard conditions yielding in two addition products **IV** (epimers) in a ratio of 13 : 7 (Scheme 4 (top)).²⁹ The extension of this reaction to other aldehydes with different protecting groups, that included a solvent change, showed cleaner conversion and faster rates. Under these conditions, ethyl acrylate was added to the aldose **V** with steric more hindering protecting groups. The stereoselectivity was boosted significantly, giving almost only one of the two epimers as the product **VI** (Scheme 4 (bottom)).³⁰



Scheme 4. Two examples for the Baylis-Hillman reaction of sugar-derived aldehydes

Upon ozonolysis followed by reduction with NaBH_4 the terminal olefin in the adduct **IV** can be converted into a hydroxy group. This reaction shows substrate controlled diastereoselectivity, too, and compound **VIII** with a 2,3-*syn(threo)*-relationship can be obtained as the major product. Further deprotection of the hydroxy groups and conversion of the ester to an aldehyde gives the *L-glycero-D-altro*-heptose that is elongated by two carbon atoms compared to the starting material (Scheme 5).²⁹



Scheme 5. Reaction of the Baylis-Hillman adduct **IV** to the sugar derivative **VIII** and the corresponding unprotected aldose *L-glycero-D-altro-heptose*

Strictly speaking, the Baylis-Hillman reaction does not include an attack of the nucleophile at an anomeric centre, as only acyclic sugar derived aldehydes³⁰ can be used as a substrate. In general, this protocol for the synthesis of higher-carbon sugars is quite circumstantial as it includes many steps, mostly due to the necessity of manipulating the sugar species prior to the actual elongation reaction.

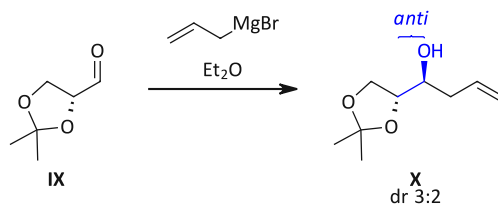
A 2.2 Organometallic addition reactions

Organometallic addition reactions are generally a useful tool to elongate the carbon chain of reducing sugars, allowing the synthesis of higher-carbon sugars.²⁶ Depending on the used organometallic species and applied reaction conditions, either fully protected carbohydrate aldehydes or carbohydrate hemiacetals in the unprotected or semi-protected form are feasible as the substrate. Due to the addition of an organometallic reagent to the aldehyde moiety, a new chiral centre is formed. The stereochemical outcome of the reaction depends on whether chelation is possible or not and further on the nature of the chelating species. Nonetheless, sometimes it is difficult to predict if either the *anti*-addition (*erythro*) or *syn*-addition (*threo*) product is favoured as the stereoselectivity is a result of the used organometallic species, the carbohydrate substrate, and the reaction conditions.²¹

A 2.2.1 Elongation with organomagnesium and -lithium reagents

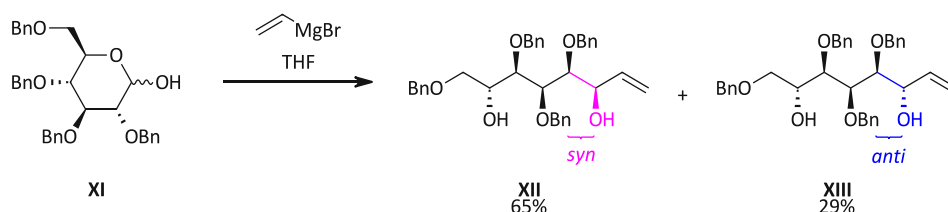
In general, organomagnesium and -lithium reagents require anhydrous reaction conditions as they are sensitive to hydrolysis and therefore, aprotic solvents as, e.g., ether or THF as well as substrates are necessary. Because of this, only protected or at least partially protected sugars can be used as a substrate, also due to solubility issues in the required solvents. When it comes to the stereochemical outcome, studies on the simplest open-chain saccharide 2,3-*O*-isopropylidene-*D*-glyceraldehyde **IX** showed that with organomagnesium and to a lesser extent -lithium reagents the *anti(erythro)*-configured

product **X** is moderately favoured over the *syn(threo)*-configured one.^{26, 31} This stereoselectivity is shown in the following Scheme 6.



Scheme 6. Elongation of the simple open-chain saccharide 2,3-*O*-isopropylidene-*D*-glyceraldehyde (IX) with an organomagnesium reagent; the *anti(erythro)*-configured product **X** is favoured

However, for the more complex carbohydrate 2,3,4,6-tetra-*O*-benzyl-*D*-glucopyranose (XI), the addition of vinylmagnesium bromide was studied by Cumpstey, et al.³², where reversed diastereoselectivity was obtained compared to the example in Scheme 6. Under standard Grignard conditions using THF as a solvent, the *syn*-addition product **XII** was formed as the major isomer with a yield of 65% and the *anti*-addition product **XIII** as the minor one with 29% yield (Scheme 7).



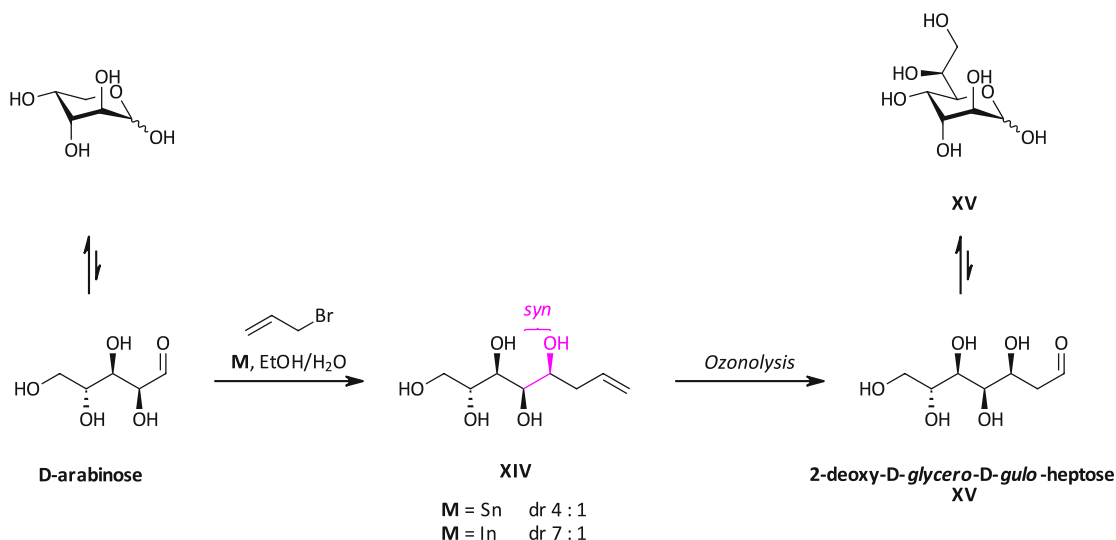
Scheme 7. Addition of vinylmagnesium bromide to the partially protected hemiacetal carbohydrate 2,3,4,6-tetra-*O*-benzyl-*D*-glucopyranose **XI** with diastereoselectivity for the *syn(threo)*-configured product **XII**

Generally, the lithium cation is not as effective in the formation of chelating species as magnesium, leading to only modest diastereoselectivity in the addition of organolithium reagents to sugars. Further, the stereochemical outcome depends less on the reaction conditions and more on the structure of the substrate.^{21,26}

A 2.2.2 Tin- and indium-mediated allylation

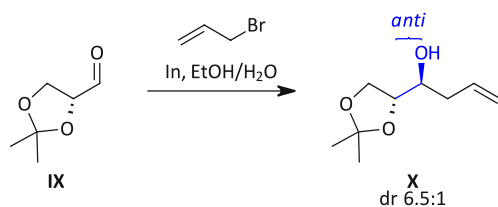
In contrast to "classical" organometallic addition reactions, allylations with indium and tin allow the use of water or alcohols as a solvent. Consequently, no full protection of the aldose hemiacetal or aldehyde is required.³³⁻³⁴ Already in early attempts, stereoselectivity was obtained in the tin-mediated allylation of aldoses (e.g. *D*-erythrose, *D*-arabinose, *D*-glucose) in which the *syn(threo)*-configured diastereomer (in respect to the formed hydroxy group and the hydroxy group in α -position to the aldehyde moiety of the starting aldose) was formed as the major product.³³ It was further shown that this diastereoselectivity was also achieved using indium instead of tin as the metal, but a change in the *threo/erythro*-ratio could be obtained.³⁴⁻³⁵ This is shown in Scheme 8 for the

unprotected pentose D-arabinose as an example, giving the enitol **XIV**.³⁴ The corresponding 2-deoxy sugar **XV** can be obtained by subsequent ozonolysis.



Scheme 8. Tin- and indium-mediated allylation of unprotected D-arabinose with diastereoselectivity for the *threo*-isomer **XIV** but different *threo/erythro*-ratios depending on the used metal

In contrast, the In-mediated allylation of aldoses, where the hydroxy groups next to the aldehyde moiety are protected (e.g. (*R*)-2,3-*O*-isopropylidene glyceraldehyde), gives the *erythro*-product as the major diastereomer.³⁶ This is shown for the (*R*)-2,3-*O*-isopropylidene glyceraldehyde **IX** in the following Scheme 9 and the diastereodivergent behaviour is in line with the chelation versus non-chelation mode explained before, giving the *anti*-product **X** as the major one.



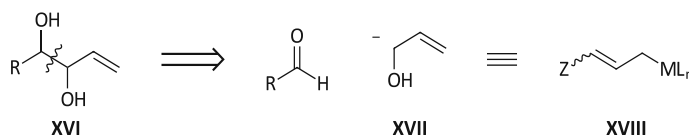
Scheme 9. In-mediated allylation of a protected aldose **IX** with diastereoselectivity for the *anti(erythro)*-isomer **X**

A 2.2.3 Indium-mediated acyloxyallylation

A 2.2.3.1 A new reagent Class and methodology

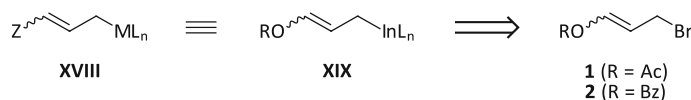
As already mentioned, the chain elongation of aldoses with allyl halides and subsequent ozonolysis of the allylation product yields 2-deoxy sugars. To get towards an elongated *normal* sugar, a different reagent is required to result in the allylation product of an alken-1-ne-3,4-diol. The retrosynthetic analysis of an alken-3,4-diol **XVI** (Scheme 10) gives synthon **XVII**, representing a 1-hydroxyallyl anion. Synthetic equivalents for this species are

3-substituted allylic organometallic reagents **XVIII**, but most of these reagents require a 2-step protocol (lithiation, then transmetallation) for preparation and anhydrous conditions.³⁷ This makes them unusable in the elongation of unprotected sugars as aqueous conditions are required for the solubility of the sugars.



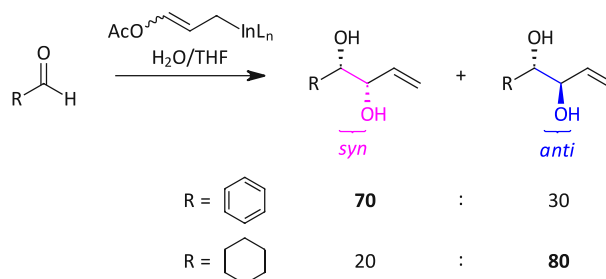
Scheme 10. Retrosynthetic analysis of an alk-1-ene-3,4-diol **XVI** giving an aldehyde and a 1-hydroxyallyl anion synthon **XVII**; the latter one can be attributed to a 3-substituted allylic organometallic compound **XVIII**

A more practical protocol was shown by Lombardo, et al.³⁸, where the organometallic species **XVIII** is obtained by oxidative addition of indium or zinc to the carbon-halogen bond of a 3-heterosubstituted allyl bromide, like, e.g., 3-bromopropenyl acetate **[1]** or the corresponding benzoate **[2]**.³⁹ This new class of organometallic reagents tolerates a wide range of experimental parameters, such as the use of protic solvents³⁸ that are required in the acyloxyallylation of reducing sugars.



Scheme 11. Analysis of the organometal species **XVIII** that can be generated from the corresponding 3-bromopropenyl ester⁴⁰

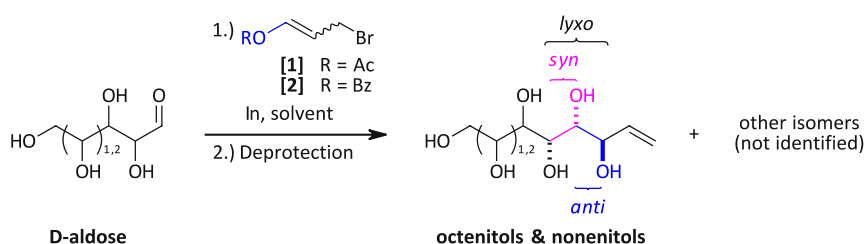
This reagent **[1]** was first used in the acyloxyallylation of simple achiral aldehydes where diastereodivergence was obtained depending on whether the aldehyde species is saturated or unsaturated. In the case of aromatic aldehydes, the product with the two newly formed hydroxy groups in an *anti*-relationship was found to be the major one. The opposite diastereoselectivity was observed for aliphatic, saturated aldehydes formed the *syn*-product preferentially.³⁸ Notably, the diastereoselectivity of the addition refers to other stereocentres compared to the simpler additions described before.



Scheme 12. Diastereoselectivity in the indium-mediated acyloxyallylation under aqueous conditions of simple aldehydes; the stereochemical outcome depends on the nature of the carbonyl compound

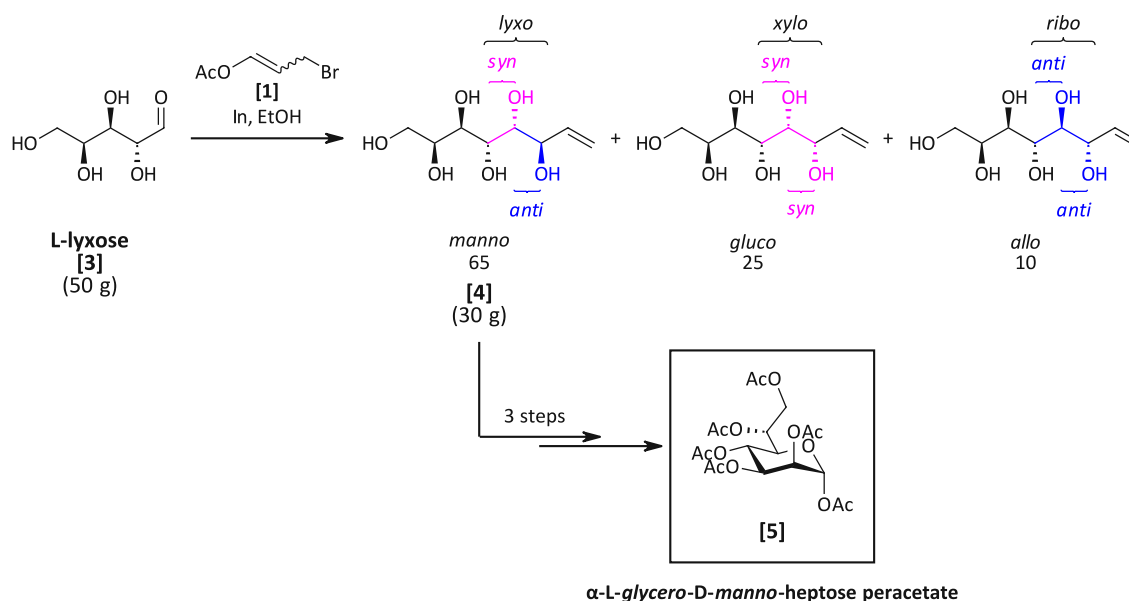
A 2.2.3.2 The implementation in carbohydrate chemistry

This new reagent class and methodology was then first introduced into carbohydrate chemistry by Palmelund and Madsen²². Their extensive proof of concept study investigated the acetic acid **[1]** and benzoic acid esters **[2]** of the reagent species for the indium-mediated elongation of several aldoses ultimately obtaining the two carbon atoms elongated heptoses and octoses *via* subsequent ozonolysis. It was shown that independent of the aldose that was used as starting material the product with *lyxo*-configuration at the reducing end was favourably formed. *Lyxo*-configuration means that the hydroxy group derived from the aldehyde functionality and the α -hydroxy group are in a *syn*-relationship (consistent with chelation) while the two new formed stereocentres are *anti* (Scheme 13) as found in Lombardo's study for saturated aldehydes.



Scheme 13. Study of the indium-mediated acyloxyallylation of aldoses with diastereomeric divergence to the *lyxo*-configured product

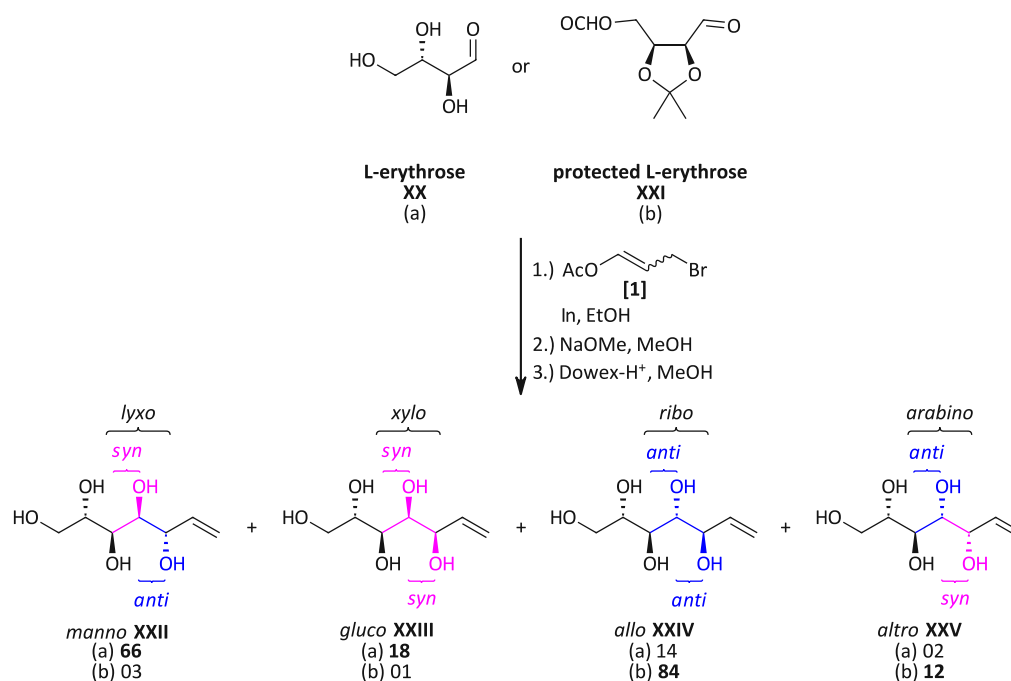
The other isomers formed in these reactions, as four diastereomers are possible in theory, were not identified within this study. This was then further investigated by Stanetty and Baxendale²³ who developed a short and scalable process for the synthesis of *L-glycero-D-manno*-heptose, an important bacterial sugar, based on the proof of concept study by Palmelund and Madsen²². Within this, they also elucidated the stereochemistry of the other formed isomers and found the following ratio of the products formed in the acyloxyallylation of *L*-lyxose **[3]** using 3-bromopropenyl acetate **[1]** as the reagent: *lyxo* (65%) > *xylo* (25%) > *ribo* (10%).



Scheme 14. Large scale synthesis of L-glycero-D-manno-heptose, a bacterial sugar, isolated as the crystalline peracetate [5], via indium-mediated acyloxyallylation of L-lyxose [3]

A 2.2.3.3 In-depth methodological study of the IMA of sugars

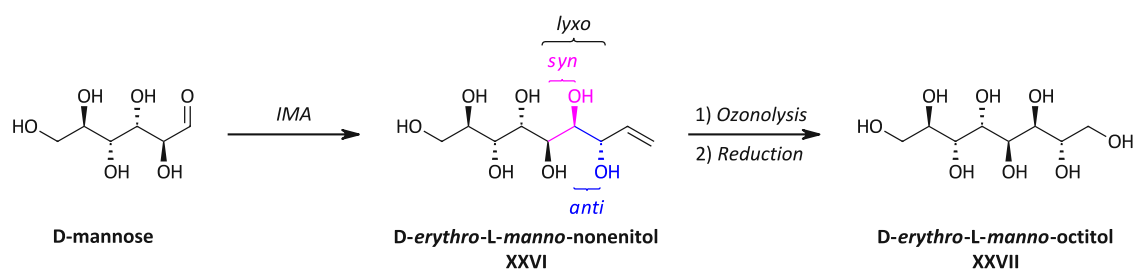
An in-depth methodological study of the indium-mediated acyloxyallylation of protected and unprotected aldotetroses was then presented by Draskovits, et al.²⁴ in which the diastereoselectivity was further investigated utilising protected and unprotected tetroses and furnishing the following results: In the unprotected case, the *lyxo*-configured product **XXII** (*syn/anti*) was obtained as the major one as expected from the earlier described acyloxyallylations of sugars by Palmelund and Madsen²² and Stanetty and Baxendale²³. The stereochemistry of the second major isomer **XXIII** was consistently found to be *xylo* (*syn/syn*), so a high degree of selectivity (85–95%) for the *si*-face (*syn*-selectivity) was obtained in the attack at the aldehyde functionality. The two minor isomers that result from a *re*-face attack are the *ribo*(*anti/anti*)- and *arabino*(*anti/syn*)-configured ones **XXIV** and **XXV**, the latter in only minute amounts. For the two new formed stereocentres, *anti*-relationship was the favoured configuration for both cases, as expected. For the protected tetroses also high facial diastereoselectivity was obtained, but for the *re*-face (*anti*-selectivity) with the *ribo*- and *arabino*-configured isomers as the major products (> 90%).²⁴ The following Scheme 15 shows the formed products and obtained ratios for the indium-mediated acyloxyallylation of the treose L-erythrose in the unprotected **XXI** and protected case **XXII**. A switch from "chelation model" versus addition following classical Cram-model was hypothesised to be the reason for the observed diastereodivergence.



Scheme 15. Product ratios in the indium-mediated acyloxyallylations of protected L-erythrose **XXII** and unprotected L-erythrose **XXI** with 3-bromopropenyl acetate **[1]**²⁴

A 2.2.3.4 Application of the IMA as a tool for the synthesis of non-natural sugar alcohols

To sum up, In-mediated acyloxyallylation is a useful tool for the elongation of reducing sugars. With 3-heterosubstituted allyl halides as the reagent, sugar enitols with a carbon chain extended by three carbon atoms are obtained in good selectivity for the *lyxo*-addition. Those can be converted into the corresponding aldoses by subsequent ozonolysis giving rise to sugars with two more carbon atoms. Further, this protocol has been investigated briefly to synthesise the non-natural sugar alcohol *D-erythro-L-manno*-octitol **XXVII** that was obtained *via* an ozonolysis protocol with reductive work-up from the corresponding *D-glycero-D-galacto*-nonenitol **XXVI**, as it is shown in Scheme 16.



Scheme 16. IMA of *D*-mannose and subsequent ozonolysis with reductive work-up of the obtained nonenitol **XXVI** towards the *D-erythro-L-manno*-octitol **XXVII**, a non-natural sugar alcohol

Compared to the pentose lyxose, *D*-mannose showed less reactivity in the IMA under the conditions displayed in Scheme 14 and Scheme 15 as it has been expected due to properties like lower solubility and also a lower open-chain content (see Chapter A 1.4.2).

A 3 Thermal energy storage

In the last decades, energy storage has become more and more important, especially when it comes to the success of any intermittent energy source.⁴¹ Currently, the interest in renewable energy sources is growing enormously due to the arising shortage of fossil fuels and the environmental damages caused by them such as global warming, air pollution, etc.⁴² A considerable problem in the field of renewable energy technologies is the irregular diurnal availability of energy. For example, solar power is not available at all times and, therefore, daily, weekly, and seasonal storage is of great interest to help offset this mismatch between the supply and demand of energy.^{41,43} There are many different methods of how energy can be stored, the three most important classes being mechanical, chemical, and thermal energy storage (TES). Mechanical energy storage includes, for example, pumped hydro systems, compressed-air energy storage systems, and flywheels, while batteries are an example for chemical energy storage systems. The major difference between these types is that mechanical and chemical energy storage are only applicable to electrical energy while thermal energy storage systems allow the storage energy before it is converted to electricity. This makes TES very attractive for the storage of solar energy or summer heat, for example.⁴¹ Economically, thermal energy storage systems can be beneficial as heat or cold electrically generated during off-peak hours can be stored and energy costs can be reduced, as off-peak electricity tariffs are cheaper. Also, the efficiency of energy use is increased, and the load on the electricity grid is more evenly distributed. The advantage of increased energy efficiency and reduced costs makes TES even an attractive technology for the industrial and commercial sectors. Additionally, the use of TES is beneficial for the environment by providing the chance of using waste heat and climatic energy resources instead of fossil fuels as energy sources.⁴¹ To sum up, the implementation of storage in an energy system promises many benefits, better economics, better efficiency, less environmental pollution and CO₂ emissions, and improved system performance and reliability being the most important ones.⁴⁴

Basically, the term thermal energy storage (TES) describes the capture and storage of thermal energy by cooling, heating, melting, solidifying, or vaporising a material for later use.^{41,43} A complete storage cycle involves three steps, namely charging, storing and discharging (Figure 7)⁴⁴, where the discharge process is the reversion of the charge process.⁴¹

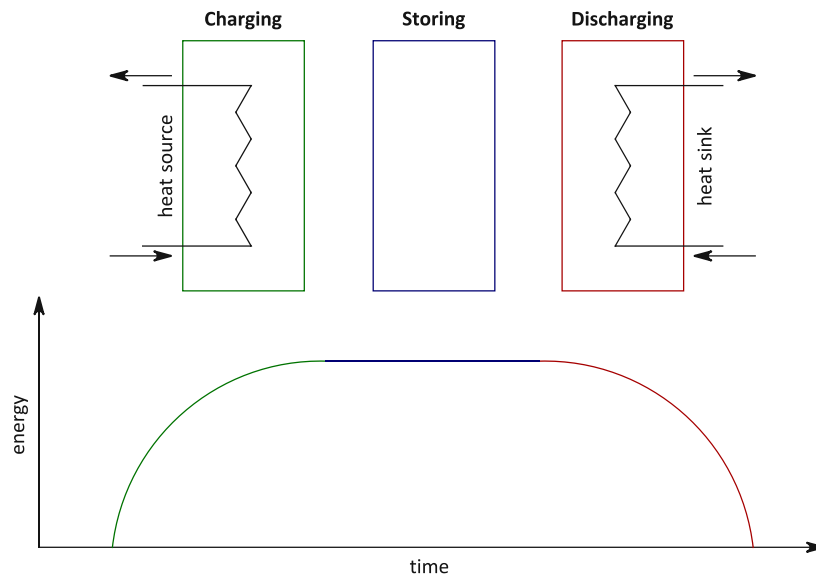


Figure 7. Working cycle of a TES system, showing the three main steps and the variation of stored energy over time (adapted from Dincer and Rosen⁴¹ and Fredi, et al.⁴⁵)

A 3.1 Types of thermal energy storage systems

There are different principles how thermal energy can be stored. In general, TES methods can use the physical or chemical change of a system providing three kinds of TES systems, namely sensible heat storage (SHS), latent heat storage (LHS) associated with phase change materials (PCM), and thermochemical storage (TCS) by chemical reactions (Figure 8).

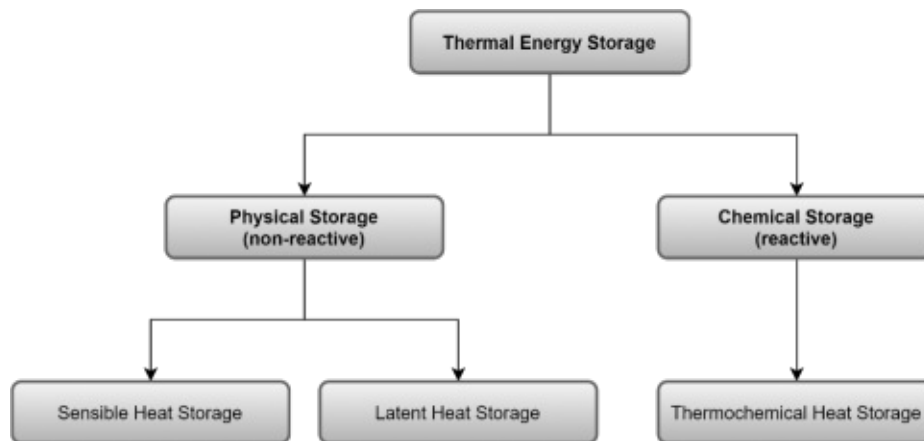


Figure 8. Classification of TES systems

A 3.1.1 Sensible heat storage systems

In sensible heat storage (SHS) systems, thermal heat is stored by heating or cooling of a storage medium that can be a liquid or solid.⁴⁶⁻⁴⁸ Commonly used storage media are rocks, ground or water, probably the oldest and most popular one.⁴¹ The choice of the material depends on its effectiveness evaluated by the specific heat and the space available for storage.⁴⁴

The amount of thermal energy that can be stored by an SHS medium is calculated by the following Equation 1, in which Q is the amount of stored thermal energy (J), m the mass of the storage medium (kg), c_p its specific heat ($\text{J kg}^{-1} \text{K}^{-1}$), T_i the initial temperature (K) and T_f the final temperature (K).

$$Q = \int_{T_i}^{T_f} m c_p dT \quad \text{Equation 1}$$

The most significant advantage of SHS is that the most commonly used storage media are cheap and non-toxic.⁴⁶ However, the energy density of sensible heat storage materials is low (11.7 kWh/m³ for a 10 °C change of water⁴⁹), which means big volumes are required to store large amounts of energy. Further, thermal energy loss at any temperature is a problem.⁵⁰

A 3.1.2 Latent heat storage systems

In latent heat storage systems, the phase transition of a material, either solid-liquid, liquid-gas or solid-solid, is used to store thermal energy. For example, by providing thermal energy, the material melts and stores the transferred heat that is released again when it solidifies. Materials that are used as LHS systems are called phase change materials (PCMs).^{41,44} The selection of a PCM is primarily made according to the required melting enthalpy and melting temperature and further based on its availability and costs.⁴⁴ The different types of PCMs and their thermal properties are further discussed in Chapter A 4 as the non-natural sugar alcohols presented within this thesis are potential PCMs.

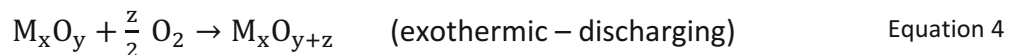
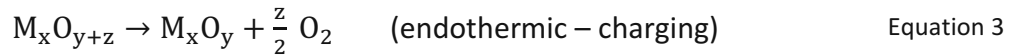
The amount of thermal energy that can be stored by an LHS medium is calculated by the following Equation 2, in which Q is the amount of stored thermal energy (J), m the mass of the storage medium (kg), T_i the initial temperature (K), T_m the melting temperature (K), T_f the final temperature (K), f the melt fraction and Δq the latent heat of fusion (J/kg).

$$Q = \int_{T_i}^{T_m} m c_p dT + m f \Delta q + \int_{T_m}^{T_f} m c_p dT \quad \text{Equation 2}$$

Compared to SHS, LHS is more efficient due to the higher energy storage density routed in the additional phase transition.⁵⁰ For example, the paraffin *n*-docosane possesses a latent heat of 194.6 kJ/kg that corresponds to an energy density of 42.4 kWh/m³ in the melting process.⁴⁹

A 3.1.3 Thermochemical heat storage systems

Thermochemical heat storage systems use reversible endothermic/exothermic reaction processes to store and release thermal energy.⁴⁶ In an endothermic reaction, the system takes heat up (charging process), that can be released in the reversed, exothermic reaction (discharging process).⁵¹ Suitable chemical reactions are, for example, decarboxylation reactions of metal carbonates, dehydration reactions of salt hydrates or metal hydrates, and redox reactions with metal oxides.⁵² The reduction (Equation 3) and oxidation of a metal oxide (Equation 4) are shown below.



In addition to chemical reactions, sorption systems can also be used to store heat. In the sorption process, the desorption of a gas or a liquid from a solid material or a liquid is the charging process of the storage cycle, and the stored heat is released upon adsorption (discharging process). Adsorbents that are commonly used as storage media are zeolites and silica gels.⁴⁴

Thermochemical storage systems provide the highest values for energy density compared to SHS and LHS, making it of great interest for TES. For example, the energy storage density of the sorption system water–LiCl is approximately 253 kWh/m³. The hydration reactions of MgSO₄ and Na₂S possess even higher values of up to 780 kWh/m³.⁴⁹ However, there are some problems with TCS like stability issues and degradation over time that need to be overcome to make TCS a usable tool.⁵⁰

A 3.2 Comparison of SHS, LHS and TCS

The following Figure 9 sums up the principles of the three types of thermal energy storage discussed in the earlier chapters A 3.1.1, A 3.1.2 and A 3.1.3.

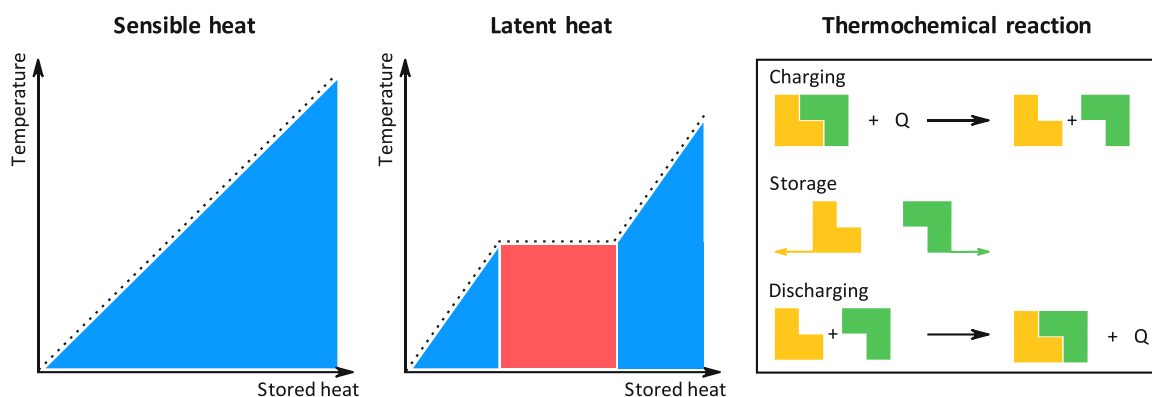


Figure 9. Methods of thermal energy storage (adapted from de Gracia and Cabeza⁵³)

The three different types of TES systems differ in characteristics like, for example, capacity, power, efficiency, and storage time. Especially, the storage time of a TES system is essential

when choosing a suitable storage technique depending on the energy source. The following Table 2 displays the named parameters of the three different types of TES systems. In general, any storage system should possess high energy storage density and also high power capacity.⁴⁶

Table 2. Comparison of the thermal energy storage systems⁴⁶

TES system	Capacity (kWh/t)	Power (MW)	Efficiency (%)	Storage time
Hot water (sensible)	10-50	0.001-10	50-90	day / year
PCM (latent)	50-150	0.001-1	75-90	hour / week
Chemical reactions	120-250	0.01-1	75-100	hour / day

A 4 Phase change materials

Of the three present types of thermal energy storage systems, latent heat storage systems, known as phase change materials (PCMs), are discussed in more detail within this chapter as the non-natural sugar alcohols presented in this thesis are potential materials within this class.

In general, PCMs are materials that store latent heat by undergoing a phase transition. Possible phase changes for energy storage are liquid-solid, liquid-gas, and solid-solid, but solid-liquid and solid-solid phase transitions are the most commonly occurring ones.⁵⁰ A solid PCM exposed to heat first absorbs energy, causing a rise of its temperature until the phase transition temperature (melting point) is reached. Then, the phase transition occurs at a constant temperature or in a narrow temperature range where a lot of energy is consumed. After the melting process, again, a temperature rise of the storage material can be obtained.⁴² This process is shown in the following Figure 10.

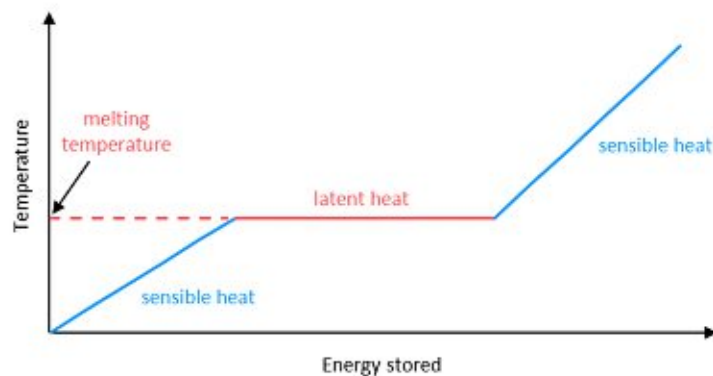


Figure 10. Temperature profile of the solid-liquid phase transition of a PCM

The latent heat stored by the PCM upon melting is then released during the solidification process.⁵⁴ In a closed system and under the assumption that no thermal energy is lost, the amount of energy released in the crystallisation process equals the absorbed energy. The

transferred energy in the melting-solidification cycle is determined by the latent heat of fusion of the material. The values for a material's latent heat of fusion are usually given in units of kJ/kg.⁵⁵

A 4.1 Classification of PCMs

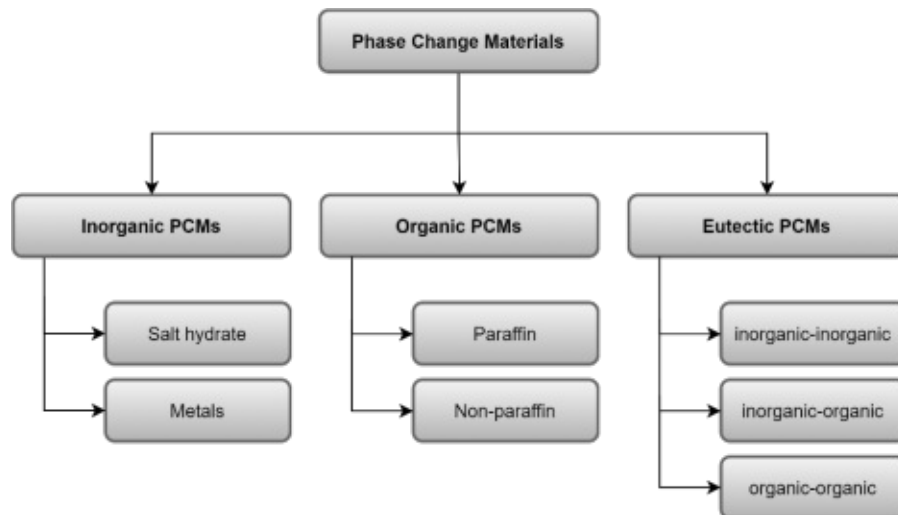


Figure 11. Classification of PCMs into inorganic, organic and eutectic

In general, PCMs are classified in inorganic, organic and eutectic PCMs, which can be mixtures of organic or inorganic compounds, or both. Organic PCMs are divided further into paraffins and non-paraffins (poly(ethylene glycol)s, fatty acids, polyalcohols etc.), inorganic PCMs into salts and metals.

Figure 12 shows the different substance classes currently known as PCMs and their melting energy (kJ/L) and melting temperature ranges (°C). In general, it can be seen here that the volumetric latent heat storage capacity of inorganic materials is significantly higher than of organic ones.⁵⁶ While the used organic materials generally show melting points below 200 °C and relatively low melting energies, inorganic salts are found in the range above 200 °C⁵⁷ with melting points up to 1000 °C.⁵⁸ More values of different physical properties of some PCM-types summarised by Peng, et al.⁵⁹ are shown in Table 3.

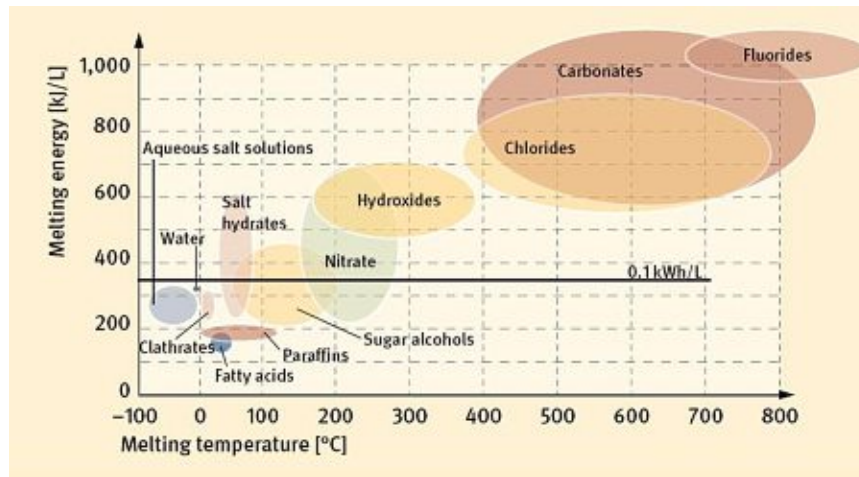


Figure 12. Different PCM-classes according to their melting energy (kJ/L) and melting temperature (°C)⁶⁰

Table 3. Physical properties of some PCMs⁵⁹

Material type	Transition	Approx. Temp. range (°C)	Latent heat (kJ/L)	Latent heat (kJ/kg)	Conductivity (W m ⁻¹ K ⁻¹)
Paraffin	S–L (dry)	–12-71	128-197	145-260	~ 0.2
Metallics	S–L (dry)	30-125	200-800	20-80	10-50
Polyalcohols	S–S (dry)	24-89	144-212	140-200	0.17-0.22
Nonparaffin organics	S–L (wet)	–13-178	131-438	80-280	~ 0.2
Salt hydrates	S–L (wet)	28-137	270-650	120-300	0.2-0.5

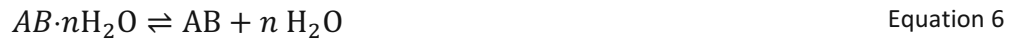
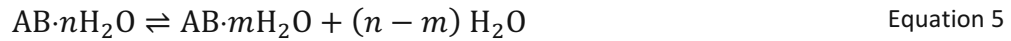
A 4.2 Inorganic phase change materials

A 4.2.1 Salts and salt hydrates

Molten salts and salt hydrates are both inorganic PCMs but have different applications due to their different temperature zones. Generally, molten salts are used in the medium to high temperature range as they possess melting temperatures of up to 1000 °C. Hydrated salts have lower phase change temperatures usually below 220 °C.⁵⁸

Molten salts used as PCMs are mainly metal nitrates, sulfates, carbonates, chlorides, and eutectic mixtures of them. As already mentioned, they are chosen for their high melting temperature and further for their relatively large thermal energy storage capacity.⁶¹

Salt hydrates can generally be described with the formula $A_xB_y \cdot n(H_2O)$.⁴² The solid-liquid transformation of these salts means that during the melting process crystallisation water is desorbed. At the same time, heat is absorbed, which leads to the formation of a salt hydrate with fewer moles of water (Equation 5) or the anhydrous salt (Equation 6). By cooling down, the inorganic salt and water recombine again, and the stored heat is released.^{46, 61}



Salt hydrates are suitable as PCMs because they have a fixed melting point, high latent heat storage density, and relatively high thermal conductivity (compared to organic PCMs). Furthermore, they show only small volume change during phase transition, are only slightly corrosive, compatible with plastics, and inexpensive. However, there are two major disadvantages: undercooling and incongruent melting.^{46, 61-62} As incongruent melting is an irreversible process, the storage efficiency is reduced significantly.⁵⁷ Undercooling is problematic as the temperature of the phase change is shifted.⁶³

Examples of salts and salt hydrates used as PCMs and their thermal properties are shown in Table 4.

Table 4. Thermal properties of salts and salt hydrates with potential use as PCMs^{42,64-65}

Salt / Salt hydrate	Melting temperature (°C)	Heat of fusion (kJ/kg)
LiNO ₃	250	370
KClO ₄	527	1253
MgCl ₂	714	452
Ba(OH) ₂ ·8H ₂ O	78	266
Mg(NO ₃) ₂ ·6H ₂ O	89.3	150
CaCl ₂ ·6H ₂ O	28	174

A 4.2.2 Metals and metal alloys

Some metals and their alloys have potential as PCMs, especially for high temperature latent heat storage because of their higher melting temperatures compared to salt hydrates and other materials used for LHS. Furthermore, the main advantages of metallic PCMs are their features of high thermal conductivity and high heat of fusion per unit volume. However, the latent heat of fusion per unit weight of metals is relatively low, and the metallic storage media are expensive.^{46, 61}

Examples for metals that have the potential to be used as PCMs are Al, Zn, Si, Cu etc., and their alloys like Al-Si alloy, Cu-Si alloy, etc.⁶¹ In Table 5, the thermal properties of some metals and alloys are shown.

Table 5. Thermal properties of metals and alloys used as PCMs⁶¹

Metal or alloy	Melting temperature (°C)	Heat of fusion (kJ/kg)
Al (Al (60 wt%)/Al ₂ O ₃ (40 wt%))	655.1	149.2
Al-Si (75:25 wt%)	576	429
Cu-Si (80:20 wt%)	802	352.2

A 4.3 Organic phase change materials

Organic materials that have been investigated as potential PCMs in the last couple of years cover a wide range, and many of them were found to have suitable melting temperature and high latent heat of fusions. In general, the classes of paraffins, fatty acids and their esters, and polyalcohol species have drawn main attention among perspective organic PCMs and are therefore further discussed within this chapter.

A 4.3.1 Paraffin waxes

Generally, the term paraffin is used for alkanes (C_nH_{2n+2}) with 14 – 40 carbon atoms⁶⁶ that possess melting points in the range of 5 – 75 °C⁵⁶. Commercial paraffin waxes are mixtures of different straight-chain *n*-alkanes.⁶⁴ The melting point and latent heat of fusion depend on the chain length and increase with the number of carbon atoms.^{46,67}

Paraffin PCMs have the advantages of being non-toxic, non-corrosive, non-hygroscopic and cheap as they are by-products of petroleum refining. Furthermore, owing to their chemical stability, no degradation occurs due to repeated phase transition cycles.⁵⁴ In contrast to inorganic salt hydrate PCMs, paraffins show good nucleating properties (no undercooling) and congruent melting, as well as little volume changes on melting. Drawbacks are that their thermal conductivity is low, they are not compatible with plastic containments and are moderately flammable.⁵⁶

Some selected paraffins with different numbers of carbon atoms and their physical properties are shown in Table 6. The latent heat of fusion of paraffins is generally in the range of 200 – 300 kJ/kg⁶⁸, and their melting points occur at approximately 5 – 75 °C⁵⁶.

Table 6. Thermal properties of paraffins with potential use as PCMs⁶²

Paraffin	Melting temperature (°C)	Heat of fusion (kJ/kg)
<i>n</i> -Tetradecane (C ₁₄)	6	228
<i>n</i> -Pentadecane (C ₁₅)	10	205
<i>n</i> -Hexadecane (C ₁₆)	18	237
<i>n</i> -Eicosane (C ₂₀)	37	246
<i>n</i> -Triacontane (C ₃₀)	66	251

A 4.3.2 Nonparaffin organic PCMs

A 4.3.2.1 Poly(ethylene glycol)s

Poly(ethylene glycol)s, short PEGs, are chains of linear dimethyl ether groups with terminal hydroxy groups. Their general formula is $HO-CH_2-(CH_2-O-CH_2-)_n-CH_2-OH$.⁶⁹

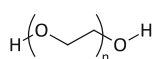


Figure 13. General structure of poly(ethylene glycol)s

PEGs are useful as PCMs because of their high heat of fusion, relatively broad and moderate melting temperature range, high thermal and chemical stability, and low vapour pressure. Furthermore, PEGs are non-flammable, biodegradable, non-toxic and inexpensive.⁶⁹⁻⁷⁰ On the other side, long PEG chains show supercooling during the melting process. The melting temperature and latent heat capacity of PEGs increase with the molecular weight of the PEG chain. Therefore, their thermal properties can be further adjusted by mixing PEGs of different molecular weights.⁶⁹

The thermal properties of some PEGs with different molecular weights are shown in the following Table 7.

Table 7. Thermal properties of PEGs with different MWs⁶⁹

Molecular weight (g/mol)	Melting temperature (°C)	Heat of fusion (kJ/kg)
400	3.2	91.4
2000	51.0	181.4
20000	68.7	187.8

The heat of fusion of poly(ethylene glycols) is approximately in the range of 90 – 190 kJ/kg⁶⁹, which are relatively low values compared to other organic PCMs.

A 4.3.2.2 Fatty acids and derivatives

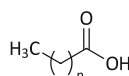


Figure 14. General structure of a saturated fatty acid

Fatty acids with the general formula $\text{CH}_3(\text{CH}_2)_{2n}\text{COOH}$ are of animal or plant origin, thus of renewable origin but currently more expensive than paraffin waxes.⁶² However, their properties make them suitable for PCM applications. Fatty acids possess high latent heat and show congruent melting. Furthermore, little or no supercooling occurs during the phase change, and thousands of melting and freezing cycles can be performed without thermal degradation. Some other superior properties of fatty acids are good thermal and chemical stability, non-toxicity and biodegradability, and their melting temperatures in a suitable range for the application in TES systems. Eutectic mixtures of fatty acids can be prepared to adjust the phase transition temperature interval for the desired application and increase the TES capacity. As fatty acids have some disadvantages like corrosivity, bad odour, and high sublimation rate, ester derivatives were prepared as a new material class of organic PCMs.⁶⁹ For example, the methyl esters of stearic and palmitic acid were studied by Nikolić, et al.⁷¹, showing high values of the enthalpy of melting/fusion reversible process with stability in a large number of cycles.

In Table 8 some fatty acids and their ester derivatives are shown together with their thermal properties.

Table 8. Thermal properties of some fatty acids and derivatives^{69,71}

Fatty acid or derivative	Melting temperature (°C)	Heat of fusion (kJ/kg)
Lauric acid (12 C)	41-44	178-183
Stearic acid (18 C)	65-70	196-253
Methyl stearate (C18)	37.8	240
Methyl palmitate (C16)	29.0	215

A 4.3.2.3 Polyalcohols and derivatives

Polyalcohols are PCMs that undergo a solid-solid transition where thermal energy in the form of latent heat is stored. At low temperatures polyalcohols like pentaerythrol (PE), pentaglycerine (PG) and neopentyl glycol (NPG) are heterogenous or amorphous but become homogeneous face-centred crystals when the temperature rises to their solid-solid phase change temperature.⁷² This phase transition gives polyalcohols the ability to absorb or release a large amount of heat and makes them attractive as organic PCMs. In addition to their high latent heat capacity above 100 kJ/kg⁷³, polyalcohols possess advantageous properties such as small volume change in the phase change, no segregation or phase separation, low temperatures of phase transition and no leakage above the melting temperature when it is, for example, microencapsulated.⁶⁴

The chemical structures of some polyalcohols are shown in Figure 15 and their thermal properties are given in Table 9.

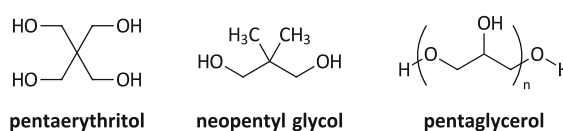


Figure 15. Structures of some polyalcohols used as PCMs

Table 9. Thermal properties of some polyalcohols as solid-solid PCMs⁶⁴

Polyalcohol	Phase transition temperature (°C)	Heat of phase transition (kJ/kg)
Pentaerythritol	185-187	289.0-339.5
Pentaglycerol	82	172.6
Neopentyl glycol	42-44	110.4-119.1

A 4.3.2.4 Sugar alcohols

Sugar alcohols (SAs) as a subclass of polyalcohols are not as intensively studied as the already presented organic PCMs but are potential candidates to serve as PCMs due to their high phase change enthalpy. Their melting point range is suitable for medium temperature application (100-200 °C)¹⁷ in, for example, solar process heat.¹⁵ Further advantages of SAs are that they are from natural origin, non-toxic, non-flammable, non-corrosive and affordable. Compared to other organic PCMs such as paraffins and fatty acids, sugar

alcohols provide a higher volumetric energy density that is in the range of the energy provided by salt hydrates.¹⁷ The most studied SAs for PCM application is erythritol with a melting temperature of 118 °C and latent heat of 340 kJ/kg. Erythritol also shows excellent thermal stability but undergoes severe undercooling as several other SAs.⁷⁴ Other sugar alcohols that have been considered as PCMs are xylitol and D-mannitol as they also show large latent heat but are also easy to handle.¹⁵

In Table 10, the thermal properties of the already mentioned sugar alcohols are shown.

Table 10. Examples for sugar alcohols used as PCMs and their thermal properties⁷⁴

Sugar Alcohol	Melting temperature (°C)	Heat of fusion (kJ/kg)
Erythritol	118	324
Xylitol	94.3	239.3
D-Mannitol	166.1	318.3

Natural sugar alcohols and mixtures possess latent heats of fusion in the range of approximately 200 – 350 kJ/kg¹⁷, which are considered as relatively high values for organic PCMs. An even higher potential as PCMs is expected for non-natural sugar alcohols with a longer carbon backbone chain as such a trend is, for example, observed for paraffins. In this context, a recent computational study by Inagaki and Ishida⁷⁵ predicted thermal storage densities of up to 450 – 500 kJ/kg for sugar alcohols with twelve carbon atoms and separately distributed hydroxy groups.

A 4.4 Non-natural sugar alcohols as potential PCMs

As already mentioned, Inagaki and Ishida⁷⁵ published a computational study in which the thermal storage densities and melting points of modelled sugar alcohols with more than six carbon atoms were predicted by molecular dynamics simulations. The design of these non-natural sugar alcohols was done following three guidelines, that were found to have a positive impact on the thermal properties (melting point, latent heat of fusion) according to an earlier theoretical study, in which the origin of differences in the enthalpy of fusion of the four natural hexitols galactitol, mannitol, sorbitol and iditol was investigated:⁷⁶

- (1) Linear elongation of the carbon backbone
- (2) 1,3-*anti*-Relationship of all hydroxy groups
- (3) Even number of carbon atoms in the carbon backbone

Following these rules, a series of non-natural sugar alcohols was designed that we refer to as the "*manno-series*", as it originated from the natural D-mannitol **XXIV**. Further, the thermal storage densities of the designed molecules were calculated and are shown in Figure 16. Compared to the best performing, existing organic PCMs, that possess thermal storage densities of up to 350 kJ/kg (red, dashed line in Figure 16), for all the investigated non-natural sugar alcohols higher values and therefore better potential performance as a PCM were observed within this study. According to the performed calculations,

outstanding thermal properties are expected for the presented C12 sugar alcohol **XXX** with thermal storage density of up to 450–500 kJ/kg.

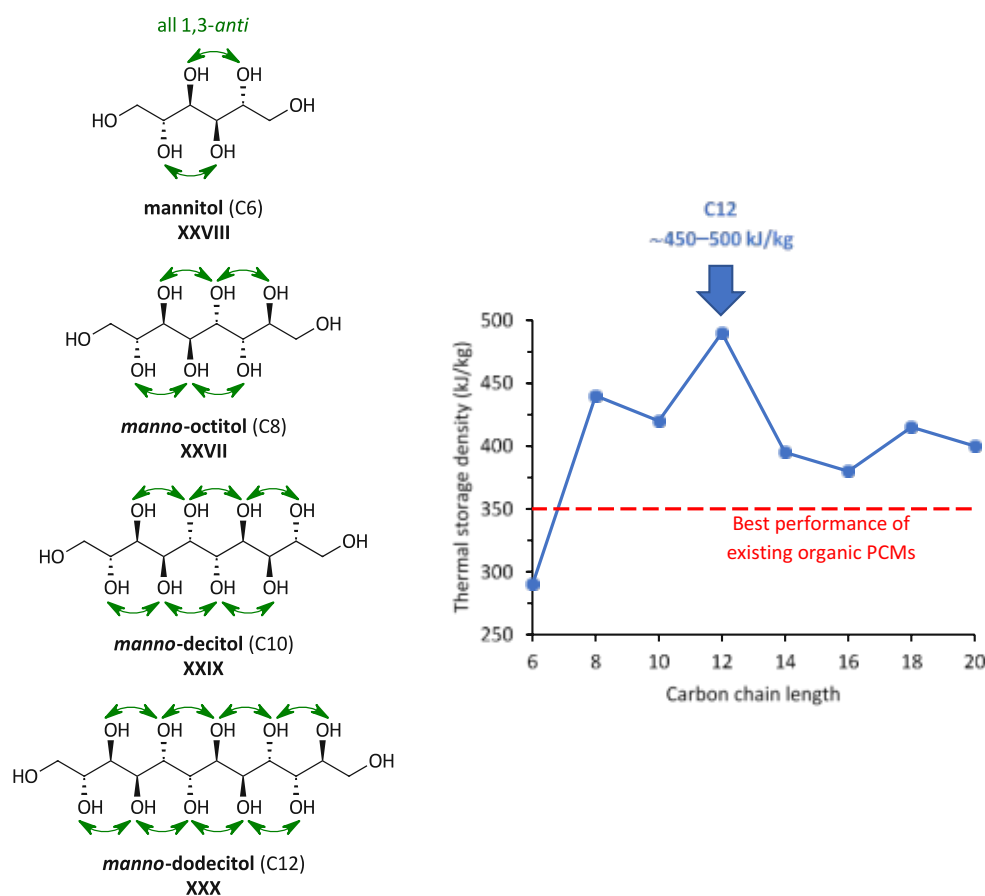


Figure 16. (Non-natural) Sugar alcohols and their calculated thermal storage densities – the best performance is predicted for the C12 sugar alcohol **XXX** with a value of 450-500 kJ/kg⁷⁵

Additional to the "perfect" C8 sugar alcohols with all hydroxy groups in a 1,3-*anti*-relationship, the melting points and thermal storage densities of "imperfect" isomers were calculated, too. For the C2-epimer **XXXI** of *manno*-octitol **XXVII**, the presence of only one 1,3-*syn* relationship between two hydroxy groups led to a significant drop of the thermal storage density from 440 kJ/kg to 257 kJ/kg, and also the melting point that was predicted to be 207 °C instead of 327 °C for the "perfect" C8 sugar alcohol. Even lower values were calculated for the C8 isomer **XXXII** in which two hydroxy groups are inverted (C2 & C6) resulting in two 1,3-*syn* relationships.⁷⁵ The structures of those sugar alcohols are shown in Figure 17, their predicted melting points and thermal storage densities in Table 11.

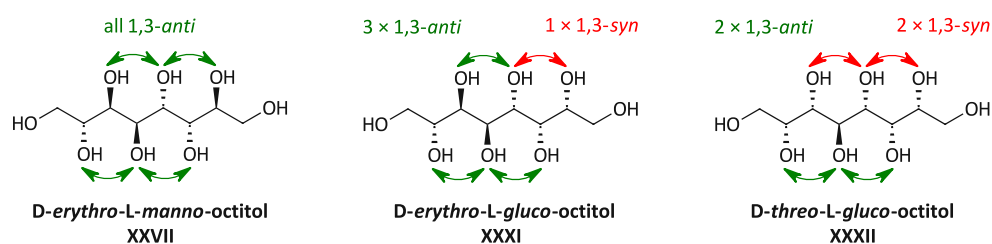


Figure 17. C8 sugar alcohols **XXVII**, **XXXI** and **XXXII** with different distributed hydroxy groups

Table 11. Melting temperatures and thermal storage densities of the non-natural sugar alcohols with eight carbon atoms (shown in Figure 17)⁷⁵

Sugar alcohol	Melting temperature (°C)	Thermal storage density (kJ/kg)
D-erythro-L-manno-octitol XXVII	327	440
D-erythro-L-gluco-octitol XXXI	207	257
D-threo-L-gluco-octitol XXXII	127	136

Some of the non-natural sugar alcohols presented here (octitols) and other sugar alcohols with an uneven number of carbon atoms (heptitols) were already successfully synthesised by Draskovits⁷⁷ (see Chapter A 2.2.3.4). Furthermore, their melting points and enthalpies were determined *via* simultaneous thermal analysis (STA), which is a technique that combines differential scanning calorimetry (DSC) and thermogravimetric analysis (TG). Within this study, the impact of the distribution of hydroxy groups on the physical properties could be shown and further, that an even number of carbon atoms is necessary to obtain high thermal storage densities. Additionally, several of the predictions and calculations by Inagaki and Ishida⁷⁵ were validated, showing, that a precise and trustworthy prediction of the physical properties was performed.

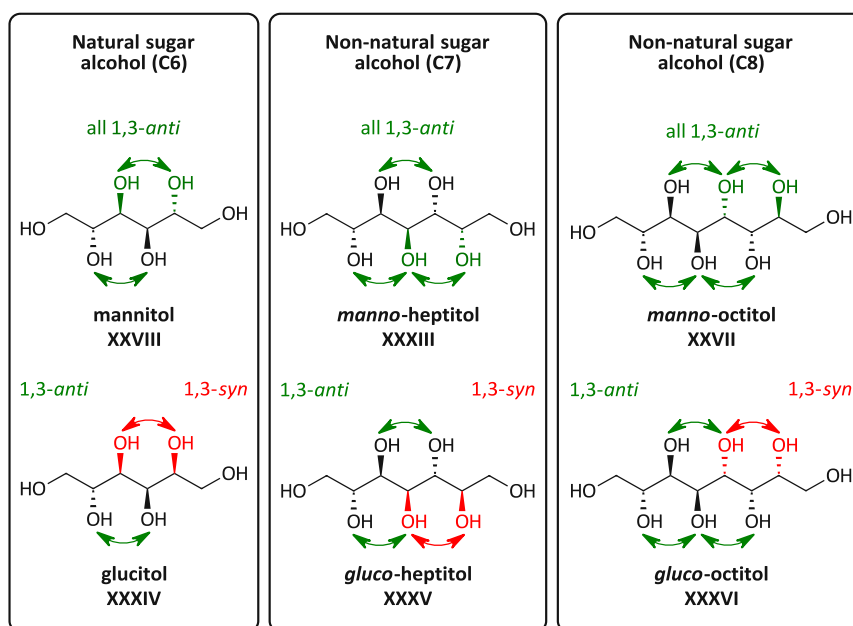


Figure 18. Sugar alcohols that have been investigated in our group according to their melting points and thermal storage densities

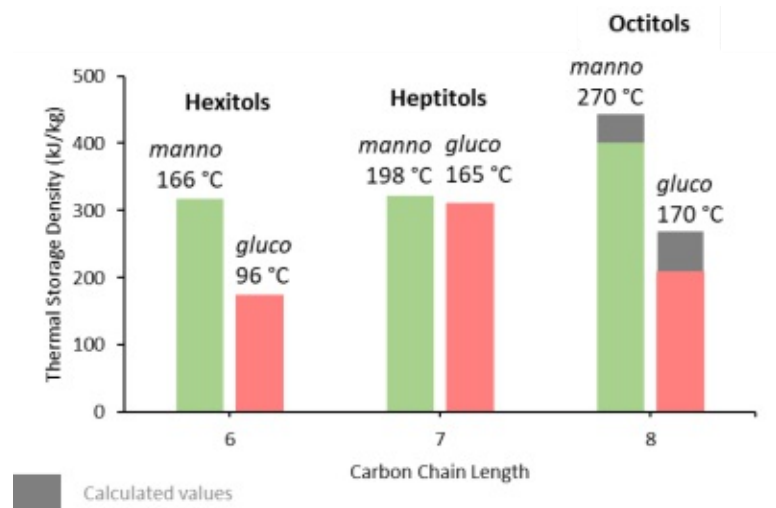


Figure 19. Thermal storage densities of natural and non-natural sugar alcohols; literature values (hexitols)⁷⁴, measured values (heptitols, octitols)⁷⁷ and calculated values (octitols)⁷⁵

A 5 Aim of the thesis

In the presented computational study on non-natural sugar alcohols⁷³, Inagaki and Ishidadeeply investigated the "*manno*-series" of sugar alcohols to evaluate their potential as PCMs and their findings for the *manno*-octitol species were already proven in our group (Chapter A 4.4). On the one hand, this match in the calculated and actually observed properties of this substance class confirmed the accuracy and reliability of their investigations and, on the other hand, fueled our interest in non-natural sugar alcohols as promising materials in the field of PCMs. According to the postulated guidelines, we designed the second series of sugar alcohols, the "*galacto*-series" (Figure 20 (bottom)). This series is formally derived from "correct" elongation of the natural sugar alcohol galactitol **XXXVII**, the second hexitol next to mannitol **XXVIII** that fulfils all stated criteria: linear carbon backbone, 1,3-*anti*-relationship of all hydroxy groups, even number of carbon atoms.⁷⁶ The only difference between mannitol and galactitol can be found in the relative configuration of the two terminal stereocentres that are in a 2,3-*anti*-relationship for the mannitol and in a 2,3-*syn*-relationship for the galactitol. The fact that the natural galactitol possesses an even higher melting point and thermal storage density than mannitol makes this series even more attractive as a potential PCMs (Figure 20 (top)).

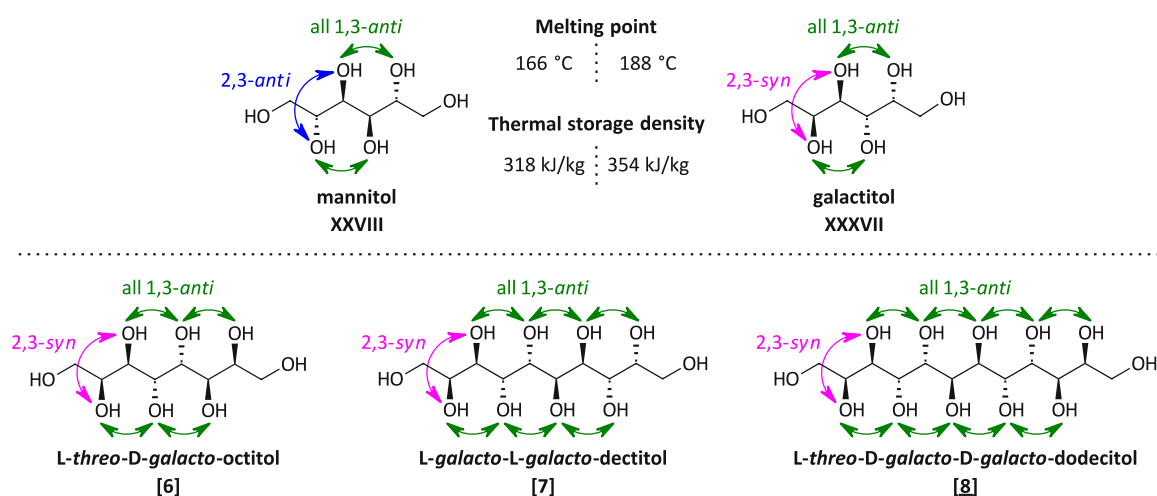
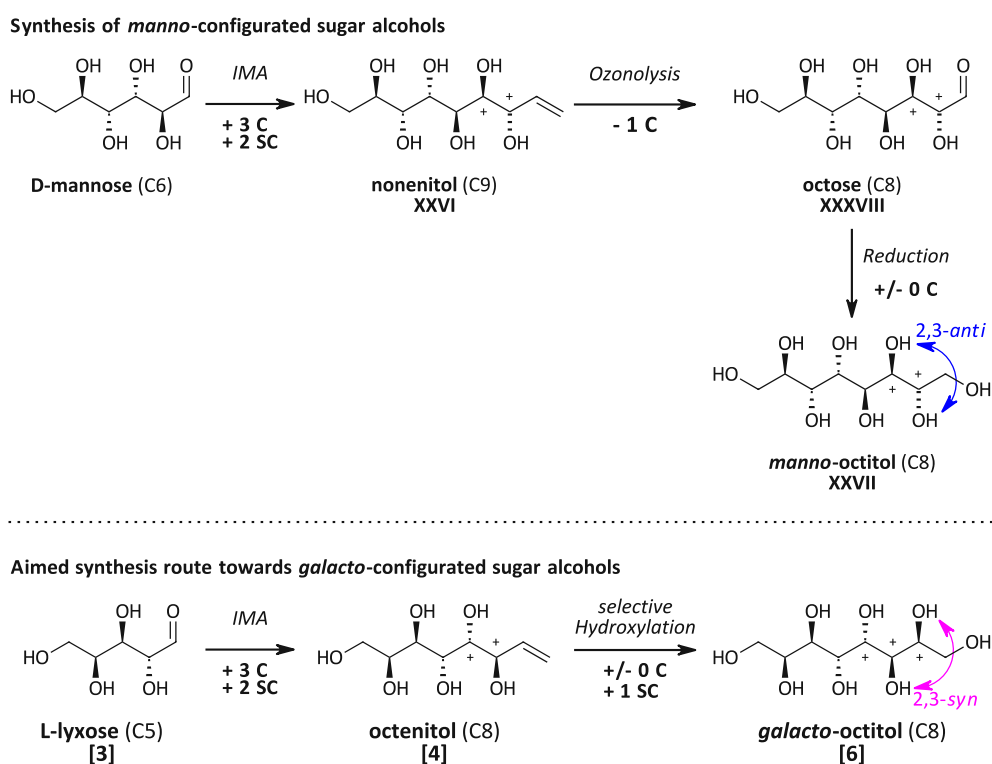


Figure 20. The natural hexitols mannitol **XXVIII** and galactitol **XXXVII** in comparison regarding structural features, melting points and thermal storage densities (top) and the "*galacto*-series" of non-natural sugar alcohols [6], [7] and [8] based on the requirements postulated by Inagaki and Ishida⁷⁵ (bottom)

With this intent, we aimed to develop an efficient enantioselective strategy to realise the synthesis of non-natural sugar alcohols with all hydroxy groups in a 1,3-*anti*-relationship and *galacto*-configuration (2,3-*syn*-relationship) for thermal analysis. The observed experimental properties will be their melting points and thermal storage densities. Further, the physical properties of this new set of high-carbon sugar alcohols are being calculated in cooperation with Inagaki and Ishida and will be compared to our experimental results.

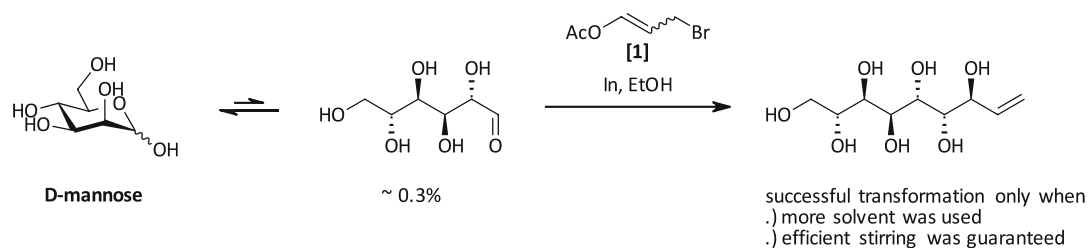
In general, the focus of this thesis can be divided into three parts covering different aspects of the synthetic challenges of the synthetic route:

- (i) As the main aspect, a synthesis protocol for the *galacto*-octitol [6] should be developed which will then serve as blueprint for the efficient synthesis of non-natural sugar alcohols with all hydroxy groups in a 1,3-*anti*-relationship and *galacto*-configuration (2,3-*syn*-relationship). So far, higher sugar alcohols were synthesised *via* IMA of the aldose and subsequent ozonolysis of the formed enitol with reductive work-up (Scheme 17 (top)). But this protocol only allows the preparation of sugar alcohols with *manno*-configuration, meaning a 2,3-*anti*-relationship. Therefore, we were looking for an adjusted route to allow a similar repetitive approach towards the *galacto*-configured sugar alcohols and suggested the general pathway shown in Scheme 17 (bottom). Starting from the aldose, the enitol species should be obtained *via* indium-mediated acyloxyallylation as in the "*manno*-series" approach. With this reaction, the sugar's backbone is elongated by three carbon atoms including the introduction of two new stereocentres with high selectivity for the desired *lxvo*-configuration at the former reducing end of the sugar. In contrast to the *manno*-route, the enitol should then directly be converted into the sugar alcohol by selective hydroxylation instead of performing ozonolysis and subsequent reduction. This approach allows the introduction of a third stereocentre while the number of carbon atoms remains the same.



Scheme 17. Synthetic route towards *manno*-configured sugar alcohols, shown for the *manno*-octitol **XXVII** (top), and aimed synthesis route towards *galacto*-configured sugar alcohols (*galacto*-series), shown for the *galacto*-octitol **[6]** (bottom) (newly formed stereocentres are marked with a +)

- (ii) As next step, we planned to use the new protocol as a blueprint for the synthesis of the *galacto*-decitol **[7]** (C10) and *galacto*-dodecenitol **[8]** (C12) (see Figure 20) in a repetitive fashion from the higher aldoses as starting materials. With the rising number of carbon atoms and present hydroxy groups, these sugars are expected to be less reactive in the IMA as lower solubility, and a lower open-chain content are predicted for them.
- (iii) According to the anticipated problem with the longer chain sugars, we wanted to optimise the indium-mediated acyloxyallylation as the standard protocol using EtOH as the solvent and 3-bromopropenyl acetate **[1]** as the reagent (Chapter A 2.2.3) was found to only be high yielding when short-chained, reactive aldoses like, e.g., erythrose and lyxose are used as starting materials. Standard sugars like mannose showed lower reaction rates in the IMA towards the corresponding enitols due to lower solubility and a lower open-chain content making the free aldehyde moiety less available. Therefore, we set out to develop an improved protocol for the IMA that allows also the transformation of less reactive aldoses required for the accomplishment of the longer-chain sugar alcohols from (ii).

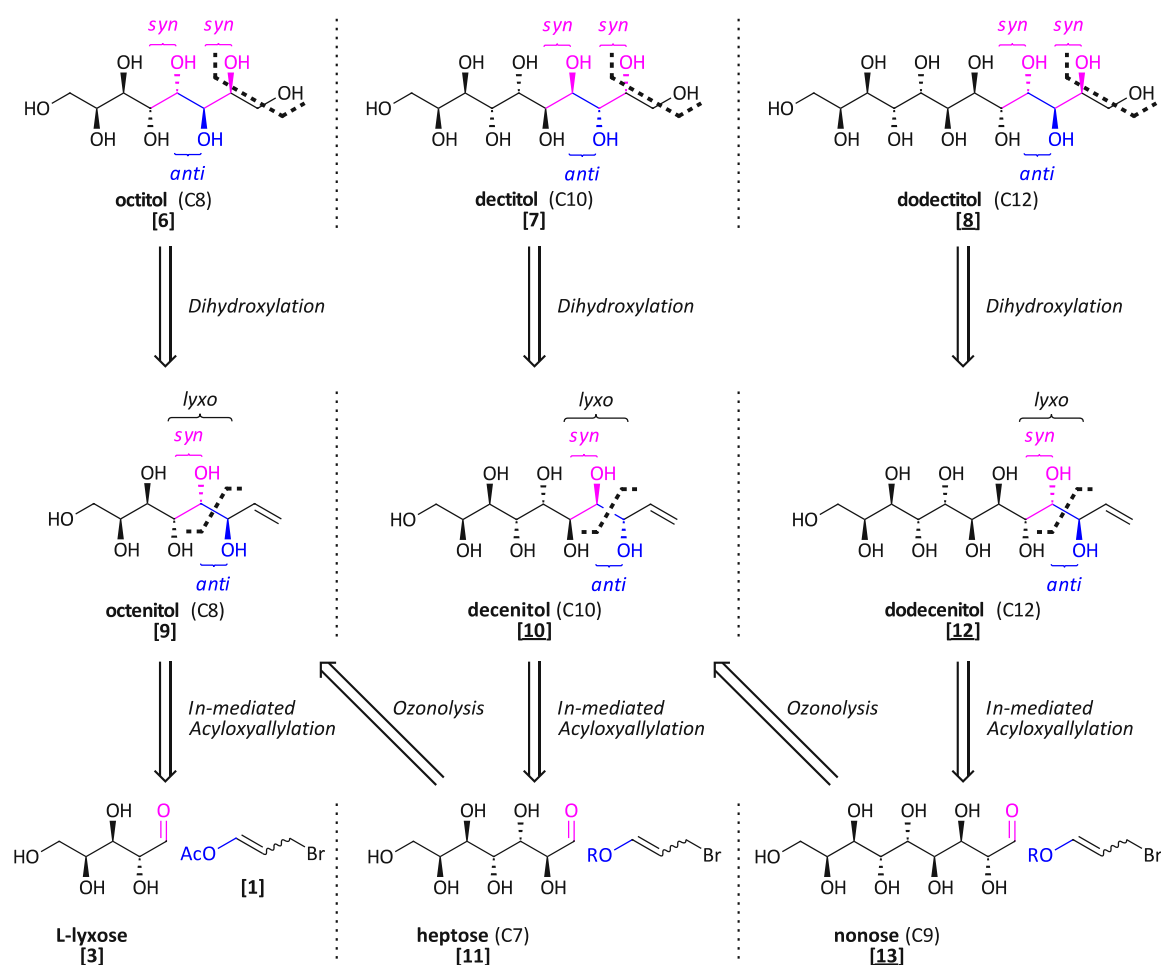


Scheme 18. IMA of D-mannose under standard conditions with 3-bromopropenyl acetate **[1]** in EtOH

B Results and discussion

B 1 Retrosynthetic analysis

To obtain higher-carbon sugars and the corresponding sugar alcohols, the indium-mediated acyloxyallylation is a handy tool, as it has already been discussed in Chapter A 2.2.3.4. In the IMA, aldoses can be elongated by three carbon atoms giving enitols that can further be transformed into the corresponding aldose due to subsequent ozonolysis. Alternatively, by performing a reductive work-up after the ozonolysis, sugar alcohols elongated by two carbon atoms compared to the starting sugar are obtained, with the two terminal stereocentres in an *anti*-relationship. However, as we were interested in sugar alcohols with a 2,3-*syn*-configuration, we thought of a different reaction sequence to obtain non-natural sugar alcohols with the desired structural features directly from sugar enitols that are accessible by IMA. The principle planning is exemplified towards the octitol [6] but can be translated to homologous sugar alcohols with longer chain length.



Scheme 19. Retrosynthetic analysis for the three targeted sugar alcohols: *L*-threo-*D*-galacto-octitol [6], *L*-galacto-*L*-galacto-decitol [7] and *L*-threo-*D*-galacto-*D*-galacto-dodecitol [8]

The retrosynthetic analysis for the C8 sugar alcohol *L-threo-D-galacto*-octitol **[6]** is shown in Scheme 19 (left). The sugar alcohol **[6]** should directly be obtained from the corresponding octenitol **[9]** *via* diastereoselective dihydroxylation of the terminal double bond, a standard method to introduce diols. In the next step, the synthesis of *L-glycero-D-manno*-octenitol **[9]** can be realised *via* indium-mediated acyloxyallylation of *L-lyxose* **[3]** with 3-bromopropenyl acetate **[1]** to form the organoindium species. This is a literature²³ known reaction that has already been described in Chapter A 2.2.3.2.

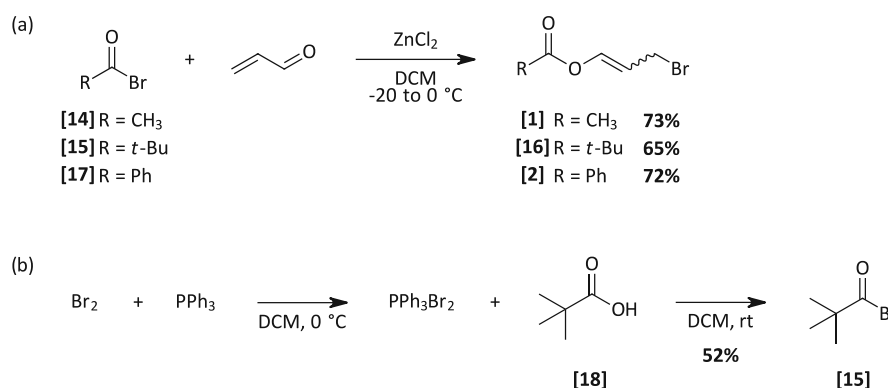
The critical step in this sequence is expected to be the dihydroxylation reaction, as high diastereoselectivity for the *2,3-syn(threo)*-configured product is required in order to obtain all hydroxy groups in a *1,3-anti*-relationship. Two standard dihydroxylation protocols are considered at this step: First, the Upjohn dihydroxylation, in which the stereochemical outcome of the reaction only depends on the substrate's nature, second, the Sharpless dihydroxylation, in which a chiral catalyst controls the face selectivity of the catalyst's coordination to the double bond. In both methods, an osmium-catalyst is used, and the introduction of the two hydroxy groups takes place from the same side of the double bond. We assumed that especially asymmetric Sharpless dihydroxylation gives us the opportunity to influence the stereochemical outcome of the introduction of the hydroxy groups and allows the selective synthesis of the targeted *2,3-syn*-octitol **[6]**.

We further considered that it might be necessary to first protect the hydroxy groups present in the enitol species and then perform the dihydroxylation reaction, according to literature research on dihydroxylation conditions used for similar polyols.⁷⁸⁻⁸⁰ The necessity of protection can be addressed to the solubility of the substrate under the aimed reaction conditions, but also disturbance of the hydroxy groups in the dihydroxylation reaction.

This principle retrosynthetic analysis can further be extended for the *galacto*-decitol **[7]** (Scheme 19 (middle)) and the *galacto*-dodecitol **[8]** (Scheme 19 (right)). The higher aldoses that are the starting materials in the sequence can be obtained *via* ozonolysis of the corresponding enitols that are intermediates in the synthetic route towards the *galacto*-octitol (heptose **[11]**) and *galacto*-decitol (nonose **[13]**), respectively.

B 2 Synthesis of the 3-bromopropenyl esters used for IMA

In the course of this work, three different bromopropenyl esters were synthesised and used as reagents in the indium-mediated acyloxyallylation of aldoses, namely the 3-bromopropenyl acetate, benzoate and pivalate. The synthesis of these compounds was carried out according to a literature protocol³⁸, in which the ester is obtained from the corresponding acid bromide and acrolein, using ZnCl_2 as a catalyst (Scheme 20 (a)).



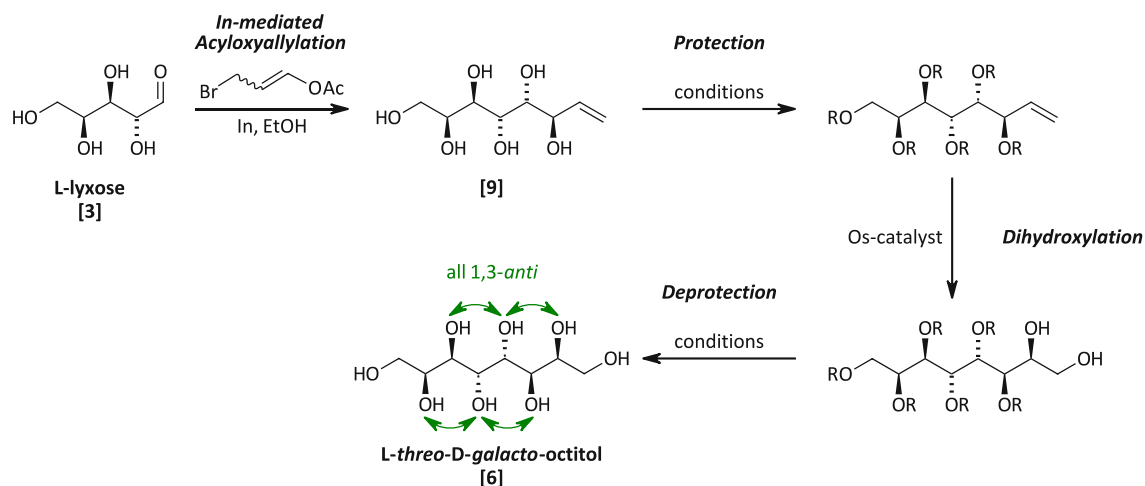
Scheme 20. Synthesis of the 3-bromopropenyl esters [1], [2] and [16] (a) and synthesis of the pivalic acid bromide [15] (b)

The bromides of the acetic acid and benzoic acids are commercially available, but the pivalic acid bromide [15] had to be synthesised following the protocol shown in Scheme 20 (b). First, the bromination reagent PPh_3Br_2 was formed from bromine and triphenylphosphine, then pivalic acid [18] was added, giving the desired pivalic acid bromide [15] that was isolated *via* distillation in good yield.

The 3-bromopropenyl esters [1], [2] and [16] were obtained by mixing the commercially available acid bromides [14] and [17] and the obtained one [15] with acrolein in DCM at lower temperatures ($< -20\text{ }^\circ\text{C}$) because of the exothermic nature of this reaction (Scheme 20 (a)). The initiation of the reaction was achieved by allowing the reaction mixture to warm up to $0\text{ }^\circ\text{C}$, where a significant jump up to $+15\text{ }^\circ\text{C}$ could be observed. Due to efficient cooling, the temperature was lowered again ($-10\text{ }^\circ\text{C}$), and kept at that temperature to achieve full conversion of the starting materials. Isolation of the 3-bromopropenyl acetate [1] and pivalate [16] was possible *via* distillation while the crystalline 3-bromopropenyl benzoate [2] was purified by flash column chromatography.

B 3 The synthetic route towards the *galacto*-octitol

This chapter deals with the development of a new synthesis route towards the *L-threo*-*D-galacto*-octitol **[6]** (C8 sugar alcohol) based on the indium-mediated acyloxyallylation of aldoses, a handy tool for the preparation of higher sugar species. According to the retrosynthetic analysis (Chapter B 1, Scheme 19), the forward synthesis for the *L-threo*-*D-galacto*-octitol **[6]** starting from the pentose *L*-lyxose **[3]** was planned as it is displayed in Scheme 21.



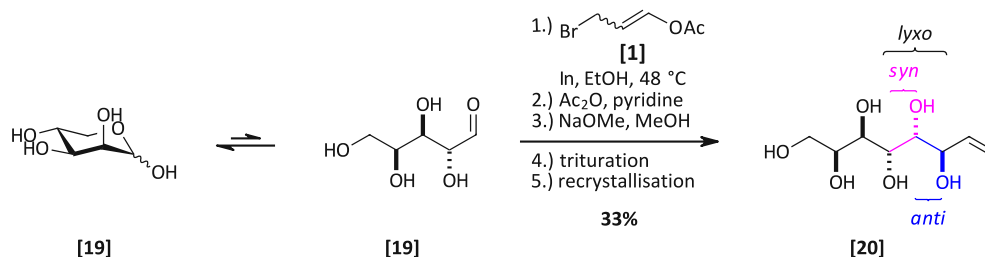
Scheme 21. Planned synthesis route towards the *L-threo*-*D-galacto*-octitol **[6]**

However, for initial investigations the enantiomeric *D*-lyxose **[19]** and the corresponding octenitol **[20]** were used as starting materials due to its lower cost and availability in large quantities in our laboratory. For the sake of clarity, only the structures for the *L*-series are depicted in the following discussion, but for the molecules of the enantiomeric *D*-series stereochemical information is shown with straight bars instead of wedges as those are used to give information about relative stereochemistry.

B 3.1 Indium-mediated acyloxyallylation of lyxose towards the *glycero-manno*-octenitol

The indium-mediated acyloxyallylation of lyxose was straight forward as this reaction was already performed for *L*-lyxose **[3]** on large scale by Stanetty and Baxendale²³. *D*-Lyxose **[19]** was dissolved in EtOH, and 3-bromopropenyl acetate **[1]** and indium were added at once under vigorous stirring (Barbier-type protocol). Efficient stirring is crucial at this stage, as the underlying reports^{23,38} showed that otherwise side reactions of the reagent are favoured (Wurtz-type dimerization), leading to incomplete conversion of the starting material. However, in this case, full conversion was observed within 15 minutes, and a mixture of enitol isomers was observed following a peracetylation – Zemplén deacetylation sequence, as it was described in the general procedure for the IMA of aldoses with 3-bromopropenyl acetate **[1]** by Draskovits, et al.²⁴. The peracetylation as an additional step facilitates separation of the product species from any inorganic components. A

mixture of isomers was obtained as the crude material with the *lyxo*-configured octenitol [20] as the major component. The ratio of the formed diastereomers was in accordance with the observations of Stanetty and Baxendale²³, being *lyxo* : *xylo* : *ribo* = 65 : 25 : 10 (according to ¹H-NMR). From this, the desired octenitol [20] with *lyxo*-configuration could be isolated upon trituration in *i*-PrOH and recrystallisation from a MeOH/H₂O mixture with a yield of 33%.



Scheme 22. Synthesis of *glycero-manno*-octenitol [20] via IMA of D-lyxose [19]

B 3.2 Introduction of protecting groups to the octenitol

As the next step, the diastereoselective dihydroxylation of the octenitol was planned. However, literature research on dihydroxylation conditions used for similar polyols⁷⁸⁻⁸¹ always showed the necessity of partial or full protection of the hydroxy groups. Therefore, different protecting groups (PG) were introduced to the octenitol to give fully protected enitol material. Four common PGs used for hydroxy groups in sugar species, each representing a different chemical class, were considered (Table 9).

Table 12. Protecting groups that were considered for the octenitol [8] and [20], respectively

Name	Abbreviation	Structure	Chemical class
acetate	Ac		ester
benzyl ether	Bn		aromatic ether
isopropylidene (acetonide)	–		cyclic ketal
<i>tert</i> -butyldimethylsilyl ether	TBS		silyl ether

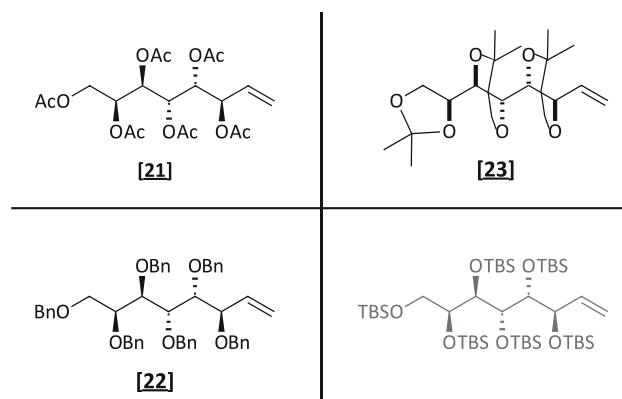
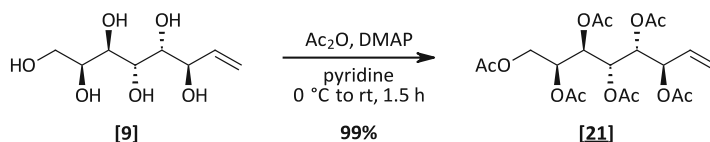


Figure 21. The four targeted, protected octenitols **[21]**, **[22]** and **[23]**

The compounds **[21]**, **[22]** and **[23]**, namely the hexaacetyl-, hexabenzyl- and triisopropylidene-octenitol, could successfully be synthesised and their preparations are shown and discussed in the following Chapters B 3.2.1 (Ac), B 3.2.2 (Bn) and B 3.2.3 (acetone). The fully TBS-protected octenitol could not be obtained under the applied conditions, using TBSCl (9 equiv.) and imidazole (18 equiv.) in DMF. Only an octenitol species with four TBS-groups present as confirmed by HPLC-MS and NMR analysis was observed and this approach was not followed up further within this work.

B 3.2.1 Introduction of acetate groups to the octenitol

The octenitol peracetate **[21]** was obtained from **[9]** with acetic anhydride and a catalytic amount of DMAP in pyridine at room temperature. An aqueous work-up upon complete conversion gave the desired product **[9]** quantitative (99%). No further purification was necessary, and the peracetylated enitol was obtained as a colourless solid.

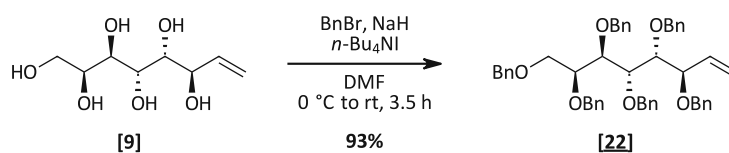


Scheme 23. Introduction of acetate protecting groups to the octenitol **[9]**

B 3.2.2 Introduction of benzyl groups to the octenitol

Another common protecting group for hydroxy groups in sugar species we were interested in was the benzyl group. The formation of benzyl ethers is usually carried out in two steps. First, the hydroxy groups of the substrate **[9]** are deprotonated using sodium hydride as a base, forming the corresponding alkoxides. Then, benzyl bromide is added that reacts with the substrate in a nucleophilic substitution reaction. Additionally, a catalytic amount of tetrabutylammonium iodide was added for the *in situ* formation of benzyl iodide. As iodides

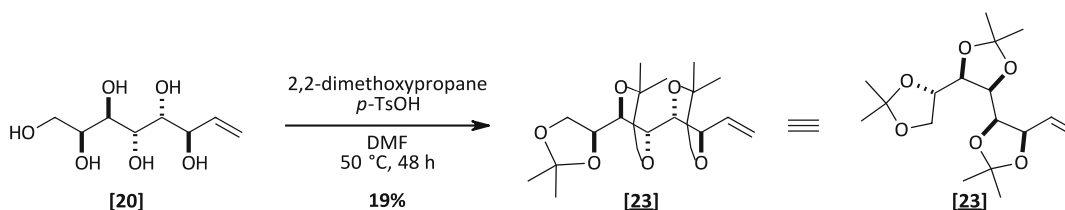
are more reactive than bromides in S_N2 reactions, the reaction rate is accelerated, and the product **[22]** was isolated after chromatographic purification in excellent yield.



Scheme 24. Introduction of benzyl protecting groups to the octenitol **[9]**

B 3.2.3 Synthesis of the 3,4:5,6:7,8-*O*-triisopropylidene-octenitol

The introduction of three acetonide protecting groups to the six hydroxy groups present in the octenitol was not as straightforward as the formation of the hexaacetyl- **[21]** and hexabenzyl-species **[22]**. However, the targeted product **[23]** was formed by treating the octenitol **[20]** with 2,2-dimethoxypropane and *p*-TsOH at 50 °C in DMF and obtained in pure form upon column chromatography in a yield of 19% only.

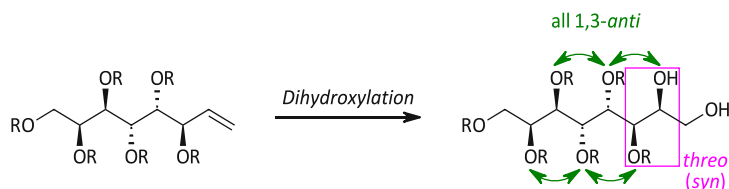


Scheme 25. Introduction of acetonide protecting groups to the octenitol **[20]**

Under the applied conditions, full conversion of the starting material was observed within 6 h, but several spots were observed on TLC. By the portionwise addition of further *p*-TsOH over 48 hours, it was tried to drive the reaction to more formation of product **[23]**, the most apolar species in the mixture. Still, the ratio of the formed products did not change according to TLC. One of the main side products showed a similar polarity as the targeted species **[23]**, but the separation of these two species could still successfully be performed *via* column chromatography. While the more apolar reaction product could be identified as the targeted 3,4:5,6:7,8-*O*-triacetonide **[23]**, the structure of the side-product could not be fully clarified by NMR analysis ($^1\text{H-NMR}$, $^{13}\text{C-NMR}$, COSY, HSQC, HMBC). However, it was confirmed that it is an octenitol species with also three isopropylidene groups present in the molecule, but the spectral data did not provide information on the very constitution. It is hypothesised that a species with 6-membered instead of 5-membered rings was formed, as a correlation between the H5 and H7 with the same quaternary carbon atom from an isopropylidene group was observed in the HMBC spectrum. As no further signals with information on the position of the isopropylidene groups were detected, the assumption could not be confirmed, and no structure could be proposed.

B 3.3 Dihydroxylation of the protected octenitol

As it was shown in the retrosynthetic analysis (Scheme 19), we wanted to perform a direct transformation of the octenitol species into the sugar alcohol by selective dihydroxylation of the olefin, as this is a standard method to introduce diols.



Scheme 26. Desired reaction outcome of the dihydroxylation reaction of the protected octenitol to obtain the partly protected octitol with all alkoxy/aryloxy groups in a 1,3-*anti*-relationship

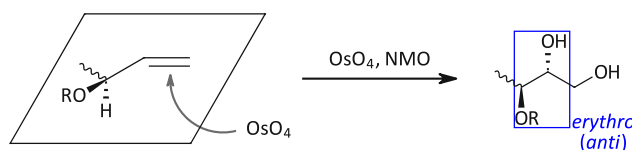
B 3.3.1 Evaluation and investigation of different dihydroxylation conditions

Two standard dihydroxylation methods were considered for the transformation of the enitol species into the corresponding partly protected sugar alcohol: the Upjohn dihydroxylation and the asymmetric Sharpless dihydroxylation.

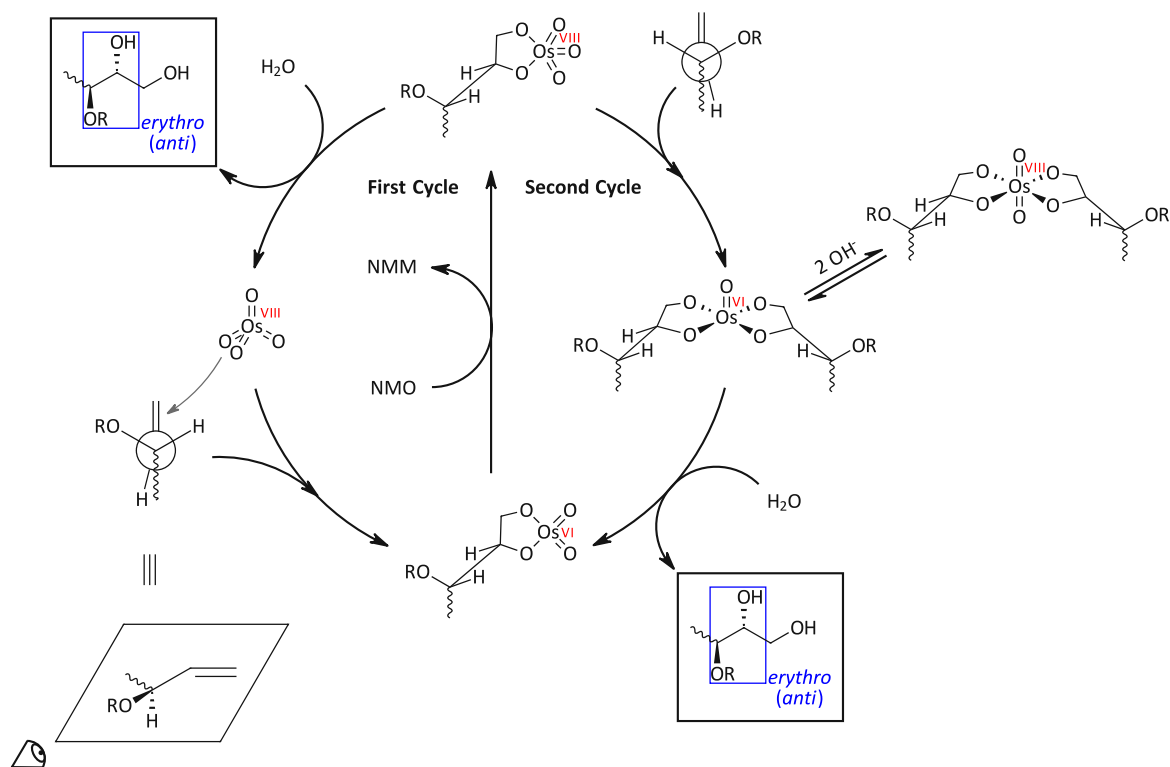
Upjohn dihydroxylation

In the general Upjohn procedure, catalytic quantities of osmium tetroxide (OsO_4), usually 0.01–2 mol%, are used together with a cheap co-oxidant, namely *N*-methylmorpholine *N*-oxide (NMO), in stoichiometric amounts.⁸² To avoid the handling of OsO_4 as it is volatile and toxic, the potassium salt $\text{K}_2[\text{OsO}_2(\text{OH})_4]$ can be used as the catalyst precursor from which is generated *in situ* by the oxidation with NMO.⁸³

In general, the product with *erythro*-configuration between the pre-existing alkyl-/ aryloxy group and the newly formed secondary hydroxy group is expected for acyclic alkenes with an allylic, oxygen-bearing stereocentre. *Erythro*-configuration means an *anti*-relationship between the two described stereocentres (Scheme 27).⁸⁴ This diastereoselectivity is assumed to arise from the preferential approach of OsO_4 to the face opposite to that of the alkyl-/aryloxyl group due to considerations of stereoelectronic ground as it is displayed in the catalytic cycle (Scheme 28).⁸⁵



Scheme 27. Expected diastereoselectivity for the *erythro*-configured product in the Upjohn dihydroxylation of acyclic alkenes with allylic, oxygen-bearing stereocentres⁸⁵



Scheme 28. Catalytic cycle of the Upjohn dihydroxylation towards the *erythro*-configured product, showing the first and second cyclic (adapted from Wai, et al.⁸⁶ and Gao and Cheun⁸⁷)

According to this, we expected the partly protected octenitol with the wrong stereochemistry (*erythro*-configuration) that is shown in Figure 22 as the major product. Still, the dihydroxylation reaction of the protected octenitols was carried out under these conditions as this has not been reported in literature on such starting materials and the presence of the other stereocentres generally complicates predictions on the stereochemical outcome. It was expected that from whatever native selectivity was found, the use of Sharpless conditions would allow tuning towards the targeted stereochemistry.

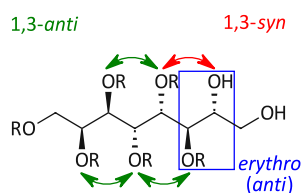
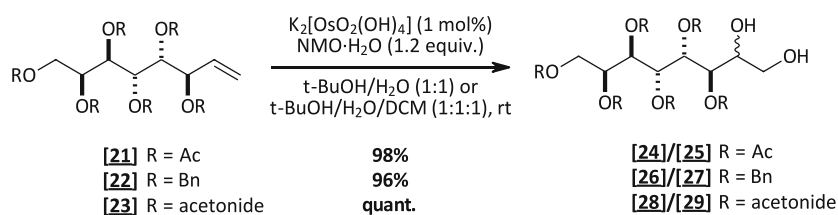


Figure 22. Structure of the expected major product from the Upjohn dihydroxylation of the protected octenitols

The protocol that was used for the octenitols **[21]**, **[22]** and **[23]** is displayed in Scheme 29. All three enitols could successfully be converted into the targeted dihydroxylated products giving mixtures of the two diastereomers.



Scheme 29. Upjohn dihydroxylation conditions that were used for the protected octenitols [21], [22] and [23]

In early attempts, only a 1:1 (v/v) mixture of *t*-BuOH and H₂O was used as the solvent but the observed reaction rates were low, and even after several days no full conversion of the starting material could be achieved in some cases. By the addition of DCM (*t*-BuOH/H₂O/DCM 1:1:1), faster reaction progress was achieved. It is assumed that solubility issues played a significant role here, and the reactions were speeded up due to the substrates' better solubility in the reaction mixture.

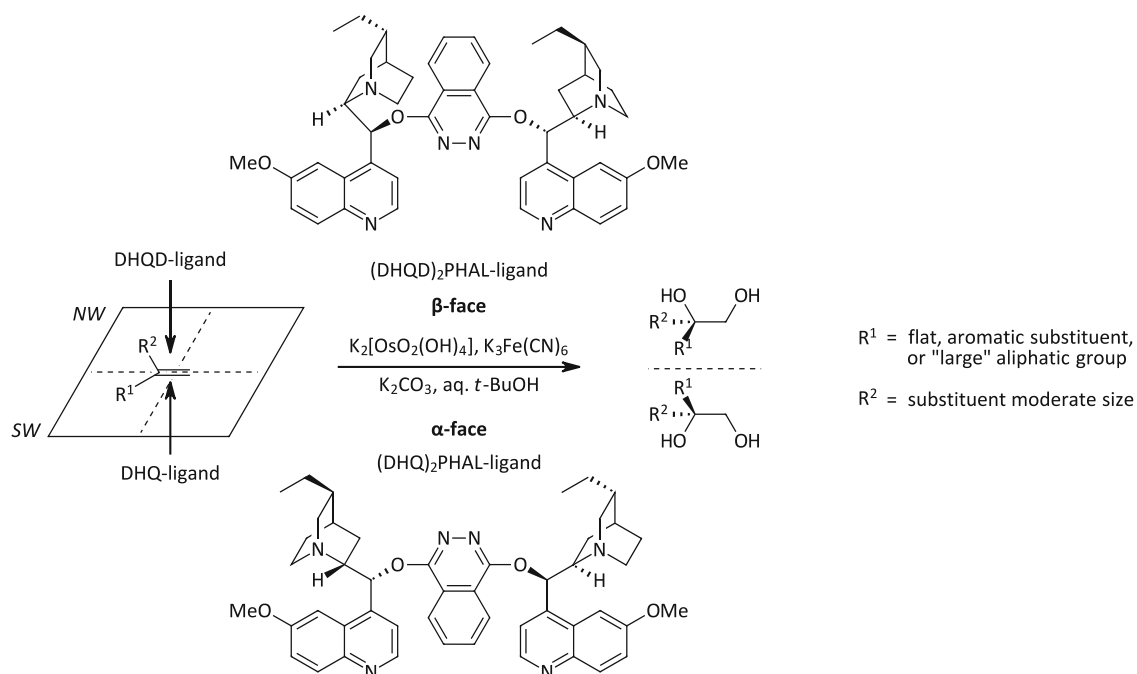
Regarding the stereochemical outcome, in all three transformations the *erythro*-configured product was obtained as the major one, as expected from literature research, but none of the two isomers was predominantly formed. The determination of the product ratios and the exact values are shown and discussed together with the results of the Sharpless AD in Chapter B 3.3.2.

Sharpless dihydroxylation

In the Sharpless dihydroxylation, facial selectivity can be induced due to the use of chiral ligands. Two different mixtures of reagents are commercially available, namely AD-mix- α and AD-mix- β , and are used depending on the substrate's structure and the targeted stereochemistry in the product. This reagent mixtures contain potassium osmate dihydrate (K₂[OsO₂(OH)₄]), potassium carbonate (K₂CO₃), the terminal oxidant potassium ferricyanide (K₃Fe(CN)₆), and either the chiral ligand (DHQ)₂PHAL (α -mix) or (DHQD)₂PHAL (β -mix).⁸⁸ Usually, methanesulfonamide (MsNH₂) is added to the reaction mixture due to its positive impact on the reaction rate as it accelerates the hydrolysis of the osmium (VI) glycolate product (see Scheme 31) considerably.⁸⁹

Generally, it is expected that the stereochemical outcome of the dihydroxylation reaction under Sharpless conditions can be controlled by the choice of the AD-mix as two sets of chiral ligands are available. Predictions on the stereoselectivity are usually made based on the mnemonic scheme that was developed by Sharpless and co-workers, in which the alkene's structure and orientation and the catalyst's coordination are considered.⁹⁰ However, for chiral substrates a matched and mismatched pairing between the substrate and the catalyst species can be observed, the later one typically resulting in low reaction rates and yields as the reagent has to overcome the intrinsic diastereofacial bias of the olefin substrate. In Scheme 30, the mnemonic scheme for 1,1-disubstituted alkenes as substrates is shown since this model is the most suitable one for the description of a terminal alkene as it is present in the octenitol species. According to the investigation by Sharpless, flat, aromatic substituents fit well in the southwest quadrant, or, in their

absence, "large" aliphatic groups (represented by R^1 in Scheme 30), whereas the northwest quadrant is more accessible for substituents of moderate size (R^2).⁸⁹ However, further investigations on the dihydroxylation of 1,1-disubstituted allyl alcohol derivatives by Hale, et al.⁹¹ showed, that oxygen-containing substituents like, e.g., BnOCH_2 or PivOCH_2 have a relatively low tendency to occupy the SW quadrant.



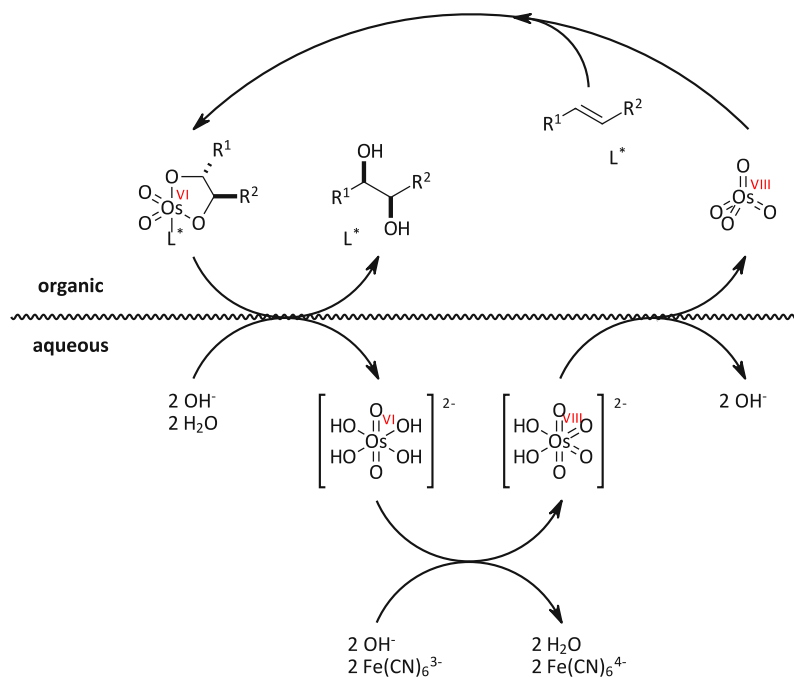
Scheme 30. Mnemonic scheme of the Sharpless dihydroxylation for 1,1-disubstituted alkenes showing alkene orientation and face selectivity (adapted from Kolb, et al.⁸⁹)

Due to the presence of only one substituent at the double bond in our enitol substrate, which possesses chiral centres and an alkoxy or aryloxy group in α -position to the olefin, it was difficult to predict the stereochemical outcome of the dihydroxylation with the two different ligands. Furthermore, Hale, et al.⁹¹ showed that the rule for face-selectivity by Sharpless cannot easily be applied for the AD of allyl alcohol derivatives. The following Figure 23 shows an example for the ambiguity of the empirical mnemonic device on two substrates with a benzyloxy group at the allylic position. For the substrate in entry **1**, the (*S*)-diol was expected with AD-mix- β according to the face-selection rule, but the (*R*)-optical antipode was predominantly formed. A similar substrate with a methyl group instead of an ethyl group as the second substituent (entry **2**) gave the (*R*)-configured product that was confirmed to the mnemonic model in the reaction with AD-mix- α .⁹¹

	Olefin	AD-mix	% yield	% ee	Product
1		β	63	31	
2		α	93	45	

Figure 23. Asymmetric dihydroxylation of 1,1-disubstituted allyl alcohol derivatives with one substituent being a benzyloxy group, the other one an alkyl chain

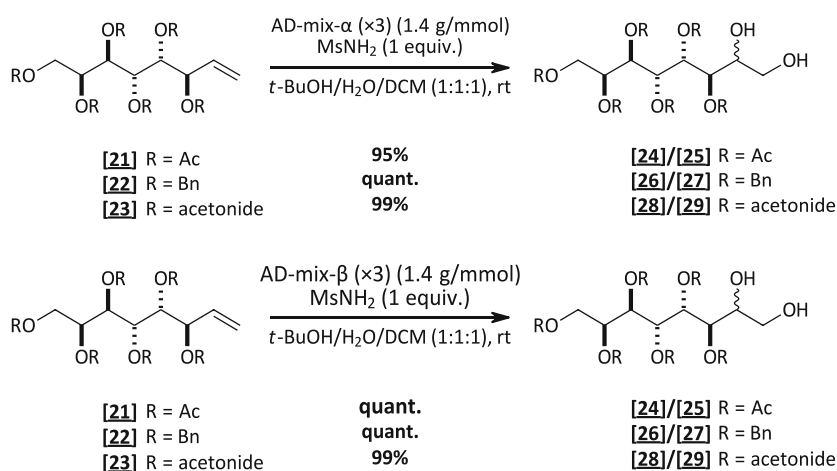
According to all these findings, no reliable prediction could be made, and in a first attempt, the dihydroxylation of the peracetylated octenitol **[21]** was conducted using commercially available AD-mix- β and MsNH_2 in a biphasic mixture of *tert*-butanol and H_2O at 0°C . Under these conditions, the substrate did not undergo any conversion to the targeted product, so the reaction was carried out again at room temperature (25°C) as this was suggested by Morikawa, et al.⁹² for sterically demanding substrates that showed low turnover numbers. Furthermore, attention was paid to efficient stirring as this is essential for the reaction's selectivity and rate since the oxidation of the substrate takes place in the organic phase, and the re-oxidation of the catalyst in the aqueous phase, as it is shown in Scheme 31.⁹³



Scheme 31. Catalytic cycle of the dihydroxylation with OsO_4 as the catalyst and Fe(CN)_6^{3-} as the re-oxidant in a biphasic mixture (adapted from Ogino, et al.⁹³ and Kolb, et al.⁸⁹)

Further, DCM was added as a co-solvent, for the same reason that has already been discussed for the dihydroxylation under Upjohn conditions. Even though the formation of hydroxylated product **[24]**/**[25]** could be observed, the reaction progress was sluggish. After 8 days, a conversion of only about 20% (according to HPLC-MS) was achieved. To

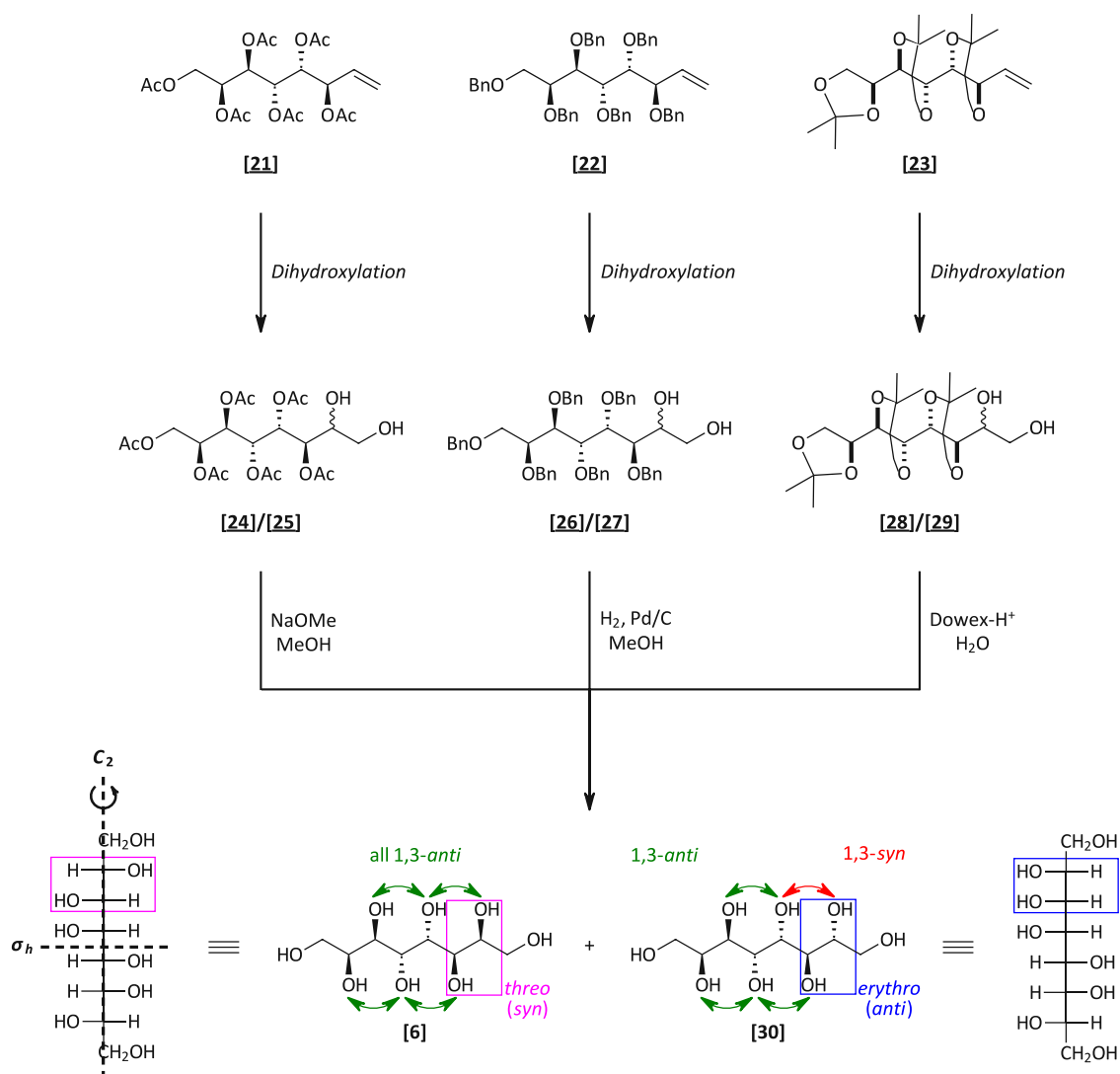
speed up the reaction, a more concentrated AD-mix was used that contained three times the standard quantity of the potassium osmate salt (0.6 mol%) and ligand (3 mol%) over the other components (AD-mix- α/β ($\times 3$)), a modification by Kobayashi, et al.⁹⁴. Using this AD-mix- β ($\times 3$) with MsNH₂ (1 equiv.) in *t*-BuOH/H₂O/DCM (1:1:1) on the peracetylated substrate **[21]**, full conversion towards the dihydroxylated species could be obtained. These conditions using both reagent mixtures in the concentrated version were applied to all three protected octenitol species **[21]**, **[22]** and **[23]** (Scheme 32).



Scheme 32. Optimised Sharpless dihydroxylation conditions with both AD-mix- α ($\times 3$) and AD-mix- β ($\times 3$) that were used for the protected octenitols **[21]**, **[22]** and **[23]**

B 3.3.2 Results for the screening of substrates and reaction conditions

The optimised dihydroxylation conditions were applied to all three substrates **[21]**, **[22]** and **[23]** to find the optimal set of protected enitol and dihydroxylation conditions to get towards the desired 2,3-*syn(threo)*-configured product. At the stage of the partly protected octitols, the two diastereomers formed in the DH reactions were always identified as one species when analytics (TLC, HPLC-MS) were performed. So, no simple preparative separation of the mixtures could be accomplished in order to get the *threo*- and *erythro*-configured partly protected octitols in enantiomerically pure form. To facilitate comparison of the ratio of the two diastereomeric products formed under different reaction conditions, the dihydroxylation products were converted into the corresponding sugar alcohols by subsequent deprotection (Scheme 33). The deprotection of the peracetate species **[24]/[25]** was successfully performed *via* Zemplén deacetylation using NaOMe in MeOH, giving the sugar alcohol in excellent yields. The benzyl ethers of the mixture **[26]/[27]** were cleaved *via* catalytic hydrogenation using palladium on activated carbon as catalyst in MeOH. Here, the addition of a catalytic amount of hydrogen chloride significantly improved the reaction rate, giving the deprotected octitol species in good yields. The acetonide groups were cleaved by treatment with Dowex-H⁺, an acidic ion exchange resin, in a solution of **[28]/[29]** in H₂O.



Scheme 33. Synthetic route towards the octitol (a mixture of the *threo(syn)*- [6] and *erythro(anti)*-configured product [30]) by dihydroxylation of the protected entitol species and subsequent cleavage of the protecting groupsⁱⁱ

The ratio of the diastereomeric mixture was determined from NMR analysis. Usually, ¹H-NMR spectroscopic integration is a powerful method for evaluating ratios of product mixtures (e.g., diastereomers or constitutional isomers). This is since ¹H-NMR spectroscopy is a fast method to determine structures at a molecular level that has been intensively investigated as a quantitative method.⁹⁵⁻⁹⁶ However, due to overlapping signals, the quantification could not be deduced from the ¹H-NMR spectra, but the two diastereomers [6] and [30] could easily be distinguished in the ¹³C-NMR spectra as almost all signals of the two diastereomers were separated. Therefore, the evaluation of the octitol ratio was done by integration of the signals in the obtained ¹³C-NMR spectra. In the case of diastereomers, sufficiently similar response factors for the ¹³C-NMR spectroscopic integration were assumed even with standard ¹³C-NMR techniques (standard pulse sequences, including broadband decoupling; short D1 values), based on the detailed study by Otte, et al.⁹⁵ on

ⁱⁱ From compound [28]/[29] the enantiomers of the displayed octitol species [6] and [30] were obtained. For clarity, only the structures of the L-series are shown in this scheme.

^{13}C -NMR spectroscopy for the quantitative determination of compound ratios. For the octitol mixture, the ^{13}C -NMR spectrum shows four signals from the targeted symmetrical *threo*-isomer [6], each representing two carbon atoms, and eight signals from the asymmetrical *erythro*-isomer [30]. In Figure 24, the ^{13}C -NMR spectrum for a roughly 1:1.6 *threo/erythro*-octitol mixture is shown, which was obtained from the acetonide protected octenitol [23] using Upjohn conditions in the dihydroxylation step. As it can be seen here, almost all signals are separated and can either be assigned to the *erythro(anti)*- or *threo(syn)*-configured octitol. The assignment of the signals was done according to ^{13}C -NMR spectra of octitol samples where one of the isomers was enriched (Figure 25).

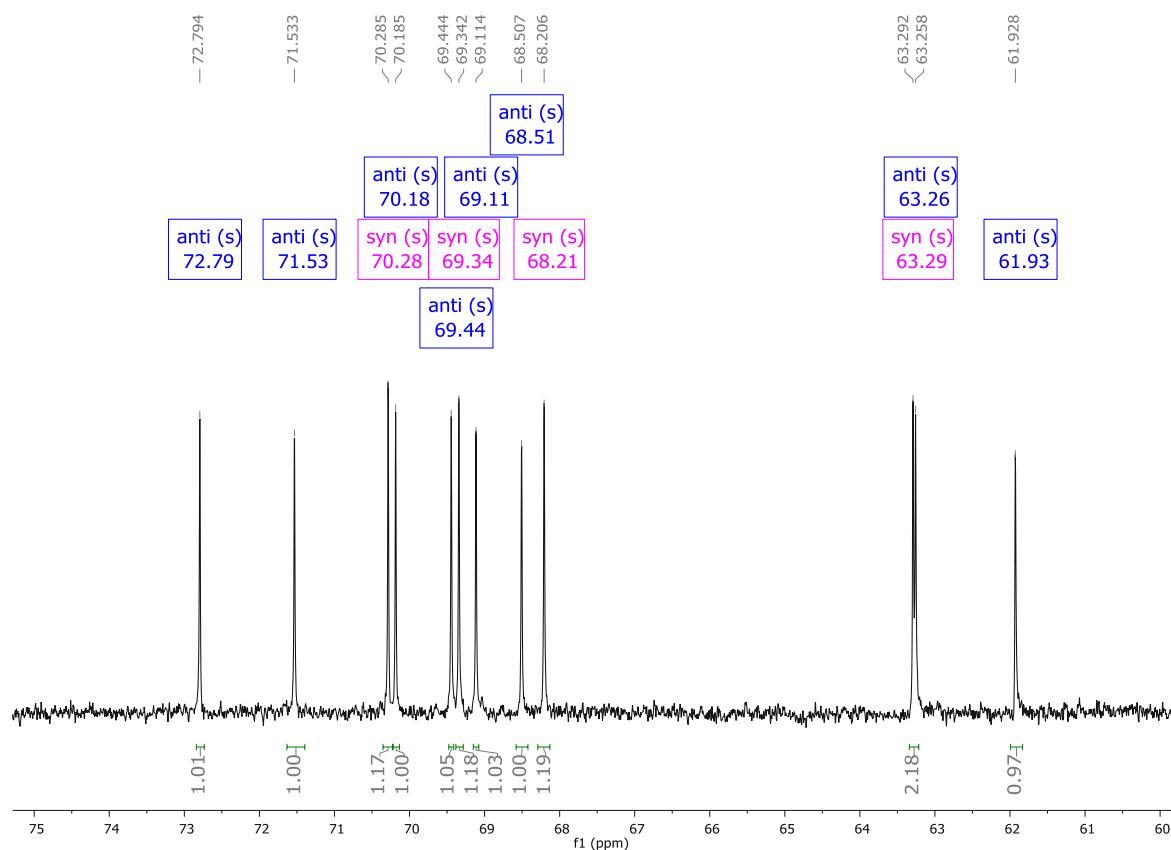


Figure 24. ^{13}C -NMR (600 MHz) assigned for a roughly 1:1.6-1.7 *threo(syn)/erythro(anti)* mixture of the two diastereomeric octitols [6] and [30]

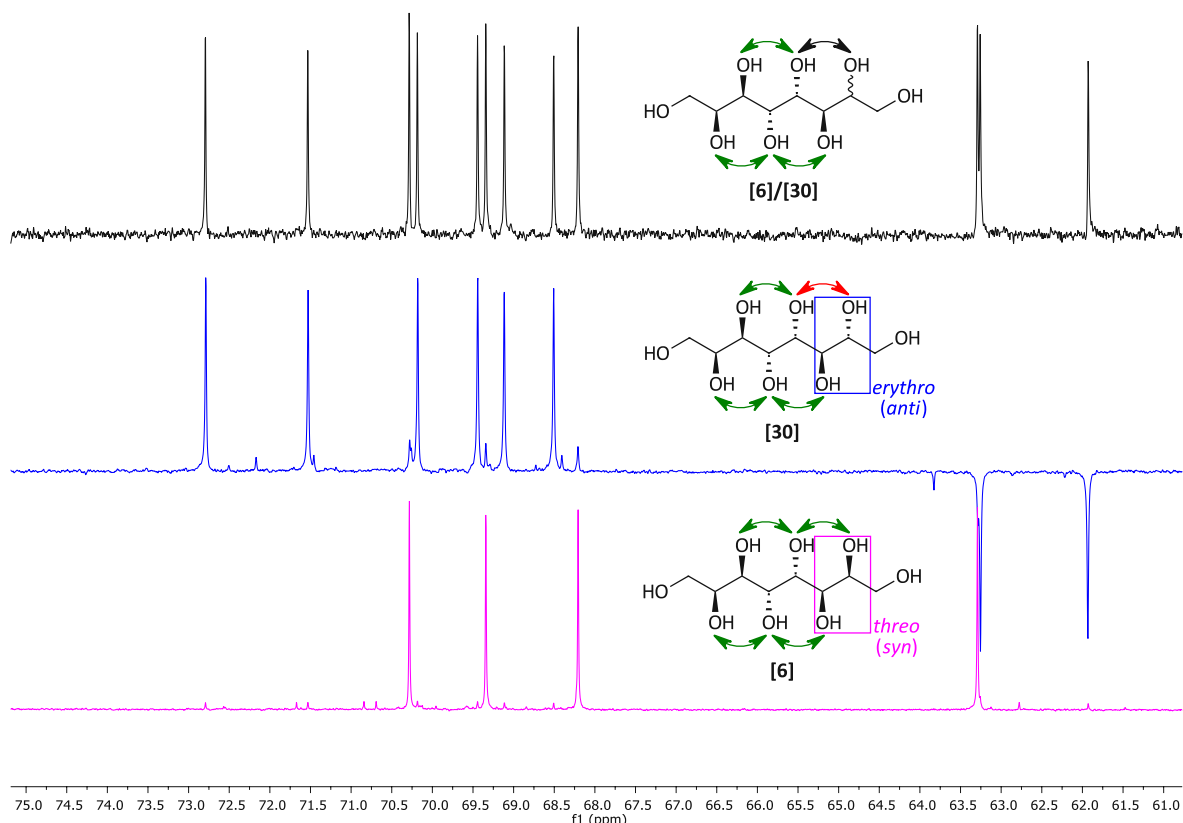


Figure 25. Comparison of the ^{13}C -NMR spectra of a *threo/erythro*-octitol mixture [6]/[30] (top, black), the *erythro*- [30] (middle, blue) and *threo*-octitol [6] (bottom, pink)

The carried out dihydroxylation reactions and the obtained *threo/erythro*-product ratios, determined by ^{13}C -NMR analysis upon deprotection, are displayed in Table 13.

Table 13. Screening results for the different dihydroxylation conditions and octenitol substrates on analytical scale

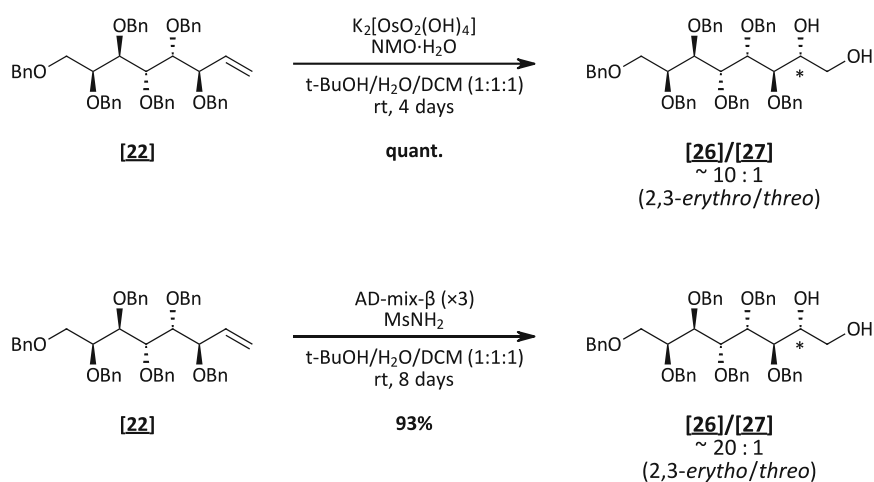
R	$\text{K}_2[\text{OsO}_2(\text{OH})_4] + \text{NMO}$		AD-mix- α (x3) + MsNH_2		AD-mix- β (x3) + MsNH_2	
	Yield (2 steps)	Ratio <i>threo/erythro</i> (^{13}C -NMR)	Yield (2 steps)	Ratio <i>threo/erythro</i> (^{13}C -NMR)	Yield (2 steps)	Ratio <i>threo/erythro</i> (^{13}C -NMR)
Ac	98%	1 : 1.4-1.5	95%	1 : 1.3	quant.	1 : 2.3-2.4
Bn	96%	1 : 10	quant.	1 : 9	quant.	1 : 20
acetone	quant.	1 : 1.6-1.7	99%	1 : 1.5	96%	1 : 1.2

In all cases, the desired product [6] with *threo*-configuration of the introduced secondary hydroxy group and the alkyl-/aryloxy group was the minor one, independent of the used substrate and dihydroxylation conditions. Surprisingly, the selectivity for the *erythro*-product [30] in the Upjohn dihydroxylation of the acetate [21] and acetonide protected octenitols [23] was not as high as expected from a related literature case⁸⁴. Furthermore, both AD-mixes containing different chiral ligands gave the *erythro*-configured product [30] as the major one, with only small deviations towards opposite sides. Outstanding high diastereoselectivity for the *erythro*-product [30] was obtained for the

benzylated octenitol **[22]** as a substrate, independent of the applied dihydroxylation conditions.

B 3.3.3 Dihydroxylation of the Bn-protected octenitol with high selectivity for the 2,3-*anti*-product

As it turned out, that under common dihydroxylation conditions the synthesis of the desired octitol with all hydroxy groups in a 1,3-*anti* relationship cannot be accomplished, an adaption of the planned synthesis strategy was necessary. The idea was to perform the dihydroxylation of benzylated octenitol **[22]** with high diastereoselectivity for the untargeted *erythro*-configured isomer **[30]**, and then invert the stereochemistry of the free secondary hydroxy group to get towards the targeted octitol species **[6]**. Therefore, the dihydroxylation of the hexabenzyl-octenitol **[22]** was carried out on larger scale under Upjohn (Scheme 34 (top)) and Sharpless conditions, using AD-mix- β ($\times 3$) (Scheme 34 (bottom)).



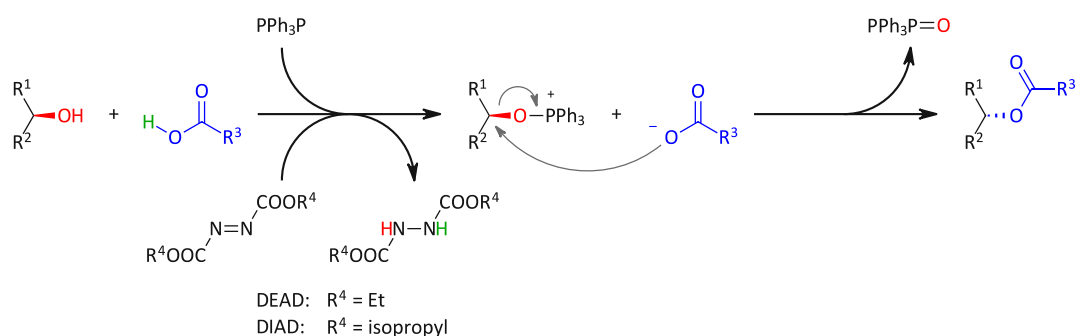
Scheme 34. Dihydroxylation of the benzylated octenitol **[22]** on larger scale under Upjohn (top) and Sharpless conditions (bottom), both with high selectivity for the 2,3-*anti*(*erythro*)-product **[26]**

Compared to the analytical experiments on small scale, significantly lower reaction rates were observed with reaction times of up to 8 days, and further, more AD-mix was necessary to obtain full consumption of the starting material in the case of the Sharpless DH.

B 3.4 Inverting the stereochemistry *via* a Mitsunobu protocol

A well-established method for the inversion of stereochemical centres is the Mitsunobu reaction. In general, the Mitsunobu reaction is a bimolecular nucleophilic substitution (S_N2) reaction where a primary or secondary alcohol is coupled with a pronucleophile (NuH). This substitution is mediated by a redox combination of a dialkyl azodicarboxylate, diethyl azodicarboxylate (DEAD) and diisopropyl azodicarboxylate (DIAD) being the most common ones, and a trialkyl- or triarylphosphine, usually triphenylphosphine (PPh_3).⁹⁷ When a chiral, secondary alcohol is used as a substrate, full inversion of the stereochemistry is observed

in the substitution of the hydroxy group with the nucleophile. Suitable pronucleophiles for the formation of the desired C-O bonds are acidic species, for example, carboxylic acids and phenols, giving the corresponding esters.⁴⁸

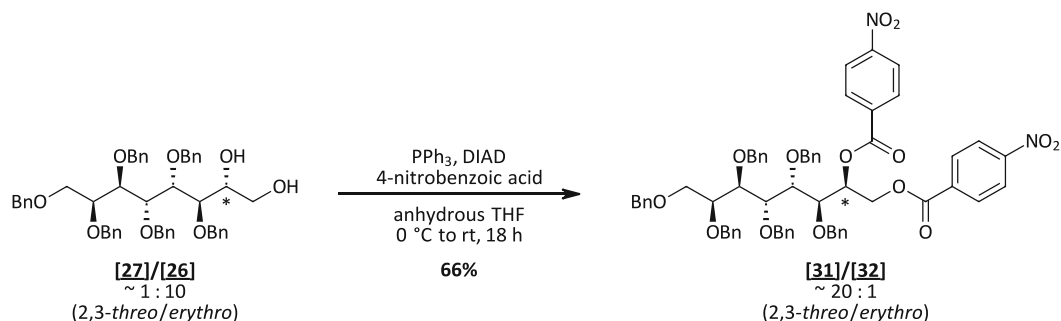


Scheme 35. General Mitsunobu reaction of a secondary alcohol with a carboxylic acid as the nucleophile, mediated by PPh₃ and a dialkyl diazocarbonylate, giving the corresponding ester

To invert the stereochemistry of the secondary hydroxy group that was introduced *via* asymmetric dihydroxylation, we considered a Mitsunobu reaction under classical conditions, using a carboxylic acid as the nucleophile. As it is shown in the general Scheme 35, the corresponding ester is formed which can be cleaved subsequently to obtain the hydroxy group again. In our case, two free hydroxy groups are present in the substrate **[8]**, a primary and a secondary one. Therefore, we thought of performing a "double Mitsunobu" reaction that leads to the esterification of both hydroxy groups by using an excess of reagents to get towards the octitol with all (protected) hydroxy groups in the desired 1,3-*anti*-relationship. Examples from literature that showed "double Mitsunobu" reactions on 1,2-diols in sterically even more demanding substrates with 4-nitrobenzoic acid as the nucleophile⁹⁸⁻⁹⁹ encouraged our intention.

In preliminary experiments, acetic acid was used as the nucleophile together with PPh₃ and DIAD in THF on a diastereomeric mixture of partly benzylated octitol **[26]**/**[27]** with a ratio of about 10:1 (*erythro*/*threo*). According to HPLC-MS of the reaction mixture, a monoester was formed under these conditions, but no full conversion of the starting material was achieved, even though all reagents were present in excessive amounts (5 equivalents). A study by Hughes and Reamer¹⁰⁰ on the effect of acid strength in Mitsunobu esterification reactions might explain the unsuccessful esterification of the substrate with acetic acid, as weaker acids react faster with the adduct formed between PPh₃ and DIAD than the alcohol. Due to this, the carboxyl is favourably activated instead of the alcohol, and the ester formation cannot occur. For stronger acids, like, for example, 4-nitrobenzoic acids, it was shown, that the rates of both activation reactions, the carboxyl and hydroxyl activation, are reduced, but the wanted hydroxyl activation leading to successful esterification is significantly favoured. This provides better yields in esterification reactions and further allows the esterification of sterically hindered alcohol substrates as it is the case for our substrate.¹⁰⁰ According to this, we switched to 4-nitrobenzoic acid as the nucleophile that is a stronger acid (pK_A 3.45¹⁰¹) than acetic acid (pK_A 4.74¹⁰¹). The reaction was then performed under anhydrous conditions in THF by mixing the starting material and an excess

of PPh₃ and 4-nitrobenzoic acid (5 equiv. each), and subsequent addition of DIAD (5 equiv.) at 0 °C. Proceeding the reaction under room temperature, the targeted "double Mitsunobu" product **[31]** could be obtained in good yield after purification *via* column chromatography (Scheme 36).

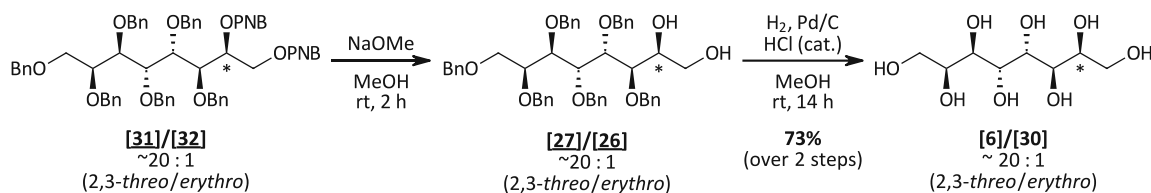


Scheme 36. "Double Mitsunobu" reaction of a diastereomeric mixture of the partly benzylated octitol with a ratio of about 1:10 of the 2,3-*threo*- and 2,3-*erythro*-configured isomer

As the starting material was a mixture of the two diastereomers **[27]/[26]**, the obtained fully protected sugar alcohol **[31]** was contaminated with a small amount of the sugar alcohol species with one 1,3-*syn* relationship (*erythro*-configuration) **[32]**, but the enantiomeric purity could be improved from 90% to 95%. This enhancement is addressed to the chromatographic purification step that was performed after the Mitsunobu reaction.

B 3.5 Deprotection towards the octitol

The targeted octitol **[6]** could then be obtained by subsequent deprotection of **[31]**. First, the 4-nitrobenzoate esters (PNB) were cleaved *via* transesterification, using NaOMe in MeOH, followed by reductive hydrogenation using palladium on activated charcoal as the catalyst. As a diastereomeric mixture was used as starting material, the octitol **[6]** was not obtained in pure form and further purification was necessary.

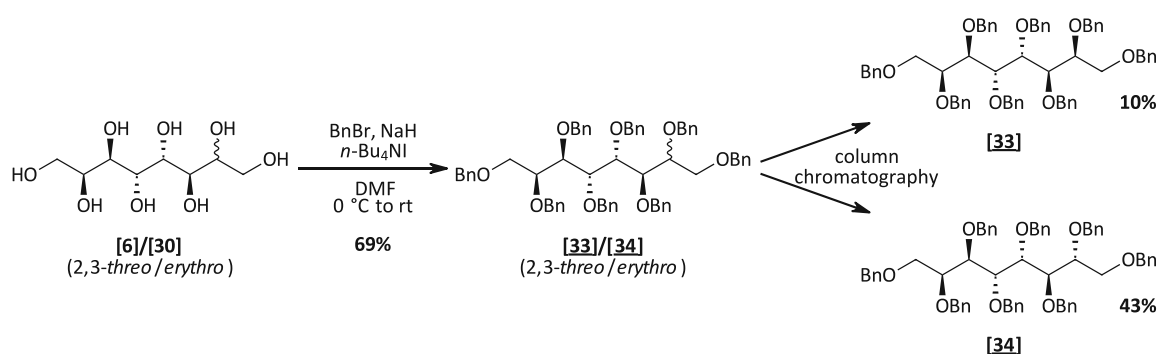


Scheme 37. Deprotection of the "double Mitsunobu" product **[31]/[32]** towards the free sugar alcohol **[6]/[30]**

B 3.6 Purification of the enantiomeric mixture

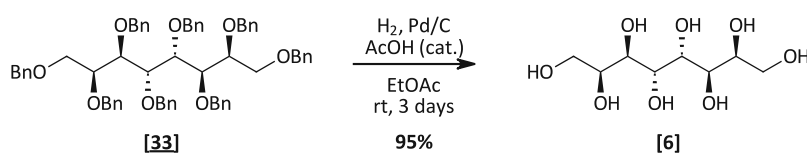
According to experiences with the separation of diastereomeric enitol mixtures, it was assumed that the fractioning of the two diastereomeric octitols **[6]** and **[30]** should be possible *via* recrystallisation. The *galacto*-isomer **[6]** was expected to be less soluble than the *talo*-isomer **[30]** due to higher crystallinity because of the perfect *1,3-anti*-distribution of all hydroxy groups. Therefore, recrystallisation was performed from several mixtures of MeOH and H₂O (4:1, 1:4, 1:8, 1:10) and also H₂O. Still, only further enrichment of the *galacto*-isomer **[6]** could be achieved, but never a complete removal of the *talo*-isomer **[30]**.

Due to new findings in the synthesis route towards the *galacto*-decitol (see Chapter B 4.3), a different attempt was chosen to get pure *L-threo-D-galacto* octitol **[6]** from the isomer mixture. Therefore, a mixture of the diastereomers *L-threo-D-galacto*- **[6]** and *L-threo-D-talo*-octitol **[30]** (major component) was transformed into the corresponding octabenzyl-species **[33]** and **[34]** which were then separated by column chromatography. Complete separation of the two diastereomers was not possible using a regular silica column, but some pure material of both could successfully be isolated.



Scheme 38. Formation of the octabenzyl octitols for separation of the two diastereomers **[33]** and **[34]** *via* column chromatography

The following deprotection *via* catalytic hydrogenation gave the *L-threo-D-galacto*-octitol **[6]** in enantiomerically pure form. Usually, MeOH was used as the solvent in the catalytic hydrogenation together with HCl in catalytic amounts. As the starting material **[33]** was insoluble in MeOH, the solvent was switched to EtOAc with a few drops of acetic acid. Under these conditions, full deprotection of the *galacto*-octitol could be achieved although in a rather sluggish fashion (see also Chapter B 4.5 for issues in the hydrogenolysis protocols and solutions thereof).

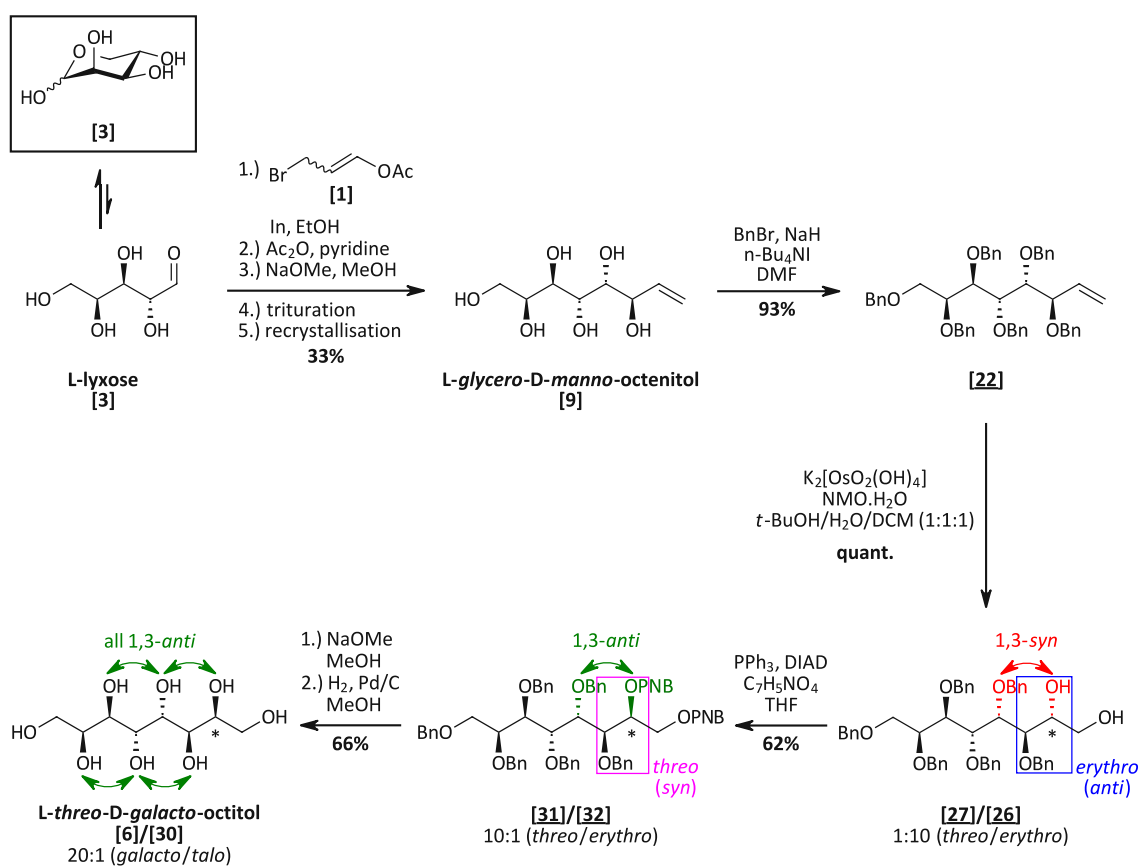


Scheme 39. Catalytic hydrogenation of octabenzyl-*galacto*-octitol **[33]** towards the desired *galacto*-configured C8 sugar alcohol **[6]**

B 3.7 Summary of the synthesis route towards the *L-threo-D-galacto*-octitol

A synthesis route towards the *L-threo-D-galacto*-octitol [6] was successfully developed. The major steps starting from the *L*-lyxose [3] are the following:

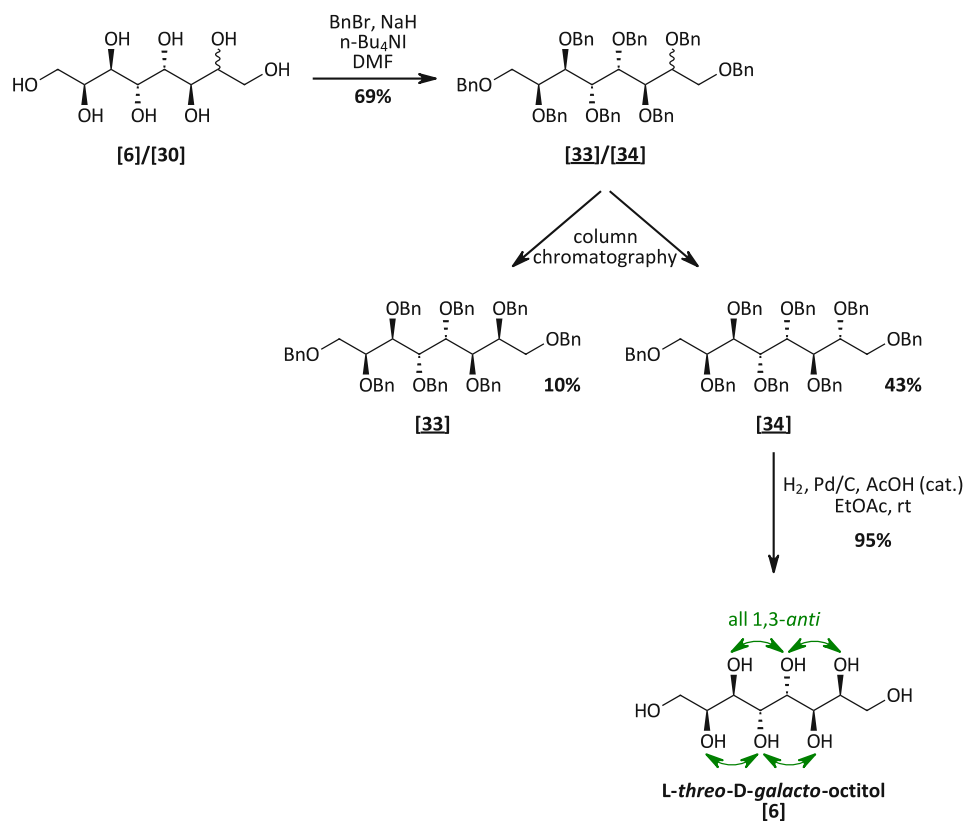
- (1) Indium mediated acyloxyallylation
- (2) Protection of the enitol species
- (3) Diastereoselective dihydroxylation
- (4) "Double Mitsunobu" reaction
- (5) Deprotection



Scheme 40. Complete synthesis route towards the *L-threo-D-galacto*-octitol [6]

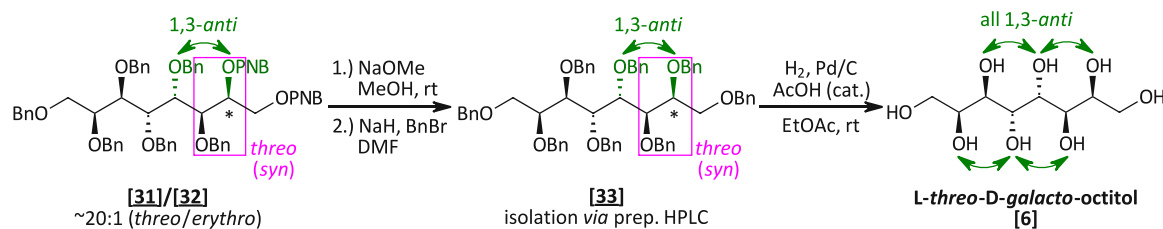
The biggest challenge in the synthesis of the *L-threo-D-galacto*-octitol [6] was that in the key steps of the sequence (IMA, dihydroxylation, Mitsunobu reaction) always a mixture of isomers was obtained as products. For the IMA, the isolation of the desired *lyxo*-configured diastereomer [9] could be performed successfully using the established trituration/recrystallisation protocol from Stanetty and Baxendale²³ Draskovits, et al.²⁴. However, the separation of diastereomeric octitol-mixtures [6]/[30] turned out to be quite challenging in the later steps, and the *talo*-configured isomer [30] could never fully be separated from the desired *galacto*-octitol [6]. It had been assumed that separation could be performed at the end of the sequence *via* recrystallisation due to their expected different physical properties, as described in Chapter B 3.6. Therefore, initially the focus

was not on the separation of the obtained diastereomer mixtures along the synthetic sequence. Besides, the isomers were always observed as one species in the analyses carried out (TLC, HPTLC, HPLC-MS) in the synthetic path. As it turned out that the purification could not successfully be performed by recrystallisation, especially on the performed scales, it was necessary to look for another option to get enantiomerically pure *galacto*-octitol [6]. To this end, the octitol isomer mixtures [6]/[30] obtained from the performed dihydroxylation reaction condition screening were transformed into the octabenzyl species [33]/[34] as at this stage separation was possible *via* column chromatography (Scheme 41).



Scheme 41. Alternative route towards enantiomerically pure *L-threo-D-galacto*-octitol [6] *via* the octabenzyl-octitol [33] as separation of the two diastereomers [33] and [34] was found to be possible at this stage *via* column chromatography

In order to lower the number of steps in the sequence, the octabenzyl-octitol **[33]** could be obtained from the hexabenzyl-octitol mixture **[6]/[30]** after the cleavage of the nitrobenzoate esters from the Mitsunobu product **[26]/[27]**. By performing preparative HPLC, the fully protected octitol **[33]** can be obtained in diastereomerically pure form, and subsequent catalytic hydrogenation then gives the desired *L-threo-D-galacto*-octitol.



Scheme 42. Assumed alternative route towards enantiomerically pure *L-threo-D-galacto*-octitol **[6]** via the octabenzyl-octitol **[33]** which should be isolated by preparative HPLC of the diastereomeric mixture

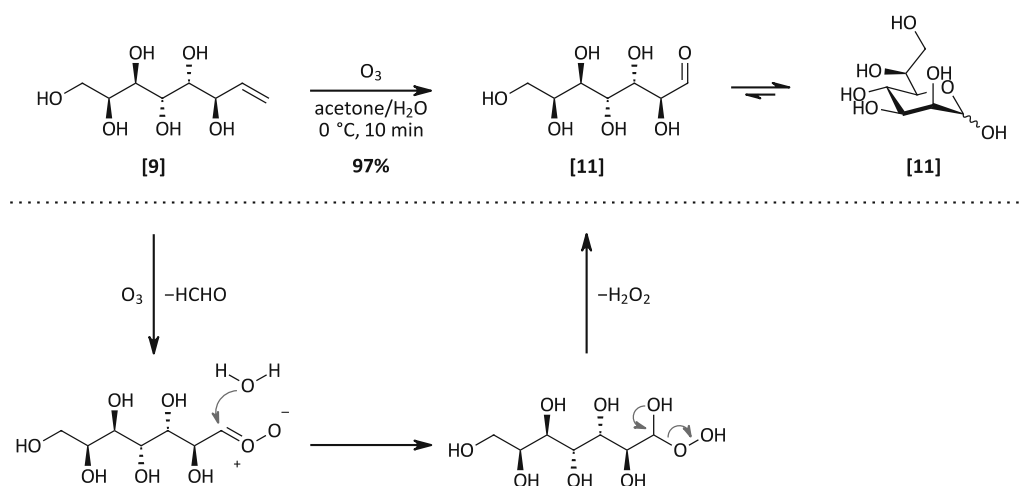
B 4 Synthesis of *galacto*-decitol – Application of the developed synthetic route

As a synthetic protocol for the *galacto*-octitol [6] could successfully be developed in which the single steps were deeply investigated and optimised, we further planned to use this route to get towards the two carbon longer *galacto*-decitol [7] (C10 sugar alcohol) in analogous manner. However, we did not expect that the investigated sequence can be easily applied as physical properties due to the presence of two more carbon atoms and therefore two more hydroxy groups might get even more "extreme" and cause problems like solubility issues, steric hindrance, etc. It was especially expected that an improved IMA protocol would be necessary as higher-carbon aldoses (above pentoses) are known to be generally less reactive in reactions at the aldehyde functionality according to a lower OCC (see Chapter A 1.4.2) in solution which has already been observed in our group for the hexose D-mannose.

In general, all steps after the indium-mediated acyloxyallylation (Chapter B 3.1) presented within this chapter have not been optimised according to the obtained yields and will be further improved in the future upon repetition.

B 4.1 Preparation of *L-glycero-D-manno*-heptose *via* ozonolysis

As the retrosynthetic analysis in Chapter B 1 shows, the synthesis of the *L-galacto-L-galacto*-decitol [7], short *galacto*-decitol, requires the reducing sugar *L-glycero-D-manno*-heptose [11] as starting point. This non-natural sugar can be obtained *via* ozonolysis of *L-glycero-D-manno*-octenitol [9], an intermediate in the synthetic route towards the *galacto*-octitol [6] (Chapter B 3.1). The ozonolysis was performed using a modern ozonolysis protocol¹⁰² that was adapted in our group for polar compounds²³⁻²⁴. In this, water is used as a solvent together with acetone and the reaction is conducted at 0 °C. Due to the presence of water, the aldehyde can directly be obtained from the organic peroxide that is formed as an intermediate leading to the formation of H₂O₂ as a by-product (putative mechanism in Scheme 43 (bottom)). The H₂O₂ and other formed peroxides are then reduced with PPh₃ which can easily be removed by extraction with organic solvents, together with the formed oxidation product PPh₃=O, allowing the isolation of pure heptose [11] from the aqueous layer. Following this protocol, the octenitol [9] was converted to the *L-glycero-D-manno*-heptose [11] with excellent yield (Scheme 43 (top)).



Scheme 43. Ozonolysis towards the *L-glycero-D-manno-heptose* **[11]** (top), including the putative mechanism of the ozonolysis with a water/acetone mixtures as a solvent (bottom)

As large quantities of the heptose peracetate **[5]** were available in our group, the ozonolysis was only carried out on a small scale. The heptose material used for the following step was obtained *via* Zémlen deacetylation of the peracetate **[5]** using NaOMe in MeOH. The obtained *L-glycero-D-manno-heptose* **[11]** was then used without further purification.

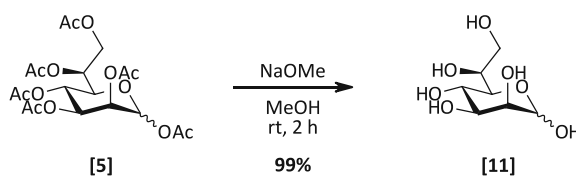


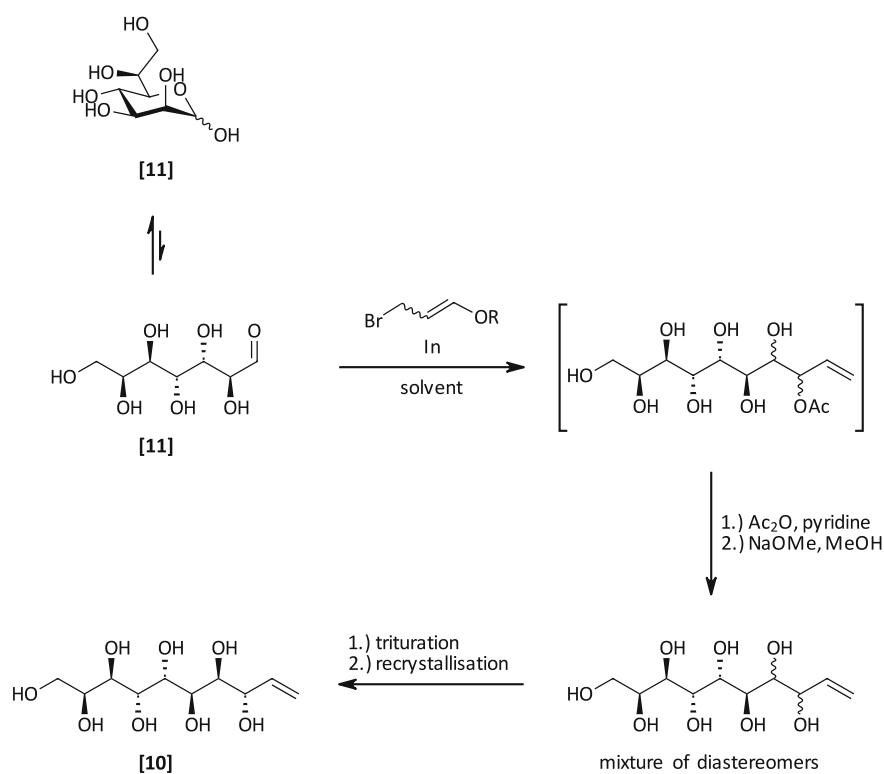
Figure 26. Preparation of *L-glycero-D-manno-heptose* **[11]** from the corresponding peracetate species **[5]**

B 4.2 Indium-mediated acyloxyallylation of *L-glycero-D-manno-heptose* towards the *manno-decenitol*

With the starting material in hand, the indium-mediated acyloxyallylation was aimed next. As already pointed out in the aim of the thesis (Chapter A 5), an improved elongation protocol was necessary at this stage due to the already known problems in the IMA of aldoses with lower solubility and reactivity under the usual IMA conditions that were described for the more reactive lyxose (see Chapter B 3.1). Therefore, the development of the indium-mediated acyloxyallylation for the unreactive aldose heptose is described in this chapter.

In general, the IMA was planned to be performed using indium and a 3-bromopropenyl ester to obtain a diastereomeric mixture of the decenitol species from the C7-sugar **[11]** that is converted into the free decenitol **[10]** by following a peracetylation – Zémlén deacetylation sequence (Scheme 44). As it has already been described in earlier chapters, this addition of organoindium reagents presented here shows high diastereoselectivity

towards the *lyxo*-configured enitol product **[10]** that can generally be isolated due to its superior crystallinity and therefore lower solubility compared to the other isomers. This observed property is addressed to the fact that in the *lyxo*-enitol all hydroxy groups are in a 1,3-*anti*-relationship, comparable to the rules of Inagaki and Ishida⁷⁶ for the sugar alcohols.



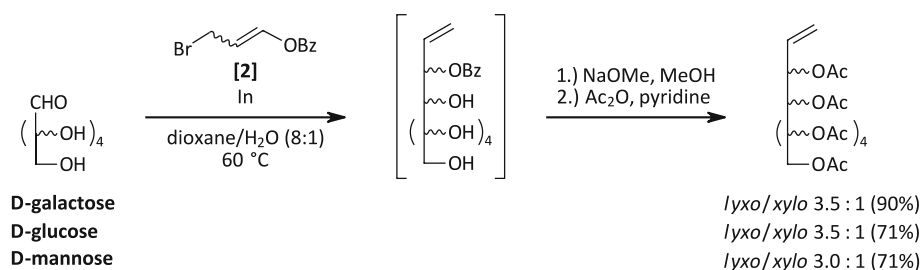
Scheme 44. General pathway of the indium-mediated acyloxyallylation of *L*-glycero-*D*-manno-heptose **[11]** towards the decenitol **[10]**

B 4.2.1 Performing the IMA using the Barbier-type protocol

Initially, the elongation of the heptose **[11]** towards the corresponding decenitol **[10]** was carried out according to the procedure for lyxose presented in Chapter B 3.1, using 3-bromopropenyl acetate **[1]** as the reagent and EtOH as the solvent. However, preliminary experiments on this, performed on a small scale (~60 μmol in 300 μL EtOH (0.2 M)), gave only little of the desired product according to TLC analysis. Compared to lyxose, the heptose **[35]** is less soluble in EtOH which slows down the reaction rate drastically. This problem was anticipated as it has already been observed earlier in our group when the acyloxyallylation of the hexose *D*-mannose was carried out (Chapter A 2.2.3.4). In that case, the drawback of low solubility could be overcome by increasing the amount of solvent (concentration <1% according to the starting material) and reagent.⁷⁷ Those changes made a quick addition of the indium as well as the reagent even more crucial together with efficient stirring, in order to suppress side reactions of the reagent. Furthermore, mannose shows a lower open-chain content than lyxose as it has been discussed in Chapter A 1.4.2. This influences the reaction rate, too, as the aldehyde functionality is not as readily

available as for aldoses with high OCCs in solution. Therefore, no full conversion had been achieved with mannose. In general, in the In-mediated acyloxyallylation, the balance between the availability of the free aldehyde moiety of the aldose and the stability of the organometallic reagent is crucial. For an aldose, that shows a low open-chain content, the reaction rate is expected to be lower than for an aldose with a high OCC in solution. This means that a longer lifetime of the elongation reagent in the reaction mixture is crucial to obtain complete conversion of aldoses like this.

To overcome the solubility issues, the solvent was changed to a dioxane/H₂O mixture (8:1) which also required the use of 3-bromopropenyl benzoate **[2]** instead of 3-bromopropenyl acetate **[1]** due to higher stability of the benzoate ester under aqueous conditions. This protocol was presented by Palmelund and Madsen²² for the less reactive hexoses D-mannose, D-galactose and D-glucose obtaining the corresponding nonenitol peracetates with diastereoselectivity for the *lyxo*-product over the *xylo*-product with good to excellent yields (Scheme 45).

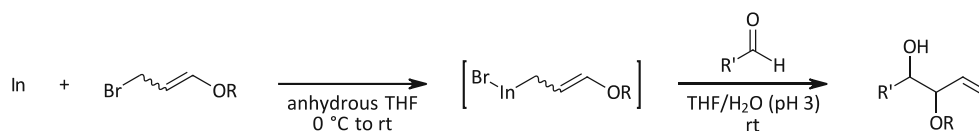


Scheme 45. IMA of hexoses with 3-bromopropenyl benzoate **[2]** in a dioxane/H₂O mixture performed by Palmelund and Madsen²²

However, applying this protocol to the *glycero-manno*-heptose **[35]** (0.1 M) with In (2.0 eq.) and 3-bromopropenyl benzoate **[2]** (3.0 eq.) in dioxane/H₂O, still, only about 20% conversion to the two main diastereomeric decenitols (*lyxo* and *xylo*) was observed. The quantification was performed *via* ¹H-NMR after the sequence IMA – acetylation – deprotection was followed, using maleic acid as an internal standard that gives a singlet at 6.40 ppm in D₂O representing two protons. For the enitol species, the diagnostic signals at 4.20 ppm (H3 *lyxo*) and 4.26 ppm (H3 *xylo*) were considered.

B 4.2.2 A two-step Grignard protocol for the IMA

As both literature-known Barbier-type protocols for the indium-mediated acyloxyallylation of aldoses did not work smoothly for the heptose, we considered a classic Grignard two-step protocol that involves the pre-formation of the organoindium-species under anhydrous conditions followed by the addition of phthalate buffer (pH 3) and the aldehyde species. This synthetic protocol was developed and investigated by Lombardo, et al.³⁸ for simple aldehydes and is shown in Scheme 46 in general.



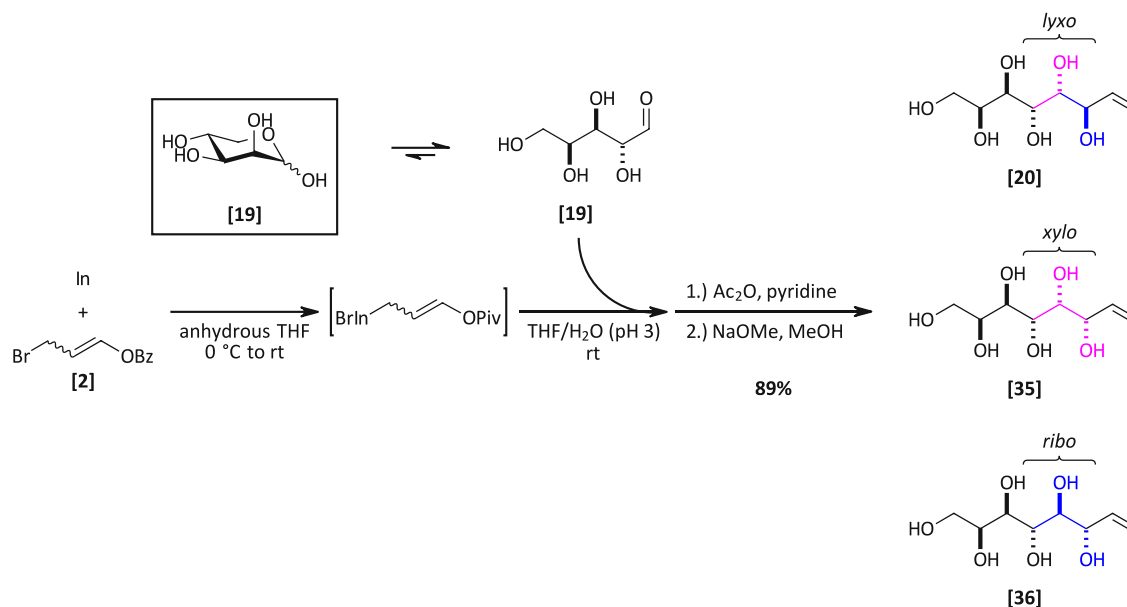
Scheme 46. General two-step Grignard protocol for the indium-mediated acyloxyallylation of aldehydes using indium in THF/H₂O (pH 3)

According to our findings so far, we assumed that this protocol could overcome the observed issues regarding the acyloxyallylation of the heptose and bring the following improvements:

- (1) The heptose **[11]** showed significantly lower reactivity than the lyxose **[3]** in the IMA under the tested conditions so far. We assume that this can be addressed to a lower open-chain content and therefore lower availability of the free aldehyde moiety of the sugar. Therefore, the two-step protocol might be beneficial as the aldose present in the open-chain form can immediately react with the organometallic species, which impacts the chemical equilibrium between the cyclic and open-chain form, leading to a faster (re)formation of the open-chain structure and therefore faster reaction rates.
- (2) In the Barbier-type protocol with aqueous reaction conditions, the added bromopropenyl ester might be hydrolysed before forming the organoindium species. Due to this, less reagent is present in the reaction mixture, which leads to lower conversion of the starting material to the desired product. Even though this is not a problem, for example, in the IMA of the reactive sugar lyxose **[3]**, it might become an issue when a less reactive aldose is used as a starting material where the reaction rate is lower (see (1)), and stability of the reagent plays a more important role. By performing the organoindium species under anhydrous conditions, the hydrolysis of the bromopropenyl ester cannot occur, and an early decomposition of the reagent precursor should not be an issue anymore.
- (3) The solubility of the heptose should be given in the aqueous buffer.

According to our knowledge, this two-step protocol has not been implemented in the IMA of aldoses so far. Therefore, we first investigated this procedure for the reactive D-lyxose **[19]**. In contrast to Lombardo, et al.³⁸, we decided to use the 3-bromopropenyl benzoate **[2]** instead of 3-bromopropenyl acetate **[1]** due to the higher stability of this reagent under aqueous conditions. Following the procedure, the organoindium species was pre-formed by stirring indium and the bromopropenyl ester vigorously in anhydrous THF at 0 °C and allowing the reaction mixture to warm up to room temperature after 5 min. As the reagent formation proceeded, a solution with only a little indium left was obtained within 40 min, to which the aldose (0.13 mmol) was added as a solution in phthalate buffer (pH 3). TLC analysis at this stage indicated complete conversion of the sugar to the desired enitol species and ¹H-NMR analysis of the crude mixture after following the peracetylation – Zemplén deacetylation sequence confirmed the applicability of this protocol for sugar species. As for the Barbier-type protocol, the *lyxo*- and *xylo*-configured octenitols **[20]** and **[35]** were the major diastereomers in the mixture and the ratio determined by ¹H-NMR

was found to be *lyxo* : *xylo* : *ribo* = 71 : 18 : 11, which represents an even slightly increased selectivity over the standard Barbier type protocol. This observation is in accordance with the findings of Draskovits, et al.²⁴, who investigated different halopropenyl esters in the IMA of L-erythrose.



Scheme 47. Indium-mediated acyloxyallylation of D-lyxose **[19]** using a two-step Grignard protocol adapted from Lombardo, et al.³⁸ with 3-bromopropenyl benzoate **[2]**, giving the *lyxo*-octenitol **[20]** as the major isomer

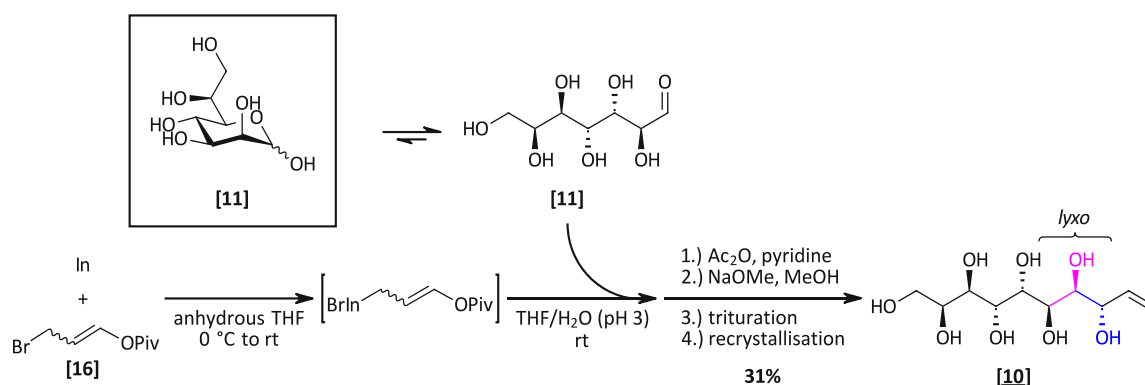
We set out to apply the new protocol for the IMA of the *glycero-manno*-heptose **[11]**. However, no full conversion of the starting material could be achieved and the overall yield for the diastereomeric mixture of decenitols was only about 40% according to ¹H-NMR analysis (quantification with maleic acid as internal standard), an improvement to the Barbier conditions but not enough to be practical.

Further, we moved on to another reagent, the 3-bromopropenyl pivalate **[16]**, that has already been investigated in the IMA of tetroses in our group⁷⁷. Compared to the acetyl and benzoyl esters, the pivaloyl ester is more stable against hydrolysis due to sterical demand of the pivalate group, enhancing the lifetime of the reagent under aqueous conditions, which has been shown by Draskovits, et al.²⁴ in a time-resolved NMR-study of the bromopropenyl acetate **[1]** and bromopropenyl pivalate **[2]** as a solution in MeOH-*d*₄. This change in the synthetic protocol finally allowed us to achieve a clean transformation of the *glycero-manno*-heptose **[11]** into the corresponding decenitol species **[10]** (see Scheme 48). ¹H-NMR analysis of the decenitol crude mixture that was obtained after the peracetylation – Zemplén deacetylation sequence showed the enitols in the usual ratio of *lyxo* : *xylo* : *ribo* = 71 : 19 : 10.

B 4.2.3 Synthesis of the L-*lyxo*-L-*manno*-decenitol

With this two-step protocol in hand, the indium-mediated acyloxyallylation of the L-*glycero*-D-*manno*-heptose **[35]** was carried out at a scale of ~10 mmol in order to have

enough material in hand for the subsequent steps towards the *L-galacto-L-galacto*-decitol [7]. The organoindium species was pre-formed by mixing indium and 3-bromopropenyl pivalate [16] in anhydrous THF as it has been described in Chapter B 4.2.2. To this, the heptose [11] was added as a solution in phthalate buffer (pH 3, THF/H₂O 6:1) to give a mixture of decenitol diastereomers upon peracetylation/deacetylation with the *lyxo*-configured species [10] as the major isomer. The isolation of the *L-lyxo-L-manno*-decenitol [10] could be achieved upon repeated trituration with MeOH and final recrystallisation from water as the *lyxo*-isomer is highly crystalline due to 1,3-*anti*-distribution of all hydroxy groups which is a huge benefit in the purification and isolation procedure. The desired product [10] was obtained in enantiomerically pure form with an overall yield of 31% over three steps.

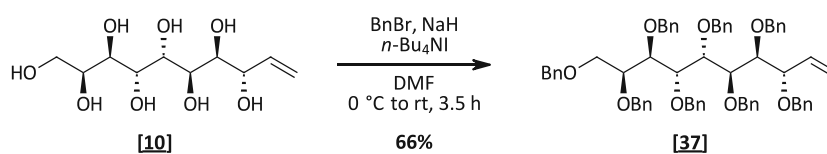


Scheme 48. Indium-mediated acyloxyallylation of *L-glycero-D-manno*-heptose [11] using a two-step Grignard protocol adapted from Lombardo, et al.³⁸ with 3-bromopropenyl benzoate [2], giving the *lyxo*-decenitol [10] as major isomer

B 4.3 Protection and dihydroxylation of the *manno*-decenitol

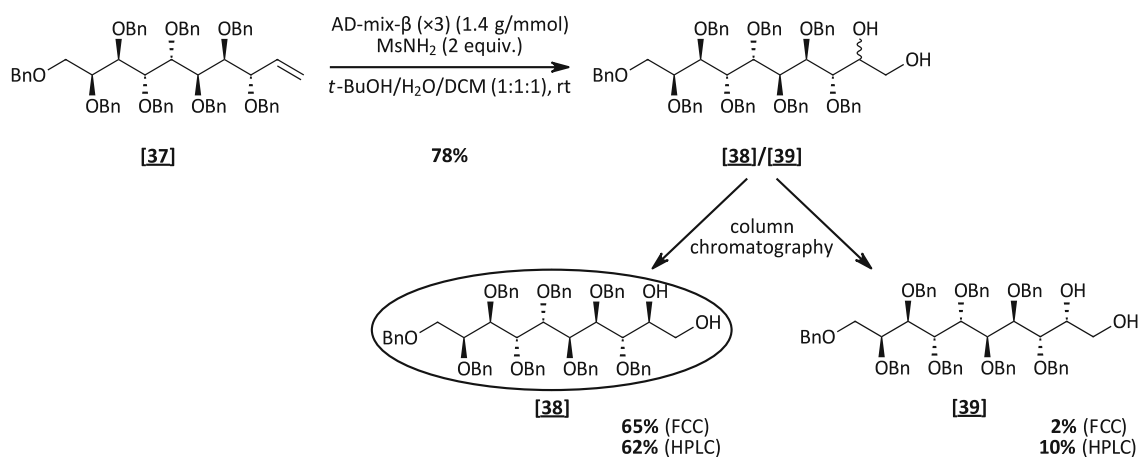
With the decenitol material in hand, the synthesis route that has been developed for the corresponding *galacto*-octitol was followed with the next steps being the benzyl-protection and subsequent diastereoselective dihydroxylation under Sharpless DH conditions.

The formation of the octabenzyl-*manno*-decenitol [37] was carried out as described in Chapter B 3.2.2. From the enitol [10], the octabenzyl-decenitol [37] was obtained by treatment with sodium hydride, benzyl bromide and a catalytic amount of tetrabutylammonium iodide. The desired product was isolated upon flash column chromatography with a yield of 66%. The low yield is to be attributed to technical losses during the workup, not to inefficiency of the used reaction protocol which suggested full conversion.



Scheme 49. Protection of the decenitol [10] with benzyl groups

With this material, the dihydroxylation reaction towards the partly benzyl-protected decitol **[37]** was performed using Sharpless dihydroxylations conditions (AD-mix- β ($\times 3$)) with high diastereoselectivity for the *L-galacto-L-talo*-configured product **[38]**, as it has been observed for the corresponding octenitol (Chapter B 3.3.2). Practically, a suspension of AD-mix- β ($\times 3$) in *t*-BuOH/H₂O (1:1) was treated with MsNH₂ to which the protected decenitol **[37]** was added as a solution in DCM (1:1:1).

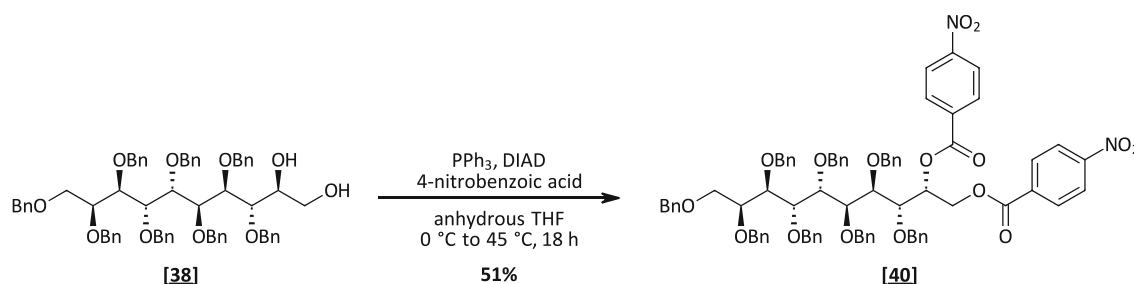


Scheme 50. Diastereoselective dihydroxylation of the octabenzyl-decenitol **[37]** using AD-mix- β ($\times 3$)

In contrast to the octitol species, TLC analysis of the reaction mixture showed two different product spots with close polarity that were assumed to be the two possibly formed diastereomers, the *talo*-decitol **[38]** and the *galacto*-decitol **[39]**. This assumption could be confirmed upon successful separation of the observed products by performing preparative normal phase HPLC on a small scale to obtain both diastereomers in pure form. Therefore, a standard flash column chromatography was performed in the case of the dihydroxylation of the octabenzyl-decenitol **[37]** at bigger scale (~ 1 mmol) subsequently to the dihydroxylation reaction to obtain a product fraction that is enriched with the *talo*-configured decitol **[38]**. This species should further be transformed into the *galacto*-configured decitol **[39]** upon Mitsunobu reaction and subsequent deprotection.

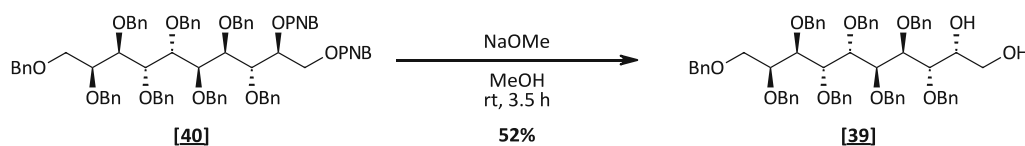
B 4.4 Mitsunobu reaction and ester cleavage towards the octabenzyl-galacto-decitol

In preliminary experiments, the "double Mitsunobu" reaction of the partly benzylated *talo*-decitol **[38]** was performed using the protocol developed for the octitol species (Chapter B 3.4). However, no full conversion could be achieved, and the synthetic procedure was further optimised regarding the order of reagent addition (according to Keith and Gomez¹⁰³) and temperature (according to Fletcher⁴⁸). In the initial protocol, the alcohol substrate, carboxylic acid and PPh₃ were mixed in the solvent (THF) and DIAD was added subsequently at 0 °C. The reaction was then conducted at room temperature. In the new protocol, the PPh₃/DIAD-complex was pre-formed at 0 °C in THF, and a mixture of the octabenzyl-*talo*-decitol **[38]** and 4-nitrobenzoic acid in THF was added. As soon as room temperature was reached, heating to 45 °C was performed to achieve full conversion of the starting material to the desired product. The "double Mitsunobu" product **[40]** was isolated upon trituration in ice-cold Et₂O (removal of PPh₃=O) and flash column chromatography with a yield of 51%. Losses of the product can be attributed to the performed trituration and difficulties in the separation *via* column chromatography due to traces of PPh₃=O that were present in the crude mixture. Likely upon repetition the achieved yields will be further improved.



Scheme 51. "Double Mitsunobu" reaction of the octabenzyl-*talo*-decitol **[38]** under optimised reaction conditions according to literature^{48,91,103}

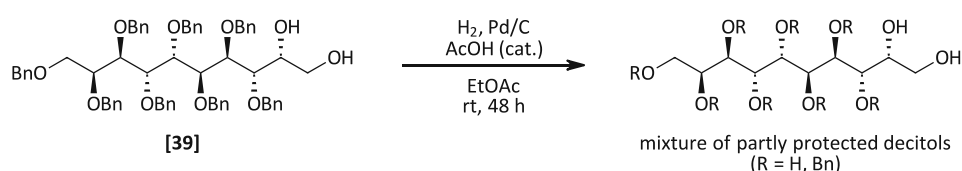
In the next step, the cleavage of the ester groups was performed *via* transesterification with NaOMe in MeOH to obtain the octabenzyl-*galacto*-decitol **[39]**. At this stage, again column chromatography was performed as traces of the octabenzyl-*talo*-decitol **[38]** were present in the obtained crude product. In the future, preparative HPLC as it has been tested for an inverse mixture of those two isomers on a smaller scale (B 4.3) will allow the isolation of pure **[39]** with a higher yield.



Scheme 52. Deprotection of the "double Mitsunobu" product **[40]** towards the octabenzyl-*galacto*-decitol **[39]**

B 4.5 Deprotection towards the L-galacto-L-galacto-decitol

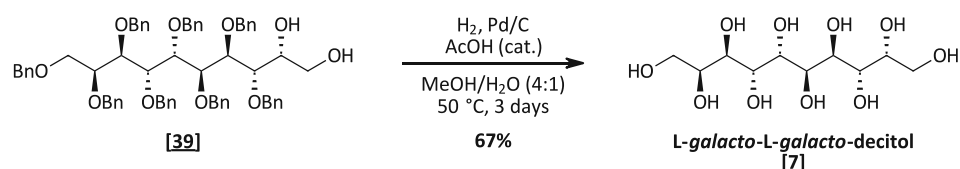
The last step in the sequence to obtain the *galacto*-decitol [7] was the deprotection of the hydroxy groups. In the octitol-case, all benzyl groups could be cleaved successfully *via* catalytic hydrogenation under standard conditions using palladium on charcoal (10 w%) as the catalyst, MeOH as the solvent, catalytic amounts of hydrochloric acid and a hydrogen balloon (see Chapter B 3.5). This protocol could not be applied here as the octabenzyl-decitol [39] was insoluble in MeOH at room temperature. Therefore, we switched to ethyl acetate instead of MeOH to achieve complete solubility of the starting material. Under these conditions, cleavage of benzyl groups could be observed, but a mixture of intermediates with a different number of benzyl groups present was obtained. According to HPLC-MS, besides products with 0 to 7 Bn-groups also starting material was left in the reaction mixture. It was assumed, that solubility issues played a major role here, as due to deprotection the material is expected to get insoluble in the organic solvent and likely precipitates, making the conversion to the free decitol impossible. Further, precipitate might coat the catalyst particles, deactivating the catalyst's surface.



Scheme 53. Catalytic hydrogenation of octabenzyl-decitol [39] in EtOAc, giving a mixture of partly protected decitols (according to HPLC-MS)

We surveyed the literature for similar cases of extreme differences in solubility between starting material and products. Following Guazzelli, et al.¹⁰⁴, who performed a global Bn-deprotection of glucuronoxylomannan (GXM) polysaccharides *via* catalytic hydrogenation, the solvent was changed to a mixture of EtOAc, water and acetic acid (4:2:1), and the reaction was conducted using a Parr hydrogenator to provide higher gas pressure (up to 5 bar). Under these conditions, no cleavage of the benzyl groups of the substrate [39] could be observed which might be addressed to the biphasic nature of the reaction mixture.

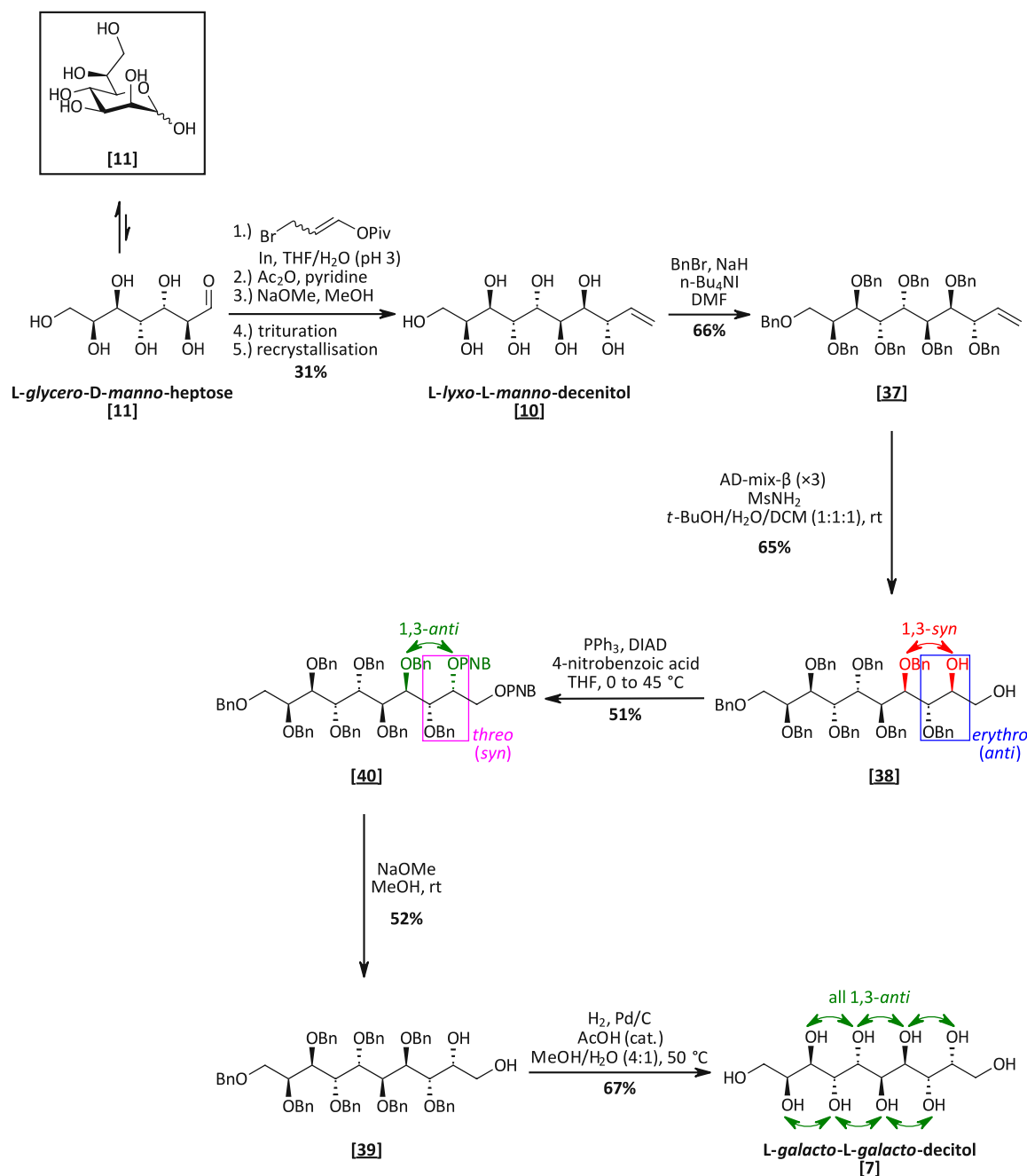
A different approach that was considered to overcome solubility issues was performing the reaction at higher temperatures. For this attempt, a mixture of MeOH and water (4:1) with acetic acid (cat.) was used as solvent and higher catalyst loading was used (1 equiv.), as the reaction was only conducted on a small scale (0.01 mmol). Performing the hydrogenation at 50 °C and atmospheric pressure, all benzyl groups could successfully be cleaved, and the targeted *galacto*-decitol **[7]** could be obtained within 3 days. This way it could be shown that the principle way is feasible and will be further optimised at larger scale in due time.



Scheme 54. Successfully performed deprotection of octabenzyl-decitol **[39]** towards the *galacto*-decitol **[7]** on small scale *via* catalytic hydrogenation at higher temperature

B 4.6 Summary of the synthesis route towards the L-galacto-L-galacto-decitol

The developed synthesis route for the *galacto*-octitol could successfully be applied to obtain the L-*galacto*-L-*galacto*-decitol [7] from the L-*glycero*-D-*manno*-heptose [11] with some necessary adaptations in the sequence.



Scheme 55. Complete synthesis route towards the L-*galacto*-L-*galacto*-decitol [7]

The main achievement herein was the development of an improved protocol for the IMA suitable for less reactive reducing sugars. By switching to a two-step Grignard protocol instead of the Barbier type protocol, a solvent change, and the use of bromopropenyl pivalate [16] instead of the corresponding acetate [1] or benzoate [2] as the reagent, the

conversion of heptose could be boosted from 20% to completion and was successfully transformed into the targeted *L-lyxo-L-manno-decenitol* [10]. Further, the octabenzyl-species [39] was obtained in diastereomerically pure form as the two diastereomeric products from the dihydroxylation step were successfully separated *via* column chromatography. This adaption in the sequence allowed the synthesis of *galacto*-configured decitol [7] without further purification at the stage of the free sugar alcohol. However, the last step of the sequence, the cleavage of the benzyl groups, turned out to be quite challenging due to solubility issues, but again the targeted product could be obtained at least on small scales upon again re-optimisation of reaction conditions (solvent, temperature). Repetition at larger scale will deliver the necessary amounts for physico-chemical evaluation.

B 5 First steps towards the *galacto*-dodecitol

We further planned to use the synthetic strategy, developed for the *galacto*-decitol [6] and already adapted on application to the *galacto*-decitol [7], to get towards the *galacto*-dodecitol [8].

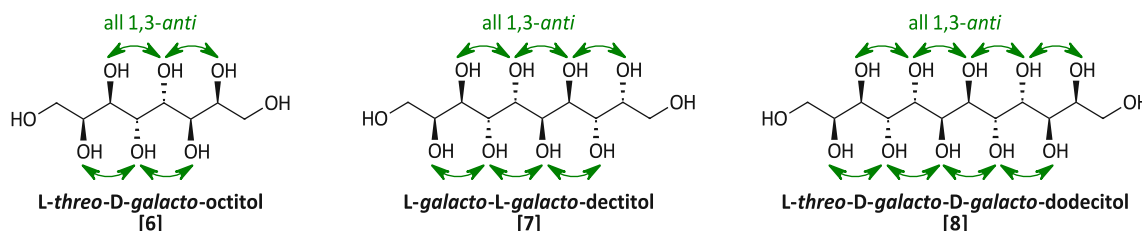
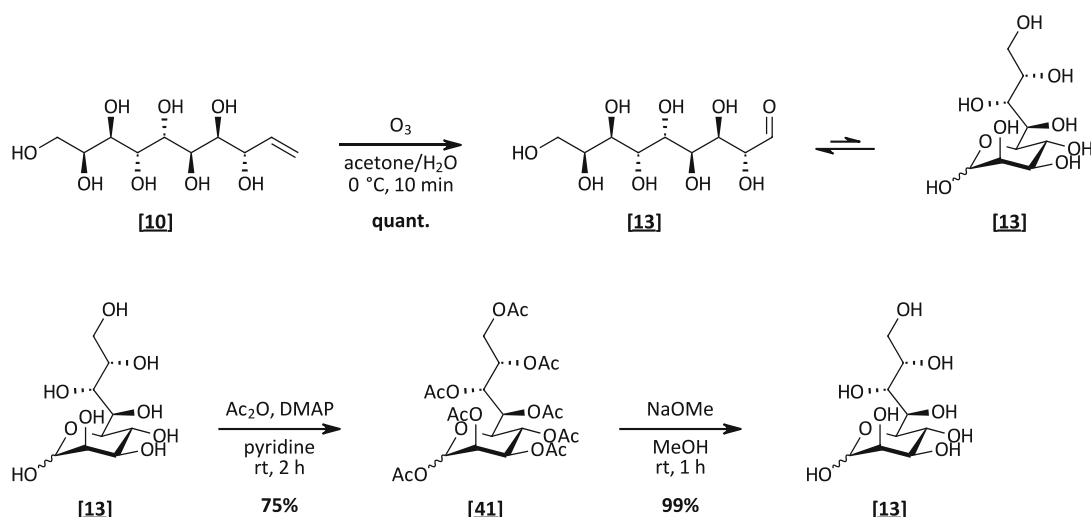


Figure 27. The three *galacto*-configured sugar alcohols of interest

According to the retrosynthetic analysis, the *L-glycero-D-manno-D-manno*-dodecenitol [8] should be obtained from the non-natural sugar *L-lyxo-L-manno*-nonose [13]. This aldose has not been described in literature yet but is accessible from *L-glycero-D-manno*-heptose [11] in the lab *via* indium-mediated acyloxyallylation with subsequent ozonolysis of the decenitol [10] that is the intermediate of the synthetic route towards the shorter decitol [7].

B 5.1 Preparation of *L-lyxo-L-manno*-nonose *via* ozonolysis

The nonose [13] could be obtained from ozonolysis of the corresponding *L-lyxo-L-manno*-decenitol [10] (Scheme 56 (top)) using the protocol that has already been described in Chapter B 4.1 for the preparation of the *L-glycero-D-manno*-heptose [11]. To dissolve the decenitol [10], the use of more water ($\text{H}_2\text{O}/\text{acetone}$ 4:1) compared to the original report²³ was necessary. Then, the ozonolysis could successfully be performed and the nonose [13] was obtained from the aqueous phase after the reduction of peroxides with PPh_3 and extraction with various organic solvents. In order to guarantee high purity of the starting material in the subsequent IMA, the nonose [13] was transformed into the corresponding peracetate [40] under classic conditions (Ac_2O , pyridine) and obtained in pure form upon flash-column chromatography ($\alpha/\beta = 2:1$ according to $^1\text{H-NMR}$ analysis). The free nonose [13] was received again *via* Zemplén deacetylation with the two anomers in a ratio of $\alpha/\beta = 6.5 : 3.5$ (Scheme 56 (bottom)).

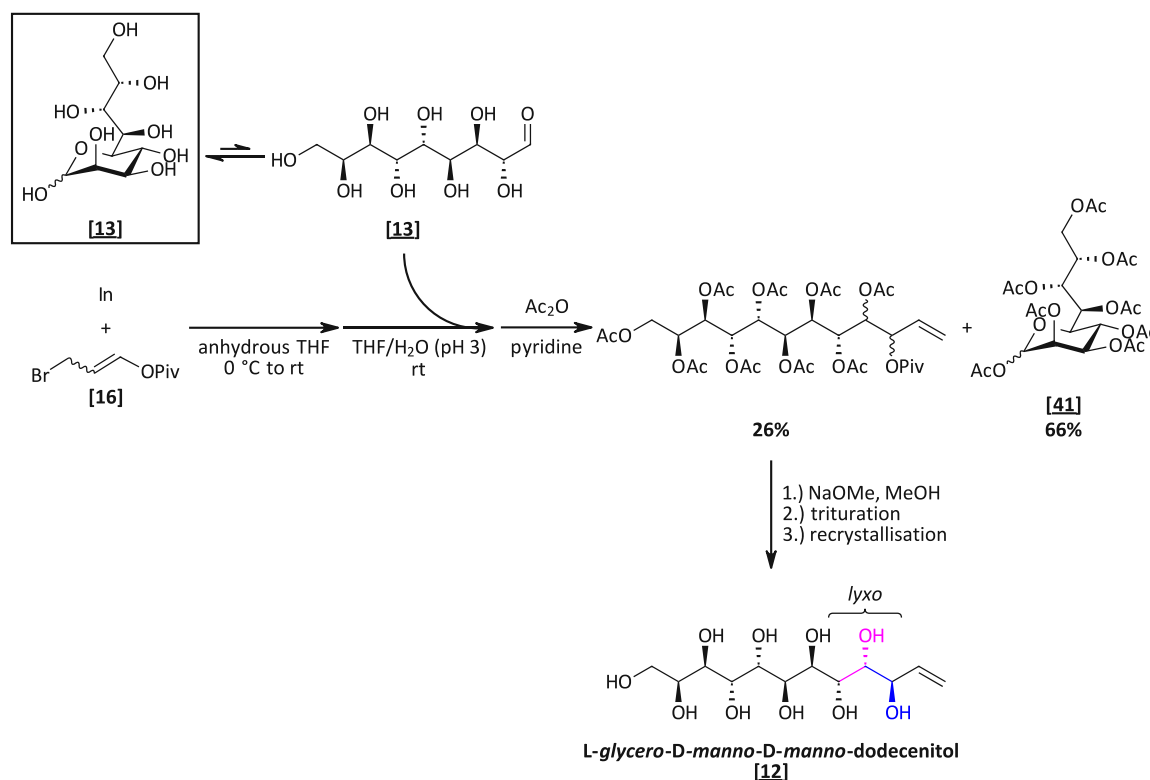


Scheme 56. Ozonolysis towards the *L*-lyxo-*L*-manno-nonose **[13]** (top) and purification via a peracetylation – Zemplén deacetylation sequence (bottom)

B 5.2 Indium-mediated acyloxyallylation of *L*-lyxo-*L*-manno-nonose towards the *manno*-dodecenitol

With the new two-step Grignard protocol for unreactive aldoses in hand, we thought that the elongation of the nonose **[13]** towards the desired dodecenitol **[12]** should be possible as it worked smoothly for the heptose **[11]**. Nevertheless, the IMA of the nonose was not successful regarding the obtained yields using the protocol described in Chapter B 4.2.3.

Preliminary experiments on the optimisation of the elongation conditions for the nonose **[13]** included the use of a higher excess of indium and bromopropenyl pivalate **[16]** and performance of the reaction at different concentrations. Still, the modified protocols did not lead to the complete conversion of the aldose to the enitol species, and the yield could not be boosted even after purification of the nonose by the described acetylation/deacetylation sequence. The IMA (0.18 mmol) was finally carried out using the Grignard two-step protocol with an excess of indium (4 equiv.) and 3-bromopropenyl pivalate **[16]** (6 equiv.) in THF/H₂O (pH 3, 5:1, 0.15 M). Isolation of the diastereomeric dodecenitol mixture was possible upon acetylation (Ac₂O, pyridine) via column chromatography but only in a yield of 26% with unreacted nonose recovered in the peracetylated form **[41]** (66%). Upon deacetylation (NaOMe, MeOH), a diastereomeric mixture of the dodecenitol species XX was obtained. To determine the diastereomeric ratio, a part of the material was taken up in D₂O to perform ¹H-NMR, which was found to be *lyxo* : *xylo* : *ribo* = 71 : 22 : 7.



Scheme 57. Indium-mediated acyloxyallylation of L-lyxo-L-manno-nonose **[13]** using the two-step Grignard protocol with 3-bromopropenyl pivalate **[16]**, giving the lyxo-configured dodecenitol **[12]** as major isomer

However, it could be proved that the synthesis of sugar species with twelve carbon atoms in the backbone is possible in general, but further investigations are necessary for a more efficient protocol. It is also expected that not only the IMA of the nonose **[13]** towards the dodecenitol **[12]** will cause troubles, but also the further steps on the path to the sugar alcohol species due to more "extrem" changes in the polarity upon protection and deprotection of the present hydroxy group, the possibility of forming more complex networks through hydrogen bond etc. as it has already been observed for the shorter decitol **[7]**.

B 5.2.1 The open-chain contents of *L-glycero-D-manno*-heptose and *L-lyxo-L-manno*-nonose

According to the findings in the performed elongations of the non-natural sugar *L-glycero-D-manno*-heptose **[11]** and *L-lyxo-L-manno*-nonose **[13]**, we were looking for an explanation for the low reactivity of those species. As already mentioned earlier, the open-chain content of sugars is assumed to impact the reactivity of the sugar in the IMA, as a low OCC means that the aldehyde functionality is less readily available to react with the organoindium species.

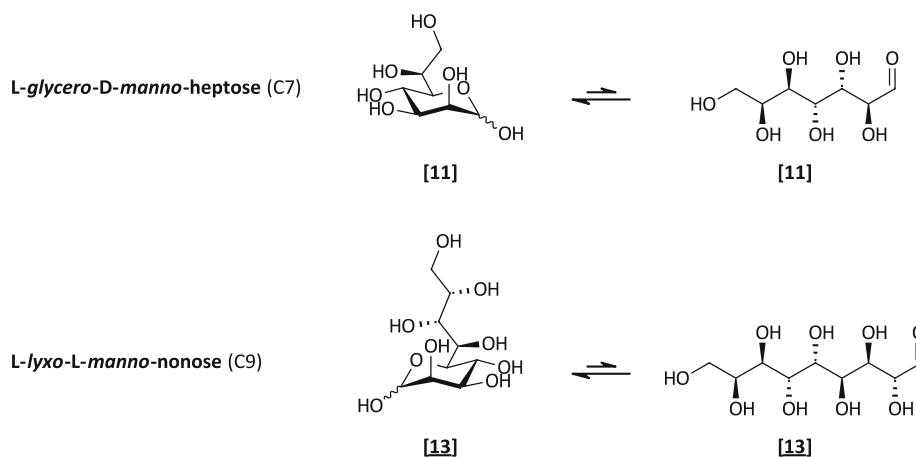


Figure 28. The aldoses *L-glycero-D-manno*-heptose **[11]** and *L-lyxo-L-manno*-nonose **[13]** in the cyclic pyranose and open-chain form

Therefore, the OCC values of the two reducing aldoses were determined using a kinetic photometric assay that was developed in the group, in which the formation of an adduct between the aldose and ABAO is followed⁷. The results of the measurements are shown in Table 14 together with the OCCs of *D*-lyxose and *D*-mannose for comparison, also determined using the same assay.

Table 14. Measured OCCs of the non-natural sugars used as starting materials for the IMA and the natural aldoses *D*-lyxose and *D*-mannose

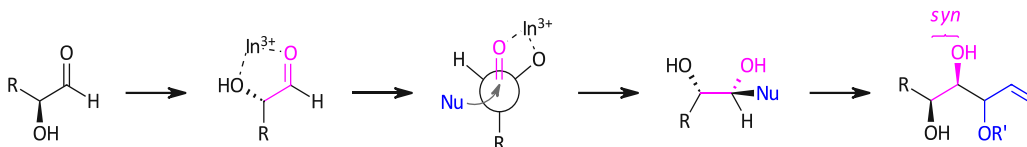
Entry	Name	No. of C-atoms	OCC (%) (ABAO assay)
1	<i>D</i> -lyxose	5	0.11
2	<i>D</i> -mannose	6	0.032
3	<i>L-glycero-D-manno</i> -heptose [11]	7	0.0344
4	<i>L-lyxo-L-manno</i> -nonose [13]	9	0.0343

It turned out, that the OCCs of the heptose (Entry **3**) and nonose (Entry **4**) were quite similar and also in the range of the hexose *D*-mannose (Entry **2**) that has already been investigated in the IMA in our group. Even though the aldehyde moiety is only little available in the mannose and heptose, those two aldoses could successfully be converted into the corresponding enitols elongated by three carbon atoms in our group (see Chapter A 4.4 for mannose and B 4.2.3 for heptose) by adaption of the used reaction conditions. According

to this, the observed behaviour of the nonose in the performed IMA cannot be explained by its low OCC.

B 5.2.2 Considerations on the low reactivity of the *L-lyxo-L-manno*-nonose in the performed IMA

As the OCC of the C9 aldose [13] turned out to be quite similar to the ones of the heptose [11] and D-mannose, we were looking for another explanation for the observed low reactivity of the nonose in the IMA. Considering the mechanism of the IMA of aldoses, that is shown in Scheme 58, the attack of the nucleophile at the aldehyde moiety takes place upon chelation of indium to the oxygen atom of the carbonyl group and the hydroxy group in α -position. In the D-mannose, one out of five hydroxy groups is involved in the IMA to give the desired enitol species with high diastereomeric selectivity. In the nonose, eight hydroxy groups are present so there is more competition to the O2/aldehyde chelation of other hydroxy groups. As the aldehyde moiety is not readily available anyways, a slower chelation of the indium further leads to slowed down reaction rates. Slow rates in the IMA are always disadvantageous due to the fate of the organoindium species upon hydrolysis and Wurtz-type dimerization.



Scheme 58. Cram-chelate model for the nucleophilic attack at the aldehyde moiety with *syn*-selectivity (adapted from Draskovits, et al.²⁴)

However, further investigation on the IMA of non-natural aldoses are necessary and ongoing in our group to obtain higher yields in the transformation of even these sugars with very long side-chains.

B 6 Physical properties of mannitol, galactitol and *galacto*-octitol

With the synthesised *galacto*-octitol [6] in hand (Chapter B 3), STA was performed to determine its physical properties. Additionally, commercially available galactitol **XXXVII** and mannitol **XXVIII** were investigated, too, to evaluate the accuracy of the used method and compare the obtained values.

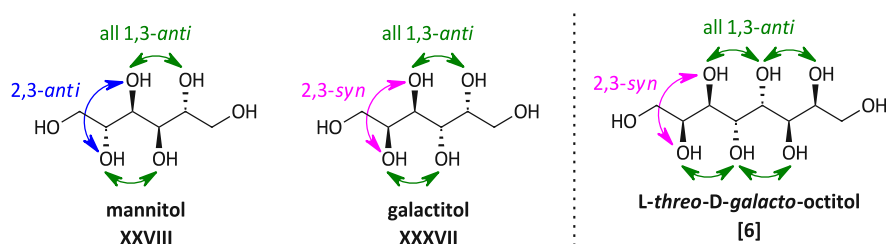
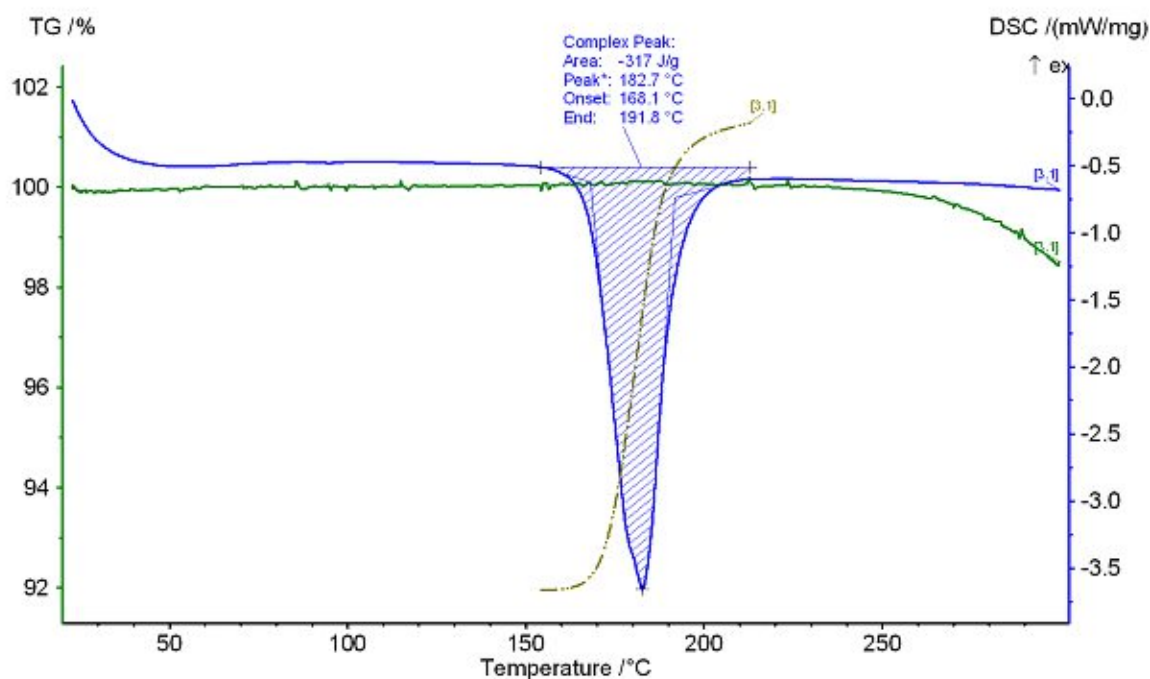
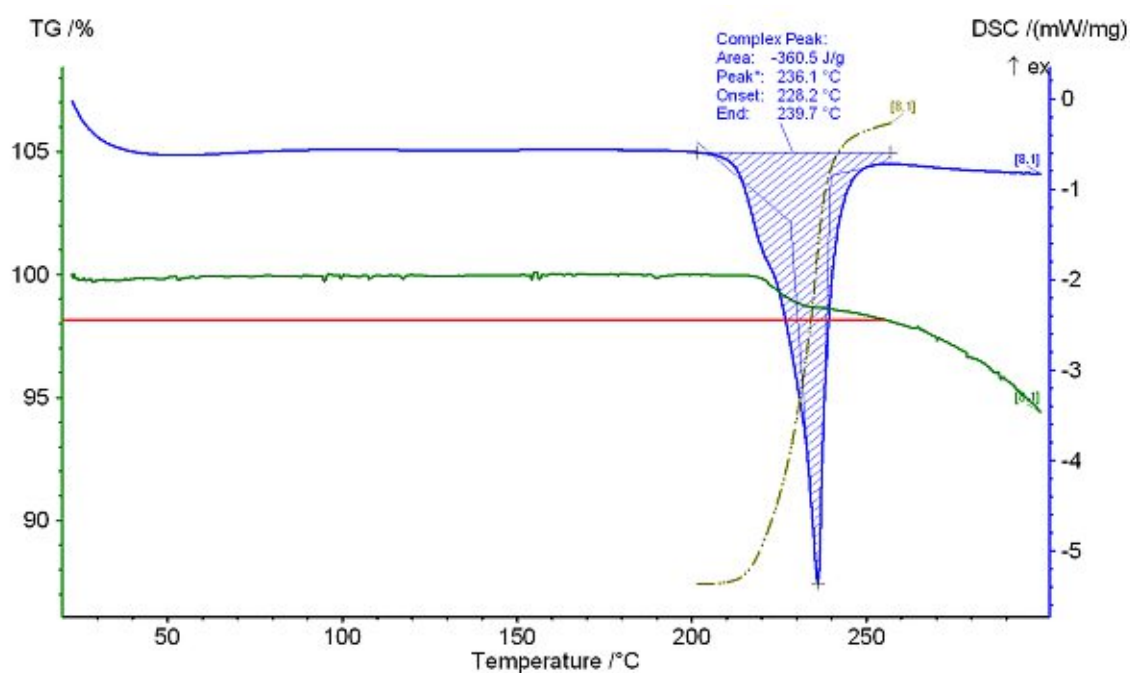


Figure 29. Sugar alcohols that were investigated by STA

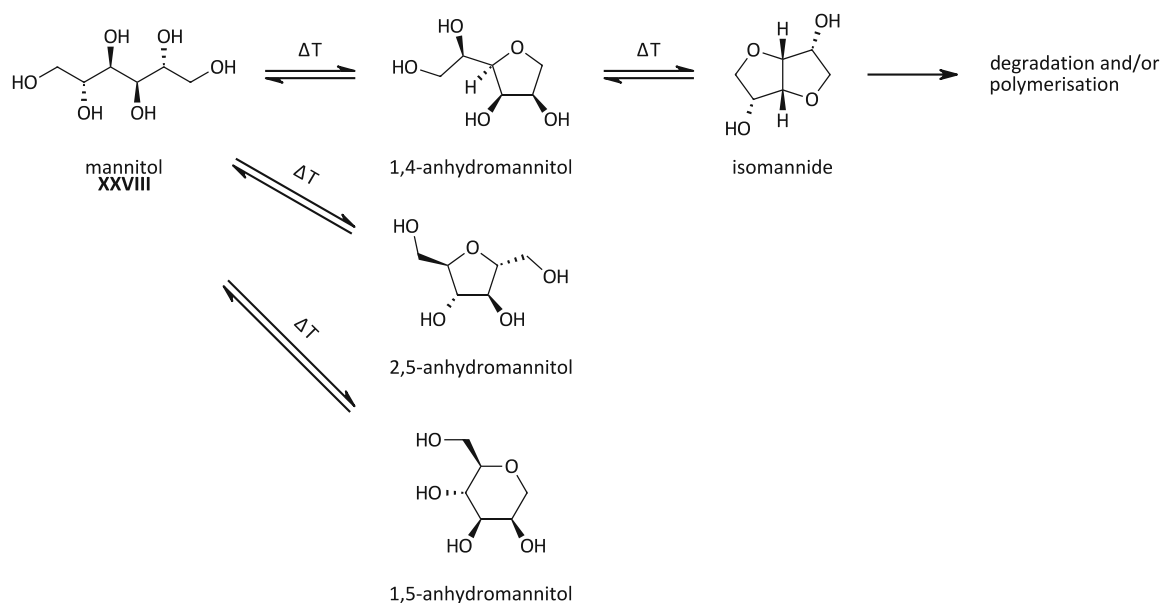
The physical properties of these compounds were measured by simultaneous thermal analysis (STA). This technique combines differential scanning calorimetry (DSC) and thermogravimetric analysis (TG) which allows the evaluation of decomposition during the melting process as these two processes cannot be distinguished unambiguously using only DSC.¹⁰⁵ In general, it is assumed that the amount of latent heat stored in a molten PCM which is released upon cooling and crystallisation is the same that was taken up by this material in the melting process.¹⁰⁶ Therefore, only the latent heat that is needed for melting was determined *via* STA.

In Figure 30, the recorded STA curve of commercially available D-mannitol **XXVIII** is displayed. The curve of the DSC (blue line) shows a negative peak starting at 168 °C and ending at 192 °C that indicates a melting process in which heat was taken up by the material. The area of this peak corresponds to the thermal storage density. The TG curve (green line) shows that decomposition at temperatures above 250 °C took place which has already been reported for mannitol in literature¹⁰⁷.

In contrast, the synthesised *galacto*-octitol [6] showed weight loss degradation process, as it can be seen in Figure 31. The red line indicates the weight loss which was found to be approximately 2%. Due to this, the calculated value for the thermal storage density by integration of the obtained peak is not trustworthy. Taking this weight loss into account, the thermal storage density was corrected to 368 kJ/kg instead of 361 kJ/kg.

Figure 30. STA measurement of commercially available mannitol **XXVIII**Figure 31. STA measurement of *galacto*-octitol [6]

A mechanism for the degradation of D-mannitol **XXVIII** under thermal treatment (Scheme 59) has already been presented by Bayón and Rojas¹⁰⁸ based on the report of Yamaguchi, et al.¹⁰⁹, who investigated the dehydration of mannitol in hot water at temperatures between 250–300 °C under argon atmosphere.



Scheme 59. Reaction pathways of mannitol dehydration proposed by Yamaguchi, et al.¹⁰⁹

The obtained melting points and thermal storage densities of the three sugar alcohols **XXVIII**, **XXXVII** and **[6]** are summarised in Table 15 and graphically displayed in Figure 32 together with the values presented in literature^{74,110}. The melting points were determined using the extrapolated onset temperature in the transition region of the DSC curves, according to Jia, et al.²⁰. For mannitol and galactitol, the average of two performed measurements is given.

Table 15. Measured and in literature given melting temperatures and thermal storage densities of the investigated sugar alcohols

Sugar alcohol	Melting temperature (°C)		Thermal storage density (kJ/kg)	
	measured	literature	measured	literature
mannitol XXVIII	168	166 ⁷⁴	333	318 ⁷⁴
galactitol XXXVII	186	188 ⁷⁴	357	354 ⁷⁴
galacto-octitol [6]	228	233-236 ¹¹⁰	368	–

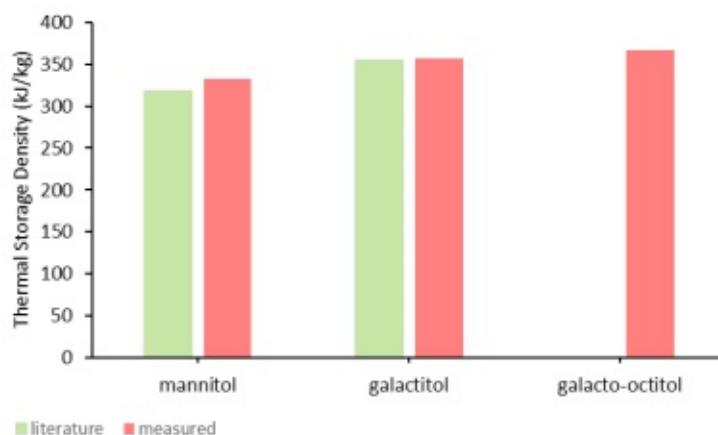


Figure 32. Measured thermal storage densities of mannitol and galactitol compared to literature values⁷⁴ and the measured value for the synthesised *galacto*-octitol

For the commercially available sugar alcohols mannitol **XXVIII** and galactitol **XXXVII** it can be seen, that the obtained melting points are in well agreement with those reported in literature⁷⁴, but the measured thermal storage densities are slightly higher. In general, those two species have already been investigated in literature several times by DSC and the values presented in different reports^{15-17,20,111-112} slightly vary. As discussed by Jia, et al.²⁰, these deviations can arise from differences in the purity of the samples, measurement conditions or the method used for data analysis.

The synthesised *galacto*-octitol **[6]** showed the highest thermal storage density of all three sugar alcohols, which was expected according to the findings in our group for the *manno*-octitol **XXVII** and based on the proposed guidelines by Inagaki and Ishida⁷⁵. However, the observed value of about 368 kJ/kg is significant lower compared to the thermal storage density of ~420 kJ/kg that was measured for the *manno*-configured octitol **XXVII** in our group (see Chapter A 4.4). This might be attributed to the different distribution of the hydroxy groups, as the first two stereocentres are in a *syn*-relationship for the *galacto*-configuration and in an *anti*-relationship for the *manno*. Furthermore, decomposition of the material took place at temperatures above the melting point which might be blamed on the sample preparation for to the STA as traces of water or acid favour dehydration reactions, as presented for mannitol in Scheme 59. Further investigations on the stability of this sugar alcohol under thermal treatment are necessary to evaluate its potential as a PCM.

The melting point observed *via* STA was 228 °C, but as the heating rate was rather high in the DSC measurement (10 °C/min) this value can only be seen as an indicative value. A more precise measurement which was additionally performed on a BÜCHI melting point apparatus with a heating rate of 1.0 °C/min, gave a melting point of 240.3–241.1 °C.

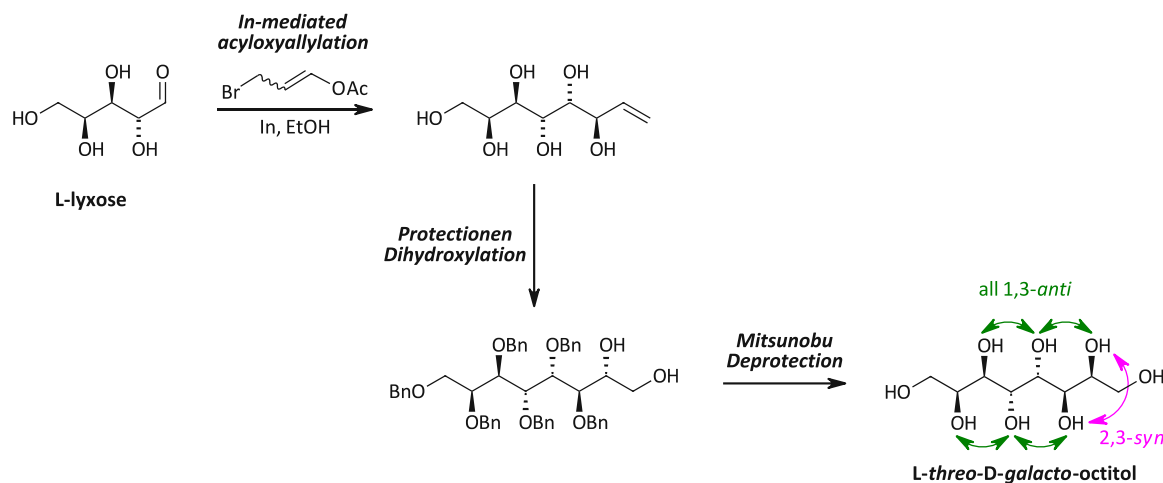
Nevertheless, these are promising preliminary results and further investigations are necessary and pending in our group. In the near future, larger amounts of the *galacto*-octitol and also sugar alcohols with differently distributed hydroxy groups and uneven numbers of carbon atoms will be synthesised and investigated *via* STA.

Die approbierte gedruckte Originalversion dieser Diplomarbeit ist an der TU Wien Bibliothek verfügbar
The approved original version of this thesis is available in print at TU Wien Bibliothek.



C Conclusion and outlook

Within this thesis, a synthetic route for higher sugar alcohols with high control of diastereoselectivity for the introduced stereocentres was successfully developed. This protocol allows the synthesis of sugar alcohols with a *syn*-relationship between the two hydroxy groups at the terminal stereocentres and a 1,3-*anti*-relationship of all hydroxy groups (*galacto*-configuration) and was used to obtain the non-natural *L-threo-D-galacto*-octitol, the corresponding decitol and partly the dodecitol as well. From the octitol already enough material was prepared for further investigations in simultaneous thermal analysis to determine its melting point and thermal storage density and evaluate its potential as an organic phase change material. Further, we were able to synthesise sugar species with ten carbon atoms in the backbone that could further be transformed into the *L-galacto-L-galacto*-deciitol, the second non-natural sugar alcohol of the *galacto*-series we were interested in. Therefore, we could show that our synthesis strategy developed for the *galacto*-octitol can also be used to obtain even longer sugar alcohols, even though some steps turned out to be quite challenging due to the physical nature of these compounds and required further investigations. As the synthesis of the *galacto*-deciitol was only performed on smaller scales, STA measurements have not been performed yet, but this sugar alcohol will be synthesised in larger quantities to further determine its physico-chemical properties.



Scheme 60. The developed synthetic route towards the non-natural sugar alcohol *L-threo-D-galacto*-octitol, that could also be applied for the synthesis of the *L-galacto-L-galacto*-deciitol with further improvements of some steps in the sequence

En route towards the *galacto*-decitol, a major achievement was the development of an improved protocol for the indium-mediated acyloxyallylation of unreactive aldoses like, for example, *L-glycero-D-manno*-heptose. Three major changes in the reaction protocol turned out to be the key for the successful transformation of such unreactive sugars to the corresponding enitol species:

(1) **Two-step Grignard protocol**

The Barbier-type protocol was replaced by a two-step Grignard protocol in which the organoindium species is pre-formed under anhydrous conditions, and the aldose is added to the reagent solution. This guaranteed that hydrolysis of the bromopropenyl ester cannot take place in the first place and the reagent is present in higher quantities. Further, it is assumed, that the reaction rate of the aldose was accelerated as the sugar molecules present in the open-chain form can immediately react with the organometallic species, fastening the (re)formation of the open chain structure from the cyclic hemiacetal that is dominantly present. Additionally, the reaction mixture turned homogeneous in the first step which also positively impacted the reaction rate.

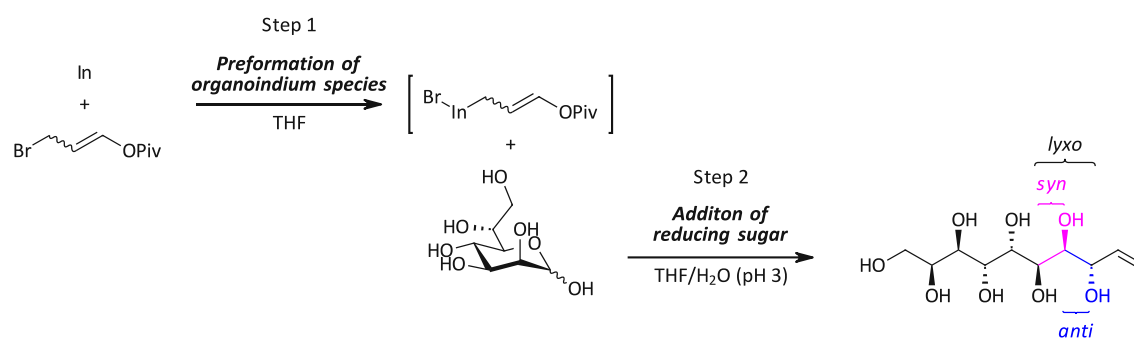
(2) **Change of the solvent system**

Instead of EtOH, THF together with an aqueous buffer as a co-solvent in the 2nd step was used which guaranteed full solubility of the sugar species.

(3) **Change of the used 3-bromopropenyl ester as reagent**

Instead of 3-bromopropenyl acetate or benzoate, which have deeply been investigated in the IMA of aldoses so far, 3-bromopropenyl pivalate was used as the reagent in this protocol. The benefits of the pivaloyl ester over the mentioned acetyl and benzoyl esters were the following:

- The 3-bromopropenyl pivalate showed higher stability under aqueous conditions as hydrolysis of the ester is less likely to occur. Due to this, the lifetime of the reagent is extended which is crucial in the transformation of sugars with a low OCC and therefore low reactivity.
- Slightly higher selectivity for the *lyxo*-configured enitol product is achieved due to increased preference for the *si*-face in the nucleophilic attack at the aldehyde and 3,4-*anti* stereo-preference which is addressed to the bulkiness of the ester group.



Scheme 61. The improved protocol for the IMA of the unreactive sugar *L-glycero-D-manno*-heptose with a two-step Grignard protocol giving the *lyxo*-configured enitol as the major isomer

In the future, our interests will also be on the synthesis of the *galacto*-dodecitol and other non-natural sugar alcohols that do not fulfil the established guidelines by Inagaki and Ishida⁷⁵ to show the impact of the structural features on the physical properties of this substance class. In cooperation with the authors of the presented computational study on non-natural sugar alcohols, the melting points and thermal storage densities of the sugar alcohols from the "*galacto*-series" are being calculated and will be compared to our experimental results.

Further, the "*manno*-series" (Figure 33) will be completed based on the gained knowledge in the IMA, attempting the synthesis of the *manno*-decitol **XXIX** (C10) and *manno*-dodecitol **XXX** (C12) sugar alcohols (Figure 33) and measure their thermal storage densities to evaluate the accuracy of the computational method.

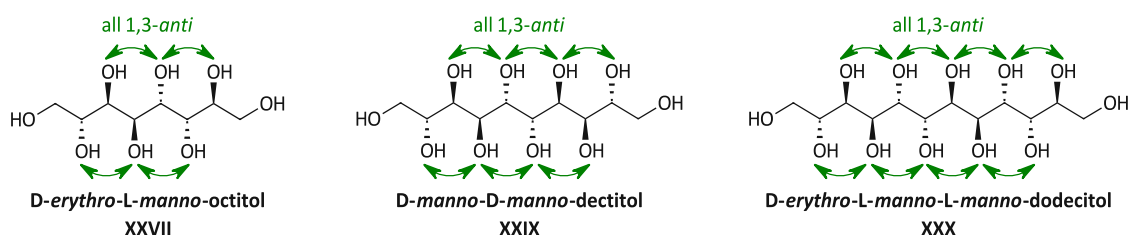


Figure 33. The "*manno*-series" of non-natural sugar alcohols that have already been investigated as potential PCMs in a theoretical study by Inagaki and Ishida⁷⁵

Die approbierte gedruckte Originalversion dieser Diplomarbeit ist an der TU Wien Bibliothek verfügbar
The approved original version of this thesis is available in print at TU Wien Bibliothek.



D Experimental part

D 1 Materials and methods

Reagents

The used reagents and solvents were bought from commercial sources with a purity of > 95% if not stated different and used without further purification.

Solvents

Water-free solvents were available at the institute from a PureSolv solvent purification system by Innovative Technology, or commercial sources that were stated as water-free and stored in bottles with a septum and over molecular sieve. Dowex-H⁺ was washed with the respective solvent before use.

TLC analysis

TLC analysis for reaction monitoring and fraction analysis from column chromatography was performed with silica gel 60 F₂₅₄ plates or HPTLC-plates (silica gel 60 F₂₅₄ with concentration zone 20 × 2.5 cm). Visualization of the spots was done using UV light (254 nm) followed by staining the plates with anisaldehyde solution (180 mL EtOH, 10 mL anisaldehyde, 10 mL H₂SO₄ (conc.), 2 mL AcOH), permanganate solution (3.0 g KMnO₄, 20.0 g K₂CO₃, 250 mg KOH, 300 mL H₂O) or cerium molybdate ("Mostain", 21 g (NH₄)₆Mo₇O₂₄·2H₂O, 1 g Ce(SO₄), 31 mL H₂SO₄ (conc.), 500 mL H₂O).

Column chromatography

Chromatography columns were packed with silica gel from Merck with a pore size of 40–63 μm. The used column sizes and eluents were adapted to the corresponding separation problem.

HPLC-MS

HPLC-MS analysis was performed on a Nexera X2[®] UHPLC system (Shimadzu[®], Kyoto, Japan) comprised of LC-30AD pumps, a SIL-30AC autosampler, CTO-20AC column oven, DGU-20A_{5/3} degasser module. Detection was accomplished by concerted efforts of SPD-M20A photo diode array, a RF-20Ax fluorescence detector, an ELS-2041 evaporative light scattering detector (JASCO[®]) and finally via a LCMS-2020 mass spectrometer. Separations were either performed using a Waters[®] XSelect[®] CSH™ C18 2.5 μm (3.0 × 50 mm) Column XP at 40 °C, a flowrate of 1.7 mL/min and with UHPLC grade water and acetonitrile containing 0.1% formic acid as the mobile phase, or a Waters[®] XBridge[®] BEH Amide 2.5 μm (3.0 × 50 mm) Column XP at 40 °C, a flowrate of 1.3 mL/min and with UPLC grade water (pH 8.5, 2.5 mM NH₄COOH) and acetonitrile as the mobile phase.

HR-MS

Accurate mass analysis was performed on an Agilent 6230 AJS ESI-TOF mass spectrometer with ESI ionisation method or Q Exactive Focus, ESI, FIA injection, mobile phase 18% MeCN with 0.1% formic acid.

NMR spectroscopy

The analysis of substances was done *via* NMR spectroscopy at 297 K in the solvent indicated using a Bruker Avance Ultra Shield 400 MHz and an Avance III HD 600 MHz spectrometer with TMS as internal standard. Processing of the data was performed with standard software and all spectra were calibrated to the solvent residual peak¹¹³ if not stated different. All assignments are based on 2D-spectra (COSY, phase sensitive HSQC, HMBC – depending on the molecule).

Melting points

Melting points were recorded on a BÜCHI melting point apparatus Model B-545 with a 40%/90% threshold and a heating rate of 1.0 °C/min.

Ozone generator

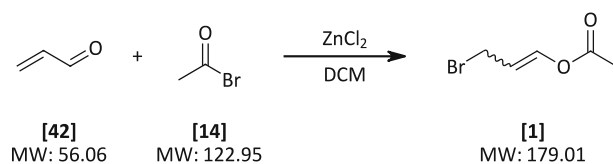
Ozone enriched oxygen was generated using a Triogen LAB2B Ozone generator.

Simultaneous thermal analysis (STA)

Simultaneous thermal analysis (STA) including differential scanning calorimetry (DSC) and thermogravimetric analysis (TG) measurements were performed on a STA 449 F1 JUPITER Netzsch under nitrogen atmosphere with a heating rate of 10 K/min.

D 2 Synthetic procedures and analytical data

D 2.1 3-Bromoprop-1-en-1-yl acetate [1]



Procedure

According to a literature protocol^{23,77}, acrolein [42] (90%, 4.7 g, 5.6 mL, 84 mmol, 1.0 equiv.) was dissolved in dry DCM (65 mL), cooled to $-20\text{ }^\circ\text{C}$ using an acetone/liquid N_2 cooling bath and acetyl bromide [14] (9.8 g, 6.0 mL, 80 mmol, 0.95 equiv.) was added to the solution under stirring. Then, after the addition of anhydrous ZnCl_2 (0.11 g, 0.84 mmol, 1.0 mol%), the reaction mixture was allowed to warm up to $-15\text{ }^\circ\text{C}$ by lowering the cooling bath as the exothermic reaction started and a temperature jump to $+12\text{ }^\circ\text{C}$ could be observed. The flask was then re-immersed in the cooling bath, and the reaction mixture was stirred for 1 hour, keeping the temperature below $-10\text{ }^\circ\text{C}$. As $^1\text{H-NMR}$ -analysis (micro work-up with Et_2O and aq. sat. NaHCO_3 , drying over Na_2SO_4) confirmed full conversion of the starting material to the targeted product, H_2O (30 mL) was added which led to the formation of a white precipitate and a temperature rise to $-10\text{ }^\circ\text{C}$.

The layers were separated, and the organic layer was washed with water (30 mL) followed by sat. aq. NaHCO_3 (2×40 mL – until pH remained basic). The greenish organic phase was further washed with brine, dried over anhydrous Na_2SO_4 and evaporated, giving a brown, oily liquid.

Purification

The pure product [1] was obtained by distillation *in vacuo* (bp $85\text{--}92\text{ }^\circ\text{C}$, 26-30 mbar) as a colourless to slightly yellow liquid (9.9 g, 73%) in a ratio of $E/Z = 1:1.6$ (according to $^1\text{H-NMR}$).

Yield

9.9 g, 73%

Appearance

colourless/slightly yellow liquid

Boiling point

$85\text{--}92\text{ }^\circ\text{C}$, 26-30 mbar (lit³⁸ $69\text{--}71\text{ }^\circ\text{C}$, 22 Torr)

$^1\text{H-NMR}$ (200 MHz, CDCl_3)

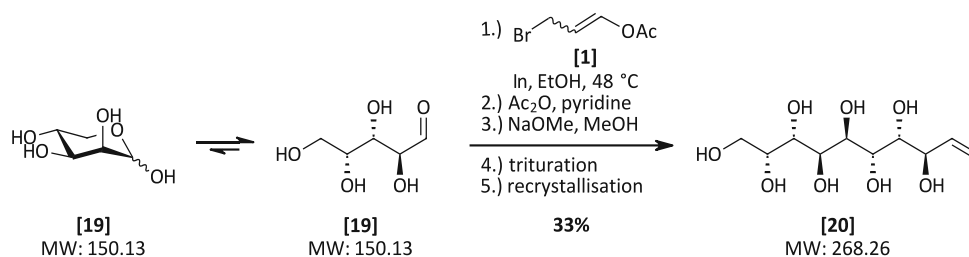
(*E*)-isomer: $\delta = 7.41$ (d, $J = 12.4$ Hz, 1H, =CH-O), 5.69 (dt, $J = 12.4, 8.4$ Hz, 1H, =CH-CH₂), 3.97 (d, $J = 8.4$ Hz, 2H, CH₂-Br), 2.14 (s, 3H, CH₃) ppm.

(*Z*)-isomer: $\delta = 7.17$ (d, $J = 6.3$ Hz, 1H, =CH-O), 5.22 (td, $J = 8.4, 6.3$ Hz, 1H, =CH-CH₂), 4.07 (d, $J = 8.4$ Hz, 2H, CH₂-Br), 2.19 (s, 3H, CH₃) ppm.

$^{13}\text{C-NMR}$ (101 MHz, CDCl_3) (*E*)-isomer: $\delta = 168.0$ (C=O), 139.6 (=CH-O), 111.7 (=CH-CH₂), 28.9 (CH₂-Br), 21.0 (CH₃)
(*Z*)-isomer: $\delta = 167.6$ (C=O), 137.5 (=CH-O), 109.9 (=CH-CH₂), 24.0 (t, CH₂-Br), 21.1 (q, CH₃)

Spectral data in accordance with literature.³⁸

D 2.2 1,2-Dideoxy-D-glycero-L-manno-oct-1-enitol [20] – method A



Procedure

Step 1 – IMA

According to a modified literature protocol²⁴, D-lyxose [19] (700 mg, 4.66 mmol, 1.00 equiv.) was dissolved in dry EtOH (70 mL) in a round-bottom flask and heated to 48 °C. First indium (1.07 g, 14.0 mmol, 3.00 equiv.) followed by 3-bromoprop-1-en-1-yl acetate [1] (2.50 g, 9.33 mmol, 2.00 equiv.) was added to the solution under vigorous stirring. After 15 min, reaction monitoring *via* TLC (CHCl₃/MeOH/H₂O 14:7:1, staining reagent: anisaldehyde) indicated full conversion of the starting material (staining yellow) to a less polar spot (staining violet). Stirring was continued for 10 more minutes to allow the reaction mixture to cool down. The mixture was filtered, and the solvent was removed *in vacuo*, giving a colourless solid (3.79 g).

Step 2 – Acetylation

This material was taken up in dry pyridine (10 mL), and Ac₂O (7.9 mL, 84 mmol, 18 eq.) was added to the stirring mixture under ice-bath cooling. The mixture was stirred at rt for 20 min, then a spatula of DMAP was added. Stirring at rt was continued overnight, and a micro work-up (with EtOAc and 1N HCl) for TLC analysis was performed the next day. Since TLC (CHCl₃/MeOH/H₂O 14:7:1, LP/Et₂O 1:2, staining reagent: anisaldehyde) indicated complete conversion to a very nonpolar species, excessive reagent was quenched by the addition of MeOH (25 mL) under ice-bath cooling, and the mixture was stirred for 45 min. After diluting with EtOAc (150 mL), the organic phase was extracted with 1N HCl (2×70 mL – until pH remained acidic) and washed with aq. sat. NaHCO₃ (40 mL) and brine. After drying over anhydrous Na₂SO₄, the solution was evaporated to dryness (3.78 g).

Step 3 – Deacetylation

The residue was taken up in MeOH (HPLC grade, 30 mL) and NaOMe (30% in MeOH) was added under stirring at rt until pH was about 8. Reaction monitoring *via* TLC (LP/Et₂O 1:2) after 3 hours showed full conversion. The reaction mixture was neutralized by the addition of Dowex-H⁺, H₂O was added to dissolve the formed enitol, and the solution was filtered. Evaporation of the solvent gave a beige solid matter (2.29 g) that was a mixture of diastereomers in a ratio of *lyxo* : *xylo* : *ribo* = 65 : 25 : 10.

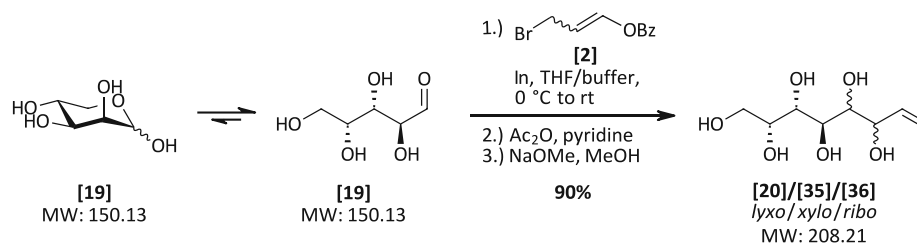
Purification

The solid was then triturated with *i*-PrOH (10 mL), and filtration gave a white solid that was further washed with small portions of MeOH (3 mL in total). The solid was further purified by recrystallisation from MeOH/H₂O (10:1), and the product **[20]** was obtained as colourless, needle-shaped crystals (320 mg, 33%).

<u>Yield</u>	320 mg, 33% (over 3 steps)
<u>Appearance</u>	white needles
<u>Melting point</u>	171.2–171.3 °C (MeOH/H ₂ O) (lit ²³ 171.9–172.7 °C (MeOH/H ₂ O))
<u>R_f</u>	0.23 (blue) (CHCl ₃ /MeOH/H ₂ O 14:7:1, staining agent: anisaldehyde)
<u>¹H-NMR (600 MHz, D₂O)</u>	δ = 6.01 (ddd, <i>J</i> = 17.3, 10.5, 6.9 Hz, 1H, H2), 5.38 (d, <i>J</i> = 17.3 Hz, 1H, H1 trans (<i>E</i>)), 5.31 (d, <i>J</i> = 10.5 Hz, 1H, H1 (<i>Z</i>)), 4.22 – 4.16 (m, 1H, H3), 4.01 – 3.96 (m, 1H, H7), 3.93 (dd, <i>J</i> = 9.4, 1.0 Hz, 1H, H5), 3.75 (dd, <i>J</i> = 8.2, 1.0 Hz, 1H, H4), 3.71 – 3.65 (m, 3H, H8a, H8b, H6) ppm.
<u>¹³C-NMR (151 MHz, D₂O)</u>	δ = 136.7 (C2), 116.8 (C1), 71.5 (C3), 70.6 (C4), 69.3 (C7), 68.4 (C6), 67.4 (C5), 62.3 (C8) ppm.

Spectral data in accordance with literature.²³

D 2.3 1,2-Dideoxy-D-glycero-L-manno-dec-1-enitol [20] – method B



Procedure

Step 1 – IMA

Based on a literature protocol³⁸, indium (36 mg, 0.31 mmol, 2.3 equiv.) was weighed in a flame dried Schlenk flask and Schlenk technique was applied. Anhydrous THF (0.40 mL) was added, and the mixture was cooled to 0 °C using an ice-bath. 3-Bromopropenyl benzoate [2] (112 mg, 0.46 mmol, 3.5 equiv.) was added dropwise to the vigorously stirring mixture. After 5 min, the ice-bath was removed, and the suspension was allowed to warm up to room temperature and stirred for another 40 min. Then, D-lyxose [19] (20 mg, 0.13 mmol, 1.0 equiv.) was added to the pre-formed reagent as a solution in phthalate buffer (pH ~3, 0.06 mL). As TLC (CHCl₃/MeOH/H₂O 14:7:1, staining reagent: anisaldehyde) indicated full conversion of the starting material (after 45 min), the reaction mixture was diluted with MeOH and H₂O and filtered. The filtrate was concentrated *in vacuo*, giving a colourless solid.

Step 2 – Acetylation

This material was taken up in pyridine (99%, 1.0 mL), and Ac₂O (0.29 g, 0.27 mL, 2.8 mmol, 21 eq.) was added to the stirring mixture under ice-bath cooling. After 10 min, the ice-bath was removed, and a spatula of DMAP was added. After 2.5 h, HPLC-MS indicated complete conversion to the fully protected species, and excessive reagent was quenched by the addition of MeOH (0.5 mL) under ice-bath cooling, and the mixture was stirred for further 30 min. After diluting with EtOAc (50 mL), the organic phase was extracted with 1N HCl (2×10 mL – until pH remained acidic) and washed with aq. sat. NaHCO₃ and brine. After drying over anhydrous Na₂SO₄, the solution was evaporated to dryness.

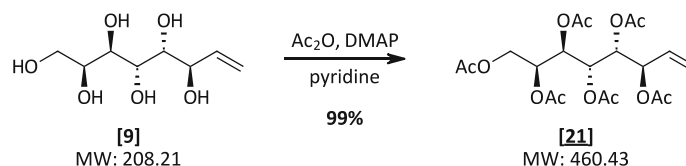
Step 3 – Deacetylation

The residue was taken up in MeOH (HPLC grade, 1.0 mL) and NaOMe (30% in MeOH) was added dropwise under stirring at rt until pH was about 10. Reaction monitoring *via* HPLC-MS after 3 hours showed full conversion. The reaction mixture was neutralized by the addition of Dowex-H⁺ (MeOH washed), H₂O was added to dissolve the formed enitol, and the solution was filtered. Evaporation of the solvent gave a beige solid matter (25 mg, 90%) that was a mixture of diastereomers in the ratio *lyxo* : *xylo* : *ribo* : 71 : 18 : 11.

As this reaction was just carried out as a proof of concept, no further purification and characterization has been performed.

<u>Yield</u>	25 mg, 90% (over 3 steps) (mixture of diastereomers)
<u>Appearance</u>	beige solid
<u>R_f</u>	0.23 (blue) (CHCl ₃ /MeOH/H ₂ O 14:7:1, staining agent: anisaldehyde)

D 2.4 3,4,5,6,7,8-Hexa-*O*-acetyl-1,2-dideoxy-*L*-glycero-*D*-manno-oct-1-enitol [21]



Procedure

The octenitol [9] (0.10 g, 0.48 mmol, 1.0 equiv.) was taken up in dry pyridine (0.5 mL), and Ac₂O (0.88 g, 0.82 mL, 84 mmol, 18 equiv.) was added to the stirring mixture under ice-bath cooling. The mixture was stirred at rt for 15 min, then a spatula tip of DMAP was added. After 1.5 hours reaction monitoring *via* TLC (micro work-up with EtOAc and 1N HCl, CHCl₃/MeOH/H₂O 14:7:1) indicated complete conversion to a very nonpolar species. Excessive reagent was quenched by the addition of MeOH (0.35 mL) under ice-bath cooling, and stirring was continued for 30 min.

The mixture was diluted with DCM (10 mL) and extracted with 1N HCl (2×5 mL – until pH remained acidic). The organic phase was further washed with aq. sat. NaHCO₃ (40 mL) and brine and dried over anhydrous MgSO₄. The solution was evaporated, giving the product [21] as white crystals (0.22 g, 99%).

Yield 0.22 g, 99%

Appearance white crystals

Melting point 127.6–127.8 °C (DCM)

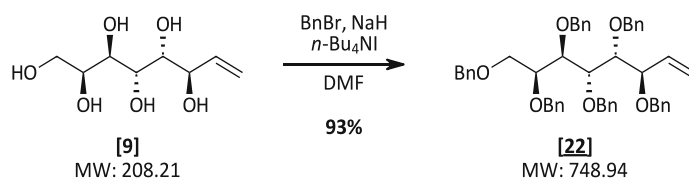
R_f 0.34 (hexane/EtOAc 1:1)

¹H-NMR (600 MHz, CDCl₃) δ = 5.68 (ddd, *J* = 17.2, 10.3, 7.9 Hz, 1H, H₂), 5.51 (dd, *J* = 10.1, 1.9 Hz, 1H, H₅), 5.34 (dd, *J* = 17.1, 0.9 Hz, 1H, H₁ (*E*)), 5.30 – 5.25 (m, 2H, H₆, H₁ (*Z*)), 5.22 (dd, *J* = 8.2, 1.9 Hz, 1H, H₄), 5.19 (ddd, *J* = 7.1, 4.9, 2.0 Hz, 1H, H₇), 5.13 (t, *J* = 8.1 Hz, 1H, H₃), 4.28 (dd, *J* = 11.7, 4.9 Hz, 1H, H_{8a}), 3.82 (dd, *J* = 11.7, 7.4 Hz, 1H, H_{8b}), 2.11 (s, 3H, COCH₃ (C₆/C₇)), 2.08 (s, 3H, COCH₃ (C₆/C₇)), 2.06 (s, 3H, COCH₃ (C₅)), 2.05 (s, 3H, COCH₃ (C₄)), 2.03 (s, 3H, COCH₃ (C₃)), 2.01 (s, 3H, COCH₃ (C₈)) ppm.

¹³C-NMR (101 MHz, CDCl₃) δ = 170.6, 170.4, 170.2, 170.0, 169.7, 169.7 (6×COCH₃), 132.4 (C₂), 121.2 (C₁), 72.1 (C₃), 69.4 (C₄), 67.7 (C₆, C₇), 66.5 (C₅), 62.4 (C₈), 21.2, 21.0, 20.9, 20.8, 20.8 (6×COCH₃) ppm.

HRMS (⁺ESI-TOF) *m/z* [M+NH₄]⁺ calc. for C₂₀H₃₂NO₁₂ 478.1918, found 478.1921

D 2.5 3,4,5,6,7,8-Hexa-*O*-benzyl-1,2-dideoxy-*L*-glycero-*D*-manno-oct-1-enitol [22]



Procedure

The enitol [9] (0.50 g, 2.4 mmol, 1.0 equiv.) was suspended in dry DMF (5 mL) and NaH (60% in paraffin oil, 1.4 g, 36 mmol, 15 equiv.) was added portionwise to the stirring mixture under ice-bath cooling (formation of H₂). After stirring for 15 min at 0 °C, benzyl bromide (4.9 g, 3.4 mL, 29 mmol, 12 equiv.) was added dropwise. The formation of a beige precipitate was obtained, and further DMF (15 mL) was added to guarantee efficient stirring while completing the addition of BnBr. The mixture was allowed to warm up to rt, and *n*-Bu₄NI (0.44 g, 1.2 mmol, 0.50 equiv.) was added. After 3.5 hours TLC (CHCl₃/MeOH/H₂O 14:7:1, LP/EtOAc 2:1, staining reagent: anisaldehyde) indicated full conversion to a single very nonpolar species. Excessive reagent was quenched by the addition of MeOH (3 mL) and aq. NH₄Cl (10%, 30 mL), and the mixture was diluted with Et₂O (50 mL).

The phases were separated, and the aqueous phase was extracted with Et₂O (3×70 mL). The pooled organic phase was washed with H₂O (3×20 mL) and brine. After drying over anhydrous Na₂SO₄, the solvent was evaporated. The residue was taken up in acetonitrile (40 mL), washed with *n*-hexane (3×20 mL) and vaporised again, giving a yellow, oily crude material (2.6 g).

Purification

The pure product [22] was obtained by flash column chromatography (250 g SiO₂, LP/EtOAc 10:1 → 4:1, fraction size: 700 mL) as a colourless oil (1.7 g, 93%).

Yield	1.7 g, 99%
Appearance	colourless oil
R_f	0.44 (hexane/EtOAc 3:1)
¹H-NMR (600 MHz, CDCl₃)	δ = 7.33 – 7.18 (m, 30H, 30×Ph CH), 5.94 (ddd, <i>J</i> = 17.4, 10.4, 8.0 Hz, 1H, H2), 5.40 – 5.22 (m, 2H, H1 (<i>Z</i>), H1 (<i>E</i>)), 4.74 (dd, <i>J</i> = 11.6, 7.8 Hz, 2H, OCH ₂ -Ph), 4.67 – 4.54 (m, 6H, 3×OCH ₂ -Ph), 4.51 (d, <i>J</i> = 11.7 Hz, 1H, H8a), 4.47 – 4.35 (m, 2H, OCH ₂ -Ph), 4.10 (d, <i>J</i> = 11.7 Hz, 1H, H8b), 4.08 – 4.02 (m, 2H, H3, H7), 3.99 – 3.90 (m, 3H, H5, H6, H4), 3.70 (d, <i>J</i> = 5.3 Hz, 2H, OCH ₂ -Ph) ppm.

¹³C-NMR (151 MHz, CDCl₃) δ = 139.2, 139.2, 139.0, 138.9, 138.8, 138.4 (6×Ph C1), 136.1 (C2), 128.6 – 127.2 (30×Ph CH), 119.8 (C1), 81.3 (C3), 81.2 (C4), 78.8 (2×CH (C5/C6/C7)), 78.8 (C5/C6/C7), 74.0, 73.9, 73.3, 73.3, 73.0, 70.9 (6×OCH₂-Ph), 70.0 (C8) ppm.

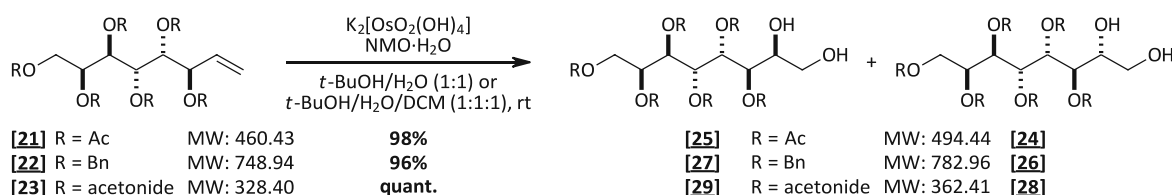
HRMS (+ESI-TOF) m/z [M+H]⁺ calc. for C₅₀H₅₃O₆ 749.3761, found 749.3835

HRMS (-ESI-TOF) m/z [M-H]⁻ calc. for C₅₀H₅₁O₆ 747.3688, found 747.2446

D 2.7 Screening of octenitol substrates and dihydroxylation conditions, followed by deprotection to determine the ratio of the octitol isomers (¹³C-NMR)

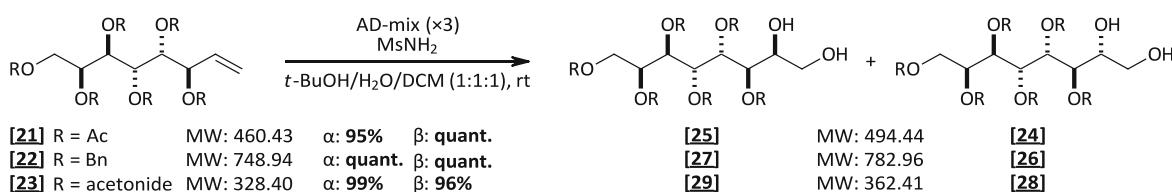
D 2.7.1 Dihydroxylation of the protected octenitols [21], [22] and [23] on analytical scale

Upjohn dihydroxylation conditions



The protected octenitol (0.10-0.22 mmol) was suspended in *t*-BuOH/H₂O (1:1, 0.1-0.3 M) at room temperature. Then, NMO·H₂O (1.0 equiv.) was added, followed by K₂[OsO₂(OH)₄] (1.0 mol%). For octenitol [22] (Bn) and [21] (acetonide), DCM (final ratio 1:1:1) was added, too. Reaction monitoring was performed *via* TLC (LP/Et₂O) and HPLC-MS. As soon as complete consumption of the starting material was obtained (1–3 days), the reaction mixture was quenched by the addition of Na₂S₂O₅. After stirring for 1 h, extraction of the aqueous phase was performed with DCM or EtOAc. The pooled organic phase was washed with brine, dried over anhydrous Na₂SO₄ and evaporated.

Sharpless dihydroxylation conditions



AD-mix-α (×3) or AD-mix-β (×3) (1.4 g/mmol substrate) was suspended in *t*-BuOH/H₂O (1:1, 0.4 M (with respect to the substrate)) and MsNH₂ (1.0 equiv.) was added. After stirring for 1 hour, the starting material was added as a solution in DCM (0.8 M). Reaction monitoring was performed *via* TLC (LP/Et₂O) and HPLC-MS. As soon as complete conversion was obtained (days), the reaction mixture was quenched by the addition of Na₂S₂O₅. After stirring for 1 h, it was diluted with DCM and H₂O, and extraction of the aqueous phase was performed with DCM. The pooled organic phase was washed with brine, dried over anhydrous Na₂SO₄ and evaporated.

sample (~5-10 mg) was prepared in D₂O (~0.7 mL), and ¹³C-NMR analysis was performed to determine the ratio of the two isomers [6] and [30].

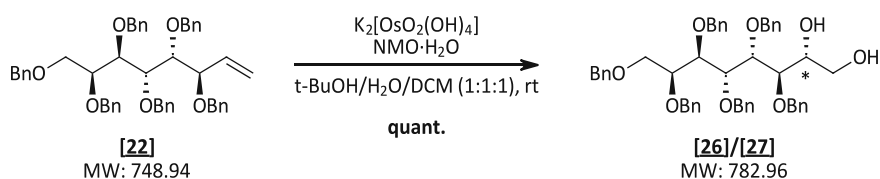
D 2.7.3 Results of the substrate and method screening, including obtained yields and product ratios [6]/[30]

The following table summarises the results of the dihydroxylation reactions of the octenitol substrates [21], [22] and [23] conducted under different reaction conditions, including the obtained yields and product ratios [6]/[30].

R	K ₂ [OsO ₂ (OH) ₄] + NMO		AD-mix-α (x3) + MsNH ₂		AD-mix-β (x3) + MsNH ₂	
	Yield (2 steps)	Ratio [6]/[30] (¹³ C-NMR) ⁱⁱⁱ	Yield (2 steps)	Ratio [6]/[30] (¹³ C-NMR) ⁱⁱⁱ	Yield (2 steps)	Ratio [6]/[30] (¹³ C-NMR) ⁱⁱⁱ
Ac	98%	1 : 1.4-1.5	95%	1 : 1.3	quant.	1 : 2.3-2.4
Bn	96%	1 : 10	quant.	1 : 9	quant.	1 : 20
acetonide	quant.	1 : 1.6-1.7	99%	1 : 1.5	96%	1 : 1.2

ⁱⁱⁱ Determined upon deprotection.

D 2.8 3,4,5,6,7,8-Hexa-*O*-benzyl-*L*-threo-*D*-talo octitol [26] – method A



Procedure

The protected octenitol **[22]** (1.0 g, 1.3 mmol, 1.0 equiv.) was suspended in $t\text{-BuOH}/H_2O$ (1:1, 4 mL) and DCM (2 mL) was added to dissolve the starting material. Then, $NMO \cdot H_2O$ (0.22 g, 1.6 mol, 1.2 equiv.) was added to the vigorously stirring mixture followed by $K_2[OsO_2(OH)_4]$ (5.0 mg, 13 μmol , 1.0 mol%). Reaction monitoring *via* HPLC-MS did not confirm full conversion of the starting after 3 days, so further $NMO \cdot H_2O$ (0.11 g) and $K_2[OsO_2(OH)_4]$ (3.0 mg) were added, and stirring was continued for another day. After 4 days in total, HPLC-MS indicated complete conversion to the targeted product. The reaction mixture was quenched by the portionwise addition of $Na_2S_2O_5$ (1.5 g), stirred for one hour and diluted with H_2O and DCM.

The layers were separated, and the aqueous phase was extracted with DCM (3×70 mL). The pooled organic phase was washed with brine, dried over anhydrous Na_2SO_4 and evaporated, giving an enantiomeric mixture of hexabenzyl-*L*-threo-*D*-talo/galacto-octitol **[26]/[27]** (*talo/galacto* ~10:1 (screening Chapter D 2.7)) as a colourless oil (1.2 g, quant.) that was not further purified.

Yield 1.2 g (crude material), quant.

Appearance colourless oil

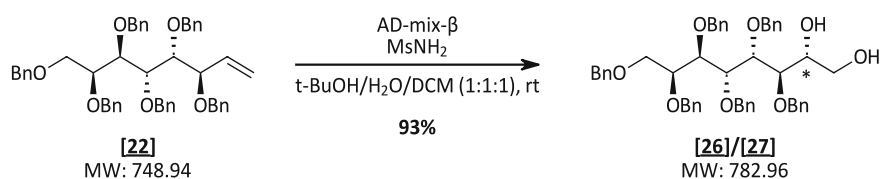
3,4,5,6,7,8-Hexa-*O*-benzyl-*L*-threo-*D*-talo-octitol [6]

R_f 0.51 (LP/EtOAc 1:1)

¹H-NMR (400 MHz, CDCl₃) 7.69 – 6.67 (m, 30H, 30×Ph CH), 4.69 – 4.46 (m, 8H, 4×OCH₂-Ph), 4.42 – 4.20 (m, 4H, 2×OCH₂-Ph), 4.01 (dd, $J = 5.3, 2.8$ Hz, 1H, CH), 3.88 (tq, $J = 7.5, 3.8, 3.1$ Hz, 3H, 3×CH), 3.71 (dt, $J = 8.0, 4.2$ Hz, 1H, CH), 3.69 – 3.48 (m, 5H, CH, H1a, H1b, H8a, H8b).

HRMS (⁺ESI-TOF) m/z [M+H]⁺ calc. for C₅₀H₅₅O₁₀ 783.3889, found 783.3909

D 2.9 3,4,5,6,7,8-Hexa-*O*-benzyl-*L*-threo-*D*-talo-octitol [26] – method B



Procedure

AD-mix- β (x3) (1.16 g, 1.40 g/mmol starting material.) was suspended in *t*-BuOH/H₂O (1:1, 2 mL) and MsNH₂ (158 mg, 1.66 mmol, 2.00 equiv.) was added under vigorous stirring. After one hour, the protected octenitol [22] (620 mg, 0.828 mmol, 1.00 equiv.) was added as a solution in DCM (1 mL). As TLC analysis (LP/EtOAc 1:1) and HPLC-MS did not show full conversion of the starting material after 7 days, more solvent (*t*-BuOH/H₂O/DCM 1:1:1, 3 mL) and AD-mix- β (580 mg) was added. After an additional day, full conversion was observed, and the reaction mixture was quenched by the addition of solid Na₂S₂O₅ which caused heavy foaming.

After dilution with H₂O (20 mL) and DCM (50 mL) the phases were separated, and the aq. phase extracted with DCM (3×30 mL). The pooled organic phase was washed with brine, dried over Na₂SO₄ and vapourised, giving an enantiomeric mixture of hexabenzyl-*L*-threo-*D*-talo/galacto-octitol [26]/[27] (*talo/galacto* ~20:1 (screening Chapter D 2.7)) as a yellow oil (600 mg, 93%) that was not further purified.

Yield 600 mg (crude material), 93%.

Appearance colourless oil

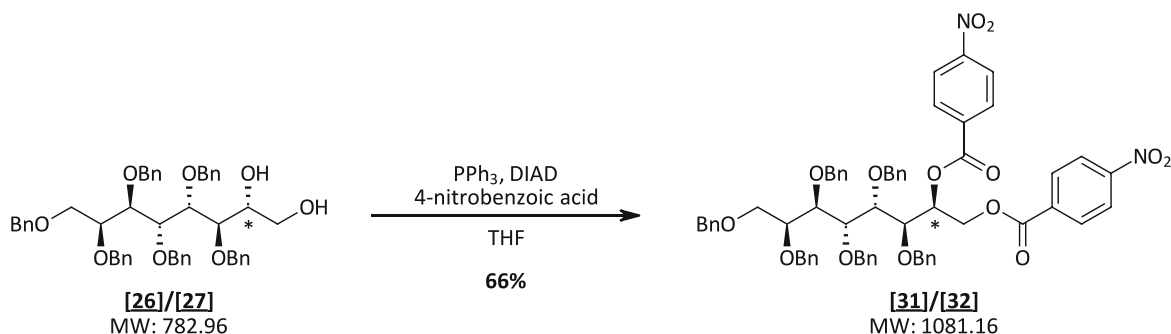
3,4,5,6,7,8-Hexa-*O*-benzyl-*L*-threo-*D*-talo-octitol [26]

R_f 0.51 (LP/EtOAc 1:1, staining agent: Mostain)

¹H-NMR (400 MHz, CDCl₃) δ = 7.69 – 6.67 (m, 30H, 30×Ph CH), 4.69 – 4.46 (m, 8H, 4×OCH₂-Ph), 4.42 – 4.20 (m, 4H, 2×OCH₂-Ph), 4.01 (dd, *J* = 5.3, 2.8 Hz, 1H, CH), 3.88 (tq, *J* = 7.5, 3.8, 3.1 Hz, 3H, 3×CH), 3.71 (dt, *J* = 8.0, 4.2 Hz, 1H, CH), 3.69 – 3.48 (m, 5H, CH, H1a, H1b, H8a, H8b).

HRMS (*ESI-TOF) *m/z* [M+H]⁺ calc. for C₅₀H₅₅O₁₀ 783.3889, found 783.3909

D 2.10 3,4,5,6,7,8-Hexa-*O*-benzyl-1,2-di-*O*-(*p*-nitrobenzoyl)-*L*-threo-*D*-galacto-octitol [31]



Procedure

The starting material **[26]/[27]** (~10:1) (180 mg, 0.230 mmol, 1.00 equiv.) was weighed in a flame dried Schlenk flask. The flask was flushed with Ar three times *via* Schlenk technique, and dry THF (3.6 mL) was added. Then, 4-nitrobenzoic acid (192 mg, 1.15 mmol, 5.00 equiv.) and PPh₃ (302 mg, 1.15 mmol, 5.00 equiv.) were added to the stirring solution under Ar stream. The reaction mixture was cooled to 0 °C using an ice-bath, and DIAD (180 μL, 234 mg, 1.15 mmol, 5.00 equiv.) was added dropwise. The flask was left in the ice-bath allowing slow warming up to rt and stirring was continued overnight. Reaction monitoring *via* HPLC-MS the next day confirmed full consumption of the starting material and the formation of the targeted product but also side products. TLC (LP/EtOAc 3:1) analysis was performed, too. The reaction mixture was evaporated, giving a yellow, oily crude material (950 mg).

Purification

The crude material was purified *via* column chromatography (95 g SiO₂, LP/EtOAc 10:1 → 2:1) giving the targeted product (164 mg) as a mixture of the two diastereomers **[31]/[32]** (*galacto/talo* ~20:1 – determined upon deprotection) and mixed fractions with a side-product with similar polarity (45 mg).

Yield 164 mg, 66%

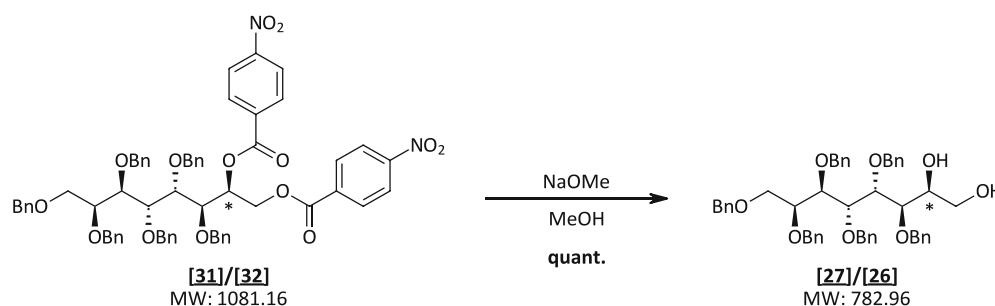
Appearance slightly yellow oil

R_f 0.52 (LP/EtOAc 2:1, staining agent: Mostain)

¹H-NMR (400 MHz, CDCl₃) δ = 8.19 – 8.13 (m, 2H, 2×PNB CH), 8.05 – 7.94 (m, 6H, 6×PNB CH), 7.35 – 7.05 (m, 30H, 30×Ph CH), 5.96 (dt, *J* = 8.0, 3.2 Hz, 1H, H₂), 4.77 (d, *J* = 11.7 Hz, 1H, OCH₂-Ph), 4.72 – 4.49 (m, 9H, 4×OCH₂-Ph, H_{1a}), 4.45 (d, *J* = 2.3 Hz, 2H, OCH₂-Ph), 4.36 (d, *J* = 11.6 Hz, 1H, OCH₂-Ph), 4.20 (dd, *J* = 11.6, 3.6 Hz, 1H, H_{1b}), 4.16 – 4.09 (m, 2H, H₄, H₅/H₆), 4.08 – 3.98 (m, 3H, H₇, H₃, H₅/H₆), 3.72 (d, *J* = 4.0 Hz, 2H, H_{8a}, H_{8b}) ppm.

¹³C-NMR (101 MHz, CDCl₃) δ = 164.3, 164.2 (2×PNB C=O), 150.7, 150.5 (2×PNB Ph C6), 138.8, 138.7, 138.4, 138.2, 138.2, 137.8 (6×Bn Ph C1), 135.4, 135.1 (2×PNB Ph C1), 130.8 (2×PNB Ph CH), 130.8 (2×PNB Ph CH), 128.8 – 127.0 (30×Bn Ph CH), 123.6 (2×PNB Ph CH), 123.5 (2×PNB Ph CH), 79.7 (C4/C5/C6), 79.6 (C4/C5/C6), 79.1 (C3/C5/C6/C7), 77.4 (C3/C5/C6/C7), 74.7, 74.1, 73.5, 73.5, 73.4, 72.7 (6×OCH₂-Ph), 71.9 (C2), 70.5 (C8), 65.4 (C1) ppm.

D 2.11 3,4,5,6,7,8-Hexa-*O*-benzyl-*L*-threo-*D*-galacto-octitol [27]



Procedure

The starting material [31]/[32] (164 mg, 0.152 mmol, 1.00 equiv.) was taken up in MeOH (HPLC grade, 2.0 mL) and NaOMe (30% in MeOH) was added dropwise under stirring at rt until pH was about 10. After 2 hours, HPLC-MS indicated full conversion and the reaction mixture was neutralized by the addition of Dowex-H⁺. After filtration and evaporation, the residue was taken up in DCM (40 mL), extracted with sat. aq. NaHCO₃ (2×10 mL) and washed with brine. After drying over anhydrous Na₂SO₄, the organic phase was evaporated, giving the crude product (120 mg) as a yellow oil that was used for the next step without further purification.

Yield 120 mg, crude

Appearance yellow oil

3,4,5,6,7,8-Hexa-*O*-benzyl-*L*-threo-*D*-galacto-octitol [27]

R_f 0.50 (LP/EtOAc 1:1, staining agent: Mostain)

¹H-NMR (400 MHz, CDCl₃) 7.37 – 7.16 (m, 30H, 30×Ph CH), 4.79 – 4.57 (m, 8H, 4×OCH₂-Ph), 4.47 (d, *J* = 11.5, 1H, OCH₂H-Ph), 4.44 – 4.38 (m, 2H, OCH₂-Ph), 4.35 (d, *J* = 11.5, 1H, OCH₂H-Ph), 4.12 (m, 3H, H₄, H₅, H₆), 4.04 – 3.97 (m, 2H, H₂, H₇), 3.87 (dd, *J* = 6.6, 1.9 Hz, 1H, H₃), 3.75 – 3.61 (m, 4H, H_{8a}, H_{8b}, H_{1a}, H_{1b}).

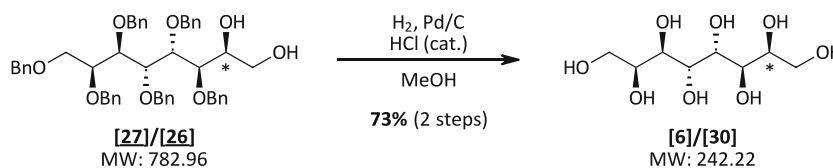
¹³C-NMR (101 MHz, CDCl₃) δ = 141.8 – 140.2 (6×Bn Ph C1), 128.2 – 127.3 (30×Ph CH), 78.8 (C₄/C₅/C₆), 78.7 (C₇), 78.5 (C₄/C₅/C₆), 78.3 (C₄/C₅/C₆), 77.9 (C₃), 73.9, 73.2, 73.1, 72.9, 72.8, 72.7 (6×OCH₂-Ph), 71.4 (C₂), 69.9 (C₈), 63.1 (C₁)

HRMS (⁺ESI-TOF) *m/z* [M+H]⁺ calc. for C₅₀H₅₅O₁₀ 783.3889, found 783.3909

Note

The given shifts for the ¹³C-NMR were determined from the recorded HSQC spectrum.

D 2.12 L-Threo-D-galacto-octitol [6] – method A

**Procedure**

The crude material **[27]/[26]** (120 mg) was taken up in MeOH (HPLC grade, 1.0 mL) and Pd/C (10 w%, 12 mg, 7 mol%) was added followed by a drop of 2N HCl. Hydrogen atmosphere was guaranteed using a balloon, and the reaction mixture was stirred at rt for 14 hours, as HPLC-MS indicated full deprotection. The mixture was diluted with H₂O, filtered over Celite®, and the filter cake washed with fresh water. Evaporation of the aqueous phase gave a colourless solid (27 mg) with a ratio of 20:1 **[6]/[30]** (*galacto/talo*) according to ¹³C-NMR.

Yield 27 mg, 73% (over 2 steps from **[31]/[32]**)

Product ratio *galacto/talo* 20:1 (according to ¹³C-NMR)

Appearance colourless solid

L-Threo-D-galacto-octitol [6]

R_f 0.17 (red) (CHCl₃/MeOH/H₂O 14:7:1, staining agent: anisaldehyde)

Melting point 240.3–241.1 °C (H₂O) (lit¹¹⁰ 233–236 °C)

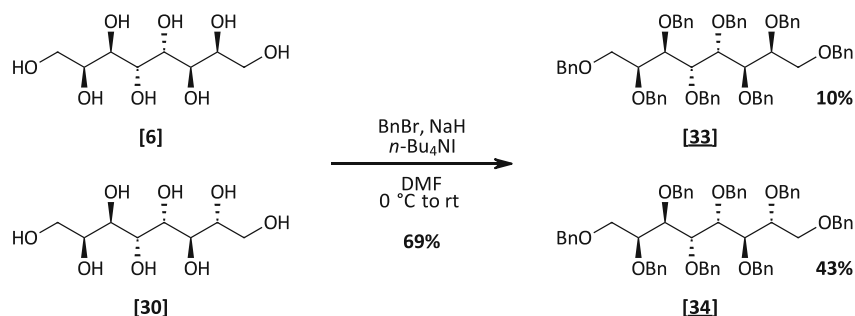
¹H-NMR (600 MHz, CDCl₃) δ = 4.01 – 3.98 (m, 2H, H2, H7), 3.95 (d, *J* = 9.3 Hz, 2H, H4, H5), 3.72 – 3.68 (m, 6H, H1, H8, H3, H6) ppm.

¹³C-NMR (151 MHz, CDCl₃) δ = 70.3 (C2, C7), 69.3 (C3, C6), 68.2 (C4, C5), 63.3 (C1, C8) ppm.

HRMS (+ESI-TOF) *m/z* [M+H]⁺ calc. for C₈H₁₉O₈ 243.1075, found 243.1135

HRMS (-ESI-TOF) *m/z* [M-H]⁻ calc. for C₈H₁₇O₈ 241.0929, found 241.1002

D 2.14 1,2,3,4,5,6,7,8-Octa-*O*-benzyl-*L*-threo-*D*-galacto-octitol [33] & 1,2,3,4,5,6,7,8-octa-*O*-benzyl-*L*-threo-*D*-talo-octitol [34]



Procedure

A mixture of [6] and [30] (0.370 g, 1.53 mmol, 1.00 equiv.) was suspended in dry DMF (3 mL) and NaH (60% in paraffin oil, 1.22 g, 30.6 mmol, 20.0 equiv.) was added portionwise to the stirring mixture under ice-bath cooling (formation of H₂). After stirring for 30 min at 0 °C, benzyl bromide (4.18 g, 2.90 mL, 24.4 mmol, 15.0 equiv.) was added dropwise. The formation of a beige precipitate was obtained. The mixture was allowed to warm up to rt, and *n*-Bu₄NI (0.28 g, 0.76 mmol, 0.50 equiv.) was added. As TLC (CHCl₃/MeOH/H₂O 14:7:1, LP/EtOAc 3:1, staining reagent: anisaldehyde, Mostain reagent) indicated full conversion of the starting material to a very nonpolar species, excessive reagent was quenched by the addition of MeOH (2 mL) under ice-bath cooling, and aq. NH₄Cl (10%, 20 mL) was added. After 15 min, the mixture was diluted with Et₂O (50 mL) and transferred into a separation funnel.

The phases were separated, and the aqueous phase was extracted with Et₂O (3×30 mL). The pooled organic phase was washed with H₂O (3×20 mL) and brine. After drying over anhydrous Na₂SO₄, the solvent was evaporated (2.7 g). The residue was taken up in acetonitrile (50 mL), washed with *n*-hexane (3×20 mL) and vaporised again, giving a yellow, oily crude material (2.0 g).

Purification

The crude material was purified by flash column chromatography (200 g SiO₂, LP/EtOAc 10:1 (800 + 800 + 400 mL) → 5:1 (700 + 800 mL) giving the following product fractions:

fr2: 636 mg – [34] according to HPTLC (LP/EtOAc 3:1) and NMR

fr3: 240 mg – mixture of [33] and [34]

fr4: 135 mg – [33] according to HPTLC (LP/EtOAc 3:1) and NMR

With mixed fraction 3 (240 mg) column chromatography was performed again (17 g SiO₂, LP/EtOAc 10:1), giving 16 mg of [33].

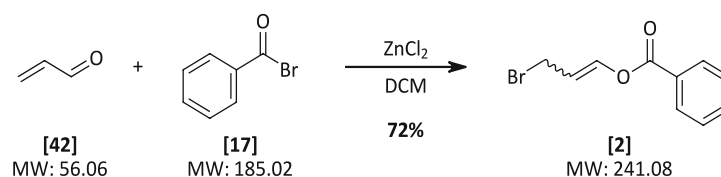
1,2,3,4,5,6,7,8-Octa-O-benzyl-L-threo-D-galacto-octitol [33]

Yield	151 mg, 10%
Appearance	colourless oil
R_f	0.44 (hexane/EtOAc 3:1, staining agent: Mostain)
¹H-NMR (400 MHz, CDCl₃)	δ = 7.46 – 6.85 (m, 40H, 40×Ph CH), 4.66 – 4.47 (m, 8H, 4×OCH ₂ -Ph), 4.44 (d, <i>J</i> = 1.6 Hz, 4H, 2×OCH ₂ -Ph), 4.36 – 4.27 (m, 4H, 2×OCH ₂ -Ph (C1, C8)), 4.09 (d, <i>J</i> = 4.9 Hz, 2H, 2×CH (H3/H6/H4/H5)), 3.94 (dd, <i>J</i> = 7.3, 4.1 Hz, 4H, 4×CH (H2/H7H3/H6/H4/H5)), 3.62 (d, <i>J</i> = 5.2 Hz, 4H, H1a, H1b, H8a, H8b) ppm.
¹³C-NMR (101 MHz, CDCl₃)	δ = 139.4 (2×Ph C1), 139.1 (2×Ph C1), 138.9 (2×Ph C1), 138.5 (2×Ph C1), 128.7 – 126.9 (m(40×Ph CH)), 78.7 (2×CH (C2/C7/C3/C6/C4/C5)), 78.7 (2×CH (C2/C7/C3/C6/C4/C5)), 78.4 (2×CH (C3/C6/C4/C5)), 73.3 (4×OCH ₂ -Ph), 73.1 (2×OCH ₂ -Ph), 73.0 (2×OCH ₂ -Ph), 71.0 (C1, C8) ppm.
HRMS (+ESI-TOF)	<i>m/z</i> [M+H] ⁺ calc. for C ₆₄ H ₆₇ O ₈ 963.4726, found 963.4857

1,2,3,4,5,6,7,8-Octa-O-benzyl-L-threo-D-talo-octitol [34]

Yield	636 mg, 43%
Appearance	colourless oil
R_f	0.51 (hexane/EtOAc 3:1, staining agent: Mostain)
¹H-NMR (400 MHz, CDCl₃)	δ = 7.42 – 6.91 (m, 40H, 40×Ph CH), 4.72 – 4.60 (m, 2H, OCH ₂ -Ph), 4.61 – 4.53 (m, 3H, OCH ₂ H-Ph, OCH ₂ -Ph), 4.52 – 4.49 (m, 4H, 2×OCH ₂ -Ph), 4.39 – 4.29 (m, 3H, OCH ₂ H-Ph, OCH ₂ -Ph), 4.29 – 4.12 (m, 4H, 2×OCH ₂ -Ph), 4.11 – 4.04 (m, 1H, H4/H5), 3.95 (ddt, <i>J</i> = 19.6, 8.0, 5.0 Hz, 4H, 4×CH (H2/H3/H4/H5/H6/H7)), 3.80 (p, <i>J</i> = 7.6, 5.1 Hz, 1H, H2/H7), 3.66 (dd, <i>J</i> = 10.5, 2.6 Hz, 1H, H1a/H8a), 3.58 (dd, <i>J</i> = 10.5, 5.3 Hz, 1H, H1b/H8b), 3.58 – 3.45 (m, 2H, H1a/H1b/H8a/H8b) ppm.
¹³C-NMR (101 MHz, CDCl₃)	δ = 139.5 (Ph C1), 139.4 (Ph C1), 139.1 (Ph C1), 139.0 (Ph C1), 138.9 (Ph C1), 138.8 (Ph C1), 138.7 (Ph C1), 138.5 (Ph C1), 129.1 – 126.7 (40×Ph CH), 80.1, 79.8, 79.5, 79.2, 79.2, 78.7 (6×CH), 74.3, 73.4, 73.3, 73.1, 73.0, 72.8, 72.3, 72.2 (8×OCH ₂ -Ph), 70.7 (C1/C8), 70.5 (C1/C8) ppm.
HRMS (+ESI-TOF)	<i>m/z</i> [M+H] ⁺ calc. for C ₆₄ H ₆₇ O ₈ 963.4726, found 963.4851

D 2.15 3-Bromoprop-1-en-1-yl benzoate [2]

**Procedure**

According to a literature protocol^{38,77}, acrolein [42] (90%, 1.50 g, 1.79 mL, 26.8 mmol, 1.00 eq.) was dissolved in dry DCM (60 mL), cooled to $-20\text{ }^{\circ}\text{C}$, using an acetone/liquid N_2 cooling bath. Then, benzoyl bromide [17] (4.70 g, 25.4 mmol, 0.95 equiv.) was followed by anhydrous ZnCl_2 (36 mg, 0.27 mmol, 0.01 equiv.). The reaction mixture was allowed to warm up to $-15\text{ }^{\circ}\text{C}$ by lowering the cooling bath, and stirring was continued for one hour, keeping the temperature below $-10\text{ }^{\circ}\text{C}$. As $^1\text{H-NMR}$ -analysis (micro work-up with Et_2O and aq. sat. NaHCO_3 , drying over Na_2SO_4) did not show any formed product but Just starting material the stirring mixture was allowed to warm up to $0\text{ }^{\circ}\text{C}$ and kept as this temperature for 2 hours. Within this time, the solution turned orange and $^1\text{H-NMR}$ -analysis confirmed full conversion of the starting material to the targeted product. Aq. sat. NaHCO_3 (40 mL) was slowly added to the mixture, followed by further DCM (200 mL).

The layers were separated, and the aqueous phase was extracted again with another portion of DCM (150 mL). The combined organic phase was dried over anhydrous Na_2SO_4 and evaporated giving a brown, oily liquid (5.5 g).

Purification

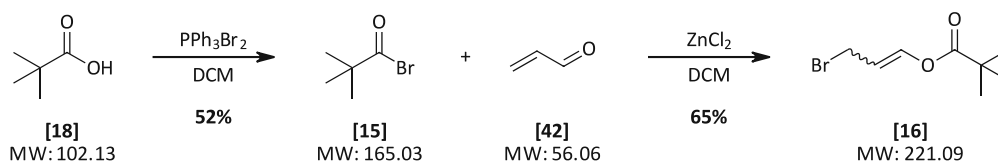
The pure product [2] was obtained by flash column chromatography (100 g SiO_2 , LP/EtOAc 9:1, fraction size 150 mL) as a colourless liquid (4.2 g, 72%) in a ratio of $E/Z = \sim 0.4:0.6$ (according to $^1\text{H-NMR}$) that solidified in the freezer ($-18\text{ }^{\circ}\text{C}$).

Yield	4.2 g, 72%
Appearance	white needles
Melting point	41.8-42.5 $^{\circ}\text{C}$ (LP/EtOAc)
R_f	0.48 (LP/EtOAc 2:1)
$^1\text{H-NMR}$ (400 MHz, CDCl_3)	$\delta = 8.20 - 8.03$ (m, 2H, Ph-CH (E/Z)), 7.67 (dt, $J = 12.4, 1.1$ Hz, 0.6H, =CH-O (Z)), 7.65 – 7.58 (m, 1H, Ph-CH (E/Z)), 7.54 – 7.45 (m, 2H, Ph-CH (E/Z)), 7.44 (dt, $J = 6.2, 0.8$ Hz, 0.4H, =CH-O (E)), 5.90 (dt, $J = 12.3, 8.4$ Hz, 0.4H, =CH-CH ₂ (E)), 5.39 (td, $J = 8.4, 6.2$ Hz, 0.6H, =CH-CH ₂ (Z)), 4.21 (dd, $J = 8.4, 0.8$ Hz, 1.2H, CH ₂ -Br (Z)), 4.07 (dd, $J = 8.4, 1.0$ Hz, 0.8H, CH ₂ -Br (E)) ppm.

$^{13}\text{C-NMR}$ (151 MHz, CDCl_3) δ = 163.3 (C=O (Z)), 162.9 (C=O (E)), 139.5 (=CH-O (Z)), 137.7 (=CH-O (E)), 134.1, 134.0, 130.2, 130.2, 128.8, 128.7 (6 \times Ph-CH (E/Z)), 128.7, 128.5 (2 \times Ph-CH (E/Z)), 112.0 (=CH-CH₂ (Z)), 110.2 (=CH-CH₂ (E)), 28.7 (CH₂-Br (Z)), 23.7 (CH₂-Br (E)) ppm.

Spectral data in accordance to literature.^{38,77}

D 2.16 3-Bromoprop-1-en-1-yl pivalate [16]



Step 1 – Synthesis of pivaloyl bromide

Procedure

According to a literature protocol²⁴, PPh₃ (89.9 g, 343 mmol, 1.00 equiv) was dissolved in dry DCM (170 mL) and cooled to –10 °C, using an ice/NaCl-mixture (3:1). Then, Br₂ (54.8 g, 17.6 mL, 343 mmol, 1.00 equiv) was added dropwise as a solution in dry DCM (170 mL) in a way that the temperature stayed below 0 °C. The formation of a white precipitate (PPh₃Br₂) was obtained. Further, a solution of pivalic acid **[18]** (35.0 g, 343 mmol, 1.00 equiv.) in dry DCM (170 mL) was prepared that was quickly added to the reaction mixture after complete addition of Br₂. The mixture turned into a clear, orange solution and was stirred at rt for 1.5 hours. Then, the solvent was removed, and the precipitate was taken up in dry Et₂O that led to the formation of more precipitate. The solid was removed *via* filtration, and the filtrate was concentrated *in vacuo*.

Purification

The pure product **[15]** was obtained by distillation *in vacuo* (bp 27-29 °C, 10 mbar) as a colourless liquid (29.4 g, 52%).

Yield 29.4 g, 52%

Appearance colourless liquid

Boiling point 27-29 °C, 10 mbar (lit¹¹⁴ 65 °C, 15 Torr)

¹H-NMR (400 MHz, CDCl₃) δ = 1.31 (s, 3×CH₃)

¹³C-NMR (101 MHz, CDCl₃) δ = δ = 178.8 (COBr), 52.8 (C(CH₃)₃), 27.2 (3×C(CH₃))

Step 2 – Synthesis of 3-bromoprop-1-en-1-yl pivalate

Procedure

Acrolein **[42]** (90%, 11.1 g, 13.2 mL, 198 mmol, 1.00 eq.) was dissolved in dry DCM (100 mL), cooled to –20 °C using an acetone/liquid N₂ cooling bath, and pivaloyl bromide **[15]** (29.3 g, 178 mmol, 0.90 equiv.) was added to the solution under stirring. Then, after the addition of anhydrous ZnCl₂ (269 mg, 1.98 mmol, 0.01 equiv.), the reaction mixture was allowed to warm up to –10 °C by lowering the cooling bath as the exothermic reaction started and a temperature jump to +10 °C could be observed. The flask was then re-immersed in the cooling bath, and the reaction mixture was stirred for one hour, keeping the temperature below –10 °C. As ¹H-NMR-analysis (micro work-up with Et₂O and

aq. sat. NaHCO₃, drying over Na₂SO₄) confirmed full conversion of the starting material to the targeted product, H₂O (40 mL) was added which led to the formation of a white precipitate and the temperature rose to -10 °C.

The layers were then separated, and the organic layer was washed with sat. aq. NaHCO₃ (2×30 mL – until pH remained basic). The greenish organic phase was further washed with brine, dried over anhydrous Na₂SO₄ and evaporated giving a brown, oily liquid.

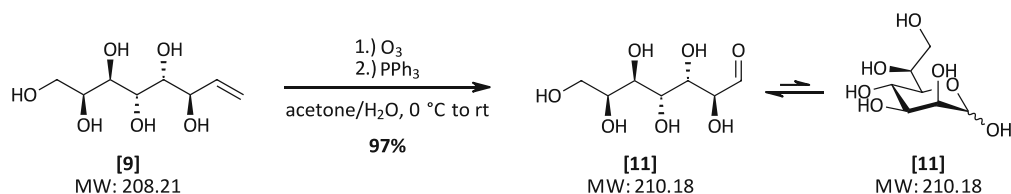
Purification

The pure product **[16]** was obtained by distillation *in vacuo* (bp 73 °C, 3.2 mbar) as a colourless to slightly yellow liquid (25.6 g, 65%) in a ratio of *E/Z* = ~0.4:0.6 (according to ¹H-NMR).

<u>Yield</u>	25.6 g, 65%
<u>Appearance</u>	colourless/slightly yellow liquid
<u>Boiling point</u>	73 °C, 3.2 mbar (lit ²⁴ 38 °C, 0.2 mbar)
<u>¹H-NMR (400 MHz, CDCl₃)</u>	<i>(E)</i> -isomer: δ = 7.43 (d, <i>J</i> = 12.4 Hz, 1H, =CH-O), 5.71 (dt, <i>J</i> = 12.4, 8.4 Hz, 1H, =CH-CH ₂), 4.00 (dd, <i>J</i> = 8.4, 1.0 Hz, 2H, CH ₂ -Br), 1.24 (s, 9H, 3×CH ₃) ppm. <i>(Z)</i> -isomer: δ = 7.19 (d, <i>J</i> = 6.2 Hz, 1H, =CH-O), 5.26 (td, <i>J</i> = 8.4, 6.2 Hz, 1H, =CH-CH ₂), 4.08 (dd, <i>J</i> = 8.4, 0.7 Hz, 2H, CH ₂ -Br), 1.29 (s, 9H, 3×CH ₃) ppm.
<u>¹³C-NMR (101 MHz, CDCl₃)</u>	<i>(E)</i> -isomer: δ = 175.2 (C=O), 139.7 (=CH-O), 111.1 (=CH-CH ₂), 38.9 (C(CH ₃) ₃), 28.9 (CH ₂ -Br), 27.0 (3×C(CH ₃) ₃) ppm. <i>(Z)</i> -isomer: δ = 174.7 (C=O), 137.9 (=CH-O), 109.6 (=CH-CH ₂), 39.2 (C(CH ₃) ₃), 27.1 (3×C(CH ₃) ₃), 23.6 (CH ₂ -Br) ppm.

Spectral data in accordance with literature.²⁴

D 2.17 L-Glycero-D-manno-heptose [11] – method A

**Procedure**

According to a literature protocol²³⁻²⁴, octenitol [9] (100 mg, 0.480 mmol, 1.00 equiv.) was dissolved in water/acetone (3:2, 2 mL) and a small amount of Sudan red (III) in acetone was added, staining the reaction mixture pink (for indication). The solution was cooled to 0 °C using an ice-bath, and ozone was bubbled through a gas inlet tube. At the outlet, the gas was passed through a gas washing bottle with aq. KI (10% w/w) solution. Bubbling of ozone was performed until the pink colour diminished and TLC analysis (CHCl₃/MeOH/H₂O 14:7:1, staining agent: anisaldehyde) indicated full conversion of the starting material.

The ozone generator was switched off and oxygen was bubbled through the solution for ~15 min. PPh₃ (252 mg, 0.961 mmol, 2.00 equiv.) was added followed by further acetone (to dissolve PPh₃) and stirring was continued at rt overnight. The next day, the reduction of all peroxides and H₂O₂ was confirmed (peroxide test stripe) and the reaction mixture was concentrated. The remaining aqueous layer was washed with DCM (20 mL), EtOAc (20 mL) and Et₂O, concentrated *in vacuo* and co-evaporated from MeOH twice. The heptose [11] was obtained as a yellow oil as an anomeric mixture with a ratio of $\alpha/\beta = 2:1$ (¹H-NMR).

Yield 98 mg, 97%

Appearance yellow, sticky oil

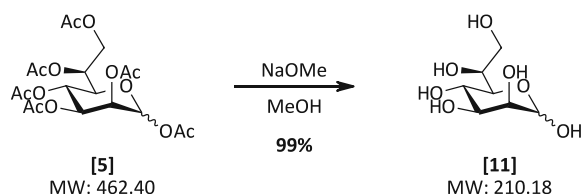
R_f 0.13 (yellow/brown) (CHCl₃/MeOH/H₂O 14:7:1, staining agent: anisaldehyde)

¹H-NMR (400 MHz, D₂O, ref. to MeOH = 3.34) $\delta = 5.16$ (d, $J = 1.7$ Hz, 2H, H-1 α), 4.86 (d, $J = 1.1$ Hz, 1H, H1 β), 4.02 (ddd, $J = 7.1, 5.7, 1.4$ Hz, 2H, H6 α), 3.97 (td, $J = 6.6, 1.7$ Hz, 1H, H6 β), 3.92 (ddd, $J = 5.1, 3.3, 1.0$ Hz, 1H, H2 β), 3.91 (dd, $J = 3.1, 1.7$ Hz, 2H, H2 α), 3.88 – 3.78 (m, 5H, H3 α , H4 α , H4 β), 3.76 – 3.72 (m, 2H, H5 α), 3.71 – 3.68 (m, 2H, H7a (β), H7b (β)), 3.68 – 3.64 (m, 4H, H7a (α), H7b (α)), 3.64 – 3.61 (m, 1H, H3 β), 3.32 (dd, $J = 9.8, 1.7$ Hz, 1H, H5 β) ppm.

¹³C-NMR (101 MHz, D₂O, ref. to MeOH = 49.5) $\delta = 94.8$ (C1 α), 94.5 (C1 β), 75.2 (C5 β), 73.9 (C3 β), 71.8 (C2 β), 71.6 (C5 α), 71.3 (C2 α), 71.2 (C3 α), 69.4 (C6 α), 69.3 (C6 β), 66.8 (C4 α), 66.5 (C4 β), 63.6 (C7 α), 63.4 (C7 β) ppm.

Spectral data in accordance with literature.²³

D 2.18 L-Glycero-D-manno-heptose [11] – method B



Procedure

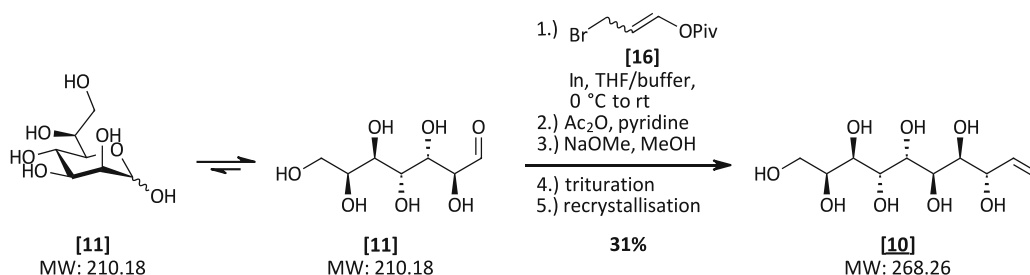
The LD-heptose peracetate [5] (650 mg, 1.41 mmol, 1.00 equiv.) was taken up in MeOH (HPLC grade, 10 mL) and NaOMe (30% in MeOH) was added dropwise until pH was about 9. After 2 hours, TLC (CHCl₃/MeOH/H₂O 14:7:1, LP/EtOAc 1:1, staining agent: anisaldehyde) indicated full conversion and the reaction mixture was diluted with H₂O.

Dowex-H⁺ resin (MeOH washed) was added until pH 7, and the solution was filtered and evaporated to dryness, giving the heptose [11] (293 mg, 99%) as a yellow, sticky oil. The obtained product was a mixture of the two anomers with a ratio of $\alpha/\beta = 2:1$ (according to ¹H-NMR). The obtained material was used without further purification.

Yield	293 mg, 99%
R_f	0.13 (yellow/brown) (CHCl ₃ /MeOH/H ₂ O 14:7:1, staining agent: anisaldehyde)
Appearance	yellow oil

For spectral data see Chapter D 2.17.

D 2.19 1,2-Dideoxy-L-lyxo-L-manno-dec-1-enitol [10]

**Procedure****Step 1 – IMA**

Based on a literature protocol³⁸, indium (2.19 g, 19.0 mmol, 2.00 equiv.) was weighed in a flame dried Schlenk flask and Schlenk technique was applied. Anhydrous THF (25.0 mL) was added, and the mixture was cooled to 0 °C using an ice-bath. 3-Bromopropenyl pivalate [16] (6.31 g, 28.5 mmol, 3.00 equiv.) was added dropwise to the vigorously stirring mixture. After 15 min, the ice-bath was removed, and the suspension was allowed to warm up to room temperature and stirred for another 45 min. Then, L-glycero-D-manno-heptose [11] (2.00 g, 9.50 mmol, 1.00 equiv.) was added to the pre-formed reagent as a solution in phthalate buffer (pH ~3, 4.0 mL). To guarantee efficient stirring, further THF (5.0 mL) was added 30 min after the addition of the starting material. As TLC (CHCl₃/MeOH/H₂O 14:7:1, staining reagent: anisaldehyde) indicated full conversion of the starting material (after 45 min), the reaction mixture was diluted with MeOH and H₂O and filtered. The filtrate was concentrated *in vacuo*, giving a colourless solid.

Step 2 – Acetylation

This material was taken up in pyridine (99%, 40 mL), and Ac₂O (34.0 g, 31.5 mL, 333 mmol, 35 eq.) was added to the stirring mixture under ice-bath cooling. After 10 min, the ice-bath was removed, and a spatula of DMAP was added. Stirring at rt was continued overnight. Next day, HPLC-MS indicated complete conversion to the fully protected decenitol. Excessive reagent was quenched by the addition of MeOH (20 mL) under ice-bath cooling, and the mixture was stirred for further 30 min. After diluting with DCM (200 mL), the organic phase was extracted with 1N HCl (3×50 mL – until pH remained acidic) and washed with aq. sat. NaHCO₃ (3×80 mL – foaming!) and brine. After drying over anhydrous Na₂SO₄, the solution was evaporated to dryness.

Step 3 – Deacetylation

The residue was taken up in MeOH (HPLC grade, 50 mL) and NaOMe (30% in MeOH, ~3 mL) was added under stirring at rt until pH was about 10. Reaction monitoring *via* HPLC-MS after 3 hours showed full conversion. The reaction mixture was neutralized by the addition of Dowex-H⁺ (MeOH washed), H₂O was added to dissolve the formed enitol, and the

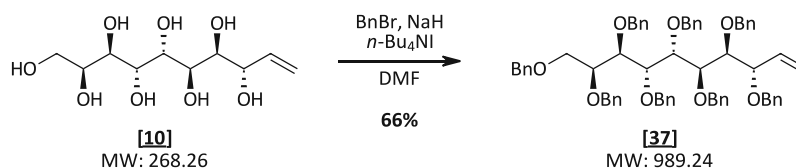
solution was filtered. Evaporation of the solvent gave a beige solid matter (3.85 g) that was a mixture of diastereomers in the ratio *lyxo* : *xylo* : *ribo* : 71 : 19 : 10.

Purification

The solid was then triturated with MeOH (10 mL), and the remaining solid was isolated by centrifugation. The residue was washed twice with further MeOH (2×10 mL). As the last step, washing with Et₂O was performed, and the solid material was dried *in vacuo* at 40 °C. This first crop (1.07 g) was recrystallized from water, and the obtained solid was washed with MeOH (8 mL) followed by Et₂O (8 mL). After drying, the *L-lyxo-L-manno*-decenitol **[10]** was obtained as a colourless solid (395 mg, 15%). A second crop of solid was isolated from the methanol phase of the trituration by centrifugation and was further washed with MeOH (2×5 mL) and Et₂O (180 mg). This was combined with the material that was obtained from evaporation of the mother liquid from the first recrystallisation (660 mg). Another recrystallisation with H₂O (9 mL) gave further product, that was washed with MeOH (2×5 mL) and Et₂O, and dried. A second crop of enantiomerically pure *lyxo*-decenitol **[10]** was obtained (395 mg, 15%).

<u>Yield</u>	790 mg, 31% (over 3 steps)
<u>Appearance</u>	colourless solid
<u>Melting point</u>	220.4 – 224.2 °C (H ₂ O)
<u>R_f</u>	0.17 (blue) (CHCl ₃ /MeOH/H ₂ O 14:7:1, staining agent: anisaldehyde)
<u>¹H-NMR (600 MHz, D₂O)</u>	δ = 6.03 (ddd, <i>J</i> = 17.3, 10.5, 6.9 Hz, 1H, H2), 5.39 (dt, <i>J</i> = 17.3, 1.2 Hz, 1H, H1 (<i>E</i>)), 5.32 (dt, <i>J</i> = 10.5, 1.1 Hz, 1H, H1 (<i>Z</i>)), 4.23 – 4.17 (m, 1H, H3), 4.00 (td, <i>J</i> = 6.5, 6.0, 1.4 Hz, 1H, H9), 3.96 (d, <i>J</i> = 9.1 Hz, 3H, H5, H6, H7), 3.78 (d, <i>J</i> = 8.1 Hz, 1H, H4), 3.73 – 3.68 (m, 3H, H10a, H10b, H8) ppm.
<u>¹³C-NMR (151 MHz, D₂O)</u>	δ = 137.7 (C2), 117.7 (C1), 72.5 (C3), 71.7 (C4), 70.3 (C9), 69.4 (C8), 68.4 (C5/C6/C7), 68.3 (C5/C6/C7), 68.2 (C5/C6/C7), 63.3 (C10) ppm.
<u>HRMS (ESI-TOF)</u>	<i>m/z</i> [M-H] ⁻ calc. for C ₁₀ H ₁₉ O ₈ 267.1086, found 267.1100

D 2.20 3,4,5,6,7,8,9,10-Octa-*O*-benzyl-1,2-dideoxy-*L*-lyxo-*L*-manno-dec-1-enitol [37]



Procedure

The *lyxo*-decenitol [10] (367 mg, 1.37 mmol, 1.00 equiv.) was suspended in dry DMF (7.5 mL) and NaH (60% in paraffin oil, 1.09 g, 27.4 mmol, 20.0 equiv.) was added portionwise to the stirring mixture under ice-bath cooling (formation of H₂). After stirring for 15 min at 0 °C, benzyl bromide (3.74 g, 2.60 mL, 21.9 mmol, 16 equiv.) was added dropwise. The formation of a beige precipitate was obtained. The mixture was allowed to warm up to rt, and *n*-Bu₄NI (253 mg, 0.684 mmol, 0.50 equiv.) was added. Stirring was continued overnight, and TLC (LP/EtOAc 3:1, staining reagent: Mostain) and HPLC-MS indicated full conversion to a very nonpolar species. Excessive reagent was quenched by the addition of MeOH (4 mL).

The mixture was diluted with Et₂O (50 mL) and extracted with water. As the flask with the organic phase was dropped at this point, the material was taken up from the floor and evaporated (2.2 g). Column chromatography (220 g SiO₂, LP/EtOAc 10:1 (1.7 L) → 7:1 (600 mL) → 5:1 (600 mL)) was performed to get rid of contamination. The fractions containing the desired product were combined, vaporised, and the residue was taken up in acetonitrile (30 mL), extracted with hexane (2×10 mL), and vaporised again (978 mg).

Purification

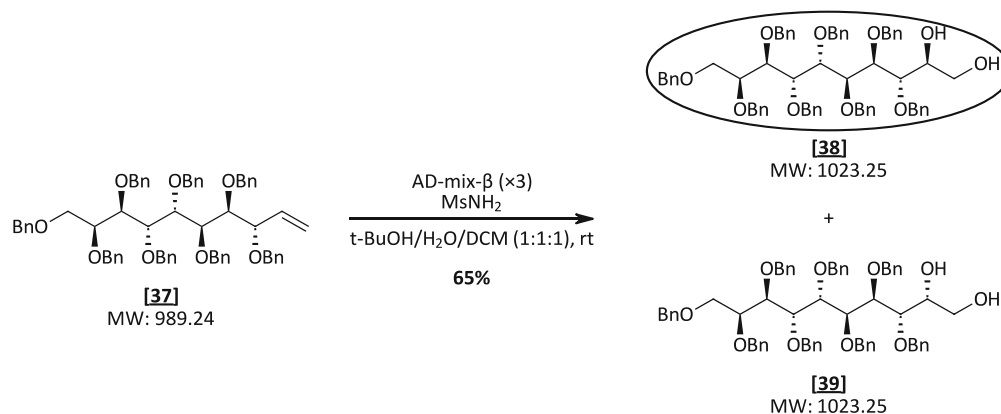
The pure product was obtained by flash column chromatography (100 g SiO₂, LP (1 L) → LP/EtOAc 10:1), giving the desired product [37] as a colourless oil (895 mg, 66%).

Yield	895 g, 66%
Appearance	colourless oil
R_f	0.53 (LP/EtOAc 3:1, staining agent: Mostain)
¹H-NMR (600 MHz, CDCl₃)	$\delta = 7.32 - 7.14$ (m, 40H, 40×Ph CH), 5.89 (ddd, $J = 17.1, 10.5, 7.8$ Hz, 1H, H2), $5.34 - 5.27$ (m, 2H, H1a, H1b), $4.73 - 4.66$ (m, 4H, 2×OCH ₂ -Ph), 4.63 (q, $J = 11.2, 10.0$ Hz, 2H, OCH ₂ -Ph (C4)), $4.59 - 4.54$ (m, 5H, 2.5×OCH ₂ -Ph), $4.53 - 4.48$ (m, 2H, OCH _H -Ph (C3), OCH _H -Ph), $4.46 - 4.32$ (m, 2H, OCH ₂ -Ph (C10)), $4.22 - 4.18$ (m, 2H, H5, H6/H7/H8), 4.16 (d, $J = 11.7$ Hz, 2H, OCH _H -Ph (C3), H6/H7/H8), 4.08 (dd, $J = 7.8, 6.8$ Hz, 1H, H3), $4.06 - 4.01$ (m, 2H, H6/H7/H8, H9), $3.97 - 3.89$ (m, 1H, H4), $3.71 - 3.58$ (m, 2H, H10a, H10b) ppm.

¹³C-NMR (151 MHz, CDCl₃) δ = 139.3, 139.2, 139.2, 139.1, 139.1, 138.9, 138.7, 138.4 (8×Ph C1), 136.4 (C2), 128.6 – 127.0 (40×Ph CH), 119.7 (C1), 81.2 (C4), 81.1 (C3), 78.7, 78.4, 78.3, 77.8, 77.6 (5×CH), 73.8, 73.4 (2×OCH₂-Ph), 73.3 (OCH₂-Ph (C10)), 73.2, 72.9, 72.8, 72.4 (4×OCH₂-Ph), 70.8 (C10), 70.1 (OCH₂-Ph (C3)) ppm.

HRMS (+ESI-TOF) m/z [M+H]⁺ calc. for C₆₆H₆₈O₈ 989.4983, found 989.4991

D 2.21 3,4,5,6,7,8,9,10-Octa-*O*-benzyl-L-galacto-L-talo-decitol [38]



Procedure

AD-mix- β ($\times 3$) (1.35 g, 1.40 g/mmol starting material) was suspended in $t\text{-BuOH}/\text{H}_2\text{O}$ (1:1, 2 mL) and MsNH_2 (158 mg, 1.66 mmol, 2.00 equiv.) was added under vigorous stirring. After 30 min, the protected decenitol [37] (954 mg, 0.964 mmol, 1.00 equiv.) was added as a solution in DCM (1 mL). As TLC analysis (LP/EtOAc 1:1) and HPLC-MS showed full conversion of the starting material after 2 days, the reaction mixture was quenched by the addition of solid $\text{Na}_2\text{S}_2\text{O}_5$ (2.2 g).

After dilution with H_2O (40 mL) and DCM (60 mL) the phases were separated, and the aq. phase extracted with DCM (3 \times 20 mL). The pooled organic phase was washed with brine, dried over Na_2SO_4 and vapourised, giving a yellow, oily crude material (990 mg).

Purification

The crude material (990 mg) was purified *via* flash column chromatography (100 g SiO_2 , LP/EtOAc 10:1 (550 mL) \rightarrow 5:1 (1200 mL) \rightarrow 2:1 (1200 mL) \rightarrow 1:1), giving three different product fractions with an overall yield of 78%: (1) enriched octabenzyl-L-galacto-L-talo-decitol [38] (636 mg, 65%), (2) mixture of talo- [38] and galacto-decitol [39] (105 mg, 11%), (3) octabenzyl-L-galacto-L-galacto-decitol [39] (20 mg, 2%).

3,4,5,6,7,8,9,10-Octa-O-benzyl-L-galacto-L-talo-octitol [38]

Yield	636 mg, 65%
Appearance	colourless oil
R_f	0.53 (LP/EtOAc 1:1, staining agent: Mostain)
¹H-NMR (400 MHz, CDCl₃)	δ = 7.28 – 6.99 (m, 40H, 40×Ph CH), 4.75 – 4.58 (m, 6H, 4×CHH-Ph (C4, C5, C7, C9), OCH ₂ -Ph (C6)), 4.51 (s, 7H, 2×CHH-Ph (C5, C4), OCH ₂ -Ph (C8), 3×CHH-Ph (C9, C7, C3)), 4.34 (d, J = 2.5 Hz, 2H, OCH ₂ -Ph (10)), 4.26 – 4.18 (m, 2H, CHH-Ph (C3), H6), 4.15 – 4.05 (m, 2H, H5, H7), 4.05 – 3.92 (m, 3H, H4, H9, H8), 3.80 (d, J = 4.4 Hz, 1H, H2), 3.66 (dd, J = 9.9, 5.8 Hz, 1H, H10a), 3.64 – 3.57 (m, 2H, H3, H10b), 3.47 (dd, J = 11.1, 6.7 Hz, 1H, H1a), 3.39 – 3.27 (m, 1H, H1b) ppm.
¹³C-NMR (101 MHz, CDCl₃)	δ = 139.0, 139.0, 138.8, 138.8, 138.7, 138.3, 138.3, 137.9 (8×Ph C1), 128.7 – 127.2 (40×Ph CH), 79.9 (C4), 78.9 (C8), 78.3 (C7), 78.3 (C9), 78.2 (C3), 77.0 (C6), 77.0 (C5), 74.9 (OCH ₂ -Ph (C4)), 73.8 (OCH ₂ -Ph (C7/C8)), 73.8 (OCH ₂ -Ph (C7/C8)), 73.4 (OCH ₂ -Ph (C10)), 73.3 (OCH ₂ -Ph (C3)), 72.7 (OCH ₂ -Ph (C9)), 72.2 (OCH ₂ -Ph (C6)), 72.0 (OCH ₂ -Ph (C5)), 71.4 (C2), 70.7 (C10), 64.3 (C1) ppm.
HRMS (+ESI-TOF)	m/z [M+H] ⁺ calc. for C ₆₆ H ₇₁ O ₁₀ 1023.5038, found 1023.5075

Note

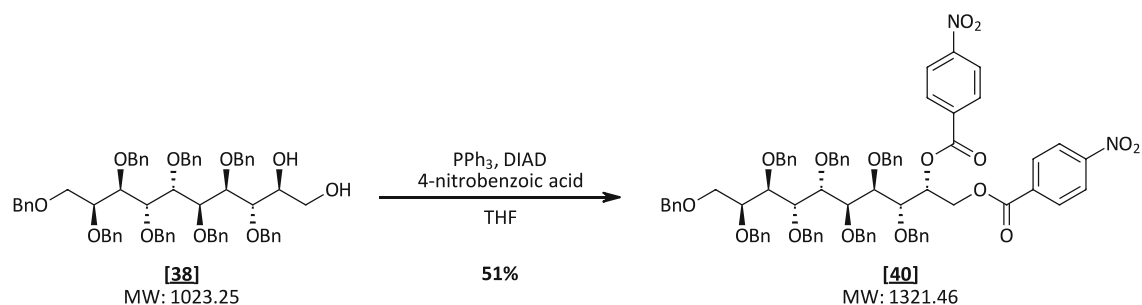
Signals for C5 and C6 overlapped with the solvent residual peak (CDCl₃ δ = 77.16 ppm) in the ¹³C-NMR spectrum. The given shifts were determined from the recorded HSQC spectrum.

3,4,5,6,7,8,9,10-Octa-O-benzyl-L-galacto-L-galacto-octitol [39]

Yield	20 mg, 2%
Appearance	colourless oil
R_f	0.45 (LP/EtOAc 1:1, staining agent: Mostain)

For spectral data see Chapter D 2.23.

D 2.22 3,4,5,6,7,8,9,10-Octa-*O*-benzyl-1,2-di-*O*-(*p*-nitrobenzoyl)-*L*-galacto-*L*-galacto-decitol [40]



Procedure

In a flame dried Schlenk flask, PPh_3 (814 mg, 3.10 mmol, 5.00 equiv.) was weighed, and the flask was flushed with Ar three times *via* Schlenk technique. Then, dry THF (3.0 mL) was added, and the mixture was cooled to 0 °C using an ice-bath. Under stirring, DIAD (627 mg, 3.10 mmol, 5.00 equiv.) was added dropwise, leading to the formation of a beige precipitate. For efficient stirring, further dry THF (0.2 mL) was added, and the mixture was stirred at 0 °C for 15 minutes. The starting material [38] (635 mg, 621 μmol , 1.00 equiv.) (evaporated from dry toluene (3 \times 3 mL) before use) and 4-nitrobenzoic acid (519 mg, 3.10 mmol, 5.00 equiv.) were mixed in dry THF (3.0 mL), and the suspension was added to the pre-formed PPh_3 /DIAD-complex at 0 °C. The reaction mixture was allowed to slowly warm up to rt, subsequently heated to 45 °C and stirred overnight.

As TLC analysis the next day (LP/EtOAc 3:1, staining agent: Mostain) showed full consumption of the starting material, the solution was concentrated *in vacuo*, and the residue stirred in cold Et_2O (3.0 mL). The formed, white precipitate was separated by centrifugation. The supernatant was diluted with further Et_2O (50 mL), extracted with aq. sat. NaHCO_3 (3 \times 20 mL) and washed with brine. After drying over anhydrous Na_2SO_4 , the solvent was vaporised giving a yellow, oily crude material (2.16 g)

Purification

The crude material was purified *via* column chromatography (220 g SiO_2 , LP/EtOAc 10:1 \rightarrow 8:1) giving the targeted product [40] (415 mg, 51%) as a yellow oil.

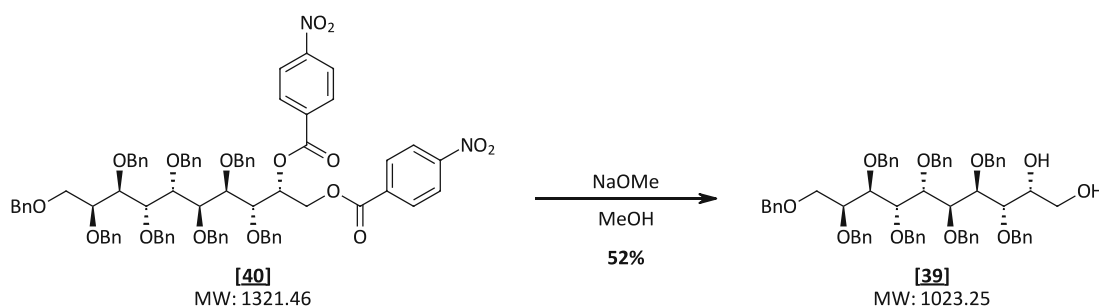
Yield 415 mg, 51%

Appearance yellow oil

R_f 0.22 (LP/EtOAc 5:1, staining agent: Mostain)

¹H-NMR (400 MHz, CDCl₃) δ = 8.12 – 8.05 (m, 2H, 2×PNB CH), 7.99 – 7.89 (m, 6H, 6×PNB CH), 7.23 – 6.99 (m, 40H, 40×Ph CH), 5.98 – 5.90 (m, 1H, H₂), 4.80 (d, J = 11.7 Hz, 1H, C \underline{H} H-Ph), 4.75 – 4.61 (m, 4H, 2×C \underline{H} H-Ph, OCH₂-Ph), 4.61 – 4.51 (m, 4H, 2×C \underline{H} H-Ph, OCH₂-Ph), 4.51 – 4.41 (m, 4H, OCH₂-Ph, C \underline{H} H-Ph, H_{1a}), 4.37 (d, J = 2.4 Hz, 2H, OCH₂-Ph), 4.35 – 4.27 (m, 4H, 2×C \underline{H} H-Ph, 2×CH), 4.19 – 4.14 (m, 1H, CH), 4.03 (dd, J = 5.6, 3.7 Hz, 1H, CH), 4.01 – 3.94 (m, 4H, H_{1b}, 3×CH), 3.77 – 3.66 (m, 2H, H_{10a}, H_{10b}).ppm.

¹³C-NMR (101 MHz, CDCl₃) δ = 164.3, 164.2 (PNB C=O), 150.7, 150.5 (PNB Ph C₆), 138.8, 138.6, 138.6, 138.4, 138.3, 138.2, 137.9, 137.6 (8×Bn Ph C₁), 135.4, 135.1 (2×PNB Ph C₁), 131.0 (2×PNB Ph CH), 130.9 (2×PNB Ph CH), 128.2 – 127.2 (40×Bn Ph CH), 123.6 (2×PNB Ph CH), 123.5 (2×PNB Ph CH), 79.1, 78.9, 78.9, 78.8, 78.7, 77.3, 76.8, 76.7 (8×CH (C₃-C₉)) 74.5, 74.4, 73.3, 73.0, 73.0, 72.8, 72.7, 71.5 (8×O \underline{C} H₂-Ph), 72.0 (C₂), 70.9 (C₁₀), 65.4 (C₁) ppm.

D 2.23 3,4,5,6,7,8,9,10-Octa-*O*-benzyl-*L*-galacto-*L*-galacto-decitol [39]**Procedure**

The starting material **[40]** (130 mg, 0.127 mmol, 1.00 equiv.) was taken up in MeOH (HPLC grade, 1.5 mL) and NaOMe (30% in MeOH) was added dropwise under stirring at rt until pH was about 10. After 3.5 hours, HPLC-MS indicated full conversion and the reaction mixture was neutralized by the addition of Dowex-H⁺. After filtration and evaporation, the residue was taken up in DCM (50 mL), extracted with sat. aq. NaHCO₃ (3×10 mL) and washed with brine. After drying over anhydrous Na₂SO₄, the organic phase was evaporated, giving the crude product (129 mg) as a yellow oil.

Purification

The diastereomerically pure octabenzyl-*galacto*-decitol **[39]** was obtained *via* column chromatography (13.0 g SiO₂, LP/EtOAc 7:1 → 2:1, fraction size: 10 mL) as a colourless solid (68 mg, 52%). Further fractions containing both diastereomers, the *galacto*- **[38]** and the *talo*-decitol **[39]**, were isolated, too.

Yield 68 mg, 52%

Appearance colourless solid

R_f 0.45 (LP/EtOAc 1:1, staining agent: Mostain)

¹H-NMR (400 MHz, CDCl₃) δ = 7.28 – 6.99 (m, 40H, 40×Ph CH), 4.75 – 4.58 (m, 6H, 4×CH₂H-Ph (C4, C5, C7, C9), OCH₂-Ph (C6)), 4.51 (s, 7H, 2×CH₂H-Ph (5, 4), OCH₂-Ph (C8), 3×CH₂H-Ph (C9, C7, C3)), 4.34 (d, *J* = 2.5 Hz, 2H, OCH₂-Ph (C10)), 4.26 – 4.18 (m, 2H, CH₂H-Ph (C3), H6), 4.15 – 4.05 (m, 2H, H5, H7), 4.05 – 3.92 (m, 3H, H4, H9, H8), 3.80 (d, *J* = 4.4 Hz, 1H, H2), 3.66 (dd, *J* = 9.9, 5.8 Hz, 1H, H10a), 3.64 – 3.57 (m, 2H, H3, H10b), 3.47 (dd, *J* = 11.1, 6.7 Hz, 1H, H1a), 3.39 – 3.27 (m, 1H, H1b) ppm.

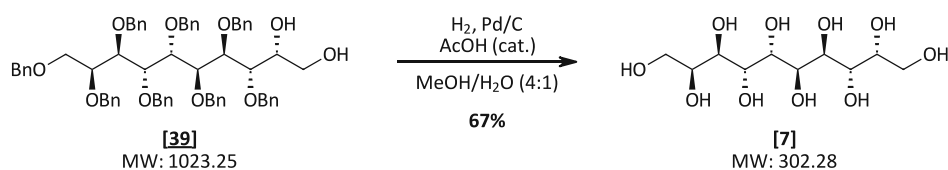
¹³C-NMR (101 MHz, CDCl₃) δ = 139.0, 139.0, 138.8, 138.8, 138.7, 138.3, 138.3, 137.9 (8xPh C1), 128.7 – 127.2 (40xPh CH), 79.9 (C4), 78.9 (C8), 78.3 (C7), 78.3 (C9), 78.2 (C3), 77.0 (C6), 77.0 (C5), 74.9 (OCH₂-Ph (C4)), 73.8 (OCH₂-Ph (C7/C8)), 73.8 (OCH₂-Ph (C7/C8)), 73.4 (OCH₂-Ph (C10)), 73.3 (OCH₂-Ph (C3)), 72.7 (OCH₂-Ph (C9)), 72.2 (OCH₂-Ph (C6)), 72.0 (OCH₂-Ph (C5)), 71.4 (C2), 70.7 (C10), 64.3 (C1) ppm.

HRMS (+ESI-TOF) m/z [M+H]⁺ calc. for C₆₆H₇₁O₁₀ 1023.5038, found 1023.5073

Note

Signals for C5 and C6 overlapped with the solvent residual peak (CDCl₃ δ = 77.16 ppm) in the ¹³C-NMR spectrum. The given shifts were determined from the recorded HSQC spectrum.

D 2.24 L-Galacto-L-galacto-decitol [7]



Procedure

The starting material **[39]** (10 mg, 0.010mmol, 1.0 equiv.) was taken up in MeOH/H₂O (HPLC grade, 4:1, 1.0 mL) with AcOH (2 drops) and Pd/C (10w%, 10 mg) was added under argon atmosphere. Then, hydrogen atmosphere was guaranteed using a balloon, and the reaction mixture was stirred at 50 °C. HPLC-MS confirmed full deprotection towards the decitol after 72 h.

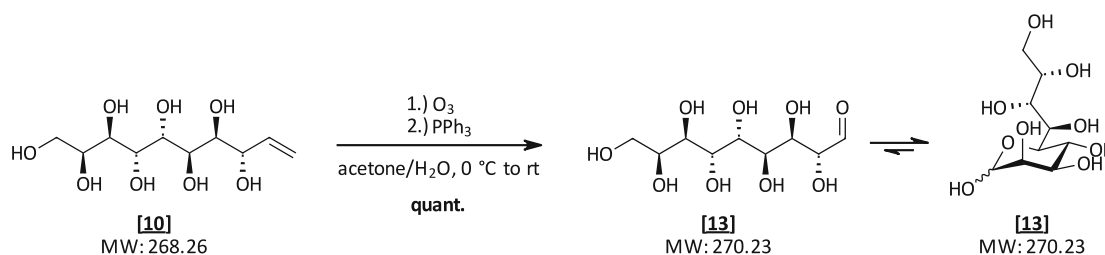
The reaction mixture was further diluted with water, filtered over Celite©, and the filtrate was concentrated

Purification

The crude material was purified by trituration with H₂O, giving the decitol **[7]** as a colourless solid (2 mg, 67%).

Yield	2 mg, 67%
Appearance	colourless solid
R_f	0.08 (red) (CHCl ₃ /MeOH/H ₂ O 14:7:1, staining agent: anisaldehyde)
¹H-NMR (400 MHz, CDCl₃)	δ = 4.01 (td, <i>J</i> = 6.4, 5.9, 1.4 Hz, 2H, H2, H9), 3.96 (m, 4H, H4, H7, H5, H6), 3.71 (m, 6H, H3, H8, H1, H10) ppm.
¹³C-NMR (101 MHz, CDCl₃)	δ = 70.3 (C2, C9), 69.4 (C3, C8), 68.3 (C4/C5, C7/C6), 68.2 (C4/C5, C7/C6), 63.3 (C1, C10) ppm.
HRMS (⁺ESI-TOF)	<i>m/z</i> [M+H] ⁺ calc. for C ₁₀ H ₂₃ O ₁₀ 303.1286, found 303.1286
HRMS (⁻ESI-TOF)	<i>m/z</i> [M-H] ⁻ calc. for C ₁₀ H ₂₁ O ₁₀ 301.1140, found 301.1140

D 2.25 L-Lyxo-L-manno-nonose [13] – method A



Procedure

According to an adapted literature protocol²³⁻²⁴, decentitol [10] (307 mg, 1.14 mmol, 1.00 equiv.) was dissolved in water/acetone (4:1, 25 mL) and a small amount of Sudan red (III) in acetone was added, staining the reaction mixture pink (for indication). The solution was cooled to 0 °C using an ice-bath, and ozone was bubbled through a gas inlet tube. At the outlet, the gas was passed through a gas washing bottle with aq. KI (10% w/w) solution. Bubbling of ozone was performed until the pink colour diminished and TLC analysis (CHCl₃/MeOH/H₂O 14:7:1, staining agent: anisaldehyde) indicated full conversion of the starting material to a more polar spot.

The ozone generator was switched off and oxygen was bubbled through the solution for ~15 min. PPh₃ (600 mg, 2.29 mmol, 2.00 equiv.) was added followed by further acetone (to dissolve PPh₃) and stirring was continued at rt overnight. The next day, the reduction of all peroxides and H₂O₂ was confirmed (peroxide test stripe) and the reaction mixture was concentrated. The remaining aqueous layer was washed with DCM (2×50 mL), EtOAc (50 mL) and Et₂O, then concentrated in vacuo and co-evaporated from MeOH twice. The nonose [13] was obtained as a viscous, colourless oil (344 mg, quant.) as an anomeric mixture with a ratio of $\alpha/\beta = 1.8:1$ (¹H-NMR).

Yield 344 mg, quant.

Appearance colourless oil

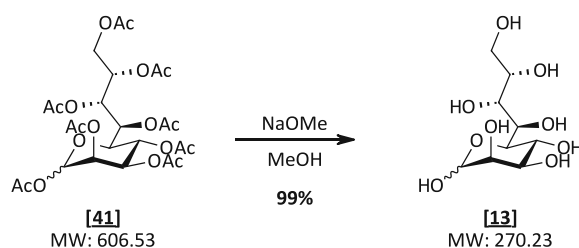
R_f 0.04 (red) (CHCl₃/MeOH/H₂O 14:7:1, staining agent: anisaldehyde)

¹H-NMR (600 MHz, CDCl₃) $\delta = 5.19$ (d, $J = 1.6$ Hz, 1.8H, H1 α), 4.90 (d, $J = 1.1$ Hz, 1H, H1 β), 4.03 – 3.97 (m, 6.4H, H6 α , H7 α , H8 α , H6 β), 3.96 – 3.94 (m, 1H, H8 β), 3.94 (d, $J = 1.1$ Hz, 1H, H2 β), 3.93 (dd, $J = 2.8, 1.6$ Hz, 1.8H, H2 α), 3.88 (d, $J = 1.2$ Hz, 3.6H, H4 α , H3 α), 3.82 (t, $J = 9.8$ Hz, 1H, H4 β), 3.76 (dd, $J = 9.6, 6.6$ Hz, 1H, H7 β), 3.73 – 3.67 (m, 4.5H, H9a (α), H9b (α), H5 α , H9a (β), H9b (β), H3 β), 3.55 (dd, $J = 9.8, 1.3$ Hz, 1H, H5 β) ppm.

¹³C-NMR (150 MHz, CDCl₃) δ = 94.2 (C1 α), 93.9 (C1 β), 73.6 (C5 β), 73.3 (C3 β), 71.2 (C2 β), 70.7 (C5 α), 70.6 (C2 α), 70.2 (C3 α), 70.2 (C6 α), 69.9 (C6 β), 68.9 (C7 α), 68.9 (C7 β), 67.1 (C8 α), 67.0 (C8 β), 66.2 (C4 α), 65.8 (C4 β), 63.2 (C9 β), 63.2 (C9 α) ppm.

HRMS (-ESI-TOF) m/z [M-H]⁻ calc. for C₉H₁₇O₉ 269.0878, found 269.0881

D 2.26 L-Lyxo-L-manno-nonose [13] – method B



Procedure

The starting material **[41]** (455 mg, 0.750 mmol, 1.00 equiv.) was taken up in MeOH (HPLC grade, 2 mL) and NaOMe (30% in MeOH) was added dropwise until pH was about 9. After 1 hour, HPLC-MS and TLC (CHCl₃/MeOH/H₂O 14:7:1, LP/EtOAc 1:1, staining agent: anisaldehyde) and the reaction mixture was diluted with H₂O to dissolve the formed nonose.

Dowex-H⁺ resin (MeOH washed) was added to neutralize the solution that was further filtered and evaporated to dryness, giving the nonose **[13]** (200 mg, 99%) as a colourless oil. The obtained product was a mixture of the two anomers with a ratio of $\alpha/\beta = 1.9:1$ (according to ¹H-NMR).

Yield 200 mg, 99%

Appearance colourless oil

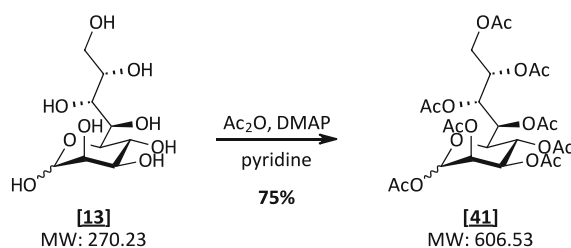
R_f 0.04 (red) (CHCl₃/MeOH/H₂O 14:7:1), staining agent: anisaldehyde)

¹H-NMR (600 MHz, CDCl₃) $\delta = 5.19$ (d, $J = 1.6$ Hz, 1.9H, H1 α), 4.90 (d, $J = 1.1$ Hz, 1H, H1 β), 4.03 – 3.97 (m, 6.7H, H6 α , H7 α , H8 α , H6 β), 3.96 – 3.94 (m, 1H, H8 β), 3.94 (d, $J = 1.1$ Hz, 1H, H2 β), 3.93 (dd, $J = 2.8, 1.6$ Hz, 1.9H, H2 α), 3.88 (d, $J = 1.2$ Hz, 3.8H, H4 α , H3 α), 3.82 (t, $J = 9.8$ Hz, 1H, H4 β), 3.76 (dd, $J = 9.6, 1.5$ Hz, 1H, H7 β), 3.73 – 3.67 (m, 8.7H, H9a (α), H9b (α), H5 α , H9a (β), H9b (β), H3 β), 3.55 (dd, $J = 9.8, 1.3$ Hz, 1H, H5 β) ppm.

¹³C-NMR (150 MHz, CDCl₃) $\delta = 94.2$ (C1 α), 93.9 (C1 β), 73.6 (C5 β), 73.3 (C3 β), 71.2 (C2 β), 70.7 (C5 α), 70.6 (C2 α), 70.2 (C3 α), 70.2 (C6 α), 69.9 (C6 β), 68.9 (C7 α), 68.9 (C7 β), 67.1 (C8 α), 67.0 (C8 β), 66.2 (C4 α), 65.8 (C4 β), 63.2 (C9 β), 63.2 (C9 α) ppm.

HRMS (⁻ESI-TOF) m/z [M-H]⁻ calc. for C₉H₁₇O₉ 269.0878, found 269.0881

D 2.27 L-Lyxo-L-manno-nonose octaacetate [41]

**Procedure**

For further purification, the nonose [13] (400 mg, 1.48 mmol, 1.00 equiv.) obtained from the ozonolysis was taken up in pyridine (99%, 5.0 mL) and acetic anhydride (3.63 g, 3.36 mL, 35.5 mmol, 24.0 equiv.) was added dropwise under ice-bath cooling. Further, a spatula tip of DMAP was added to the mixture and stirring was proceeded at room temperature. After 2 hours, HPLC-MS and TLC analysis (CHCl₃/MeOH/H₂O 14:7:1, LP/EtOAc 1:1, staining agent: anisaldehyde) indicated full conversion of the starting material to the peracetylated species and excessive reagent was quenched by the addition of MeOH (1.5 mL). Stirring was continued for 15 minutes.

The reaction mixture was diluted with EtOAc (50 mL) and extracted with ice-cold 1N HCl (3×20 mL– until pH remained acidic). Back extraction of the aqueous phase was performed with EtOAc (3×20 mL), and the pooled organic phase was washed with water (20 mL) and sat. aq. NaHCO₃ (2×25 mL). After drying over anhydrous Na₂SO₄, the solvent was removed *in vacuo* giving a yellow, oily crude material (665 mg).

Purification

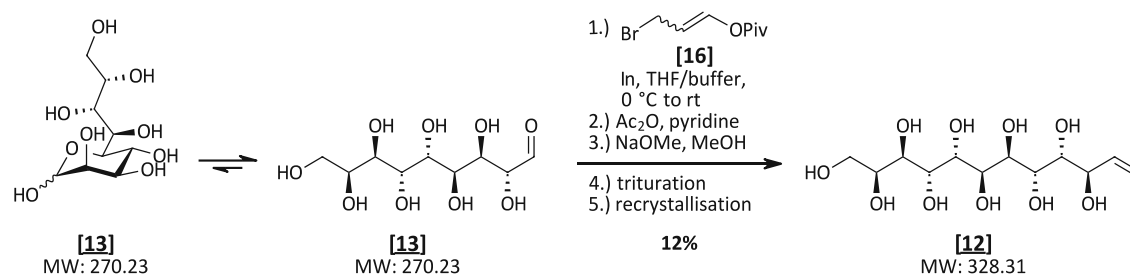
The pure product [41] was obtained by flash column chromatography (45.5 g SiO₂, LP/EtOAc 5:1 → 1:1) as a yellow oil (675 mg, 75%) in a ratio of $\alpha/\beta = 2:1$ (according to ¹H-NMR).

Yield	675 mg, 75%
Appearance	yellow oil
R_f	0.26 (red) (LP/EtOAc 1:1, staining agent: anisaldehyde)
¹H-NMR (600 MHz, CDCl₃)	$\delta = 6.15$ (d, $J = 1.7$ Hz, 2H, H1 α), 5.77 (d, $J = 1.1$ Hz, 1H, H1 β), 5.59 (dd, $J = 9.4, 1.9$ Hz, 2H, H6 α), 5.52 (dd, $J = 9.9, 1.9$ Hz, 1H, H6 β), 5.44 (dd, $J = 3.3, 1.0$ Hz, 1H, H2 β), 5.42 (dd, $J = 9.9, 2.4$ Hz, 1H, H7 β), $5.32 - 5.29$ (m, 2H, H3 α), $5.27 - 5.23$ (m, 4H, H7 α , H8 α), 5.22 (dd, $J = 3.5, 1.8$ Hz, 2H, H2 α), $5.19 - 5.13$ (m, 2H, H4 β , H8 β), $5.12 - 5.07$ (m, 3H, H4 α , H3 β), 4.25 (dd, $J = 11.7, 5.2$ Hz, 1H, H9a (β)), 4.20 (dd, $J = 11.4, 6.0$ Hz, 2H, H-9a (α)), 3.94 (dd, $J = 10.3, 1.3$ Hz, 2H, H5 α), $3.89 - 3.82$ (m, 3H, H9b (α), H9b (β)), 3.77 (dd, $J = 10.0, 2.4$ Hz, 1H, H5 β), $2.20 - 1.96$ (16×s, 72H, 8×COCH ₃ (α), 8×COCH ₃ (β)) ppm.

$^{13}\text{C-NMR}$ (151 MHz, CDCl_3) $\delta = 170.6$ ($\underline{\text{C}}\text{OCH}_3\alpha$), 170.5 ($\underline{\text{C}}\text{OCH}_3\beta$), 170.4 ($\underline{\text{C}}\text{OCH}_3\alpha$), 170.4, 170.3 ($2\times\underline{\text{C}}\text{OCH}_3\beta$), 170.3 ($\underline{\text{C}}\text{OCH}_3\alpha$), 170.1, 169.9 ($2\times\underline{\text{C}}\text{OCH}_3\beta$), 169.8, 169.8 ($2\times\underline{\text{C}}\text{OCH}_3\alpha$), 169.7 ($\underline{\text{C}}\text{OCH}_3\beta$), 169.4 ($\underline{\text{C}}\text{OCH}_3\alpha$), 169.1 ($\underline{\text{C}}\text{OCH}_3\beta$), 169.0 ($\underline{\text{C}}\text{OCH}_3\alpha$), 168.2 ($\underline{\text{C}}\text{OCH}_3\beta$), 167.7 ($\underline{\text{C}}\text{OCH}_3\alpha$), 90.5 (C1 α), 90.4 (C1 β), 73.0 (C5 β), 71.5 (C3 β), 69.9 (C5 α), 69.5 (C3 α), 68.8 (C2 α), 68.4 (C2 β), 68.1 (C8 β), 67.9 (C8 α), 67.8 (C6 β), 67.7 (C6 α), 65.9 (C7 α), 65.5 (C7 β), 64.7 (C4 α), 64.3 (C4 β), 62.3 (C9 β), 61.6 (C9 α), 21.0 – 20.6 ($8\times\underline{\text{C}}\text{OCH}_3$ (α), $8\times\underline{\text{C}}\text{OCH}_3$ (β)) ppm.

HRMS (+ESI-TOF) m/z $[\text{M}+\text{Na}]^+$ calc. for $\text{C}_{25}\text{H}_{34}\text{NaO}_{17}$ 629.5151, found 629.1691

D 2.28 1,2-Dideoxy-L-glycero-D-manno-D-manno-dodecenitol [12]

**Procedure****Step 1 – IMA**

Based on a literature protocol³⁸, indium (85 mg, 0.74 mmol, 4.0 equiv.) was weighed in a flame dried Schlenk flask and Schlenk technique was applied. Anhydrous THF (1.0 mL) was added, and the mixture was cooled to 0 °C using an ice-bath. 3-Bromopropenyl pivalate [16] (0.25 g, 1.1 mmol, 6.0 equiv.) was added dropwise to the vigorously stirring mixture. After 15 min, the ice-bath was removed, and the suspension was allowed to warm up to room temperature and stirred for another 45 min. Then, L-lyxo-L-manno-nonose [13] (50 mg, 0.19 mmol, 1.0 equiv.) was added to the pre-formed reagent as a solution in phthalate buffer (pH ~3, 0.2 mL). TLC ($\text{CHCl}_3/\text{MeOH}/\text{H}_2\text{O}$ 14:7:1, staining reagent: anisaldehyde) indicated conversion to the enitol species but also showed that starting material is left (after 45 min). The reaction mixture was diluted with MeOH and H_2O and filtered. The filtrate was concentrated *in vacuo*, giving a colourless solid.

Step 2 – Acetylation

This material was taken up in pyridine (99%, 3 mL), and Ac_2O (0.85 g, 0.79 mL, 8.3 mmol, 45 eq.) was added to the stirring mixture under ice-bath cooling. After 10 min, the ice-bath was removed, and a spatula of DMAP was added. Stirring at rt was continued overnight, and The next day, HPLC-MS indicated complete conversion to the fully protected dodecenitol and nonose, so excessive reagent was quenched by the addition of MeOH (0.5 mL) under ice-bath cooling, and the mixture was stirred for further 15 min. After diluting with EtOAc (50 mL), the organic phase was extracted with ice-cold 1N HCl (2×25 mL – until pH remained acidic). After back extraction (2×20 mL EtOAc), the pooled organic phase was washed with water (20 mL), aq. sat. NaHCO_3 (20 mL) and brine. After drying over anhydrous Na_2SO_4 , the solution was evaporated to dryness (124 mg).

From this, the protected dodecenitol could be isolated *via* column chromatography (12.5 g SiO_2 , LP/EtOAc 3:1 → 1:1) (38 mg, 26%) as a yellow oil and the nonose peracetate was recovered (65 mg, 58%).

Step 3 – Deacetylation

The dodecenitol peracetate was taken up in MeOH (HPLC grade, 0.5 mL) and NaOMe (30% in MeOH) was added under stirring at rt until pH was about 11. Reaction monitoring *via* HPLC-MS showed full conversion after 3 hours. The reaction mixture was neutralized by the addition of Dowex-H⁺ (MeOH washed), H₂O was added to dissolve the precipitated enitol, and the solution was filtered. Evaporation of the solvent gave a beige solid matter (20 mg) that is a mixture of dodecenitol diastereomers with a ratio of *lyxo* : *xylo* : *ribo* = 70 : 25 : 6.

Purification

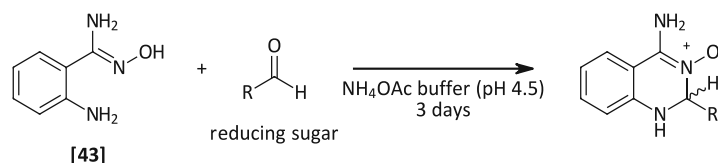
The material was then triturated in MeOH (1 mL), and the remaining solid was isolated *via* centrifugation. The residue was again washed with MeOH (2×1 mL), and further triturated in H₂O (2×1 mL). After washing with MeOH (1 mL) and Et₂O (1 mL), the remained white solid was dried at 50 °C, giving pure *L-glycero-D-manno-D-manno-dodecenitol* [12] (7 mg, 12%).

<u>Yield</u>	7 mg, 12% (over 3 steps)
<u>Appearance</u>	colourless solid
<u>¹H-NMR (600 MHz, D₂O)</u>	δ = 6.03 (ddd, <i>J</i> = 17.3, 10.5, 6.9 Hz, 1H, H2), 5.39 (dt, <i>J</i> = 17.1, 1.3 Hz, 1H, H1 (<i>E</i>)), 5.32 (dt, <i>J</i> = 10.5, 1.1 Hz, 1H, H1 (<i>Z</i>)), 4.21 (t, <i>J</i> = 7.5 Hz, 1H, H3), 4.01 (t, <i>J</i> = 6.5 Hz, 1H, H10), 3.99 – 3.96 (m, 5H, H5, H6, H7, H8, H9), 3.79 (d, <i>J</i> = 8.1 Hz, 1H, H4), 3.72 – 3.70 (m, 3H, H12a, H12b, H10) ppm.
<u>¹³C-NMR (151 MHz, D₂O)</u>	δ = 138.0 (C2), 118.1 (C1), 72.6 (C3), 72.0 (C4), 70.4 (C11), 69.5 (C10), 69.0 – 67.8 (C5, C6, C7, C8, C9), 63.4 (C12) ppm.
<u>HRMS (⁻ESI-TOF)</u>	<i>m/z</i> [M-H] ⁻ calc. for C ₁₂ H ₂₃ O ₁₀ 327.1296, found 327.1296

Note

Due to the low solubility of the final product in the used solvent (D₂O), no ¹³C-NMR spectrum could be recorded, and the given shifts for the carbon atoms were determined from the corresponding HSQC spectrum.

D 2.29 General procedure for the ABAO assay used for the determination of the OCC of *L-glycero-D-manno-heptose* [11] and *L-lyxo-L-manno-nonose* [13]



Procedure

To a solution of 2-aminobenzamidoxyamine (ABAO, [43], 42.1 mM) in NH_4OAc buffer (190 μL , 100 mM, pH 4.5) in a 96-well plate (Greiner, 96-well microplate, PS, F-bottom, clear) with lid (Greiner, with condensation rings, PS, high profile, clear), an aqueous solution of the respective sugar (10 μL , 80 mM) in H_2O was added. The plate was shaken in the plate reader, and measurements were conducted at 405 nm for 3 days at 25°C.

Blank samples with pure water (10 μL) instead of the sugar solution were performed and considered, too. All reactions and the blank samples were performed in triplicates.

Calculation of OCC

The calculation of the OCC was performed according to Kalaus, et al.⁷

Results

Entry	Name	OCC (%)
1	<i>L-glycero-D-manno-heptose</i> [11]	0.0344
2	<i>L-lyxo-D-manno-nonose</i> [13]	0.0343

Die approbierte gedruckte Originalversion dieser Diplomarbeit ist an der TU Wien Bibliothek verfügbar
The approved original version of this thesis is available in print at TU Wien Bibliothek.



E Appendix

E 1 Curriculum vitae

Education and Scholarships

02/2019 – today

Master programme Technical Chemistry

(expected graduation 03/2021)

Vienna University of Technology (TU Wien), Vienna, Austria

Specialisation in applied organic synthetic chemistry

Master thesis: Non-Natural Sugar Alcohols as Potential
Phase Change Materials

Supervised by: Prof. Dr. Michael Schnürch
Dr. Christian Stanetty

08/2019 – 01/2020

ERASMUS+ semester in Master programme Chemistry

Uppsala University, Uppsala, Sweden

Courses in biochemistry and organic chemistry

10/2015 – 01/2019

Bachelor programme Technical Chemistry

Vienna University of Technology (TU Wien), Vienna, Austria

Graduation with Distinction

Bachelor thesis: Synthesis of Oxymetholon-Metabolites

Supervised by: Prof. Dr. Peter Gärtner
Dr. Nicolas Kratena

2017/18 and 2018/19

Performance scholarship of TU Wien

2007 – 2015

Bundesrealgymnasium Waidhofen an der Thaya

Waidhofen an der Thaya, Austria

Specialisation in natural science

Graduation with Distinction

Publications

10/2019

Synthesis of a human long-term oxymetholone metabolite
Nicolas Kratena, **Nina Biedermann**, Biljana Stojanovic, Lorenz
Göschl, Matthias Weil, Valentin S. Enev*, Günter Gmeiner,
Peter Gärtner*

Steroids 150 (2019), 108430

Work Experience

11/2020 – 03/2021

Scientific co-worker

at research group Bioorganic Synthetic Chemistry

TU Wien, Vienna, Austria

Contracted NMR-analysis by cooperation partners
(academia & industry)

2018 – 2019

Tutor

at Synthesis Laboratory Course of Bachelor Programme

Technical Chemistry

TU Wien, Vienna, Austria

03/2018 – 09/2019

Student assistant

at Chemistry and Mechanical Engineering Library

TU Wien, Vienna, Austria

Additional Skills

Fond Computer Skills

MS-Office

Word, Excel, Power Point

Chemistry related software

MestreNova

ChemDraw, ChemDoodle

Scifinder, Reaxys

Language Skills

German native

English advanced high

Swedish novice high

Further Interests

Memberships

Big Band Waidhofen

Hobbies

Triathlon, winter sports, playing the saxophone

E 2 References

1. Voet, D.; Voet, J. G.; Pratt, C. W., *Lehrbuch der Biochemie*. 2., aktualisierte und erweitert Auflage ed.; Wiley-VCH: Weinheim, **2010**; p XXVI, 1253.
2. Bruice, P. Y., *Organische Chemie: Studieren kompakt*. 5th ed.; Pearson Deutschland GmbH: Hallbergmoos, **2011**; p 1166.
3. Sinnott, M., *Carbohydrate chemistry and biochemistry: Structure and mechanism*. RSC Publishing: Cambridge, **2007**.
4. Moss, G. P., Basic terminology of stereochemistry (IUPAC Recommendations 1996). *Pure Appl. Chem.* **1996**, *68* (12), 2193-2222.
5. Tentative rules for carbohydrate nomenclature. *Eur. J. Biochem.* **1971**, *21* (4), 455-477.
6. Zhu, Y.; Zajicek, J.; Serianni, A. S., Acyclic forms of [1-¹³C]aldohexoses in aqueous solution: Quantitation by ¹³C NMR and deuterium isotope effects on tautomeric equilibria. *J. Org. Chem.* **2001**, *66* (19), 6244-6251.
7. Kalaus, H.; Reichetseder, A.; Scheibelreiter, V.; Rudroff, F.; Stanetty, C.; Mihovilovic, M. D., A kinetic photometric assay for open-chain aldose quantification. *Eur. J. Org. Chem.* **2021**, submitted for publication.
8. Dworkin, J. P.; Miller, S. L., A kinetic estimate of the free aldehyde content of aldoses. *Carbohydr. Res.* **2000**, *329* (2), 359-365.
9. Serianni, A. S.; Clark, E. L.; Barker, R., Carbon-13-enriched carbohydrates. Preparation of erythrose, threose, glyceraldehyde, and glycolaldehyde with ¹³C-enrichment in various carbon atoms. *Carbohydr. Res.* **1979**, *72*, 79-91.
10. Drew, K. N.; Zajicek, J.; Bondo, G.; Bose, B.; Serianni, A. S., ¹³C-Labeled aldopentoses: Detection and quantitation of cyclic and acyclic forms by heteronuclear 1D and 2D NMR spectroscopy. *Carbohydr. Res.* **1998**, *307* (3), 199-209.
11. Godswill, A. C., Sugar alcohols: chemistry, production, health concerns and nutritional importance of mannitol, sorbitol, xylitol, and erythritol. *Int. J. Adv. Aca. Res* **2017**, *3* (2), 31-66.
12. Fischer, E., Über die Konfiguration des Traubenzuckers und seiner Isomeren. I. In *Untersuchungen Über Kohlenhydrate und Fermente (1884–1908)*, Springer Berlin Heidelberg: Berlin, Heidelberg, **1909**; pp 417-426.
13. Fischer, E., Über die Konfiguration des Traubenzuckers und seiner Isomeren. II. In *Untersuchungen Über Kohlenhydrate und Fermente (1884–1908)*, Springer Berlin Heidelberg: Berlin, Heidelberg, **1909**; pp 427-431.
14. Lawson, M. E., Sugar alcohols. In *Kirk-Othmer Encyclopedia of Chemical Technology*, John Wiley & Sons: Hoboken, **2000**; pp 1-24.
15. Solé, A.; Neumann, H.; Niedermaier, S.; Martorell, I.; Schossig, P.; Cabeza, L. F., Stability of sugar alcohols as PCM for thermal energy storage. *Sol. Energy Mater. Sol. Cells* **2014**, *126*, 125-134.
16. Kaizawa, A.; Maruoka, N.; Kawai, A.; Kamano, H.; Jozuka, T.; Senda, T.; Akiyama, T., Thermophysical and heat transfer properties of phase change material candidate for waste heat transportation system. *Heat Mass Transfer.* **2008**, *44* (7), 763-769.
17. del Barrio, E. P.; Godin, A.; Duquesne, M.; Daranlot, J.; Jolly, J.; Alshaer, W.; Kouadio, T.; Sommer, A., Characterization of different sugar alcohols as phase change materials for thermal energy storage applications. *Sol. Energy Mater. Sol. Cells* **2017**, *159*, 560-569.
18. Hühlein, S.; König-Haagen, A.; Brüggemann, D., Thermophysical characterization of MgCl₂·6H₂O, xylitol and erythritol as phase change materials (PCM) for latent heat thermal energy storage (LHTES). *Materials* **2017**, *10* (4), 444.
19. Barreneche, C.; Gil, A.; Sheth, F.; Inés Fernández, A.; Cabeza, L. F., Effect of D-mannitol polymorphism in its thermal energy storage capacity when it is used as PCM. *Solar Energy* **2013**, *94*, 344-351.

20. Jia, R.; Sun, K.; Li, R.; Zhang, Y.; Wang, W.; Yin, H.; Fang, D.; Shi, Q.; Tan, Z., Heat capacities of some sugar alcohols as phase change materials for thermal energy storage applications. *J. Chem. Thermodyn.* **2017**, *115*, 233-248.
21. Monrad, R. N.; Madsen, R., Modern methods for shortening and extending the carbon chain in carbohydrates at the anomeric center. *Tetrahedron* **2011**, *67*, 8825-8850.
22. Palmelund, A.; Madsen, R., Chain elongation of aldoses by indium-mediated coupling with 3-bromopropenyl esters. *J. Org. Chem.* **2005**, *70* (20), 8248-8251.
23. Stanetty, C.; Baxendale, I. R., Large-scale synthesis of crystalline 1,2,3,4,6,7-hexa-*O*-acetyl-*L*-glycero- α -*D*-manno-heptopyranose. *Eur. J. Org. Chem.* **2015**, *2015* (12), 2718-2726.
24. Draskovits, M.; Stanetty, C.; Baxendale, I. R.; Mihovilovic, M. D., Indium- and zinc-mediated acyloxyallylation of protected and unprotected aldotetroses—Revealing a pronounced diastereodivergence and a fundamental difference in the performance of the mediating metal. *J. Org. Chem.* **2018**, *83* (5), 2647-2659.
25. Kiliani, H., Ueber die Einwirkung von Blausäure auf Dextrose. *Ber. Dtsch. Chem. Ges.* **1886**, *19* (1), 767-772.
26. Goyorgydeak, Z.; Pelyvas, I., *Monosaccharide sugars: Chemical synthesis by chain elongation, degradation, and epimerization*. Academic Press: San Diego, **1998**.
27. Baylis, A. B.; Hillmann, M. E. D. Acrylic compounds. DE 2155113, **1972**.
28. Basavaiah, D.; Rao, K. V.; Reddy, R. J., The Baylis–Hillman reaction: a novel source of attraction, opportunities, and challenges in synthetic chemistry. *Chem. Soc. Rev.* **2007**, *36* (10), 1581-1588.
29. Krishna, P. R.; Reddy, P. V. N.; Sreeshailam, A.; Uday Kiran, M.; Jagdeesh, B., The Baylis–Hillman reaction: a strategic tool for the synthesis of higher-carbon sugars. *Tetrahedron Lett.* **2007**, *48* (37), 6466-6470.
30. Krishna, P. R.; Sachwani, R.; Reddy, P. S., Asymmetric Baylis-Hillman reaction: An enchanting expedition. *Synlett* **2008**, *2008* (19), 2897-2912.
31. McGarvey, G. J.; Kimura, M.; Oh, T.; Williams, J. M., Acyclic stereoselective synthesis of carbohydrates. *Carbohydr. Chem.* **1984**, *3* (2), 125-188.
32. Cumpstey, I.; Gehrke, S.; Erfan, S.; Cribiu, R., Studies on the synthesis of valienamine and 1-epivalienamine starting from *D*-glucose or *L*-sorbose. *Carbohydr. Res.* **2008**, *343* (10), 1675-1692.
33. Schmid, W.; Whitesides, G. M., Carbon-carbon bond formation in aqueous ethanol: Diastereoselective transformation of unprotected carbohydrates to higher carbon sugars using allyl bromide and tin metal. *J. Am. Chem. Soc.* **1991**, *113*, 6674-6675.
34. Kim, E.; Gordon, D. M.; Schmid, W.; Whitesides, G. M., Tin- and indium-mediated allylation in aqueous media: Application to unprotected carbohydrates. *J. Org. Chem.* **1993**, *58* (20), 5500-5507.
35. Prenner, R. H.; Binder, W. H.; Schmid, W., Indium-assisted allylation in carbohydrate chemistry: A convenient route to *D*-glycero-*D*-galacto- and *D*-glycero-*L*-galacto-heptose. *Liebigs Ann. Chem.* **1994**, *1994* (1), 73-78.
36. Binder, W. H.; Prenner, R. H.; Schmid, W., Indium-mediated allylation of aldehydes: a convenient route to 2-deoxy and 2,6-dideoxy carbohydrates. *Tetrahedron* **1994**, *50* (3), 749-758.
37. Lombardo, M.; Girotti, R.; Morganti, S.; Trombini, C., A new protocol for the acetoxyallylation of aldehydes mediated by indium in THF. *Org. Lett.* **2001**, *3* (19), 2981-2983.
38. Lombardo, M.; Morganti, S.; Trombini, C., 3-Bromopropenyl esters in organic synthesis: Indium- and zinc-mediated entries to alk-1-ene-3,4-diols. *J. Org. Chem.* **2003**, *68* (3), 997-1006.
39. Lombardo, M.; Gianotti, K.; Licciulli, S.; Trombini, C., An environmentally friendly α -hydroxyallylation reaction of the Garner aldehyde: a comparative assessment of alternative Barbier conditions. *Tetrahedron* **2004**, *60* (51), 11725-11732.

40. Lombardo, M.; Licciulli, S.; Trombini, C., 3-Halopropenyl esters as precursors of a new class of oxygen-substituted allylic organometallic compounds: Applications in organic synthesis. *Pure Appl. Chem.* **2004**, *76* (3), 657-669.
41. Dincer, I.; Rosen, M. A., *Thermal energy storage: Systems and applications*. 2nd ed.; Wiley: Chichester, **2011**.
42. Mohamed, S. A.; Al-Sulaiman, F. A.; Ibrahim, N. I.; Zahir, M. H.; Al-Ahmed, A.; Saidur, R.; Yılbaş, B. S.; Sahin, A. Z., A review on current status and challenges of inorganic phase change materials for thermal energy storage systems. *Renew. Sustain. Energy Rev.* **2017**, *70*, 1072-1089.
43. Liu, M.; Fernández, A. I.; Segarra, M., Chapter 8 - Materials for phase change material at high temperature. In *High Temperature Thermal Storage Systems Using Phase Change Materials*, Cabeza, L. F.; Tay, N. H. S., Eds. Academic Press: London [i.a.], **2018**; pp 195-230.
44. Cabeza, L. F.; Martorell, I.; Miró, L.; Fernández, A. I.; Barreneche, C., 1 - Introduction to thermal energy storage (TES) systems. In *Advances in Thermal Energy Storage Systems*, Cabeza, L. F., Ed. Woodhead Publishing: Cambridge, **2015**; pp 1-28.
45. Fredi, G.; Dorigato, A.; Fambri, L.; Pegoretti, A., Multifunctional structural composites for thermal energy storage. *Multifunctional Materials* **2020**, *3* (4), 042001.
46. Sarbu, I.; Sebarchievici, C., A comprehensive review of thermal energy storage. *Sustainability* **2018**, *10* (1), 191.
47. Beddoe, R. H.; Sneddon, H. F.; Denton, R. M., The catalytic Mitsunobu reaction: a critical analysis of the current state-of-the-art. *Org. Biomol. Chem.* **2018**, *16* (42), 7774-7781.
48. Fletcher, S., The Mitsunobu reaction in the 21st century. *Org. Chem. Front.* **2015**, *2* (6), 739-752.
49. Wang, R. Z.; Xu, Z. Y.; Ge, T. S., 1 - Introduction to solar heating and cooling systems. In *Advances in Solar Heating and Cooling*, Wang, R. Z.; Ge, T. S., Eds. Woodhead Publishing: Cambridge, **2016**; pp 3-12.
50. Elias, C. N.; Stathopoulos, V. N., A comprehensive review of recent advances in materials aspects of phase change materials in thermal energy storage. *Energy Procedia* **2019**, *161*, 385-394.
51. Stadler, I.; Sterner, M., 2.3 - Urban energy storage and sector coupling. In *Urban Energy Transition (Second Edition)*, Droege, P., Ed. Elsevier: Amsterdam [i.a.], **2018**; pp 225-244.
52. Block, T.; Schmücker, M., Metal oxides for thermochemical energy storage: A comparison of several metal oxide systems. *Solar Energy* **2016**, *126*, 195-207.
53. de Gracia, A.; Cabeza, L. F., Phase change materials and thermal energy storage for buildings. *Energy and Buildings* **2015**, *103*, 414-419.
54. Pause, B., 9 - Phase change materials and their application in coatings and laminates for textiles. In *Smart Textile Coatings and Laminates*, Smith, W. C., Ed. Woodhead Publishing: Cambridge, **2010**; pp 236-250.
55. Fleischer, A. S., *Thermal energy storage using phase change materials : fundamentals and applications*. Springer International Publ.: Cham [i.a.], **2015**; p X, 94 S., Ill., graph. Darst., 235 mm x 155 mm.
56. Sharma, A.; Tyagi, V. V.; Chen, C. R.; Buddhi, D., Review on thermal energy storage with phase change materials and applications. *Renew. Sustain. Energy Rev.* **2009**, *13* (2), 318-345.
57. Bruno, F.; Belusko, M.; Liu, M.; Tay, N. H. S., 9 - Using solid-liquid phase change materials (PCMs) in thermal energy storage systems. In *Advances in Thermal Energy Storage Systems*, Cabeza, L. F., Ed. Woodhead Publishing: Cambridge, **2015**; pp 201-246.
58. Nazir, H.; Batool, M.; Bolivar Osorio, F. J.; Isaza-Ruiz, M.; Xu, X.; Vignarooban, K.; Phelan, P.; Inamuddin; Kannan, A. M., Recent developments in phase change materials for energy storage applications: A review. *Int. J. Heat Mass Transfer* **2019**, *129*, 491-523.
59. Peng, S.; Fuchs, A.; Wirtz, R. A., Polymeric phase change composites for thermal energy storage. *J. Appl. Polym. Sci.* **2004**, *93* (3), 1240-1251.

60. Mehling, H.; Schossig, P.; Kalz, D.; Friedrich (ed.), U. Latent heat storage in buildings. Storing heat and cold in a compact and demnad-oriented manner *BINE themeninfo* [Online], **2009**, p. 1-20. (accessed 31/01/2021).
61. Lin, Y.; Alva, G.; Fang, G., Review on thermal performances and applications of thermal energy storage systems with inorganic phase change materials. *Energy* **2018**, *165*, 685-708.
62. Vakhshouri, A. R., Paraffin as phase change material [online first]. In *Paraffin - an Overview [Working Title]*, Soliman, F. S., Ed. Intech Open: London, **2019**.
63. Jelle, B. P.; Kalnæs, S. E., Chapter 3 - Phase change materials for application in energy-efficient buildings. In *Cost-Effective Energy Efficient Building Retrofitting*, Pacheco-Torgal, F.; Granqvist, C.-G.; Jelle, B. P.; Vanoli, G. P.; Bianco, N.; Kurnitski, J., Eds. Woodhead Publishing: Cambridge, **2017**; pp 57-118.
64. Pielichowska, K.; Pielichowski, K., Phase change materials for thermal energy storage. *Prog. Mater Sci.* **2014**, *65*, 67-123.
65. Xie, N.; Huang, Z.; Luo, Z.; Gao, X.; Fang, Y.; Zhang, Z., Inorganic salt hydrate for thermal energy storage. *Appl. Sci.* **2017**, *7* (12), 1317.
66. Abhat, A., Low temperature latent heat thermal energy storage: Heat storage materials. *Solar Energy* **1983**, *30* (4), 313-332.
67. Akeiber, H.; Nejat, P.; Majid, M. Z. A.; Wahid, M. A.; Jomehzadeh, F.; Zeynali Famileh, I.; Calautit, J. K.; Hughes, B. R.; Zaki, S. A., A review on phase change material (PCM) for sustainable passive cooling in building envelopes. *Renew. Sustain. Energy Rev.* **2016**, *60*, 1470-1497.
68. Yang, X.-H.; Liu, J., Chapter four - Advances in liquid metal science and technology in chip cooling and thermal management. In *Advances in Heat Transfer*, Sparrow, E. M.; Abraham, J. P.; Gorman, J. M., Eds. Elsevier: Amsterdam [i.a.] **2018**; Vol. 50, pp 187-300.
69. Sarier, N.; Onder, E., Organic phase change materials and their textile applications: An overview. *Thermochim. Acta* **2012**, *540*, 7-60.
70. Kou, Y.; Wang, S.; Luo, J.; Sun, K.; Zhang, J.; Tan, Z.; Shi, Q., Thermal analysis and heat capacity study of polyethylene glycol (PEG) phase change materials for thermal energy storage applications. *J. Chem. Thermodyn.* **2019**, *128*, 259-274.
71. Nikolić, R.; Marinović-Cincović, M.; Gadžurić, S.; Zsigrai, I. J., New materials for solar thermal storage—solid/liquid transitions in fatty acid esters. *Sol. Energy Mater. Sol. Cells* **2003**, *79* (3), 285-292.
72. Gao, W.; Lin, W.; Liu, T.; Xia, C., An experimental study on the heat storage performances of polyalcohols NPG, TAM, PE, and AMPD and their mixtures as solid-solid phase-change materials for solar energy applications. *Int. J. Green Energy* **2007**, *4* (3), 301-311.
73. Fallahi, A.; Guldentops, G.; Tao, M.; Granados-Focil, S.; Van Dessel, S., Review on solid-solid phase change materials for thermal energy storage: Molecular structure and thermal properties. *Appl. Therm. Eng.* **2017**, *127*, 1427-1441.
74. del Barrio, E. P.; Cadoret, R.; Daranlot, J.; Achchaq, F., New sugar alcohols mixtures for long-term thermal energy storage applications at temperatures between 70°C and 100°C. *Sol. Energy Mater. Sol. Cells* **2016**, *155*, 454-468.
75. Inagaki, T.; Ishida, T., Computational design of non-natural sugar alcohols to increase thermal storage density: Beyond existing organic phase change materials. *J. Am. Chem. Soc.* **2016**, *138* (36), 11810-11819.
76. Inagaki, T.; Ishida, T., Computational analysis of sugar alcohols as phase-change material: Insight into the molecular mechanism of thermal energy storage. *J. Phys. Chem.* **2016**, *120* (15), 7903-7915.
77. Draskovits, M. New methodologies for the interconversion of reducing sugars by activation of the anomeric carbin. Dissertation, Vienna University of Technology, Vienna, **2020**.
78. Karnekanti, R.; Hanumaiah, M.; Sharma, G. V. M., Stereoselective total synthesis of (+)-Anamarine and 8-*epi*-(-)-Anamarine from D-mannitol. *Synthesis* **2015**, *47* (19), 2997-3008.

79. Yadav, J. S.; Chinnam, V. V.; Krishna, B. B. M.; Rao, K. L. S.; Das, S., Stereoselective synthesis of vittarilide-A. *Tetrahedron Lett.* **2015**, *56* (13), 1661-1663.
80. Kumar, P.; Naidu, S. V., Enantio- and diastereocontrolled total synthesis of (+)-Boronolide. *J. Org. Chem.* **2006**, *71* (10), 3935-3941.
81. Sabitha, G.; Reddy, C. N.; Raju, A.; Yadav, J. S., Stereoselective total synthesis of the cytotoxic lactone (-)-spicigerolide. *Tetrahedron: Asymmetry* **2011**, *22* (4), 493-498.
82. Marko, I. E.; Svendsen, J. S., 11.2 - Transition metal-catalyzed oxidations: Asymmetric hydroxylation. In *Comprehensive Organometallic Chemistry II*, Abel, E. W.; Stone, F. G. A.; Wilkinson, G., Eds. Elsevier: Oxford, **1995**; pp 1137-1176.
83. Figueiredo, J. L.; Pereira, M. M.; Faria, J., *Catalysis from theory to application: An integrated course*. Imprensa da Universidade de Coimbra: Maio, **2008**.
84. Gao, Y.; Donohoe, T. J.; Harris, R. M.; Chughtai, M. J.; Yang, J. W.; Kim, S. M.; Oh, J. S.; Song, E. E., Osmium tetroxide. In *Encyclopedia of Reagents for Organic Synthesis*, Pasquette, L. A., Ed. John Wiley & Sons Ltd: Hoboken, **2013**.
85. Cha, J. K.; Christ, W. J.; Kishi, Y., On stereochemistry of osmium tetroxide oxidation of allylic alcohol systems: empirical rule. *Tetrahedron* **1984**, *40* (12), 2247-2255.
86. Wai, J. S. M.; Marko, I.; Svendsen, J. S.; Finn, M. G.; Jacobsen, E. N.; Sharpless, K. B., A mechanistic insight leads to a greatly improved osmium-catalyzed asymmetric dihydroxylation process. *J. Am. Chem. Soc.* **1989**, *111* (3), 1123-1125.
87. Gao, Y.; Cheun, Y., Osmium tetroxide-N-methylmorpholine N-oxide. In *Encyclopedia of Reagents for Organic Synthesis*, Pasquette, L. A., Ed. John Wiley & Sons Ltd: Hoboken, **2013**.
88. Ager, D., 9.6 Industrial applications of asymmetric oxidations. In *Comprehensive Chirality*, Carreira, E. M.; Yamamoto, H., Eds. Elsevier: Amsterdam, **2012**; pp 104-128.
89. Kolb, H. C.; VanNieuwenhze, M. S.; Sharpless, K. B., Catalytic asymmetric dihydroxylation. *Chem. Rev.* **1994**, *94* (8), 2483-2547.
90. Gao, Y.; Cheun, Y., Osmium tetroxide-potassium ferricyanide. In *Encyclopedia of Reagents for Organic Synthesis*, Pasquette, L. A., Ed. John Wiley & Sons Ltd: Hoboken, **2013**.
91. Hale, K. J.; Manaviazar, S.; Peak, S. A., Anomalous enantioselectivity in the Sharpless catalytic asymmetric dihydroxylation reaction of 1,1-disubstituted allyl alcohol derivatives. *Tetrahedron Lett.* **1994**, *35* (3), 425-428.
92. Morikawa, K.; Park, J.; Andersson, P. G.; Hashiyama, T.; Sharpless, K. B., Catalytic asymmetric dihydroxylation of tetrasubstituted olefins. *J. Am. Chem. Soc.* **1993**, *115* (18), 8463-8464.
93. Ogino, Y.; Chen, H.; Kwong, H.-L.; Sharpless, K. B., On the timing of hydrolysis / reoxidation in the osmium-catalyzed asymmetric dihydroxylation of olefins using potassium ferricyanide as the reoxidant. *Tetrahedron Lett.* **1991**, *32* (32), 3965-3968.
94. Kobayashi, Y.; William, A. D.; Tokoro, Y., Sharpless asymmetric dihydroxylation of *trans*-propenylphosphonate by using a modified AD-mix- α and the synthesis of fosfomycin. *J. Org. Chem.* **2001**, *66* (23), 7903-7906.
95. Otte, D. A. L.; Borchmann, D. E.; Lin, C.; Weck, M.; Woerpel, K. A., ^{13}C NMR spectroscopy for the quantitative determination of compound ratios and polymer end groups. *Org. Lett.* **2014**, *16* (6), 1566-1569.
96. Malz, F.; Jancke, H., Validation of quantitative NMR. *J. Pharm. Biomed. Anal.* **2005**, *38* (5), 813-823.
97. Kumara Swamy, K. C.; Bhuvan Kumar, N. N.; Balaraman, E.; Pavan Kumar, K. V. P., Mitsunobu and related reactions: Advances and applications. *Chem. Rev.* **2009**, *109* (6), 2551-2651.
98. El Sous, M.; Khoo, M. L.; Holloway, G.; Owen, D.; Scammells, P. J.; Rizzacasa, M. A., Total synthesis of (-)-Episilvestrol and (-)-Silvestrol. *Angew. Chem. Int. Ed.* **2007**, *46* (41), 7835-7838.

99. Zheng, W.; Seletsky, B. M.; Palme, M. H.; Lydon, P. J.; Singer, L. A.; Chase, C. E.; Lemelin, C. A.; Shen, Y.; Davis, H.; Tremblay, L.; Towle, M. J.; Salvato, K. A.; Wels, B. F.; Aalfs, K. K.; Kishi, Y.; Littlefield, B. A.; Yu, M. J., Macrocyclic ketone analogues of halichondrin B. *Bioorganic & Medicinal Chemistry Letters* **2004**, *14* (22), 5551-5554.
100. Hughes, D. L.; Reamer, R. A., The effect of acid strength on the Mitsunobu esterification reaction: Carboxyl vs hydroxyl reactivity. *J. Org. Chem.* **1996**, *61* (9), 2967-2971.
101. Reusch, W. Acidity of carboxylic acids. <https://chem.libretexts.org/@go/page/779> (accessed 15/01/2021).
102. Schiaffo, C. E.; Dussault, P. H., Ozonolysis in solvent/water mixtures: Direct conversion of alkenes to aldehydes and ketones. *J. Org. Chem.* **2008**, *73* (12), 4688-4690.
103. Keith, J. M.; Gomez, L., Exploration of the Mitsunobu reaction with tosyl- and boc-hydrazones as nucleophilic agents. *J. Org. Chem.* **2006**, *71* (18), 7113-7116.
104. Guazzelli, L.; Ulc, R.; Rydner, L.; Oscarson, S., A synthetic strategy to xylose-containing thioglycoside tri- and tetrasaccharide building blocks corresponding to *Cryptococcus neoformans* capsular polysaccharide structures. *Org. Biomol. Chem.* **2015**, *13* (23), 6598-6610.
105. Combination of thermal analysis techniques. In *Introduction to thermal analysis. Hot topics in thermal analysis and calorimetry*, Brown, M. E., Ed. Springer: Dordrecht, **2004**; Vol. 1, pp 129-137.
106. Nomura, T.; Okinaka, N.; Akiyama, T., Impregnation of porous material with phase change material for thermal energy storage. *Mater. Chem. Phys.* **2009**, *115* (2), 846-850.
107. Gallegos Lazcano, M. A.; Yu, W., Thermal performance and flammability of phase change material for medium and elevated temperatures for textile application. *J. Therm. Anal. Calorim.* **2014**, *117* (1), 9-17.
108. Bayón, R.; Rojas, E., Feasibility study of D-mannitol as phase change material for thermal storage. *AIMS Energy* **2017**, *5* (3), 404-424.
109. Yamaguchi, A.; Sato, O.; Mimura, N.; Shirai, M., Intramolecular dehydration of mannitol in high-temperature liquid water without acid catalysts. *RSC Advances* **2014**, *4* (85), 45575-45578.
110. Brimacombe, J. S.; Hanna, R.; Kabir, A. K. M. S.; Bennett, F.; Taylor, I. D., Higher-carbon sugars. Part 1. The synthesis of some octose sugars *via* the osmylation of unsaturated precursors. *J. Chem. Soc., Perkin Trans. 1* **1986**, 815-821.
111. Nomura, T.; Zhu, C.; Sagara, A.; Okinaka, N.; Akiyama, T., Estimation of thermal endurance of multicomponent sugar alcohols as phase change materials. *Appl. Therm. Eng.* **2015**, *75*, 481-486.
112. Kumaresan, G.; Velraj, R.; Iniyan, S., Thermal analysis of D-mannitol for use as phase change material for latent heat storage. *J. Applied Sci.* **2011**, *11*, 3044-3048.
113. Gottlieb, H. E.; Kotlyar, V.; Nudelman, A., NMR chemical shifts of common laboratory solvents as trace impurities. *J. Org. Chem.* **1997**, *62* (21), 7512-7515.
114. Matveeva, E. D.; Podrugina, T. A.; Sandakova, N. G.; Zefirov, N. S., Triphenylphosphine-2,4,4,6-tetrabromo-2,5-cyclohexadienone complex as a reagent for preparation of carboxylic acid bromides. *Russ. J. Org. Chem.* **2004**, *40* (10), 1469-1472.